National Library
of Canada

Canadian Theses Service

Ottawa, Canada
K1A 0N4

Bibliothèque nationale
du Canada

Services des thèses canadiennes

CANADIAN THESES

THÈSES CANADIENNES

NOTICE

The quality of this microfiche is heavily dependent upon the quality of the original thesis submitted for microfilming. Every effort has been made to ensure the highest quality of reproduction possible.

If pages are missing, contact the university which granted the degree.

Some pages may have indistinct print especially if the original pages were typed with a poor typewriter ribbon or if the university sent us an inferior photocopy.

Previously copyrighted materials (journal articles, published tests, etc.) are not filmed.

Reproduction in full or in part of this film is governed by the Canadian Copyright Act, R.S.C. 1970, c. C-30. Please read the authorization forms which accompany this thesis.

AVIS

La qualité de cette microfiche dépend grandement de la qualité de la thèse soumise au microfilmage. Nous avons tout fait pour assurer une qualité supérieure de reproduction.

S'il manque des pages, veuillez communiquer avec l'université qui a conféré le grade.

La qualité d'impression de certaines pages peut laisser à désirer, surtout si les pages originales ont été dactylographiées à l'aide d'un ruban usé ou si l'université nous a fait parvenir une photocopie de qualité inférieure.

Les documents qui font déjà l'objet d'un droit d'auteur (articles de revue, examens publiés, etc.) ne sont pas microfilmés.

La reproduction, même partielle, de ce microfilm est soumise à la Loi canadienne sur le droit d'auteur, SRC 1970, c. C-30. Veuillez prendre connaissance des formules d'autorisation qui accompagnent cette thèse.

THIS DISSERTATION
HAS BEEN MICROFILMED
EXACTLY AS RECEIVED

LA THÈSE A ÉTÉ
MICROFILMÉE TELLE QUE
NOUS L'AVONS REÇUE

Canada

NL 339 (r. 86/01)

National Library of Canada
Ottawa, Canada
K1A 0N4

Bibliothèque nationale du Canada

74

TC –

ISBN 0-315-22940-3

CANADIAN THESES ON MICROFICHE SERVICE – SERVICE DES THÈSES CANADIENNES SUR MICROFICHE

PERMISION TO MICROFILM – AUTORISATION DE MICROFILMER

- Please print or type – Écrire en lettres moulées ou dactylographier

AUTHOR – AUTEUR

Full Name of Author – Nom complet de l'auteur
Kenneth Wayne Shushkewich

Date of Birth – Date de naissance
Sept 22, 1952

Canadian Citizen – Citoyen canadien
☒ Yes / Oui ☐ No / Non

Country of Birth – Lieu de naissance
Canada

Permanent Address – Résidence fixe
178 Maryland St
Winnipeg, Manitoba
R3G 1L3

THESIS – THÈSE

Title of Thesis – Titre de la thèse
Analysis of Segmental Bridges

Degree for which thesis was presented
Grade pour lequel cette thèse fut présentée
PhD

Year this degree conferred
Année d'obtention de ce grade
1985

University – Université
U of Alberta

Name of Supervisor – Nom du directeur de thèse
SH Simmonds

AUTHORIZATION – AUTORISATION

Permission is hereby granted to the NATIONAL LIBRARY OF CANADA to **microfilm** this thesis and to **lend** or **sell copies of the film.**

The author reserves other publication rights, and neither the thesis nor extensive extracts from it may be printed or otherwise reproduced without the author's written permission.

L'autorisation est, par la présente, accordée à la BIBLIOTHÈQUE NATIONALE DU CANADA de **microfilmer** cette thèse et de **prêter** ou de **vendre des exemplaires du film.**

L'auteur se réserve les autres droits de publication; ni la thèse ni de longs extraits de celle-ci ne doivent être imprimés ou autrement reproduits sans l'autorisation écrite de l'auteur.

ATTACH FORM TO THESIS – VEUILLEZ JOINDRE CE FORMULAIRE À LA THÈSE

Signature
KW Shushkewich

Date
May 30, 1985

NL-91 (r. 84/03)

Canada

THE UNIVERSITY OF ALBERTA

ANALYSIS OF SEGMENTAL BRIDGES

by

KENNETH WAYNE SHUSHKEWICH

A THESIS
SUBMITTED TO THE FACULTY OF GRADUATE STUDIES AND RESEARCH
IN PARTIAL FULFILMENT OF THE REQUIREMENTS FOR THE DEGREE
OF DOCTOR OF PHILOSOPHY
IN
STRUCTURAL ENGINEERING

DEPARTMENT OF CIVIL ENGINEERING

EDMONTON, ALBERTA
FALL, 1985

THE UNIVERSITY OF ALBERTA

RELEASE FORM

NAME OF AUTHOR	Kenneth Wayne Shushkewich
TITLE OF THESIS	Analysis of Segmental Bridges
DEGREE FOR WHICH THESIS WAS PRESENTED	PhD
YEAR THIS DEGREE GRANTED	1985

Permission is hereby granted to THE UNIVERSITY OF ALBERTA LIBRARY to reproduce single copies of this thesis and to lend or sell such copies for private, scholarly or scientific research purposes only.

The author reserves other publication rights, and neither the thesis nor extensive extracts from it may printed or otherwise reproduced without the author's written permission.

K.W. Shushkewich
KENNETH WAYNE SHUSHKEWICH

Permanent Address:

178 Maryland St
Winnipeg, Manitoba
R3G 1L3

Date May 28, 1985

THE UNIVERSITY OF ALBERTA

FACULTY OF GRADUATE STUDIES AND RESEARCH

The undersigned certify that they have read, and recommend to the Faculty of Graduate Studies and Research, for acceptance, a thesis entitled "Analysis of Segmental Bridges" submitted by Kenneth Wayne Shushkewich in partial fulfilment of the requirements for the degree of Doctor of Philosophy in Structural Engineering.

S H Simmonds
Dr S H Simmonds (Supervisor)
Department of Civil Engineering

T. Hrudey
Dr T M Hrudey
Department of Civil Engineering

Dr J G MacGregor
Department of Civil Engineering

D W Murray
Dr D W Murray
Department of Civil Engineering

JS Kennedy
Dr J S Kennedy
Department of Mechanical Engineering

William L. Gamble
Dr W L Gamble (External Examiner)
University of Illinois
at Urbana-Champaign

Date May 28, 1985

ABSTRACT

This research provides a methodology for the analysis of prestressed concrete segmental bridges. To maximize the design efficiency, the analysis of the bridge is uncoupled into two parts; the first part considers the time-dependent analysis of a segmental bridge under construction while the second part deals with the approximate three-dimensional analysis of a completed segmental bridge. The time-dependent analysis gives the longitudinal flexural requirements at each stage of construction, while the three-dimensional analysis gives the requirements for transverse flexure as well as longitudinal shear and torsion in the completed structure. The computer programs TIMEDEP and BOXGIRD have been developed to handle the time-dependent and three-dimensional analyses respectively.

TIMEDEP gives the time-dependent effects of creep and shrinkage in the concrete as well as relaxation of the prestressing. The loadings considered are self weight, prestress, construction loads, and temperature. The program is based on the direct stiffness method. The effects of creep and shrinkage are based on the recommendations of ACI Committee 209 while relaxation is given by the expression of Magura, Sozen, and Siess. Dirichlet series are used in conjunction with the method

of superposition to handle time-dependent effects.

BOXGIRD gives a three-dimensional analysis of a box girder bridge. The loadings considered are self weight, superimposed dead load, truck loads, lane loads, temperature, and prestressing. The program utilizes folded plate theory and is based on the direct stiffness method. Element stiffnesses are evaluated by the equations of Goldberg-Leve while the loads are given by an appropriate number of Fourier series terms.

This research also provides a methodology for the analysis of partially prestressed concrete sections. Since partial prestressing can be defined as the general case whose extremes are conventional reinforced concrete and fully prestressed concrete, the development of simple analysis procedures has a wide range of application. These include (but are not limited to) the longitudinal and transverse analysis of segmental bridges having prestressed and/or conventional reinforcing. New computational techniques are developed for the (1) uncracked section analysis, (2) cracked section analysis, and (3) ultimate strength analysis. The serviceability criteria of cracking, fatigue, and deformation are examined. The computer program PREBEAM has been developed for the analysis of partially prestressed concrete sections.

ACKNOWLEDGEMENTS

The author would like to thank Dr S H Simmonds for serving as his thesis supervisor. The fact that his door was always open to discuss aspects of this work is sincerely appreciated. In addition, the guidance provided by Dr D W Murray during the early stages of this research is gratefully acknowledged.

A number of individuals have enthusiastically provided valuable information during the course of this study. These include Dr W H Dilger, Dr W L Gamble, Dr A Ghali, Dr W Podolny Jr, Dr I C Potgieter, Professor A C Scordelis, and Dr M K Tadros.

Finally, the author would like to dedicate this work to his mentor Daniel Demarthe of Paris, France.

TABLE OF CONTENTS

Page

1. INTRODUCTION 1

1.1 General remarks 1

1.2 Objectives and scope 1

1.3 Organization of report 3

2. DESIGN CONSIDERATIONS 6

2.1 Introduction 6

2.2 Methods of construction 6

2.2.1 Balanced cantilever construction 6

2.2.2 Progressive placing 22

2.2.3 Span-by-span construction 24

2.2.4 Incremental launching 27

2.3 Design sequence 29

2.3.1 Conceptual design 30

2.3.2 Preliminary design 34

2.3.3 Detailed design 37

2.3.4 Design verification 38

2.3.5 Design changes 39

2.4 Conclusions 39

3. TIME-DEPENDENT ANALYSIS 40

3.1 Introduction 40

3.2 Basic definitions 41

3.3 Material models 43

3.3.1 Introduction 43

3.3.2 ACI 209 45

3.3.3 CEB 1970 50

3.3.4 CEB 1978 54
3.3.5 Bazant-Panula 59
3.3.6 Relaxation of prestressing 60
3.3.7 Discussion 61
3.4 Analytical models 62
3.4.1 Introduction 62
3.4.2 Effective modulus method 62
3.4.3 Rate of creep method 63
3.4.4 Linear superposition method 64
3.4.5 Discussion 65
3.5 Review of existing computer programs 67
3.6 Proposed method of analysis 74
3.6.1 Introduction 74
3.6.2 Segmental analysis 74
3.6.3 Analysis for creep and shrinkage 76
3.6.4 Prestressing analysis 80
3.6.5 Thermal analysis 85
3.6.6 Direct stiffness analysis 93
3.6.6.1 Introduction 93
3.6.6.2 Coordinate systems 93
3.6.6.3 Direct stiffness method 95
3.6.6.4 Element stiffness matrices 96
3.6.6.5 Element load vectors 99
3.6.6.6 Solution of equations 99
3.7 Computer program 102
3.8 Numerical examples 107
3.8.1 Example 1 - Creep test 107

3.8.2 Example 2 - Precast segmental bridge 110

3.9 Conclusions 118

4. THREE-DIMENSIONAL ANALYSIS 119

4.1 Introduction 119

4.2 Types of structural action 120

4.2.1 Introduction 120

4.2.2 Longitudinal bending 120

4.2.3 St Venant torsion 120

4.2.4 Warping torsion 121

4.2.5 Shear lag 121

4.2.6 Local effects 122

4.2.7 Summary 122

4.3 Review of analysis methods 128

4.3.1 Introduction 128

4.3.2 Hand methods 128

4.3.3 Finite difference method 129

4.3.4 Plane grid and space frame methods 130

4.3.5 Folded plate method 131

4.3.6 Finite element method 133

4.3.7 Finite strip method 134

4.3.8 Conclusions 135

4.4 Folded plate method 136

4.4.1 Introduction 136

4.4.2 Coordinate systems 137

4.4.3 Direct stiffness method 139

4.4.4 Element stiffness matrix 140

4.4.5 Stiffness influence coefficients 142

4.4.6 Element load vectors 142
4.4.7 Element forces 149
4.5 Computer program 150
4.6 Numerical examples 156
4.6.1 Introduction 156
4.6.2 Example 1 - Box girder bridge 157
4.6.3 Example 2 - Concentrated loads 160
4.6.4 Example 3 - Prestressing analysis 165
4.6.5 Example 4 - Corpus Christi bridge 168
4.6.6 Example 5 - Islington Avenue extension ... 173
4.7 Conclusions 194
5. PARTIAL PRESTRESSING 198
5.1 Introduction 198
5.2 Why partial prestressing? 199
5.3 Load deflection response 200
5.4 Analysis procedures 205
5.4.1 Introduction 205
5.4.2 Uncracked section analysis 208
5.4.3 Cracked section analysis 213
5.4.4 Ultimate strength analysis 219
5.5 Serviceability considerations 225
5.6 Computer program 231
5.7 Numerical examples 231
5.7.1 Example 1 - Partially prestressed T beam . 231
5.7.2 Example 2 - Islington Avenue extension ... 238
5.8 Conclusions 244
6. CONCLUSIONS AND RECOMMENDATIONS 245

6.1 Conclusions 245
6.2 Recommendations for further study 248
BIBLIOGRAPHY 250
APPENDICES 268
A TIMEDEP user's guide 268
B FORTRAN listing of TIMEDEP 274
C Listing of input data for TIMEDEP 284
D Listing of output information for TIMEDEP 287
E BOXGIRD user's guide 293
F FORTRAN listing of BOXGIRD 299
G Listing of input data for BOXGIRD 307
H Listing of output information for BOXGIRD 309
I FORTRAN listing of PREBEAM 314
J Listing of output information for PREBEAM 317
K Derivation of equations 3.22 and 3.23 319
L Membrane forces acting on a box girder bridge ... 323

LIST OF TABLES

Table		Page
2.1	Range of appication of bridge type by span length	31
2.2	Average bridge lengths for various construction methods	31
3.1	Creep and shrinkage coefficients according to CEB 1978	57
3.2	Cross section properties	112
3.3	Prestressing tendon data	112
3.4	Construction stages	113
4.1	Equivalent loads vs direct treatment of prestressing	167
4.2	Nxy at 10 ft inside of interior support	171
4.3	Nxx at midspan of interior span	171
4.4	Nyy at midspan of interior span	172
4.5	Myy at midspan of interior span	172
5.1	Order of operations for the analysis of uncracked and cracked sections	218
5.2	Serviceability limit states	230

LIST OF FIGURES

Figure Page

2.1 Balanced cantilever construction (erection of cantilevers) 8

2.2 Balanced cantilever construction (establishment of continuity) 9

2.3 Moment resistant piers vs temporary supports ... 11

2.4 Launching truss (Islington Avenue extension) ... 13

2.5 Strand system 14

2.6 Bar system 15

2.7 Long line method 19

2.8 Short line method (horizontal casting) 20

2.9 Short line method (vertical casting) 20

2.10 Progressive placing 23

2.11 Span-by-span construction (cast-in-place) 25

2.12 Span-by-span construction (precast) 26

2.13 Incremental launching 28

2.14 Various types of sections 33

2.15 Various types of boxes 33

3.1 Typical creep curve for concrete 42

3.2 Concrete strains vs age and duration of loading 44

3.3 Creep according to CEB 1970 52

3.4 Creep according to CEB 1978 56

3.5 Creep according to various analysis methods 66

3.6 Equivalent load representation of prestressing . 82

3.7 Friction and anchor set losses in prestressing . 82

3.8 Thermal gradients and temperature differentials 86

3.9 Thermal study of an experimental bridge 87

3.10 General cross section subjected to an arbitrary temperature distribution 90

3.11 Element forces and displacements 94

3.12 Element load vectors 100

3.13 Solution of equations 101

3.14 Flow chart for the computer program TIMEDEP 106

3.15 Creep test no. 1 108

3.16 Creep test no. 2 109

3.17 Precast concrete segmental bridge 111

3.18 Stresses at left pier 115

3.19 Stresses at midspan of interior span 116

3.20 Deflections at midspan of interior span 117

4.1 Decomposition of an eccentric load on a box girder 123

4.2 Stresses in a box girder due to bending 125

4.3 Stresses in a box girder due to torsion 126

4.4 Node and element forces and displacements 138

4.5 Stiffness influence coefficients using folded plate theory 143

4.6 Stiffness influence coefficients using plane frame theory 144

4.7 Element load vectors 145

4.8 Fixed end forces for concentrated loads 148

4.9 Some applications for the folded plate method .. 152

4.10 Flow chart for the computer program BOXGIRD 155

4.11 Box girder bridge 158

4.12 Bending moments and axial forces 159

4.13 Mx and My at midspan for pinned-pinned case 161

4.14 Mx and My at midspan for pinned-fixed case 162

4.15 Mx and My at midspan for fixed-fixed case 163

4.16 Mx at support for fixed-fixed case and fixed-free case 164

4.17 Prestressing analysis 166

4.18 Corpus Christi bridge 170

4.19 Islington Avenue extension 175

4.20 Loading cases for transverse flexure 178

4.21 Nxx/t for self weight 180

4.22 Myy and Nyy for self weight 182

4.23 Myy and Nyy for superimposed dead load 183

4.24 Myy and Nyy for sidewalk live load 184

4.25 Myy and Nyy for truck load 1 (negative cantilever moment) 185

4.26 Myy and Nyy for truck load 2 (negative interior moment) 186

4.27 Myy and Nyy for truck load 3 (positive interior moment) 187

4.28 Myy and Nyy for temperature 1 (top surface 40 F above datum) 188

4.29 Myy and Nyy for temperature 2 (interior surface 20 F above datum) 189

4.30 Myy and Nyy for transverse prestress 190

4.31 Loading cases for longitudinal shear and torsion 193

4.32 Nxy for self weight 195

4.33 Nxy for superimposed dead load 195

4.34 Nxy for sidewalk live load 196

4.35 Nxy for lane load 1 (no eccentricity) 196

4.36 Nxy for lane load 2 (left eccentricity) 197

4.37 Nxy for lane load 3 (right eccentricity) 197

5.1 Typical load-deflection response of a prestressed concrete beam 202

5.2 Typical load-deflection response of various concrete beams 204

5.3 Segmental bridge analysis 206

5.4 General I-girder analysis 207

5.5 Uncracked section analysis 209

5.6 Cracked section analysis 214

5.7 Ultimate strength analysis 220

5.8 Typical stress-strain curve for prestressing steel 222

5.9 Idealized moment-deflection diagrams for concrete members 228

5.10 Partially prestressed T beam 232

5.11 Discretization of a box girder as an equivalent I-girder 239

5.12 Stress results for the Islington Avenue extension 241

A.1 Sign conventions for node displacements and element forces 273

E.1 Sign conventions for element loads 297

E.2 Sign conventions for node displacements and element forces 298

L.1 Membrane forces acting on a box girder bridge .. 325

L.2 Transverse membrane forces due to self weight .. 329

1. INTRODUCTION

1.1 General remarks

Prestressed concrete segmental bridge construction is undoubtedly the most important breakthrough in bridge engineering during the last twenty years. It has extended the competitive span range of concrete structures while being adaptable to almost any conceivable site condition. The only limitation to this extremely versatile method of construction is the imagination of the designer. With the emergence of this construction technology, has come a whole new set of challenging design problems. The purpose of this research is to address some of these problems.

1.2 Objectives and scope

The main objective of this research is to provide a methodology for the analysis of prestressed concrete segmental bridges which is suitable for use in an engineering design office. To maximize design efficiency, the three-dimensional time-dependent analysis of a prestressed concrete segmental bridge is uncoupled into two distinct parts.

The first part deals with the time-dependent analysis of a segmental bridge under construction. A two-dimensional (plane frame) model is used. Loadings considered are self weight, prestress, construction loads, and temperature. Time-dependent effects include creep and shrinkage of the concrete as well as relaxation of the prestressing.

The second part deals with the approximate three-dimensional analysis of a completed segmental bridge. Time-dependent effects are neglected. Loading conditions include self weight, superimposed dead load, truck loads, lane loads, temperature, and prestressing.

The time-dependent analysis gives the longitudinal flexural requirements for each stage of construction, while the three-dimensional analysis gives the requirements for transverse flexure as well as longitudinal shear and torsion in the completed structure. In addition, the three-dimensional analysis gives an indication as to the severity of shear lag effects.

A secondary objective of this research is to provide a methodology for the analysis of partially prestressed concrete sections. Since partial prestressing can be defined as the general case whose extremes are conventional reinforced concrete and fully prestressed concrete, the development of simple analysis procedures would have a wide range of application. This includes the longitudinal and transverse analysis of segmental bridges having prestressed and/or conventional reinforcing.

This study is restricted to straight bridges without skew. Stresses are limited to the working stress range.

1.3 Organization of report

Chapter 2 is included to serve as a guide for design of segmental bridges, since some kind of design must exist before an analysis can be made. The chapter discusses the various techniques used in segmental construction and defines the terminology used in this study.
Since the design process for a segmental bridge is a highly complex and interactive one, a sequence of design is proposed in this chapter.

Chapter 3 considers the time-dependent analysis of two-dimensional prestressed concrete structures in general and segmental bridges in particular. After an extensive review of existing material and analytical models for the prediction of time-dependent behaviour, a procedure is outlined for the efficient and accurate analysis of these effects. The computer program TIMEDEP is presented for the time-dependent analysis of segmental bridges.

Numerical examples show the versatility and accuracy of the method.

Chapter 4 considers the three-dimensional analysis without time-dependent effects of box girder bridges in general and segmental bridges in particular. After an extensive review of the types of structural action which occur and suitable methods of analysis, the folded plate method is recommended as being both reasonably accurate and computationally efficient. The computer program BOXGIRD is presented for the transverse analysis of box girder bridges. The versatility and accuracy of the method is illustrated by a number of numerical examples.

Chapter 5 discusses the application of partial prestressing to the design of segmental bridges and offers some new computational techniques for the analysis of partially prestressed concrete sections. Behaviour in both the working stress (uncracked or cracked section) and ultimate strength ranges is considered. Some serviceability aspects of partial prestressing (including cracking, fatigue, and deformation) are studied. The computer program PREBEAM is presented for the analysis of partially prestressed concrete beams, subjected to axial force as well as bending moment. Numerical examples show the versatility and accuracy of the method.

The final chapter lists the conclusions reached in this study and makes some recommendations for further study.

2. DESIGN CONSIDERATIONS

2.1 Introduction

In order to conduct an analysis of a segmental bridge, some kind of design must first be made. Consequently, this chapter is included to serve as a guide for the design of segmental bridges. It is divided into two parts. The first part discusses various techniques of segmental construction and defines the terminology used in this study, while the second part proposes a design sequence to be followed in a typical design.

2.2 Methods of construction

Construction is commonly categorized by one of the following four methods: (1) balanced cantilever construction, (2) progressive placing, (3) span-by-span construction, and (4) incremental launching. Balanced cantilever construction has been the most common form of construction and consequently will be discussed in some detail while the other three methods will be summarized in general terms.

2.2.1 Balanced cantilever construction

In the balanced cantilever method of construction, segments are simply cantilevered from each side of a pier in a balanced sequence until midspan is reached (Figure 2.1). Then a cast-in-place closure is made with the half-span cantilever from the previous pier (Figure 2.2). The procedure is repeated until the structure is completed. In essence, balanced cantilever construction consists of two distinct operations: (1) erection of cantilevers and (2) establishment of continuity.

During cantilever erection of precast structures (Figure 2.1), epoxy is applied to the joint surfaces of the segments to be attached. The segments are slowly brought together ensuring that the horizontal and vertical alignment is correct. Then temporary prestressing bars are stressed to squeeze out the excess epoxy and hold the segments in place (Figure 2.1(a)). An unbalanced moment equal to the segment weight multiplied by its eccentricity from the centerline of the pier must be transmitted through the cantilever to the pier and foundations. This procedure is repeated on the other side of the cantilever (Figure 2.1(b)) whereby the unbalanced moment is removed. Top cantilever cables are stressed and the temporary prestressing is removed (Figure 2.1(c)). This procedure is repeated until midspan is reached.

With regard to the establishment of continuity, the operations required for the construction of a three span

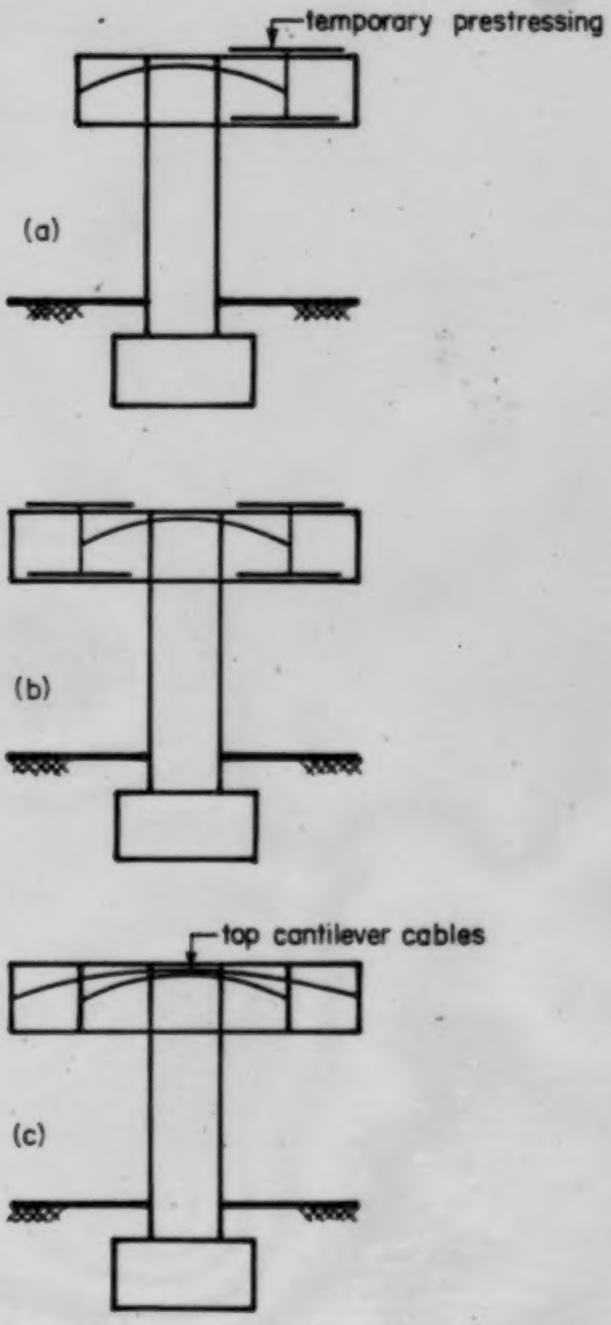
temporary prestressing
(a)
(b)
top cantilever cables
(c)

Figure 2.1 Balanced cantilever construction
(erection of cantilevers)

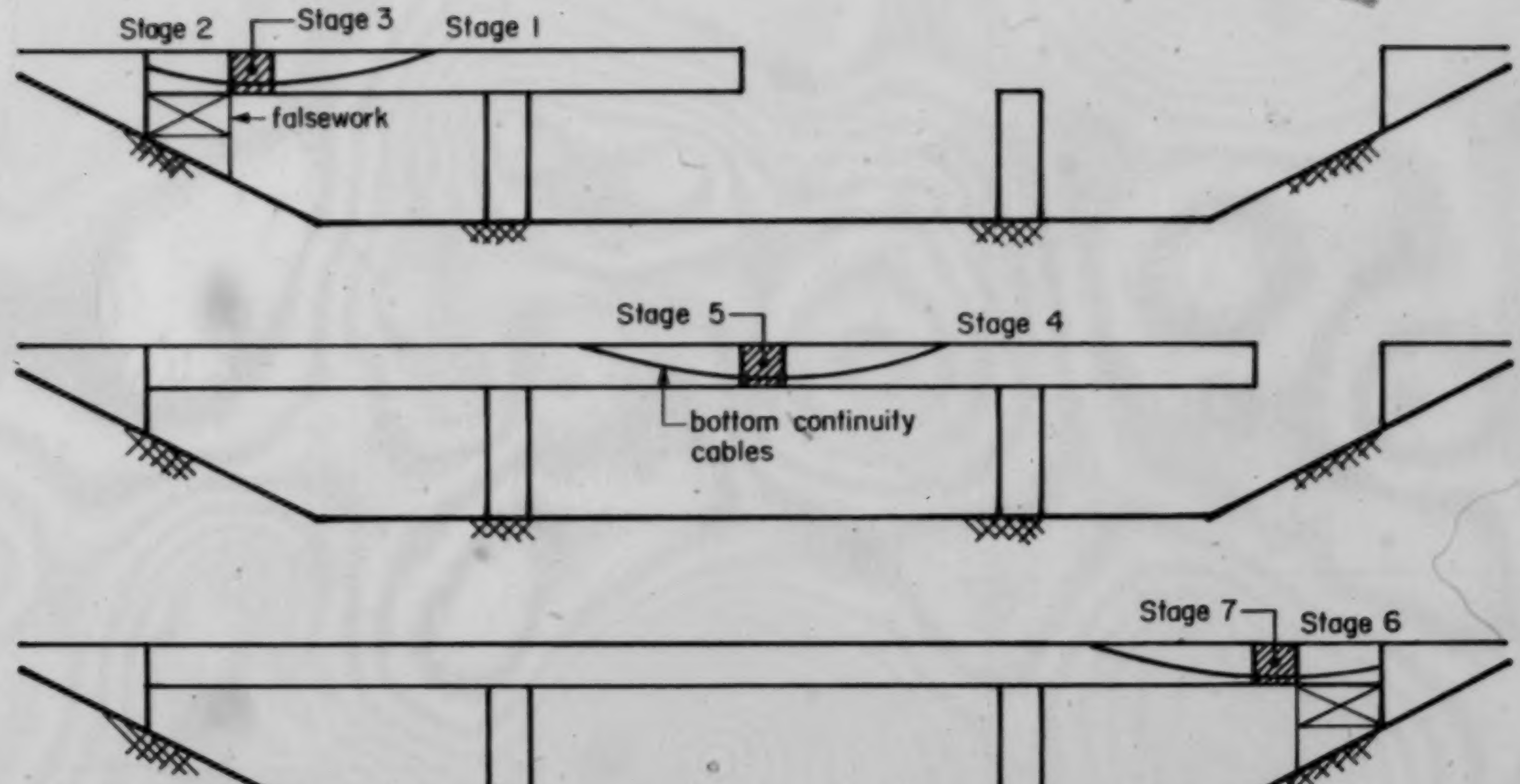
Stage 2
Stage 3
Stage 1
falsework
Stage 5
Stage 4
bottom continuity cables
Stage 7
Stage 6

Figure 2.2 Balanced cantilever construction (establishment of continuity)

bridge are shown in Figure 2.2. Segments are erected in cantilever in stage 1 while additional end-span segments are assembled on falsework in stage 2. Stage 3 involves the pouring of a cast-in-place closure segment, the stressing of the bottom continuity cables, and the modification of the support conditions. Segments are again erected in cantilever in stage 4 while another closure segment is cast in stage 5 (as per stage 3). Segments are again assembled on falsework in stage 6 and the final closure segment is cast in stage 7 (as per stage 3).

In precast construction, the pier will normally be out of balance by one segment. This unbalance must be carried by either moment resistant piers or temporary supports. Figure 2.3(a) shows how vertical prestressing can be used to create a moment resistant pier for a situation where the superstructure and pier are not monolithic. In the case where the unbalanced moment exceeds the capacity of the cantilever, pier, and/or foundation, temporary supports, as shown in Figure 2.3(b), must be used. Note that the temporary support is located on the side of the unbalance, and that it is attached to the superstructure with a small amount of vertical prestressing. For cast-in-place construction, moveable formwork is supported from the previously cast segment on each side of the cantilever. Consequently, only a small unbalance due to construction

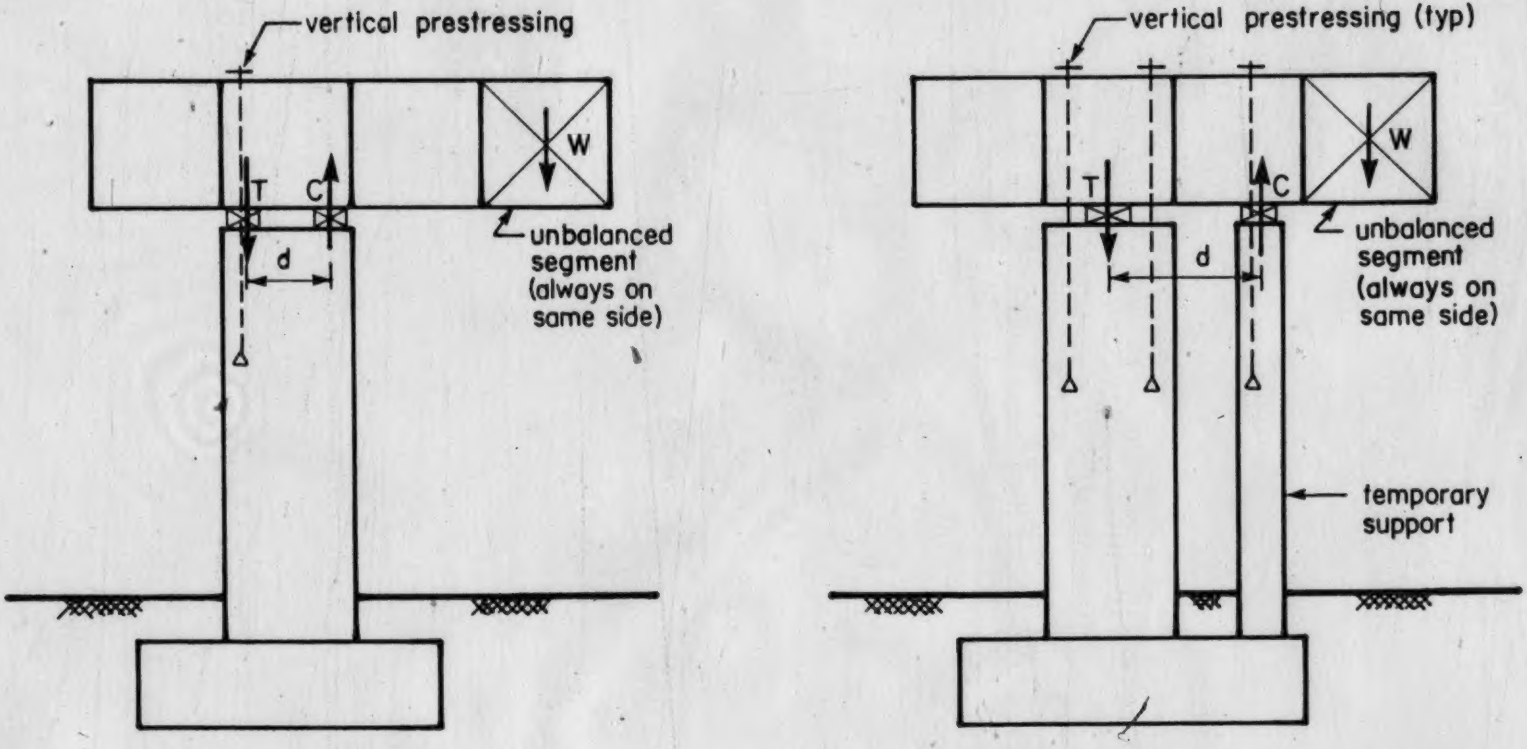
vertical prestressing
T
C
W
d
unbalanced segment (always on same side)
vertical prestressing (typ)
T
C
W
d
unbalanced segment (always on same side)
temporary support

(a) moment resistant pier

(b) temporary supports

Figure 2.3 Moment resistant piers vs temporary supports

loads occurs.

Erection may be carried out by cranes on land or barges, winches on the completed portion of the structure, or by a launching truss. Figure 2.4 shows a typical launching truss which propells itself across the structure by virtue of three moveable legs. Segments are delivered by a flat-bed trailer to the launching truss, where a trolley picks up and transfers them to the end of the truss. A special mechanism allows the segments to be rotated and attached to the end of the cantilever. In general, the reactions of the launching truss are transmitted to the structure as unbalanced moments, although self-equilibrating launching trusses have been built which transfer no unbalance to the cantilevers.

Longitudinal post-tensioning tendons are commonly grouped as either cantilever tendons (top) to be stressed during cantilever construction or continuity tendons (bottom) which are stressed after continuity is achieved. Traditionally, stranded cables (Figure 2.5) have been used for precast construction while high-alloy bars (Figure 2.6) have been used for cast-in-place construction. One exception to this is the Kishwaukee River bridge in Illinois which was precast and stressed with Dywidag bars.

In the strand system, anchorages for the cantilever cables

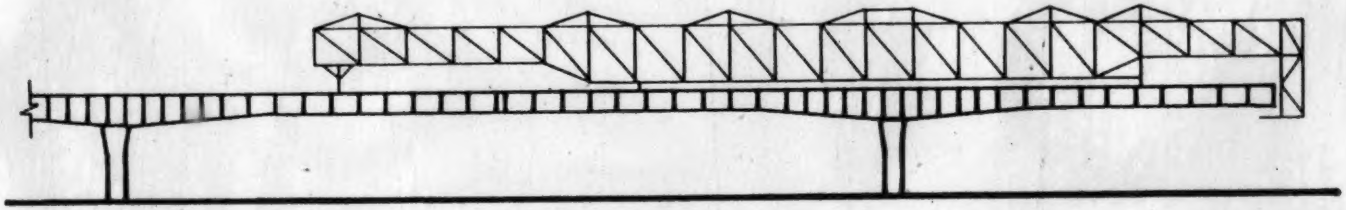

Figure 2.4 Launching truss (Islington Avenue extension)

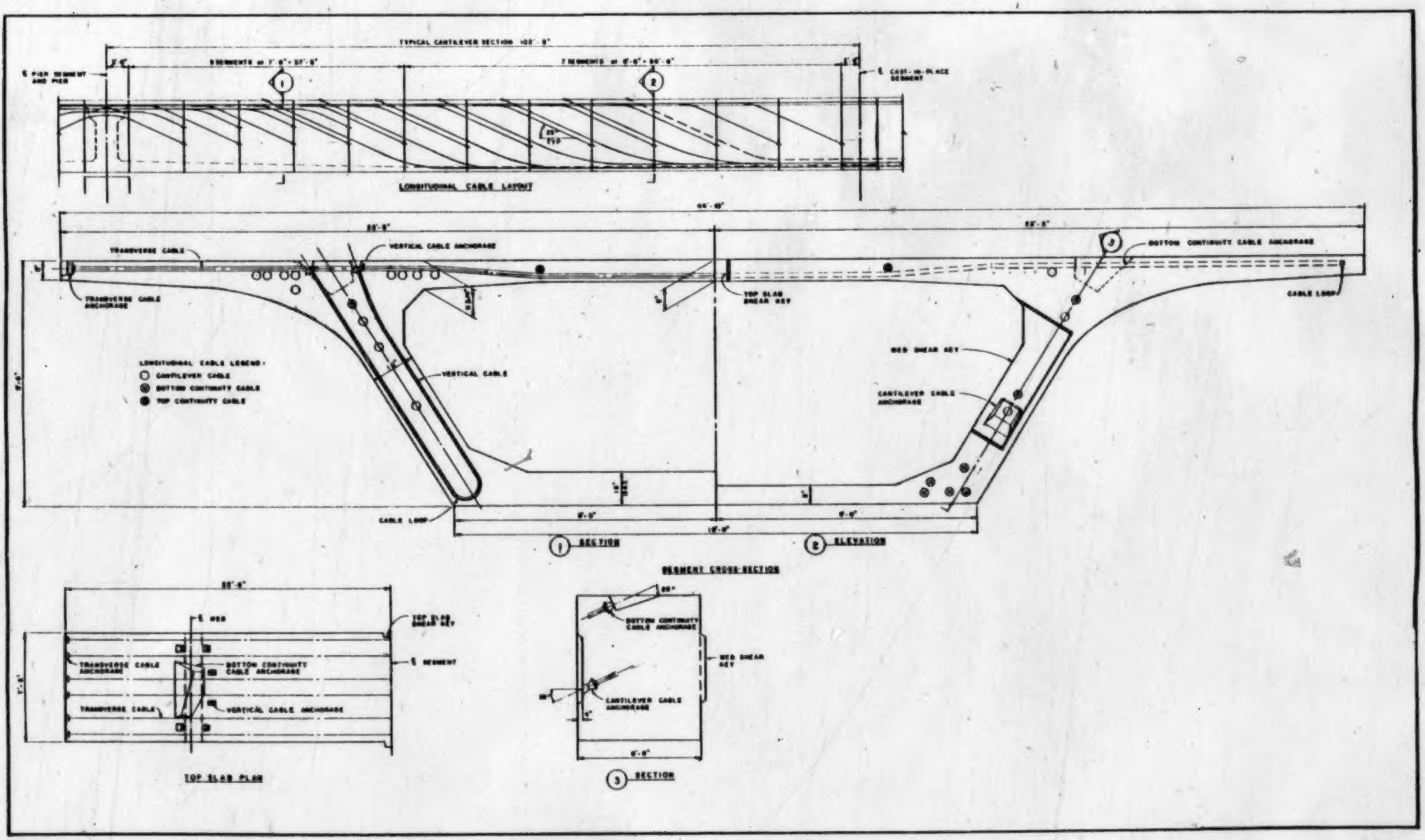
TYPICAL CANTILEVER SECTION
℄ PIER SEGMENT AND PIER
℄ CAST-IN-PLACE SEGMENT
1
2
LONGITUDINAL CABLE LAYOUT
TRANSVERSE CABLE
VERTICAL CABLE ANCHORAGE
TRANSVERSE CABLE ANCHORAGE
LONGITUDINAL CABLE LEGEND:
○ CANTILEVER CABLE
⊗ BOTTOM CONTINUITY CABLE
● TOP CONTINUITY CABLE
VERTICAL CABLE
CABLE LOOP
TOP SLAB SHEAR KEY
3
BOTTOM CONTINUITY CABLE ANCHORAGE
CABLE LOOP
WEB SHEAR KEY
CANTILEVER CABLE ANCHORAGE
1 SECTION
2 ELEVATION
℄ WEB
TOP SLAB SHEAR KEY
℄ SEGMENT
TRANSVERSE CABLE ANCHORAGE
BOTTOM CONTINUITY CABLE ANCHORAGE
TRANSVERSE CABLE
VERTICAL CABLE ANCHORAGE
TOP SLAB PLAN
SEGMENT CROSS-SECTION
BOTTOM CONTINUITY CABLE ANCHORAGE
WEB SHEAR KEY
CANTILEVER CABLE ANCHORAGE
3 SECTION

Figure 2.5 Strand system

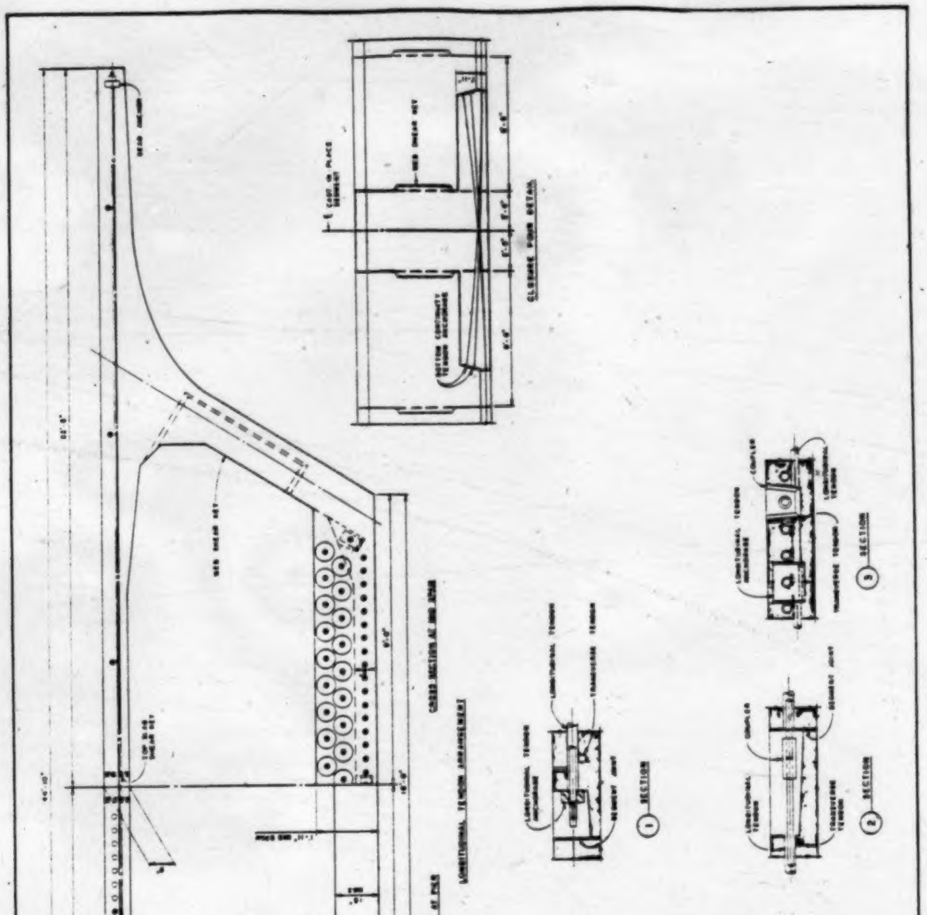
CROSS SECTION AT PIER
CROSS SECTION AT MID SPAN
LONGITUDINAL TENDON ARRANGEMENT
CLOSURE POUR DETAIL
TOP SLAB PLAN

Figure 2.6 Bar system

may be located in the web at the face of the segment (Figure 2.5) or in special web stiffeners cast in the segment. Web stiffeners allow stressing to be independent of erection but add a degree of complexity to the casting. Continuity cables may be anchored in block-outs in the top slab (Figure 2.5) or in the web stiffeners. Another possibility is to anchor the continuity cables in build-outs in the bottom slab. However, these build-outs are complicated and expensive to form. It is not uncommon to add a little extra compression at the top by virtue of top continuity cables. The cables run the entire length of the span and are anchored in the diaphragms at the piers or abutments.

In the bar system (Figure 2.6), the cantilever and continuity cables are anchored in recesses in the top and bottom slabs respectively. One advantage to this system is that the permanent post-tensioning provides the temporary compression required to squeeze out the excess epoxy during erection. A possible disadvantage is that a large number of bars and couplers are required, and the stressing and restressing operations become quite complex. Another advantage is that since there is no curvature in the tendons, the friction losses are low. However, since there is no curvature in the tendons, there is also no vertical component of prestressing to help carry the shear.

Transverse post-tensioning is recommended in the top slab to improve the response of the deck to cracking and fatigue. A transversely prestressed slab will not crack due to the application of normal loads, and any cracks which may occur due to the application of severe loads will be tightly closed upon removal of the loads. Fatigue is not a problem in prestressed decks since the stress change is very small compared to the strength of the tendons. The increased cost of transverse post-tensioning is offset by the reduced volume of concrete and conventional reinforcing. Furthermore, the economy of the structure is improved by the weight reduction. In multiple box sections, transverse prestressing provides continuity between the boxes.

Vertical post-tensioning can be used to resist high shear stresses near the piers. In this way, a minimum web thickness can be used throughout, allowing a substantial saving in weight. Figures 2.5 and 2.6 show how transverse and vertical prestressing can be used with the strand system and bar system respectively. Diaphragm post-tensioning can be used to transfer the shear from the webs through the diaphragm to offset bearings, thereby replacing large amounts of conventional reinforcing.

Precast segments are match-cast (each segment is cast against the segment which will be adjacent to it in the completed structure) by the long-line or short-line methods. Match-casting is critical for balanced cantilever construction since small discrepancies in the geometry of a joint near the pier are magnified by the lever arm of the cantilever to produce large variations at midspan.

In the long-line method, (Figure 2.7), segments are cast on a long-line bed having the profile of the bottom soffit·of the bridge, and a length slightly greater than one-half of the longest span. Each segment is cast in interior and exterior forms against a bulkhead on one side and the previously cast segment on the other. One possibility with this system is that if there are several sets of forms, portions of several cantilevers can be cast concurrently. Although this scheme is simple to set up and requires a minimum of geometric control, it has been used almost exclusively for bridges having parabolic soffits, since it requires a large amount of space.

For the short-line method (Figure 2.8), segments are cast against the previously cast segment in stationary forms. After curing, the previously cast segment is removed to storage, the segment just cast is put in its place, and a new segment is cast. Horizontal and vertical curves are obtained by adjusting the relative positions of the segments in the forms. Unfortunately, geometric control becomes quite complicated for this system; elevation and alignment

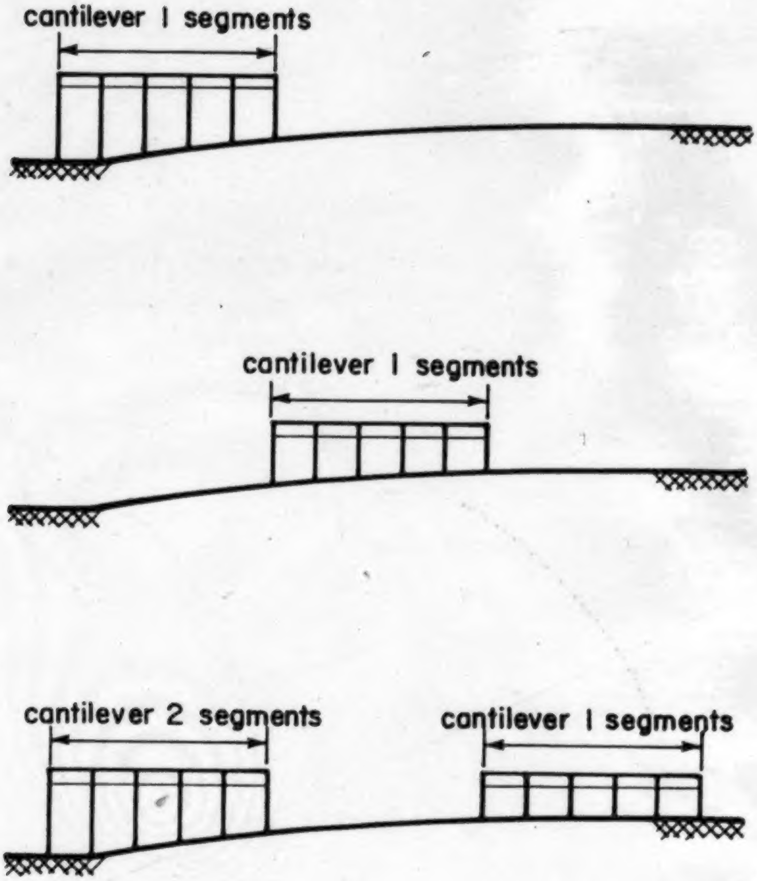
cantilever 1 segments
cantilever 1 segments
cantilever 2 segments
cantilever 1 segments

Figure 2.7 Long line method

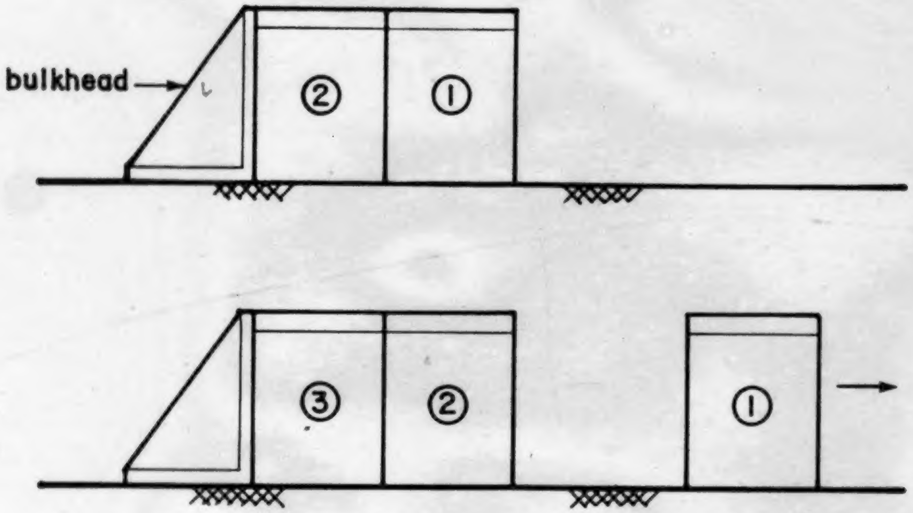
bulkhead
②
①
③
②
①

Figure 2.8 Short line method (horizontal casting)

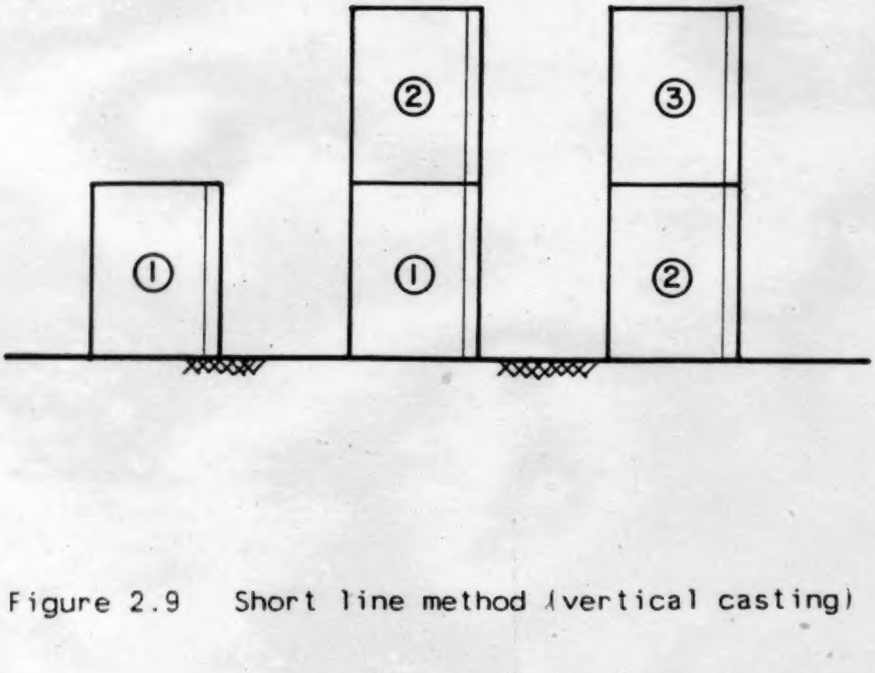

Figure 2.9 Short line method (vertical casting)

readings must be taken with surveying equipment before and after each cast and corrections must be made for each subsequent cast.

The previous discussion pertains to casting a segment in the horizontal position. For very shallow structures, it is desirable, from the viewpoint of placing and vibrating concrete, to cast in the vertical position using the short-line method (Figure 2.9). After the first segment is cast, the forms are moved upward so that each succeeding segment can be cast above the previous one. This scheme requires special equipment to rotate the segment from the vertical to the horizontal position.

These three methods of casting have all been used successfully on various projects in Ontario. A long-line casting bed having a parabolic soffit was set up at the site of the Credit River and Mullet Creek bridges. Two horizontal short-line forms were set up in the precasting plant to handle the linear variation in depth of the Islington Avenue Extension. A vertical short-line set up was constructed at the precasting plant to cast the 4'-6" deep segments of the Elora Gorge bridge.

2.2.2 Progressive placing

Progressive placing is a derivative of the balanced cantilever concept. Precast segments are placed continuously from one end of the structure to the other in successive cantilevers on the same side of the pier rather than by balanced cantilever on both sides of the pier (Figure 2.10). Since the lengths of the cantilevers become excessive, a temporary moveable tower and cable-stay arrangement must be employed to keep the stresses within reasonable limits. Segments are typically rolled to the end of the completed portion of the structure where a swivel crane picks up and rotates them to their final position. The method was pioneered by Jean Muller of Campenon Bernard and Figg & Muller.

Although this technique has been used on numerous structures in France, its only application in North America has been on the Linn Cove Viaduct in North Carolina. This environmentally sensitive area in the Blue Ridge mountains does not allow access to the piers; consequently, the piers were constructed from the tip of the cantilever, with men and equipment being lowered down to construct the foundations and piers. Since the alignment of this structure is an "s-shape" with extreme curvature, temporary towers and stays were impractical. Instead temporary bents were erected at midspan in the same manner as the permanent piers.

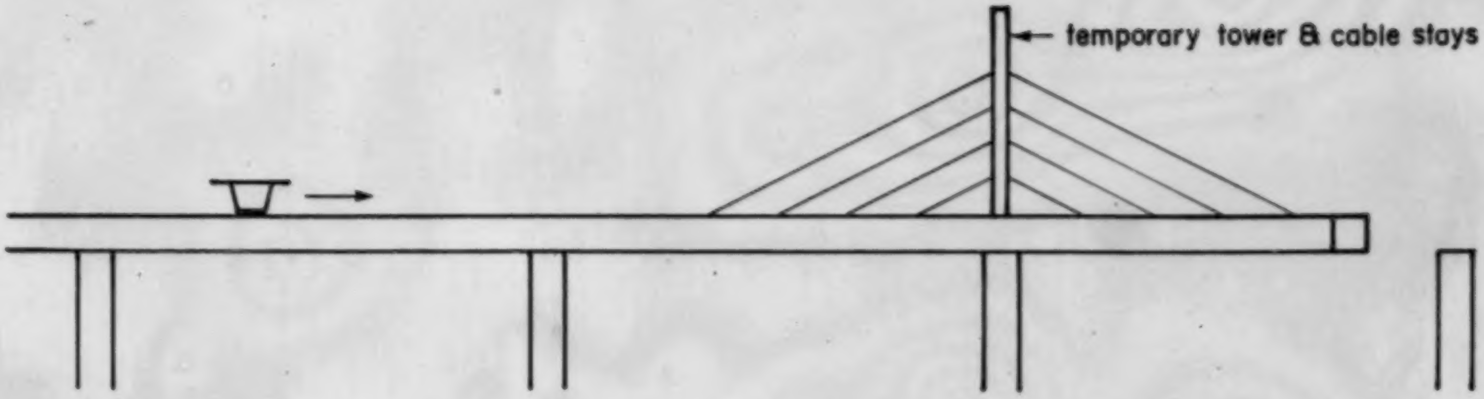
temporary tower & cable stays

Figure 2.10 Progressive placing

2.2.3 Span-by-span construction

In the span-by-span method of construction, work progresses in span increments from one end of the structure to the other. The German firm of Dyckerhoff and Widmann pioneered a system whereby a long span cast-in-place structure could be erected by means of a moveable form carrier (Figure 2.11). The moveable form carrier is comprised of a self-propelled launching truss at the deck level and three sets of forms corresponding to the three stages of casting. The bottom slab and webs are cast in the first stage while the top slab spanning between the webs is cast in the second stage. The cantilevers are completed in the third stage. These three stages can proceed concurrently. Once the concrete reaches the specified strength, the truss can be launched to the next span. The Denny Creek bridge in Washington has been built by this procedure.

Another type of span-by-span construction has been developed by Figg and Muller for short span viaduct type structures built with precast segments (Figure 2.12). This system requires that a steel assembly truss be fastened between two piers. The segments are then rolled along the truss to their final position. A six inch closure joint is poured at the beginning of each span before the tendons are stressed and the truss is moved to the next span. The Long Key and Seven Mile bridges in Florida have been built in this way.

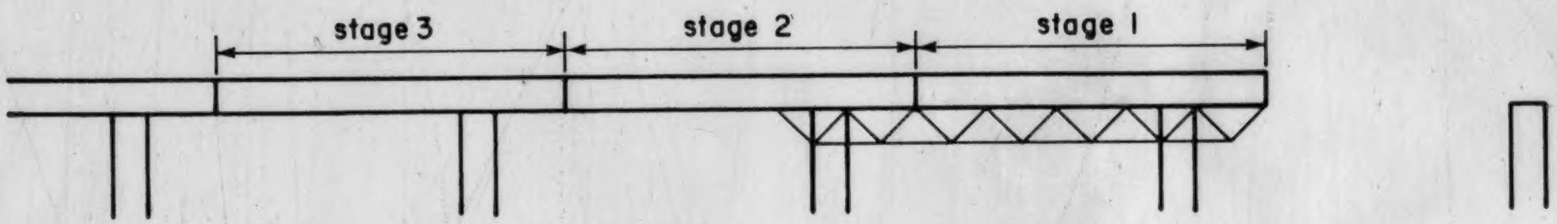
stage 3
stage 2
stage 1

(a) elevation

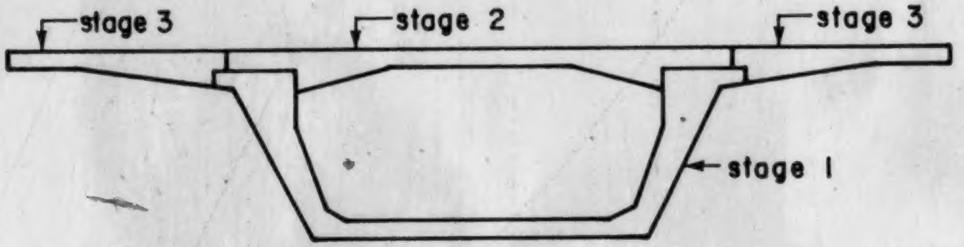
stage 3
stage 2
stage 3
stage 1

(b) cross-section

Figure 2.11 Span-by-span construction (cast-in-place)

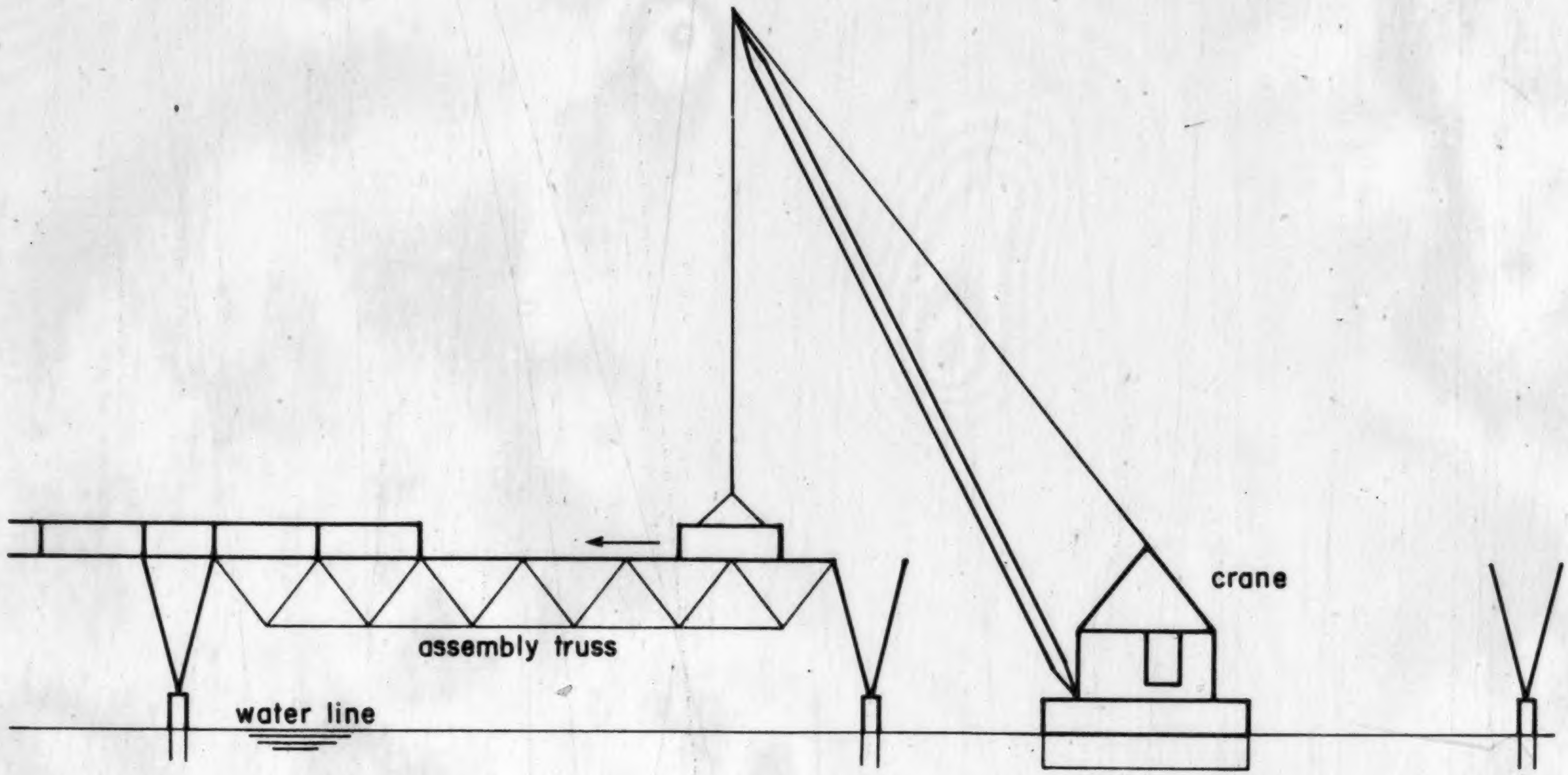
crane
assembly truss
water line

Figure 2.12 Span-by-span construction (precast)

2.2.4 Incremental launching

Incremental launching or "Taktschiebeverfahren", as it is known in its native Germany, was pioneered by the firm of Leonhardt and Andra (Figure 2.13). The superstructure is cast in stationary forms at an on-site factory behind the abutment, in lengths of 30 to 100 ft (10 to 30 m). After the segment reaches sufficient strength, it is prestressed to the previous segment and the entire superstructure is pushed out longitudinally to permit casting of the next segment. Normally casting and launching a segment is based on a one week cycle. Segments can be cast in stages (as per span-by-span construction).

Obviously, only constant depth sections can be used. In addition, the bridge alignment for this scheme must either be straight or a circular curve. A dramatic example of this type of construction is the Val Ristel bridge in Italy which was launched with a radius of 500 ft (150 m).

To counteract the varying bending moments that occur during the launching operation, the superstructure is concentrically prestressed. To reduce the large negative bending moments that occur just before the superstructure touches a new pier, a steel launching nose is installed. Long spans may be subdivided by providing temporary piers or stayed towers.

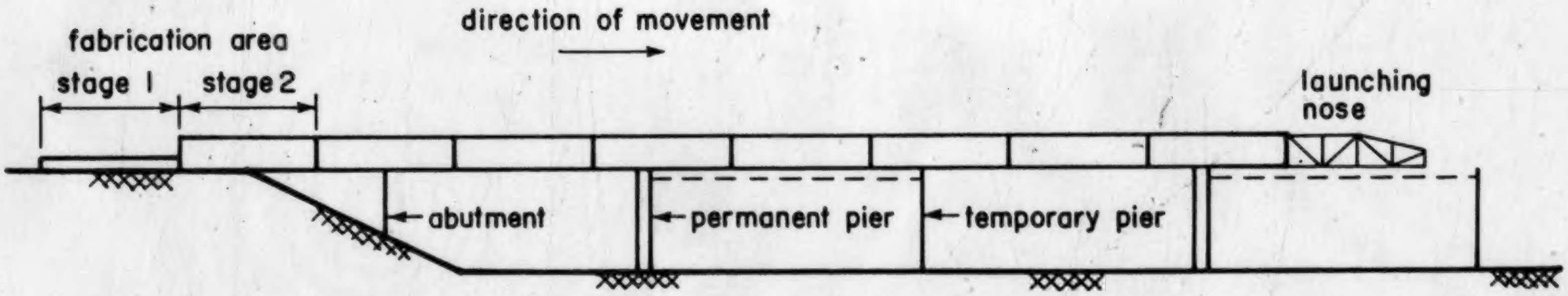
fabrication area
stage I
stage 2
direction of movement
launching nose
abutment
permanent pier
temporary pier

Figure 2.13 Incremental launching

The concentrically prestressed superstructure is jacked vertically and then pushed horizontally in successive increments by means of hydraulic jacks. To allow the superstructure to move longitudinally, special low friction teflon and stainless steel bearings are provided at the piers. When the opposite abutment has been reached, additional prestressing is installed to accommodate service load moments in the final structure.

This technique has been used for spans of up to 200 ft (60 m) without temporary supports and 330 ft (100 m) with temporary supports. The Wabash River bridge in Indiana was built by this procedure.

2.3 Design sequence

A segmental bridge must be designed for the loads acting on the completed structure as well as the loads acting on the partially erected structure during any stage of construction. Consequently, the design process is a highly complex and interactive one. It can, however, be simplified by dividing the sequence of design into the following stages:

(1) conceptual design - select type and method of construction
(2) preliminary design - select span lengths and cross

sectional dimensions

(3) detailed design - proportion prestressing and reinforcing in the longitudinal and transverse directions

(4) design verification - check construction stresses and deformations by virtue of a detailed analysis

(5) design changes - evaluate alternate designs, field changes, etc.

Each of these will be considered in some detail.

2.3.1 Conceptual design

A number of major conceptual decisions must be made at a stage when relatively little hard information is known. For instance, the designer must decide whether to use precast or cast-in-place concrete. This decision is a function of many variables but the location and climate of the site are important factors.

The type of construction and method of construction must also be chosen. Podolny and Muller (16) have determined the range of application of various types of construction. These are given in Table 2.1. It should be noted that there is enough overlap in this table that two or more bridge types may be suitable for a particular span length. A recent study conducted by T Y Lin International (6) for

Table 2.1 - Range of application of bridge type by span length

Span (ft)	Bridge type
0- 150	I-type pretensioned girder
100- 300	Cast-in-place post-tensioned box girder
100- 300	Precast balanced cantilever (constant depth)
250- 600	Precast balanced cantilever (variable depth)
200-1000	Cast-in-place balanced cantilever
800-1500	Cable-stay with balanced cantilever

Table 2.2 - Average bridge lengths for various construction methods

Construction method	Average bridge length for a 40 ft roadway (ft)
Incremental launching	1087
Progressive placing	1165
Balanced cantilever (cast-in-place)	2818
Balanced cantilever (precast)	3133
Span-by-span construction	5347

the Federal Highway Administration has found the average length of bridge for various methods of construction. Table 2.2 gives these requirements. Incremental launching requires the lowest overall length of structure, because it requires the least amount of specialized equipment i.e. casting cells, launching trusses, etc. It should be mentioned that although span-by-span construction requires the longest minimum length of superstructure, it also happens to be the cheapest method of construction for this length.

The designer must decide whether to have a constant or variable depth section and also whether to increase the bottom slab thickness near the supports (see Figure 2.14). This decision will depend a great deal on the span/depth ratios discussed in the next section. Finally, he must determine whether to use a single box, multiple box, or multicell box (see Figure 2.15). This decision is based on the overall roadway width as well as size and weight restrictions for transporting the segments (in the case of precast construction).

All the decisions mentioned in this section are interdependent; they must all be considered together. For example, you cannot have a variable depth incrementally launched structure.

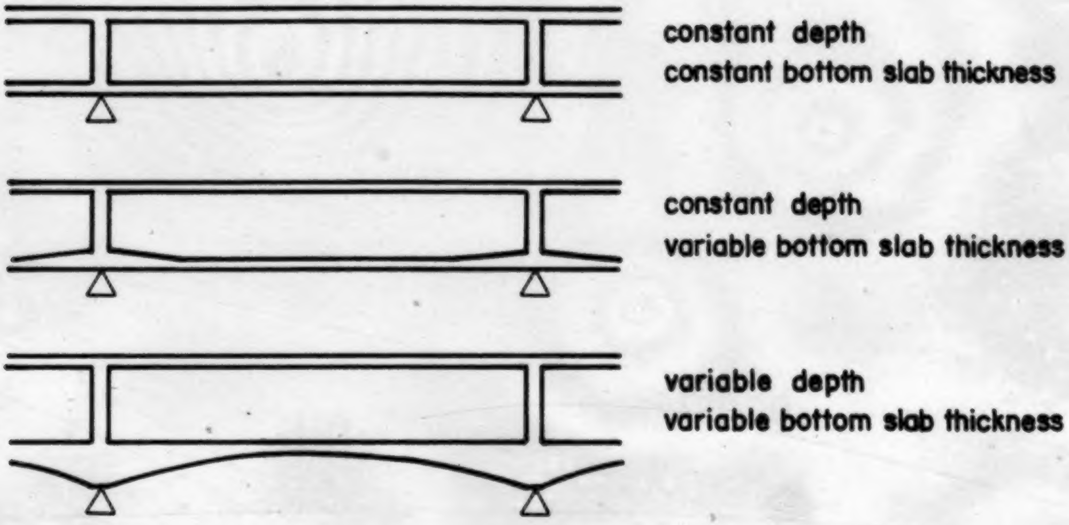
constant depth
constant bottom slab thickness
constant depth
variable bottom slab thickness
variable depth
variable bottom slab thickness

Figure 2.14 Various types of sections

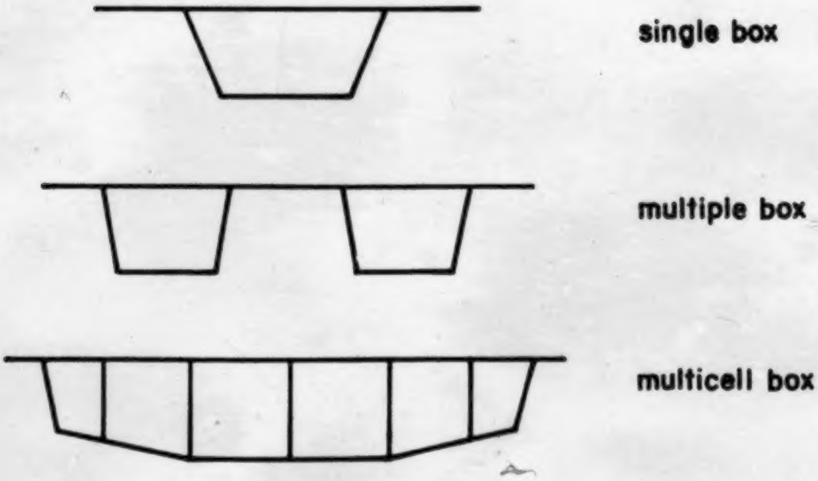
single box
multiple box
multicell box

Figure 2.15 Various types of boxes

2.3.2 Preliminary design

The following basic parameters must be determined before a detailed design can be performed. The span ratio (ratio of the exterior span to the interior span) must be chosen. The conventional span ratio of 0.80 for cast-in-place structures is too high for balanced cantilever construction since it requires extensive falsework in the end span. Also, the ideal span ratio of 0.50 for balanced cantilever construction is too low since it would have uplift at the abutments and require special detailing. A span ratio of 0.65 appears to be a reasonable compromise. Once the span ratio has been chosen, the span lengths can be found, given the overall length and number of spans.

According to Podolny and Muller (16), the span/depth ratio should be in the range of 15 to 30 for constant depth sections with an optimum value of 18 to 20. Variable depth (parabolic) sections should have a span/depth ratio in the range of 30 to 50 at midspan and 16 to 20 at the pier. The optimum value would again be 18. Knowing the span/depth ratios and span lengths, the depth of the section can be found.

Mathivat (15) has determined that, based on European experience, a single box is suitable up to a width of 13 m (43 ft) while a two cell multicell box is reasonable for widths of 13m to 18 m (43 ft to 59 ft). A multiple box can be used for widths of 18 m to 25 m (59 ft to 82 ft).

Cross section dimensions may now be determined; for the most part, they are a function of detailing procedures and not stress levels. The web thickness is, in general, a function of the shear stress due to shear and torsion, placing of concrete around the longitudinal tendons, and bursting stresses due to concentrated reactions at the anchorages. The minimum web thickness is 10" for the bar system and 14" for the strand system with cables anchored in the web. Personal experience has indicated that 18" is not an unreasonable minimum from the viewpoint of placing concrete in a strand system. The absolute minimum web thickness for a section having no prestressing ducts in the webs is 8".

A minimum top slab thickness of 6" is required to prevent punching shear due to concentrated wheel loads. For top slabs having transverse prestressing, 7" will span up to 10 ft, 8" will span from 10 to 15 ft, 10" will span from 15 to 25 ft, and stiffening ribs are required for spans greater than 25 ft. The minimum bottom slab thickness at midspan should be in the vicinity of 8 to 10" while the thickness at the pier should be based on the compressive force to be developed in the concrete. Fillets must be provided at all slab/web junctions to permit transverse moments to be transmitted around corners and also to accommodate all longitudinal tendons. If non-vertical webs are desired, the slope of the webs should be from 4:1 to 5:1.

Permanent hinges and intermediate expansion joints complicate the construction of segmental bridges immensely. It is therefore recommended that hinges be avoided and expansion joints be restricted to the extreme ends of the structure. It should be noted that bridges have been built up to lengths of 2000 ft without intermediate expansion joints. The bearings must obviously be capable of handling substantial longitudinal movements.

Since the torsional rigidity of a box girder is high, intermediate diaphragms (as are usually provided for in I-girder bridges) are not necessary. Of course, diaphragms must be provided at the abutments and piers to transmit the bearing reactions.

2.3.3 Detailed design

The detailed design of a segmental bridge includes the following:

1. determine section properties
2. design for longitudinal flexure during cantilever construction (determine configuration and number of cantilever cables for each stage)
3. design for longitudinal flexure during establishment of continuity (determine configuration and number of continuity cables for each stage)
4. design for longitudinal flexure after completion of structure (determine configuration and number of any additional cables)
5. design for transverse flexure (proportion transverse reinforcing)
6. design for shear and torsion (proportion longitudinal stirrups)
7. check service stresses
8. check ultimate strength
9. design piers (for maximum unbalanced moment as well as vertical and lateral load)
10. design abutments
11. design foundations
12. design bearings (for movements due to creep and shrinkage as well as temperature)

13. design expansion joints (same as above)
14. design railing and barrier curb
15. determine casting and erection schedule (necessary for detailed analysis with computer program TIMEDEP)
16. compute quantities
17. estimate cost

2.3.4 Design verification

Once the detailed design has been completed, it is necessary to take a comprehensive look at the stresses and deformations that occur at each stage of construction. The deformations must be predicted very accurately, so that the camber diagram can be determined, and the structure will fit together when continuity is established. It is therefore necessary to accurately account for the time-dependent effects due to creep and shrinkage of the concrete and relaxation of the prestressing. To facilitate this end, the computer program TIMEDEP has been developed. This program accounts for the time-dependent behaviour as well as the effects of self weight, prestress, construction loads, and temperature. Due to large expense associated with running the program, it is only undertaken after the detailed design has been completed.

2.3.5 Design changes

Changes are often made to the design for a number of reasons. A contractor may propose an alternate design during the tender process. After award of the tender, the contractor may wish to modify the construction sequence. New information on the site may necessitate some alterations to the design. All these changes must be evaluated, and a new verification analysis must be made if they differ significantly from the original design.

2.4 Conclusions

This chapter has described the various techniques for segmental construction and has suggested an appropriate sequence of design. Once a reasonable design has been made, the procedures discussed in the following chapters can be used to evaluate the design.

3. TIME-DEPENDENT ANALYSIS

3.1 Introduction

This chapter discusses the time-dependent analysis of two-dimensional prestressed concrete structures in general and segmental bridges in particular. Time-dependent effects include creep and shrinkage of the concrete as well as relaxation of the prestressing. Loadings considered are self weight, prestress, construction loads, and temperature at each stage of construction.

The existing material and analytical models for the prediction of time-dependent behaviour are summarized, after which, a number of existing computer programs are reviewed. After careful examination of all this information, the methodology for a time-dependent analysis is formulated for this study. A new efficient computer program is developed. The accuracy of any new features as well as the versatility of the program are illustrated by a series of numerical examples.

3.2 Basic definitions

Three distinct but inter-related time-dependent effects must be considered in the analysis of segmental bridges. These are creep and shrinkage of the concrete and relaxation of the prestressing:

(1) Creep is the change in strain with time due to constant stress.

(2) Shrinkage is the change in strain with time not due to stress.

(3) Relaxation is the change in stress with time due to constant strain.

Concrete under constant axial compressive stress (Figure 3.1) undergoes a gradual increase of strain with time due to creep deformation. The final creep strain may be several times as large as the initial elastic strain. The rate of creep decreases with time. When the load is removed, a portion of the elastic strain is recovered immediately while a portion of the creep strain is recovered with time. The final portion of the strain is never recovered and results in a permanent deformation.

Although creep has little effect on the ultimate strength of the structure, it does cause a redistribution of stress at service load levels. Furthermore, creep causes an

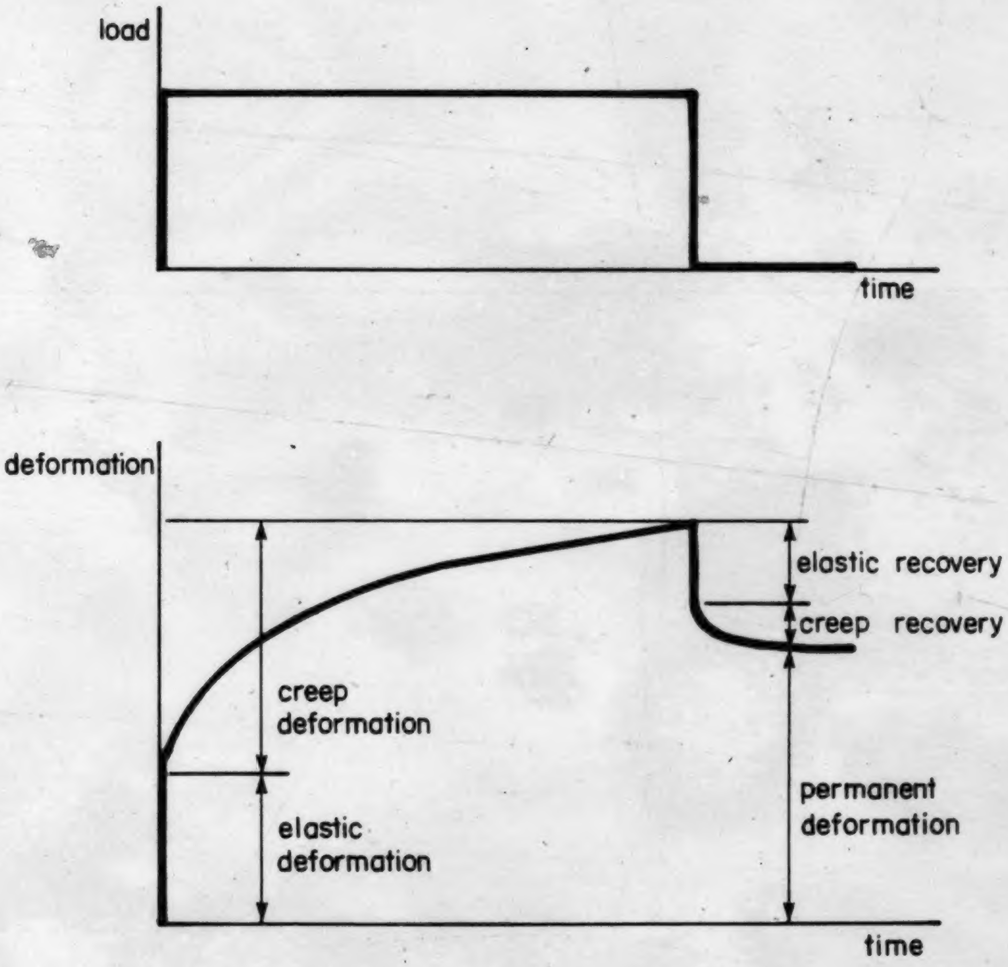
load
time
deformation
elastic recovery
creep recovery
creep
deformation
elastic
deformation
permanent
deformation
time

Figure 3.1 Typical creep curve for concrete

increase in service load deflections. As one can imagine, the accurate prediction of deflections is critical for cantilever construction. It is normal to use a linear relationship between creep strain and applied stress for service load stresses in the range of 0.4 fc′ and 0.5 fc′.

Shrinkage is the shortening of concrete due to the loss of moisture by evaporation. Shrinkage strain rates decrease with time, in a manner similar to that of creep.

Creep and shrinkage are functions of the relative humidity, the dimensions of the element, the composition of the concrete, and the ambient temperature. Creep is also a function of the rate of hardening (age at loading) of the concrete. Figure 3.2 shows the total elastic and creep strain (normalized with respect to the 28 day elastic strain) as a function of the age at loading and duration of loading.

3.3 Material models

3.3.1 Introduction

Creep and shrinkage are commonly predicted by one of the following material models: (1) ACI 209 (70,71), (2) CEB 1970 (73), (3) CEB 1978 (74), and (4) Bazant-Panula (76). Relaxation of prestressing is normally given by the expression of Magura, Sozen, Siess (77).

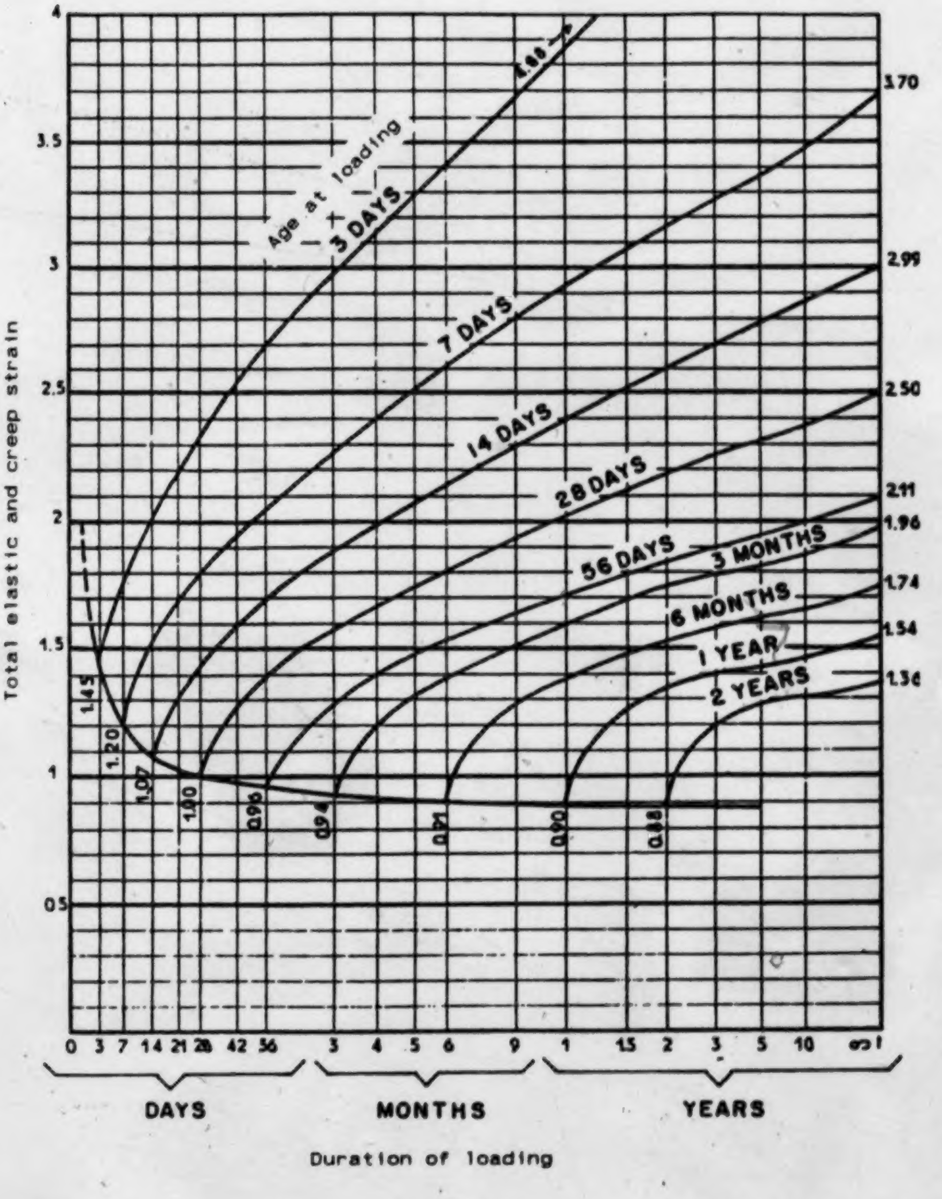

Figure 3.2 Concrete strains vs age and duration of loading (l)

3.3.2 ACI Committee 209

(a) Strength and elasticity properties

The compressive strength of the concrete fc(t) in psi at time t in days is a function of the age, curing conditions, and cement type as shown below

$$fc(t) = \frac{t}{4.00 + 0.85\,t}\,fc(28) \quad \text{for moist cured type I cement} \qquad (3.1a)$$

$$fc(t) = \frac{t}{2.30 + 0.92\,t}\,fc(28) \quad \text{for moist cured type III cement} \qquad (3.1b)$$

$$fc(t) = \frac{t}{1.00 + 0.95\,t}\,fc(28) \quad \text{for steam cured type I cement} \qquad (3.1c)$$

$$fc(t) = \frac{t}{0.70 + 0.98\,t}\,fc(28) \quad \text{for steam cured type III cement} \qquad (3.1d)$$

The modulus of elasticity Ec(t) in psi at time t in days is determined as follows

$$Ec(t) = 33\,w^{1.5}\sqrt{fc(t)} \qquad (3.2a)$$

$$Ec(t) = 57{,}000\sqrt{fc(t)} \quad \text{for } w = 145 \text{ pcf} \qquad (3.2b)$$

(b) Creep

The creep coefficient Ct for standard conditions may be written as

$$Ct = \frac{t^{0.60}}{10 + t^{0.60}} Cu \qquad (3.3)$$

where t is the time after loading in days and Cu is the ultimate creep coefficient. This coefficient ranges from 1.30 to 4.15 with an average value of 2.35. Standard conditions are defined as loading at 7 days for moist cured concrete and 1 - 3 days for steam cured concrete, ambient relative humidity of 40% or less, minimum member thickness of 6 in or less, and slump of 4 in or less.

For nonstandard conditions, the creep coefficient must be multiplied by the following correction factors:

(1) Loading age

$(CF)LA = 1.25\ tLA^{-0.118}$ for moist cured concrete

$(CF)LA = 1.13\ tLA^{-0.095}$ for steam cured concrete

where tLA is the loading age in days

(2) Humidity

$(CF)H = 1.27 - 0.0067\ H$ for $H > 40\ \%$

where H is the relative humidity in percent

(3) Minimum thickness of member

$(CF)T = 1.14 - 0.023\ T$ for < one year loading

$(CF)T = 1.10 - 0.017\ T$ for ultimate value

where T is the minimum thickness in inches

(4) Slump

$(CF)S = 0.82 + 0.067\ S$

where S is the slump in inches

(5) Cement content

$(CF)B = 1.00$

(6) Percent fines

$(CF)F = 0.88 + 0.0024\ F$

where F is the percent of fine aggregate by weight

(7) Air content

$(CF)A = 1.00$ for $A < 6\ \%$

$(CF)A = 0.46 + 0.090\ A$ for $A > 6\ \%$

where A is the air content in percent

(c) Shrinkage

The shrinkage strain (esh)t for standard conditions may be written as

$$(esh)t = \frac{t}{a + t} (esh)u \qquad (3.4)$$

where t is the time after curing in days and (esh)u is the ultimate shrinkage strain. This coefficient ranges from 0.000415 to 0.00107 with average values of 0.00080 for moist cured concrete and 0.00073 for steam cured concrete. The coefficient "a" has a value of 35 for moist cured concrete after 7 days and 55 for steam cured concrete after 1 - 3 days. Standard conditions are defined as ambient relative humidity of 40% or less, minimum member thickness of 6 in or less, and slump of 4 in or less.

For nonstandard conditions, the shrinkage strain must be multiplied by the following correction factors:

(1) Loading age

Shrinkage is not a function of loading

(2) Humidity

$(CF)H = 1.40 - 0.010\,H$ for $40\,\% < H < 80\,\%$

$(CF)H = 3.00 - 0.030\,H$ for $80\,\% < H < 100\,\%$

where H is the relative humidity in percent

(3) Minimum thickness of member

$(CF)T = 1.23 - 0.038\ T$ for < one year drying

$(CF)T = 1.17 - 0.029\ T$ for ultimate value

where T is the minimum thickness in inches

(4) Slump

$(CF)S = 0.89 + 0.041\ S$

where S is the slump in inches

(5) Cement content

$(CF)B = 0.75 + 0.034\ B$

where B is the number 94 lb sacks of cement per cubic yard of concrete

(6) Percent fines

$(CF)F = 0.30 + 0.0140\ F$ for $F < 50\ \%$

$(CF)F = 0.90 + 0.0020\ F$ for $F > 50\ \%$

where F is the percent of fine aggregate by weight

(7) Air content

$(CF)A = 0.95 + 0.0080\ A$

where A is the air content in percent

3.3.3 CEB 1970

(a) Creep

The creep strain ef at time t is given by

$$ef = \frac{fo}{Ec(28)} \varnothing t \qquad (3.5)$$

The creep coefficient 0t is expressed as the product of five coefficients

$$\varnothing t = Kc\ Kd\ Kb\ Ke\ Kt \qquad (3.6)$$

where

Kc - depends on the environmental conditions ie relative humidity of air (Figure 3.3(a))

Kd - depends on the age of the concrete at the time of loading and the type of cement (Figure 3.3(c))

Kb - depends on the composition of the concrete in terms of water/cement ratio and cement content (Figure 3.3(d))

Ke - depends on the theoretical thickness of the member (Figure 3.3(f))

Kt - covers the development of the deferred deformation with time - depends on the theoretical thickness (Figure 3.3(e))

(b) Shrinkage

The shrinkage strain er at time t is expressed as the product of five coefficients

$$er = ec\ Kb\ Ke\ Kp\ Kt \qquad (3.7)$$

where

ec - depends on the environmental conditions ie relative humidity of air (Figure 3.3(b))

Kb - depends on the composition of the concrete in terms of water/cement ratio and cement content (Figure 3.3(d))

Ke - depends on the theoretical thickness of the member (Figure 3.3(g))

Kp - depends on the geometric percentage (p) of longitudinal reinforcement area (Ast) with respect to the cross-sectional area of the member (Ac)

$$Kp = \frac{100}{100 + n\ p}$$

note that $p = 100 \frac{Ast}{Ac}$ and $n = 20$ for creep

Kt - covers the development of shrinkage with time - depends on the theoretical thickness (Figure 3.3(e))

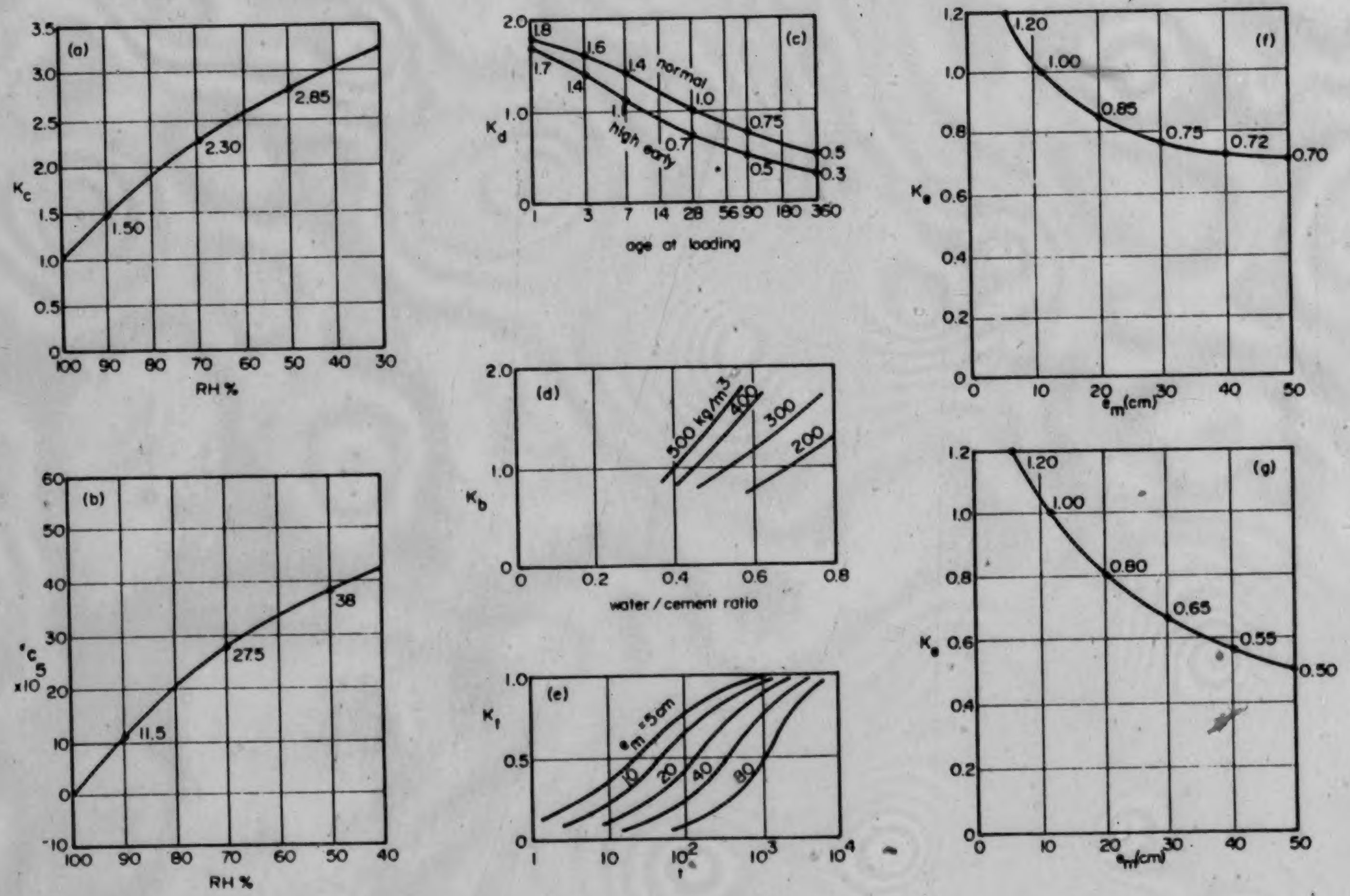

Figure 3.3 Creep according to CEB 1970

Some notes:

(1) The theoretical thickness em is defined as the area of the cross-section divided by one-half of the perimeter in contact with the atmosphere.

(2) If the concrete hardens at a temperature other than 20°C, the age at loading is replaced by the corresponding degree of hardening D

$$D = \Sigma \Delta t \ (T + 10) \qquad (3.8)$$

where Δt represents the number of days during which hardening has taken place at T °C.

3.3.4 CEB 1978

(a) Creep

The total strain e at time t for a specimen loaded at time to is comprised of an elastic component and a component due to creep.

$$e(t,to) = fo \left[\frac{1}{Ec(to)} + \frac{\phi(t,to)}{Ec(28)}\right] \quad (3.9)$$

The creep coefficient ϕ is given by

$$\phi(t,to) = Ba(to) + \phi d\ Bd(t-to) + \phi f\ [Bf(t) - Bf(to)] \quad (3.10)$$

The first term is due to the irreversible initial deformation, the second term is due to recoverable delayed deformation sometimes called delayed elasticity, and the third term is due to irreversible delayed deformation also known as plastic flow.

The various terms in this expression are defined as follows

$Ba = 0.8\ [1 - fc(to) / fc(\infty)]$

ϕd - delayed elasticity coefficient (usually taken as 0.4)

Bd - function corresponding to the development with time of delayed elasticity (Figure 3.4(b))

Øf - plastic flow coefficient

  Øf = Øf1 x Øf2

  Øf1 - depends on ambient environment (Table 3.1)

  Øf2 - depends on notional (theoretical) thickness (Figure 3.4(a))

Bf - function corresponding to the development with time of plastic flow - depends on notional thickness (Figure 3.4(c))

(b) Shrinkage

The shrinkage strain es at time t for which shrinkage is considered from time to is

$$es(t,to) = eso\,[Bs(t) - Bs(to)] \tag{3.11}$$

The various terms in this expression are defined as follows

eso - shrinkage coefficient

  eso = es1 x es2

  es1 - depends on ambient environment (Table 3.1)

  es2 - depends on notional (theoretical) thickness (Figure 3.4(d))

Bs - function corresponding to change of shrinkage with time - depends on notional thickness (Figure 3.4(e))

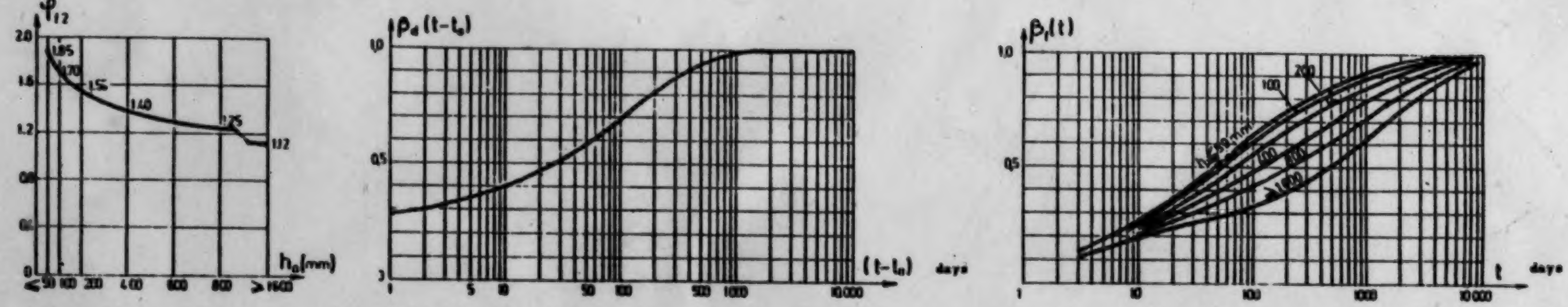

(a) influence of notional thickness on creep

(b) development of delayed elastic strain with time

(c) development of delayed plastic strain with time

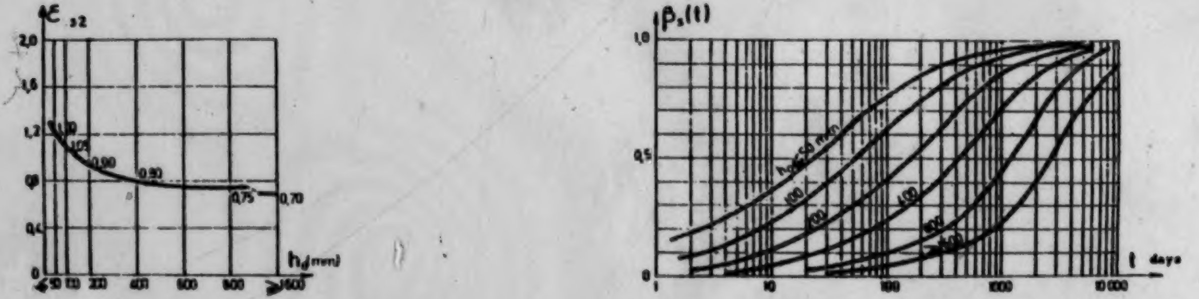

(d) influence of notional thickness on shrinkage

(e) development of shrinkage with time

Figure 3.4 Creep according to CEB 1978 (74)

Table 3.1 - Creep and shrinkage coefficents according to CEB 1978

Ambient environment	Relative humidity	Øf1	es1	λ
Water		0.8	+0.00010	30
Very damp atmosphere	90%	1.0	-0.00013	5
Outside in general	70%	2.0	-0.00032	1.5
Very dry Atmosphere	40%	3.0	-0.00052	1

Some notes:

(1) The notional thickness mentioned in the previous sections is given by the following expression

$$ho = \lambda \frac{2\ Ac}{u} \qquad (3.12)$$

where

λ - coefficient depending on ambient environment (Table 3.1)

Ac - area of concrete section (mm^2)

u - perimeter of concrete section in contact with the atmosphere (mm)

(2) A corrected age must be used for cements other than type I and temperatures other than 20°C as follows:

$$t = \frac{\alpha}{30} \Sigma\ [[T(tm) + 10]\Delta tm] \qquad (3.13)$$

where

α - 1 for slow and normal hardening cements (Type I)
2 for rapid-hardening cements (Type III)
3 for rapid-hardening high-strength cements

T - mean daily temperature of concrete (°C)

Δtm - number of days when the mean daily temperature has been T

(3) The values given for Øf1 and es1 in Table 3.1 relate to concrete of plastic consistence; they should be reduced 25% for concretes of stiff consistence and increased 25% for concretes of semi-fluid consistence. A plastic concrete has a slump of 1 to 2 inches, while a stiff concrete has a slump of 1/2 to 3/4 inches. A semi-fluid concrete has a slump of 3 to 6 inches (without a super-pasticizer).

3.3.5 Bazant-Panula

Bazant and Panula (76) have recently developed a model which they claim gives a more accurate prediction of creep and shrinkage, when applied to available test data, than either the ACI or CEB approaches.

This model is found to be quite complicated, since a large number of factors have been considered in its development and because it has a wide range of applicability. It is also found to be very empirical, since its development consisted of extensive curve fitting to available test data. For this reason, some physical significance is lost when the method is applied. However, the accuracy of the method cannot be denied and it is probably a suitable basis for the development of a code, although it is too cumbersome to use in its present state.

3.3.6 Relaxation of prestressing

Intrinsic relaxation is defined as the reduction in stress with time of a prestressing tendon which is stretched between two points, or simply the change in stress at constant strain. This is not to be confused with reduced relaxation which pertains to a prestressing tendon embedded in a continually shortening concrete member. The reduced relaxation is normally computed while the intrinsic relaxation must be defined.

In the absence of manufacturers' data, the expression developed by Magura, Sozen, and Siess (77) can be used to determine the intrinsic relaxation:

$$fs(t2) = \frac{fsi}{k}\left[\frac{fsi}{fsy} - 0.55\right](\log 24\ t2 - \log 24\ t1) \qquad (3.14)$$

where

fs(t2) = intrinsic relaxation at time t2 for a tendon stressed at time t1 (in days)

fsi = initial stress (usually 0.7 fsu)

fsy = yield stress (usually 0.85 fsu)

k = 10 for stress-relieved strands
45 for stabilized (low relaxation) strands
36 for Dywidag bars

It is obvious from the factor k that stabilized strands will have about one quarter of the relaxation of stress relieved strands. Note that fsi/fsy must be greater than 0.55; relaxation is negligible below this value.

3.3.7 Discussion

The basic philosophical differences between the different material models should be noted.

The ACI 209 model and CEB 1970 model represent the creep function as a product of age at loading and duration under load functions.

$$\phi(t,to) = \frac{1}{E(to)} [1 + C\ f(to)\ g(t-to)] \tag{3.15}$$

The CEB 1978 model represents the creep function as the sum of delayed elastic and plastic flow components. The delayed elastic component is assumed to be independent of the age at loading.

$$\phi(t,to) = \frac{1}{E(to)} [1 + C1\ f(t-to) + C2\ [g(t)-g(to)]] \tag{3.16}$$

The Bazant-Panula model separates creep into basic creep and drying creep.

3.4 Analytical models

3.4.1 Introduction

The analytical models for the prediction of creep that will be discussed here are the (1) effective modulus method, (2) rate of creep method, and (3) linear superposition method.

3.4.2 Effective modulus method

This simple and widely used method replaces the conventional modulus of elasticity Ec(t) by an effective modulus of elasticity Eeff(t) which includes the effects of both elastic and creep strains as a function of time.

$$E_{eff}(t) = \frac{E_c(t)}{1 + \phi(t)} \tag{3.17}$$

The method does not take the stress history and the aging of the concrete into account. Moreover, the method incorrectly predicts that all creep is fully recoverable.

An age-adjusted effective modulus, originated by Trost and further developed by Bazant, is a modification of the effective modulus method to include an aging coefficient X(t).

$$Eeff(t) = \frac{Ec(t)}{1 + X(t)\phi(t)} \tag{3.18}$$

The aging coefficient depends on the age at first loading and duration under load as well as the magnitude of the creep coefficient.

3.4.3 Rate of creep method

The rate of creep method is based on the assumption that the creep rate is completely independent of the age at loading of the concrete (and hence the previous stress history).

A single creep curve, based on the age at first loading, is used to predict the creep strain over the entire range of loading. Hence the previous stress history is ignored. Computationally, the method is attractive since only the current values of stress have to be stored. However, since only a single creep curve is defined, creep recovery is not possible. The widely used Dischinger equation is based on this method.

3.4.4 Linear superposition method

The linear superposition method is based on the assumption that the total strain due to two or more stresses can be obtained by calculating the strain from each stress separately and superimposing them.

Although the results from this method are superior to those given by the previous methods, the computational effort and storage requirements are significantly increased. This is because the entire previous stress history must be stored and used for each subsequent calculation. As well, a new creep curve must be defined for each stress change.

3.4.5 Discussion

Let us evaluate each of the three methods outlined with reference to a particular example. A concrete specimen (Figure 3.5) is subjected to a unit stress at time to; this stress is removed at time t1. Whereas the effective modulus predicts that all creep is fully recoverable, the rate of creep method predicts no creep recovery. These two methods seem to bound the real situation, which is approximated by the linear superposition method. It should be obvious that all three methods give identical results up to the point where the stress is removed.

Each of these three methods has its own range of application. The effective modulus method gives good results when the concrete stress does not vary appreciably and aging effects are minimal. This method is used extensively for the prediction of deflections in beams and creep effects in columns. The rate of creep method gives good results under similar conditions. The linear superposition method is the only procedure which can accurately predict the creep effects due to the complex stress history of a segmental bridge.

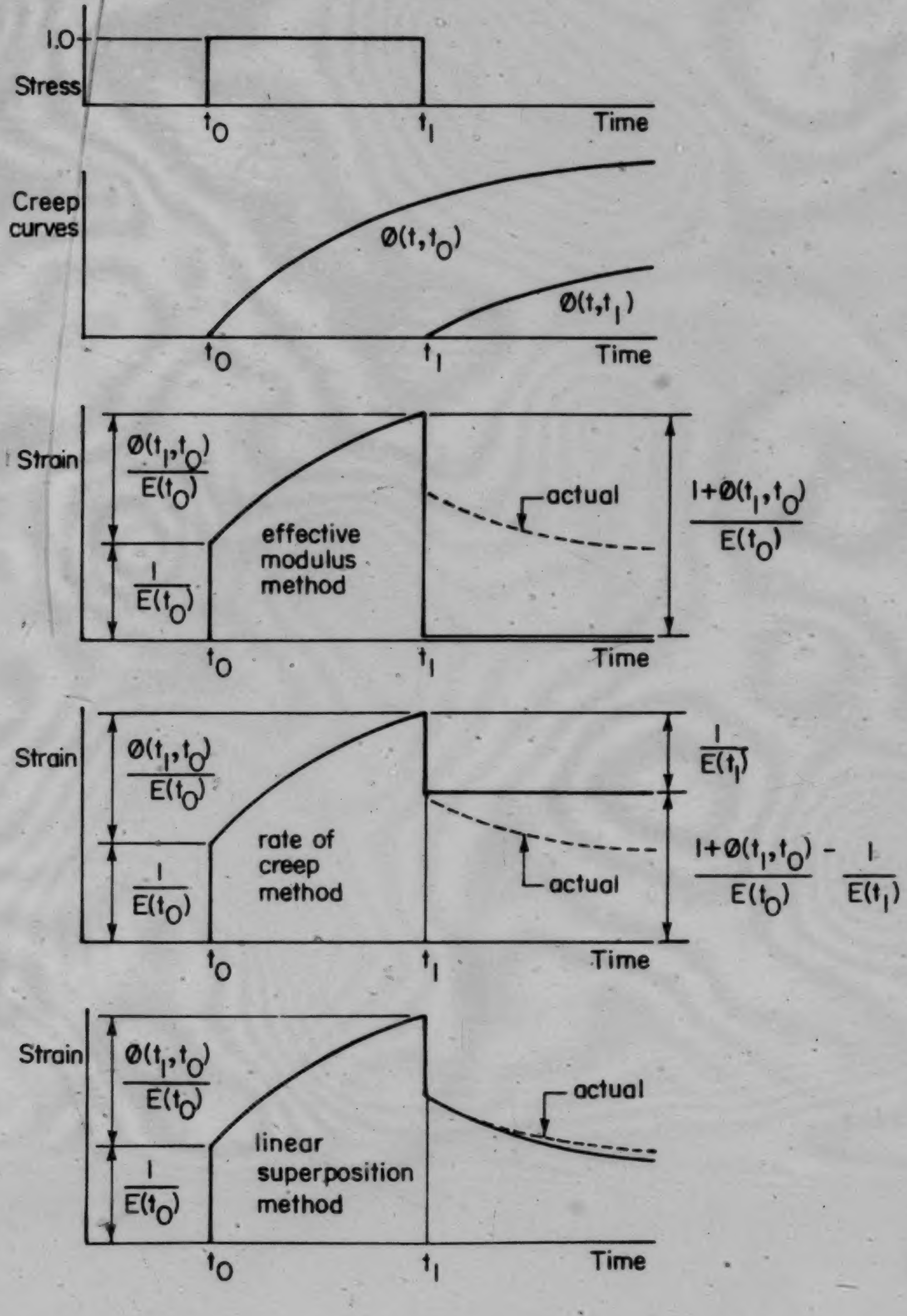
1.0
Stress
t_0
t_1
Time
Creep curves
$\emptyset(t,t_0)$
$\emptyset(t,t_1)$
t_0
t_1
Time
Strain
$\frac{\emptyset(t_1,t_0)}{E(t_0)}$
$\frac{1}{E(t_0)}$
effective modulus method
actual
$\frac{1+\emptyset(t_1,t_0)}{E(t_0)}$
t_0
t_1
Time
Strain
$\frac{\emptyset(t_1,t_0)}{E(t_0)}$
$\frac{1}{E(t_0)}$
rate of creep method
actual
$\frac{1}{E(t_1)}$
$\frac{1+\emptyset(t_1,t_0)}{E(t_0)} - \frac{1}{E(t_1)}$
t_0
t_1
Time
Strain
$\frac{\emptyset(t_1,t_0)}{E(t_0)}$
$\frac{1}{E(t_0)}$
linear superposition method
actual
t_0
t_1
Time

Figure 3.5 Creep according to various analysis methods

3.5 Review of existing computer programs

Surprisingly few computer programs have been developed for the analysis of segmental bridges. All programs can be classified as either institutional or commercial. Institutional programs are normally written at universities as part of research projects. Source code is available to the general public at the cost of duplication and use of the programs is unrestricted. Programs of this type have been developed by the following universities:

(1) University of Texas at Austin,
(2) University of Illinois at Urbana-Champaign,
(3) University of Calgary,
and (4) University of California at Berkeley.

Commercial programs are developed by private companies. Source code is not available; however, object code can be accessed at various service bureaus where a royalty fee is paid for the usage of the program. The following organizations have developed programs of this type:

(5) Europe Etudes,
(6) BVN/STS,
(7) Dyckerhoff and Widmann,
and (8) Engineering Computer Corporation.

Each of the above programs will be briefly discussed.

(1) University of Texas at Austin

Brown, Burns, and Breen (20,24) developed program SIMPLA2 for the three-dimensional analysis of segmental bridges without time-dependent effects. At the time this program was developed, the significance of time-dependent effects was not fully appreciated, and the effects of shear lag and cross sectional distortion and warping were deemed to be more important. This program was part of an extensive research program conducted jointly by the University of Texas at Austin and the Texas Highway Department (17-24). This research culminated in the construction of the first segmental bridge in the United States at Corpus Christi, Texas.

The program is based on the finite segment method of Scordelis and Lo (26,38). In this method, segments are first connected in the transverse direction to form the full cross-section, and then in the longitudinal direction segment-by-segment. In this way, stage construction, including the effects of self weight and prestressing, can easily be handled.

(2) University of Illinois at Urbana-Champaign

Danon and Gamble (66) developed a program for the time-dependent analysis of cantilevers erected segmentally. The program was written specifically so that parametric studies could be conducted on the effects of creep, shrinkage, and relaxation. The program is based on simple beam theory. Both the ACI 209 and CEB 1970 recommendations are considered. The rate of creep method and the method of superposition are both used. The analysis stops at the point where two cantilevers are joined by a closure segment to form a continuous structure.

Marshall and Gamble (67) used the force method to extend the above program to consider the effects of continuity. This program was specifically developed for the analysis of the Kishwaukee River bridge in Illinois. Analyses were conducted using both experimentally determined material properties and the CEB 1970 recommendations, and the results were compared against deformations measured during the construction of the bridge. The rate of creep method and the method of superposition have been combined by Marshall and Gamble to form the revised rate of creep method. It is important to note that, of all the programs currently available, these are the only ones not based on the direct stiffness method.

(3) University of Calgary

Tadros, Ghali, and Dilger (59,61) developed the program SEGCON for the two-dimensional time-dependent analysis of segmental bridges. The CEB 1970 recommendations are used and the program is based on the method of superposition (without Dirichlet series). Relaxation is based on the expression of Magura, Sozen, and Siess. Nonprestressed reinforcing can be included in the analysis.

Khalil, Dilger, and Ghali (53,63,64) developed a program for the time-dependent analysis of precast concrete cable-stayed bridges. The CEB 1978 recommendations are expressed as a Dirichlet series and used with the method of superposition. The model includes both material and geometric nonlinearities.

(4) University of California at Berkeley

Van Zyl and Scordelis (46,48) have developed program SEGAN for the three-dimensional time-dependent analysis of curved segmental bridges. The cross-section is limited to single box sections with cantilever flanges and vertical or inclined webs. The width and depth of the structure can vary along the length and the plate thicknesses can vary from element to element. Each curved element in plan or elevation is approximated by a straight skew-ended element which possesses eight degrees of freedom per node. A transverse distortional and a longitudinal warping degree of freedom are included in addition to the standard degrees of freedom for a space frame (three translations and three rotations).

The ACI 209 recommendations are used for the prediction of creep and shrinkage while the expression of Magura, Sozen, and Siess is used for prediction of relaxation. The program is based on the method of superposition with Dirichlet series.

(5) Europe Etudes

Europe Etudes Gecti of Paris, France has developed the program BC (Bridge Construction). Time-dependent effects are based on the recommendations of CEB 1978. The analytical technique is based on the method of superposition. A substantial amount of effort has been spent to simplify the input/output for this program. A user-oriented language allows input to be read directly from the tender drawings while a post-processor allows the results to be plotted.

(6) BVN/STS

BVN/STS of Indianapolis, Indiana has developed the program BRUCO (Bridge Under Construction). This program operates in much the same way as the Europe Etudes program.

(7) Dyckerhoff and Widmann

Dyckerhoff and Widmann of New York have developed a program suitable for the analysis of structures constructed with Dywidag bars. Material properties are based on the CEB recommendations and the analytical model is based on the Dischinger equation.

(8) Engineering Computer Company

The Engineering Computer Company of Sacramento, California (62) have developed a program which they call STDS (Segmental Time Dependent System). Creep and shrinkage are predicted using the CEB 1970 model while relaxation is based on the work of Magura, Sozen, and Siess. The analytical method is that given by Tadros, Ghali, and Dilger (59,61). This program can include nonprestressed reinforcing in the analysis.

Discussion:

Let us see which of the institutional programs can suitably be used for this study. The University of Texas program can immediately be eliminated from consideration since it does not include time-dependent effects. Similarly, the University of California program can be eliminated since it goes against the philosophy of this study, which is to uncouple the three-dimensional behaviour and time-dependent effects. Also, the University of Illinois programs can be eliminated since they were written for one specific analysis. This leaves the University of Calgary programs. The program of Tadros, Ghali, and Dilger does not use Dirichlet series and consequently is not as efficient as it could be. The program of Khalil, Dilger, and Ghali is quite general and some improvements can be made to the numerical efficiency by making it more specific.

Hence, the decision is made to develop a new program incorporating the desirable features of all the programs while trying to keep the numerical efficiency at a high level. It should be noted that these programs will be used as a source of comparison for the program to be developed.

3.6 Proposed method of analysis

3.6.1 Introduction

This section proposes a method for the analysis of segmental bridges. The basic requirements of a segmental analysis are reviewed, and a new model for creep and shrinkage is presented. The general requirements of a prestressing analysis are considered and some simplifying assumptions are made. Temperature is an important loading which has long been ignored, and consequently some discussion is devoted to it. Finally, the direct stiffness method, as it pertains to segmental analysis, is described.

3.6.2 Segmental analysis

A computer program for segmental analysis requires a tremendous amount of input data. This is because the final structure is the end result of an evolutionary process in which a different structure is subjected to different loads at each stage of construction. Careful organization of the input data is critical if the computer program is to have any practical significance.

It is therefore convenient to divide the input into two parts. The first part defines the overall geometry of the completed structure. It consists of material information, section properties, node coordinates, element data, and prestressing tendon data. The second part describes the events that occur at each stage of construction. This consists of segments assembled, tendons stressed, support conditions, construction loads, and temperature effects.

Two things can be done to reduce the amount of input for the construction stages even further. First of all, the stage at which each segment is assembled and tendon is stressed can be defined in the element data and prestressing tendon data respectively. Secondly, once the support conditions, construction loads, and temperature effects are defined, they remain in effect until they are redefined or removed.

In summary, the structure must be analysed at each stage of construction for the effects of self weight, prestressing, construction loads, temperature, and time-dependent effects. In addition, the completed structure must be analysed for the effects of self weight, prestressing, superimposed dead load (overlay, curbs, railing, etc.), live load (truck and lane load), and temperature.

3.6.3 Analysis for creep and shrinkage

The analysis for creep and shrinkage requires the selection of both an analytical and a material model. The linear superposition method with Dirichlet series is chosen as the analytical model while the recommendations of ACI Committee 209 are used as the material model. Dirichlet series allow the entire stress history to be stored in a set of hidden state variables. Since only the running total of the stresses need to be stored and used in the computations, a significant reduction in computational effort and storage requirements over other methods can be realized. The ACI Committee 209 recommendations have been chosen since aging effects can be incorporated directly.

Let us express the recommendations of ACI Committee 209 (equations 3.3 and 3.4) in a form more suitable for this analysis. The creep coefficient Ø(t,t') may be written as

$$Ø(t,t') = \frac{(t - t')^{0.60}}{10 + (t - t')^{0.60}} \; CFla(t') \; Cu \qquad (3.19)$$

where t is the current age in days, t' is the age at loading in days, CFla(t') is the correction factor for the age at loading, and Cu is the ultimate creep coefficient. The shrinkage strain esh(t,t0) may be written as

$$esh(t,t0) = \frac{(t - t0)}{a + (t - t0)} \; eshu \qquad (3.20)$$

where t is the current age in days, t0 is the age at the completion of curing in days, and eshu is the ultimate shrinkage strain. "a" has a value of 35 or 55 depending on whether moist-cured or steam-cured concrete is used. Note that the ultimate creep and shrinkage coefficients must be modified for nonstandard conditions as before.

The creep compliance or specific creep C(t,t') is defined as the creep function Ø(t,t') divided by the modulus of elasticity Ec(t') and can be expressed as a Dirichlet series as follows

$$C(t',t) = \sum_{i=1}^{m} ai(t') \, [1 - e^{-\lambda i(t-t')}] \qquad (3.21)$$

where ai and λi are coefficients determined by least-squares curve-fitting.

The determination of the coefficients ai and λi have been discussed in great detail by Kabir (44), Kang (45,49), Van Zyl (46,48), and Khalil (53), and it is not necessary to repeat this discussion here. The coefficients used in the computer program of Van Zyl have been found to correlate the best with the ACI Committee 209 recommendations and consequently will be used here.

Van Zyl determined the following:

$m = 3 \quad , \quad \lambda 1 = 0.1 \quad , \quad \lambda 2 = 0.01 \quad , \quad \lambda 3 = 0.001$

$$ai(tJ) = ai(tK) \; \frac{Ec(tK)}{Ec(tJ)} \; \frac{CFla(tJ)}{CFla(tK)} \; \frac{Cu}{2.35}$$

where

$t0 = 28$ days

$Ec(tK) = 3.834 \times 10^{6}$ psi

$a1(tK) = 1.88313 \times 10^{-7}$

$a2(tK) = 1.76834 \times 10^{-7}$

$a3(tK) = 1.29512 \times 10^{-7}$

During the time interval ΔtJ, the increments in free axial strain and curvature due to creep and shrinkage are given by the following equations. (Appendix K shows how the creep part of these equations can be derived from equation 3.21).

$$\Delta\varepsilon = \sum_{i=1}^{3} Ai,J^{N} \left[1 - e^{-\lambda i \Delta tJ}\right] + \Delta\varepsilon sh \qquad (3.22a)$$

$$\Delta\phi = \sum_{i=1}^{3} Ai,J^{M} \left[1 - e^{-\lambda i \Delta tJ}\right] \qquad (3.22b)$$

where

$$Ai,J^{N} = Ai,J{-}1^{N} \, e^{-\lambda i \Delta tJ-1} + \frac{\Delta N^{J}}{Ac} \, ai(tJ) \qquad (3.23a)$$

$$Ai,J^{M} = Ai,J{-}1^{M} \, e^{-\lambda i \Delta tJ-1} + \frac{\Delta M^{J}}{Ic} \, ai(tJ) \qquad (3.23b)$$

$$\Delta\epsilon sh = \epsilon sh(tJ+1,t0) - \epsilon sh(tJ,t0) \qquad (3.24)$$

Note that $\Delta tJ = tJ+1 - tJ$ is the length of the present time interval while $\Delta tJ+1 = tJ - tJ-1$ is the length of the previous time interval. ΔN^{J} and ΔM^{J} are the increments in axial force and bending moment due to initial strains in the present time interval ΔtJ. Of course, Ac and Ic are the area and moment of inertia of the concrete section.

The increments in axial force and bending moment due to creep and shrinkage on a restrained section are found as

$$\Delta N = \Delta\epsilon \ Ac \ Ecef(tJ) \qquad (3.25a)$$

$$\Delta M = \Delta\phi \ Ic \ Ecef(tJ) \qquad (3.25b)$$

where the effective modulus of elasticity Ecef(tJ) is given as

$$Ecef(tJ) = \frac{Ec(tJ)}{1 + \phi(tJ+1,tJ)} \qquad (3.26)$$

3.6.4 Prestressing analysis

Prestressing is a difficult feature to incorporate into a computer program for the time-dependent analysis of segmental bridges. This is because there are a large number of tendons, each of which has a different profile, and is stressed at a different time. Each tendon profile must be defined with a minimum amount of input, and this information must be converted into equivalent loads for each segment that the tendon crosses. The equivalent loads are influenced by the instantaneous losses due to friction, anchor set, and elastic shortening. Keeping track of whether the tendon is stressed from one-end or both-ends complicates the issue even more. The time-dependent losses due to creep, shrinkage, and relaxation are inter-dependent and vary with each stage of construction. Grouting an unbonded tendon to create a bonded tendon adds another degree of complexity. Consequently, there is a significant demand on the computer with respect to both number of operations and storage required. Let us look at each of these items individually.

In order to give the computer program any practical importance, the tendon profiles should be defined with a minimum amount of input. This implies that two points should be used to describe a straight tendon, while three points should be used to define a parabolic tendon.

Alternatively, a parabolic tendon should have the option of being defined by two points and a tangent at one of the points. More complex profiles should be specified as a combination of straight and parabolic segments.

Once a minimum amount of input has been used to define the tendon, a substantial amount of information must be generated. Ultimately, the equivalent loads must be determined for each segment that the tendon crosses. Figure 3.6 shows that the determination of equivalent loads for a segment can become quite complex.

In addition to the time-dependent losses due to creep, shrinkage, and relaxation, prestressing tendons are also subjected to instantaneous losses due to friction, anchor set, and elastic shortening. Friction losses are due to both intentional and unintentional curvature. The tendon profile comprises the intentional curvature while deviations from the theoretical profile constitutes the unintentional curvature. Anchor set losses are associated with the slip that occurs at the jacking end of the tendon, when the tendon is locked into position. Although anchor set losses will significantly reduce the overall prestressing force for short tendons, they are usually small for long tendons. Since concrete shortens as prestressing forces are applied to it, tendons previously stressed also shorten, and consequently lose part of their

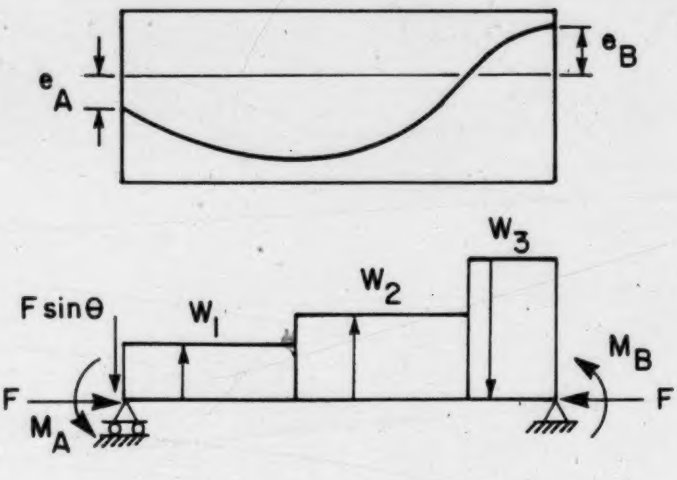
e_A
e_B
W_3
W_2
W_1
F sinθ
M_B
F
F
M_A

Figure 3.6 Equivalent load representation of prestressing

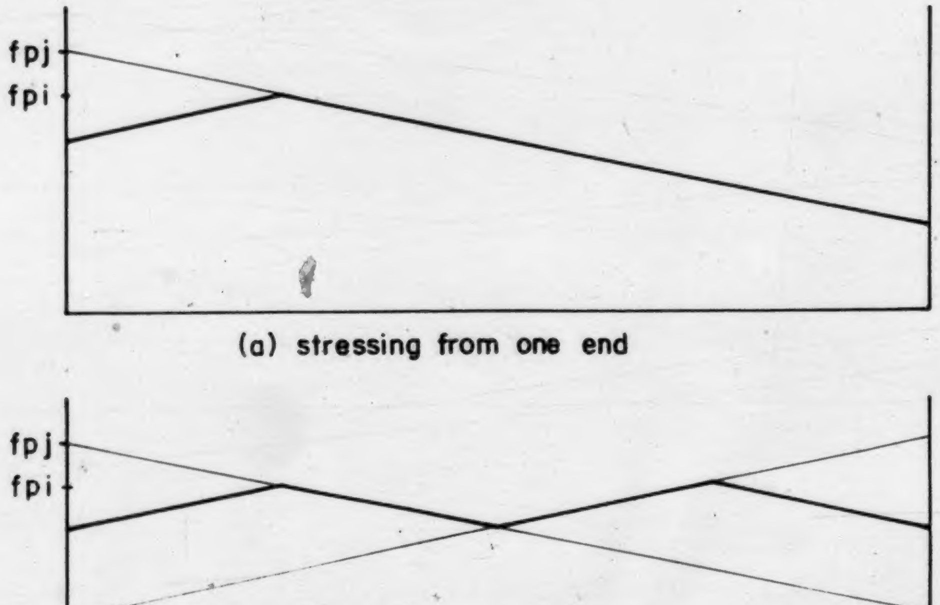

(a) stressing from one end

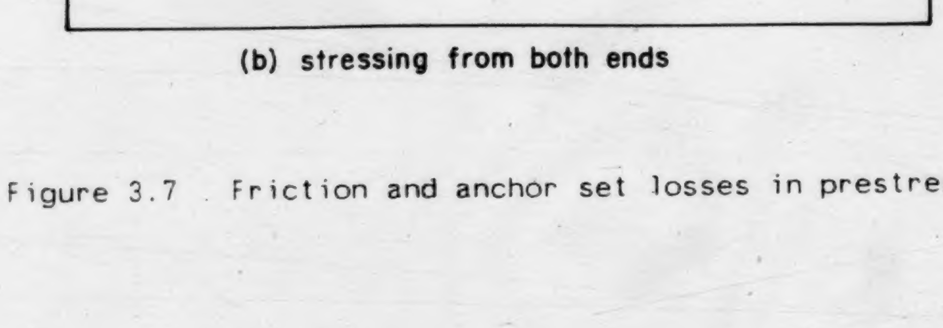

(b) stressing from both ends

Figure 3.7 Friction and anchor set losses in prestressing

stress. This is known as elastic shortening. Note that elastic shortening (and elastic recovery losses) are automatically taken into account when transformed section properties are used in the analysis (67).

Friction and anchor set losses are shown in Figure 3.7 for tendons stressed from one-end and both-ends. The stress in a tendon varies with the distance from the jacking end as given by the following equation:

$$fpi(x) = fpj\, e^{-(u\alpha + kx)} \qquad (3.27)$$

where

fpi = steel stress at a distance x from the jacking end
fpj = steel stress at the jacking end
u = curvature friction coefficient (per unit angle change)
α = total angular change from the jacking end to the point under consideration
k = wobble friction coefficient (per unit length)
x = total distance from the jacking end to the point under consideration

Prestressing tendons can be grouted only after all the tendons in a particular region have been stressed. This is to prevent grout migration into the ducts of tendons which have not yet been stressed. Before the tendons have been grouted, they are considered to be unbonded. This implies that the displacements in the tendon are independent of those in the surrounding concrete except at the anchors, and the strains in the tendon are uniformly distributed. After the tendons have been grouted, they are considered to be bonded to the concrete, and the displacements of the tendon and concrete coincide. Most of the existing computer programs ignore unbonded tendons and treat strictly bonded tendons.

Since this entire project is quite an ambitious one, there is not enough time available to give prestressing the type of consideration that it deserves. Consequently, some simplifications are made to the present method of analysis (and computer program). First of all, only straight tendons are considered; parabolic tendons are not possible at this time. Secondly, the instantaneous prestress losses are not determined, but rather, the initial stress in each tendon is assumed to be 0.7 of the ultimate tensile strength. Thirdly, only bonded tendons are considered. By making these simplifications, the number of operations and storage required by the computer is greatly reduced. Since the program is coded in a modular form, these additional features could easily be added at a later date.

3.6.5 Thermal Analysis

Temperature is an important loading, which has all but been ignored in the past. Consequently, it deserves some special attention. The analysis for thermal effects requires two parameters - the thermal gradient and temperature differential. This information can be determined by a detailed heat-flow analysis or given as code requirements.

The recommendations of the PCI-PTI (10) and New Zealand specification (135), as shown in Figure 3.8, are commonly used. The PCI-PTI suggests a constant gradient over the top slab with a temperature differential of 18°F (10°C). Meanwhile, the New Zealand specification considers a fifth order parabola over a depth of 1200 mm (47.2 in) with a temperature differential of 32°C (57.6°F). An additional linear portion is specified in the bottom slab while modifications are made to include the effects of blacktop.

Hoffman, McClure, and West (121) have conducted a thermal study on an experimental bridge in Pennsylvania (Figure 3.9). They have found that the stresses predicted by the New Zealand specification compare favourably with the experimental results. They have also found that the stress at the bottom of the section predicted by the PCI-PTI recommendation can be made to agree with the

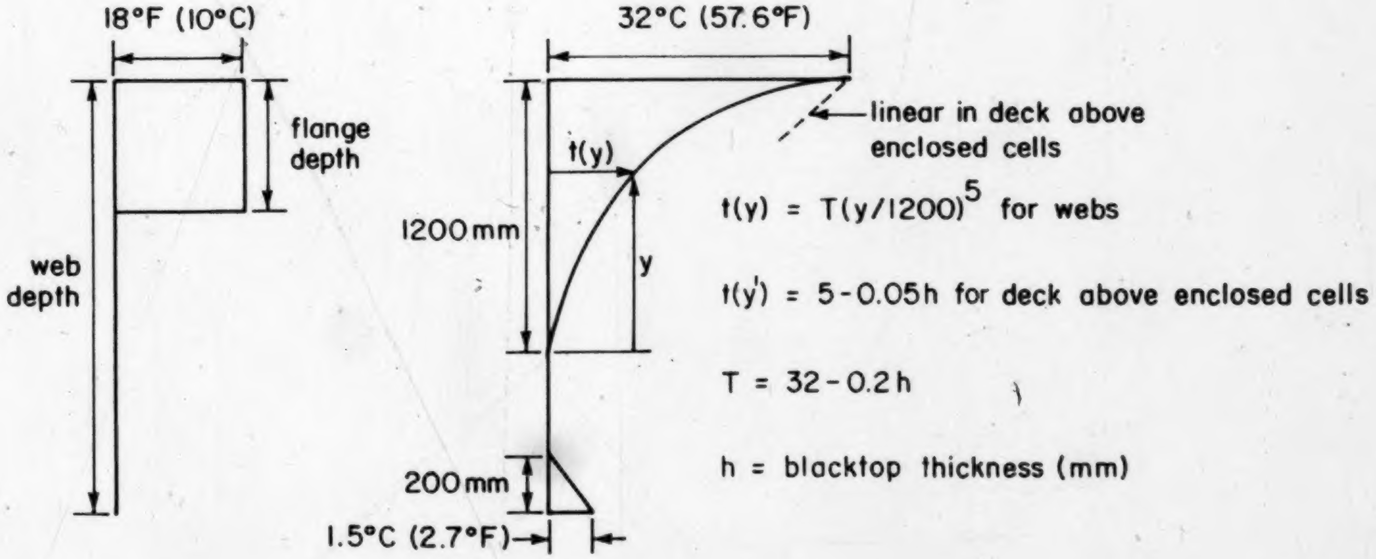
18°F (10°C)
flange depth
web depth
32°C (57.6°F)
linear in deck above enclosed cells
t(y)
1200 mm
y
t(y) = T(y/1200)^5 for webs
t(y') = 5-0.05h for deck above enclosed cells
T = 32-0.2h
h = blacktop thickness (mm)
200 mm
1.5°C (2.7°F)

(a) PCI-PTI recommendation

(b) New Zealand specification

Figure 3.8 Thermal gradients and temperature differentials

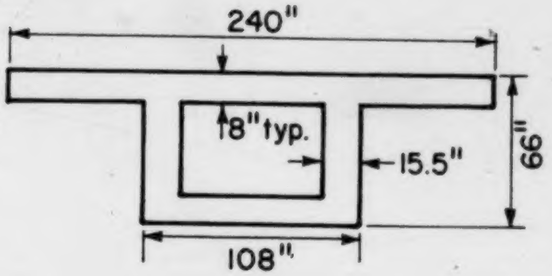
240"
8" typ.
15.5"
66"
108"

(a) cross-section

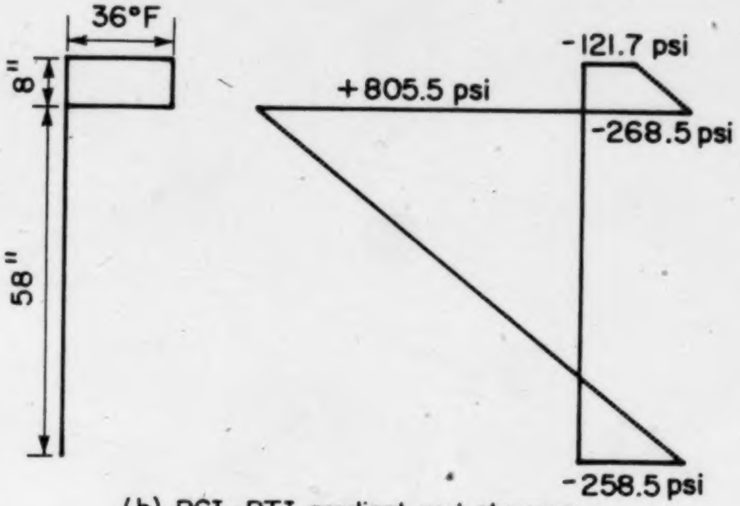
36°F
8"
58"
+805.5 psi
-121.7 psi
-268.5 psi
-258.5 psi

(b) PCI-PTI gradient and stresses

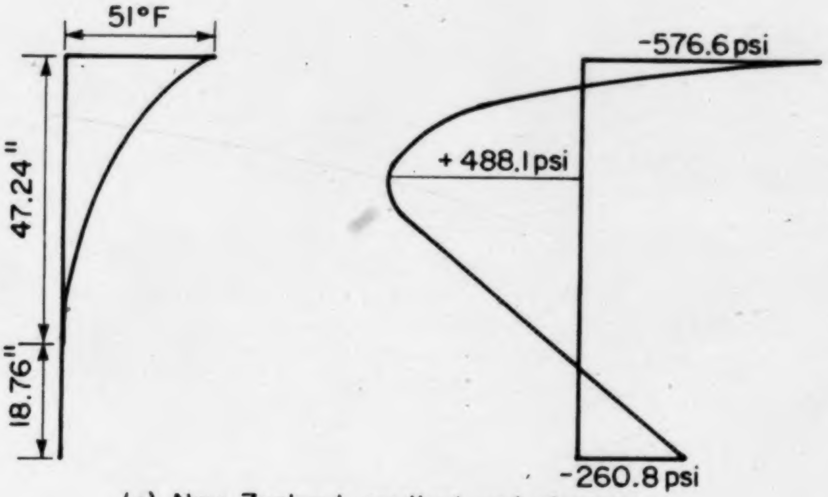
51°F
47.24"
18.76"
-576.6 psi
+488.1 psi
-260.8 psi

(c) New Zealand gradient and stresses

Figure 3.9 Thermal study of an experimental bridge

experimental results if a temperature differential of 36°F (20°C) is used instead of the specified 18°F (10°C). Although the stress at the bottom can be made to agree with the experimental data, the distribution will still be wrong.

Since calculations using the fifth-order parabola of the New Zealand specification become quite cumbersome, and the stress distribution given by the PCI-PTI recommendation is somewhat unrealistic, let us propose a linear gradient over the top slab with a temperature diffential of 72°F (40°C). The linear gradient predicts the stress distribution much more accurately than the constant gradient, while requiring essentially the same amount of computational effort. The 72°F (40°C) temperature differential correlates favourably with experimental data.

Thermal stresses are induced by restraint to expansion and rotation, and not by temperature changes directly. Restraint can be provided by the cross-section itself or by the support conditions. If the structure is statically determinate, only the cross-section provides restraint; whereas if the structure is statically indeterminate, restraint is provided by both the cross-section and support conditions.

It is convenient to separate the thermal response of a statically indeterminate structure into primary and secondary components. The primary component is due to the temperature distribution acting on the cross-section while the secondary component is due to the redistribution of stress due to the support conditions. In the direct stiffness method, the primary calculations involve the determination of the fixed end restraining forces for the element while the secondary calculations involve the analysis of the structure for the fixed end forces. Figure 5.12(a) shows how the thermal stress distribution acting on a section can be broken down into its component form.

Consider the general cross-section shown in Figure 3.10 which is subjected to an arbitrary vertical temperature distribution. Based on the equations of equilibrium, assuming that plane sections remain plane, Priestley (132) derived expressions for the average strain and curvature in the unrestrained section (note: α=thermal coefficient)

$$\epsilon = \alpha/A\ (T1-T2) \int t(y)\ b(y)\ dy \qquad (3.28)$$

$$\varnothing = \alpha/I\ (T1-T2) \int t(y)\ b(y)\ (y-yb)\ dy \qquad (3.29)$$

as well as an expression for the stress

$$f(y) = E\ [\epsilon + \varnothing\ y - \alpha\ t(y)] \qquad (3.30)$$

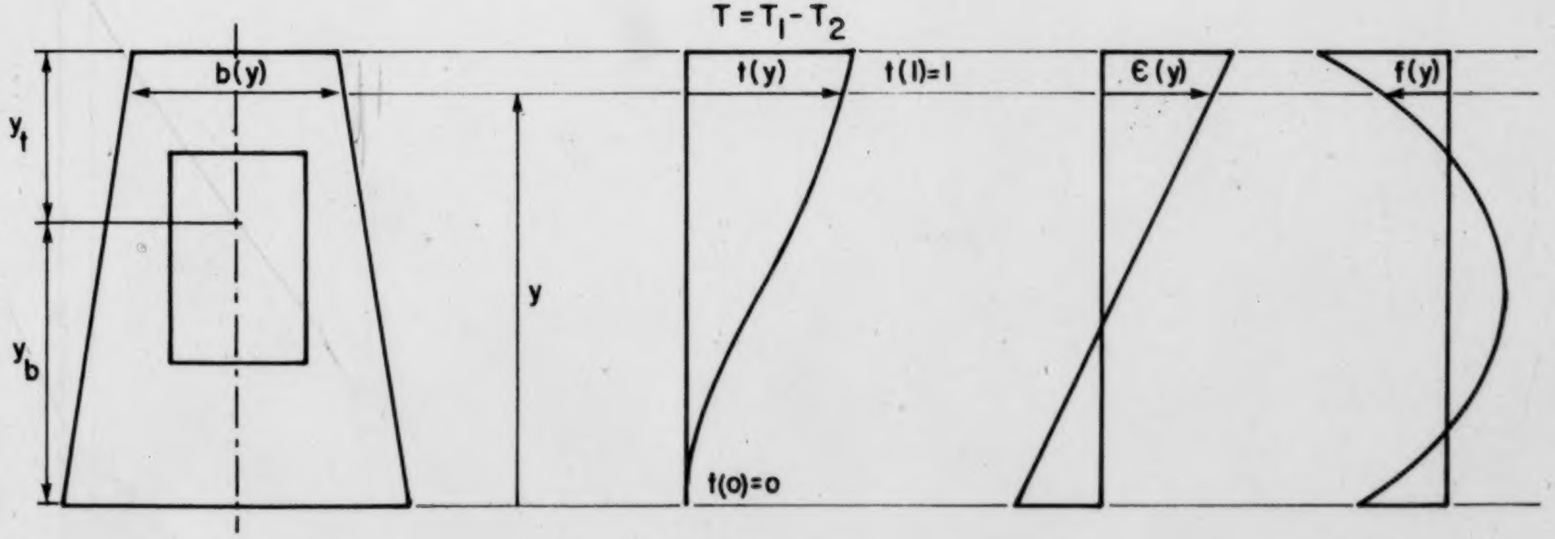
$T = T_1 - T_2$
b(y)
y_t
y_b
y
t(y)
t(1)=1
t(o)=o
ε(y)
f(y)

(a) general cross section

(b) temperature distribution

(c) strain distribution

(d) stress distribution

Figure 3.10 General cross section subjected to an arbitrary temperature distribution

Since ϵ = N/EA and ϕ = M/EI, the axial force and bending moment can easily be found for the restrained section.

$$N = E \alpha (T1-T2) \int t(y)\, b(y)\, dy \tag{3.31}$$

$$M = E \alpha (T1-T2) \int t(y)\, b(y)\, (y-yb)\, dy \tag{3.32}$$

It is convenient to rewrite the expressions in the following form

$$N = E \alpha (T1-T2)\, S1 \tag{3.33}$$

$$M = E \alpha (T1-T2)\, S2 \tag{3.34}$$

where

$$S1 = \int t(y)\, b(y)\, dy \tag{3.35}$$

$$S2 = \int t(y)\, b(y)\, (y-yb)\, dy \tag{3.36}$$

The integrals S1 and S2 can be considered as section properties for a particular temperature profile. They can be input into a computer program in the same way as the area and moment of inertia are usually input. For a rectangular section, the evaluation of the integrals is very simple, even for complex temperature profiles. For more complex shapes, the evaluation becomes somewhat more demanding.

The previous discussion assumes that the reference temperature is T2. If the reference temperature is TR, an additional term must be added to the axial restraining force.

$$N = E \alpha (T1-T2)\, S1 + E \alpha (T2-TR)\, A \tag{3.37}$$

$$M = E \alpha (T1-T2)\, S2 \tag{3.38}$$

Consider the special case of a linear gradient on a rectangular section with TR = 0. Since $S1 = A/2 = bd/2$ and $S2 = I/d = bd^2/12$, the restraining forces can be expressed as follows

$$N = E \alpha (T1 + T2)\, bd/2 \tag{3.39}$$

$$M = E \alpha (T1 - T2)\, bd^2/12 \tag{3.40}$$

These equations are used in Chapter 4 (see Figure 4.7).

3.6.6 Direct stiffness analysis

3.6.6.1 Introduction

The development of the direct stiffness method of analysis has been well documented in the past. Consequently, it will only be briefly summarized, as it pertains to segmental bridges.

3.6.6.2 Coordinate systems

As with any direct stiffness assemblage procedure, two right handed Cartesian coordinate systems are defined (Figure 3.11).

(1) Global system (X,Y,Z) - An arbitrary point is chosen as the origin such that the structure lies in the X-Y plane. Nodal displacements and support reactions are expressed in the global system.

(2) Local system (x,y,z) - Each element has a local coordinate system whose x axis is directed along the centroidal axis of the element from node I to node J. The global Z axis and local z axis have the same direction. The local x and z directions define the direction of the local y axis. Element forces are expressed in the local system.

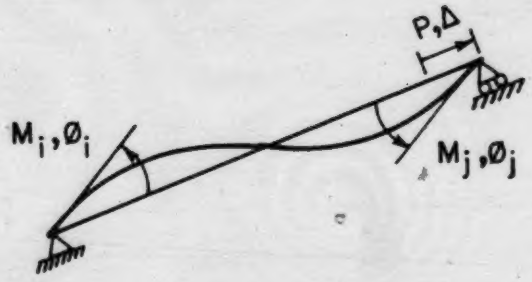
P, Δ
M_i, ϕ_i
M_j, ϕ_j

(a) independent degrees of freedom in the local coordinate system

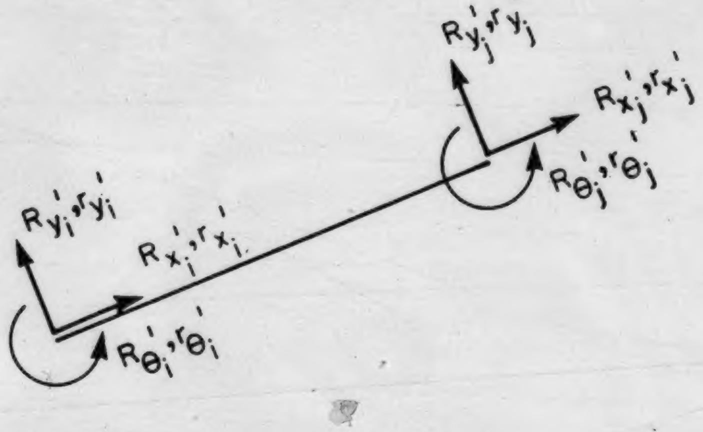
$R_{y_j'}, r_{y_j'}$
$R_{x_j'}, r_{x_j'}$
$R_{\theta_j'}, r_{\theta_j'}$
$R_{y_i'}, r_{y_i'}$
$R_{x_i'}, r_{x_i'}$
$R_{\theta_i'}, r_{\theta_i'}$

(b) complete degrees of freedom in the local coordinate system

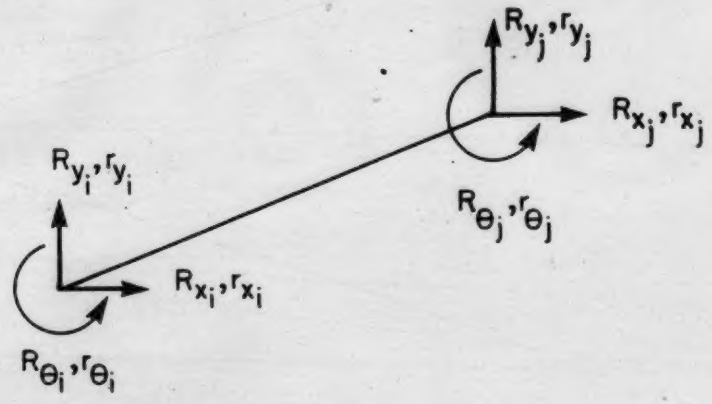
R_{y_j}, r_{y_j}
R_{x_j}, r_{x_j}
$R_{\theta_j}, r_{\theta_j}$
R_{y_i}, r_{y_i}
R_{x_i}, r_{x_i}
$R_{\theta_i}, r_{\theta_i}$

(c) complete degrees of freedom in the global coordinate system

Figure 3.11 Element forces and displacements

3.6.6.3 Direct stiffness method

The direct stiffness method consists of the following sequence of matrix operations:

(1) Form element stiffness matrix in local coordinate system

$$[s] = [K]\,[v] \tag{3.41}$$

(2) Form element translation matrix (transforms independent dof to complete dof)

$$[v] = [T]\,[v'] \tag{3.42a}$$

$$[s'] = [T]^T\,[s] \tag{3.42b}$$

(3) Form element rotation matrix

$$[v'] = [R]\,[\bar{v}] \tag{3.43a}$$

$$[\bar{s}] = [R]^T\,[s'] \tag{3.43b}$$

(4) Form element transformation matrix

$$[v] = [T]\,[v'] = [T]\,[R]\,[\bar{v}] = [a]\,[\bar{v}] \tag{3.44a}$$

$$[\bar{s}] = [R]^T\,[s'] = [R]^T\,[T]^T\,[s] = [a]^T\,[s] \tag{3.44b}$$

(5) Form element stiffness matrix in global coordinate system

$$[s] = [K]\,[a]\,[\bar{v}] \tag{3.45a}$$

$$[\bar{s}] = [a]^T\,[K]\,[a]\,[\bar{v}] \tag{3.45b}$$

$$[\bar{s}] = [\bar{K}]\,[\bar{v}] \tag{3.45c}$$

(6) Add element stiffness matrix and element load vector to structure stiffness matrix keeping in mind that a banded equation solver is being used.

$$[R] = [K]\,[r] \tag{3.46}$$

(7) Solve for node displacements

$$[r] = [K]^{-1}[R] \tag{3.47}$$

(8) Find element forces

$$[s] = [k]\,[a]\,[\bar{v}] \quad \text{where} \quad [\bar{v}] = [r] \tag{3.48a}$$

$$[s] = [T]^{T}\,[k]\,[a]\,[\bar{v}] \tag{3.48b}$$

3.6.6.4 Element stiffness matrices

The element stiffness matrix [k] in the local coordinate system is given as follows

$$\begin{bmatrix} P \\ Mi \\ Mj \end{bmatrix} = \begin{bmatrix} K11 & 0 & 0 \\ 0 & K22 & K23 \\ 0 & K32 & K33 \end{bmatrix} \begin{bmatrix} \Delta \\ \phi i \\ \phi j \end{bmatrix} \tag{3.49}$$

The stiffness coefficients are

$$K11 = \frac{EA}{L} \qquad K22 = K33 = \frac{4EI}{L} \qquad K23 = K32 = \frac{2EI}{L} \tag{3.50}$$

If shear deformations are included, the coefficients are modified as follows

$$K22 = K33 = \frac{4EI}{L}\left[\frac{1 + B/2}{1 + 2B}\right] \tag{3.51a}$$

$$K23 = K32 = \frac{2EI}{L}\left[\frac{1 - B}{1 + 2B}\right] \tag{3.51b}$$

$$\text{where} \quad B = \frac{6EI}{L}\,\frac{1}{G\bar{A}L} \quad (\bar{A} \text{ is the shear area}) \tag{3.51c}$$

The element translation matrix [T] is given as follows

$$\begin{bmatrix} \Delta \\ \text{Ø}i \\ \text{Ø}j \end{bmatrix} = \begin{bmatrix} -1 & 0 & 0 & 1 & 0 & 0 \\ 0 & 1/L & 1 & 0 & -1/L & 0 \\ 0 & 1/L & 0 & 0 & -1/L & 1 \end{bmatrix} \begin{bmatrix} rxi' \\ ryi' \\ r\theta i' \\ rxj' \\ ryj' \\ r\theta j' \end{bmatrix} \qquad (3.52)$$

The element rotation matrix [R] is given as follows

$$\begin{bmatrix} rxi' \\ ryi' \\ r\theta i' \\ rxj' \\ ryj' \\ r\theta j' \end{bmatrix} = \begin{bmatrix} C & S & 0 & 0 & 0 & 0 \\ -S & C & 0 & 0 & 0 & 0 \\ 0 & 0 & 1 & 0 & 0 & 0 \\ 0 & 0 & 0 & C & S & 0 \\ 0 & 0 & 0 & -S & C & 0 \\ 0 & 0 & 0 & 0 & 0 & 1 \end{bmatrix} \begin{bmatrix} rxi \\ ryi \\ r\theta i \\ rxj \\ ryj \\ r\theta j \end{bmatrix} \qquad (3.53)$$

where C=cos(a) and S=sin(a)

The element transformation matrix [a] is determined as

$$\begin{bmatrix} \Delta \\ \text{Ø}i \\ \text{Ø}j \end{bmatrix} = \begin{bmatrix} -C & -S & 0 & C & S & 0 \\ -S/L & C/L & 1 & S/L & -C/L & 0 \\ -S/L & C/L & 0 & S/L & -C/L & 1 \end{bmatrix} \begin{bmatrix} rxi \\ ryi \\ r\theta i \\ rxj \\ ryj \\ r\theta j \end{bmatrix} \qquad (3.54)$$

This matrix can easily be modified for hinges at the i and/or j ends of the element

The use of untransformed section properties is recommended for the time-dependent analysis of segmental bridges. Although many of the existing programs consider the contribution of both prestressed and nonprestressed steel to the transformed section properties, the fact of the matter is that creep can only be accurately predicted to plus or minus 20%, while the difference between untransformed and transformed section properties for real structures is generally within 5%.

The advantage of using untransformed section properties is that the element stiffness matrices can be found once for the entire structure and stored. If the transformed section properties are used, the element stiffness matrices must be reformulated at each stage of construction to accommodate the addition of prestressing tendons. Calculating the element stiffness matrices once represents a significant reduction in computational effort. Of course, the effective modulus of elasticity varies from stage to stage as the concrete gets older, but this can be accounted for when the element stiffness matrices are assembled into the structure stiffness matrix.

3.6.6.5 Element load vectors

Four different element load vectors are considered in this study. They are self weight, prestressing, temperature, and time-dependent effects (Figure 3.12). The analysis procedure is the same as that traditionally used. The fixed end forces are found in the local coordinate system and transformed into the global coordinate system, after which they are added to the structure load vector. When the displacements have been found, the fixed end forces are subtracted from the forces calculated to give the actual forces.

3.6.6.6 Solution of equations

Most programs for segmental analysis are inefficiently organized because they are written to accommodate existing equation solvers. By making a slight modification to the equation solver, the analysis can be substantially simplified.

Consider the structure shown in Figure 3.13. If we were to simply check for nodes connected to assembled elements, we would find that node 2 is the first equation and node 12 is the last equation to be solved. In reality, equations corresponding to nodes 2 to 6 should be solved independently of equations corresponding to nodes 7 to 12.

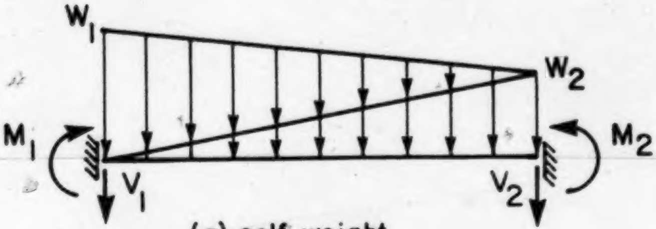
W1
W2
M1
M2
V1
V2

(a) self weight

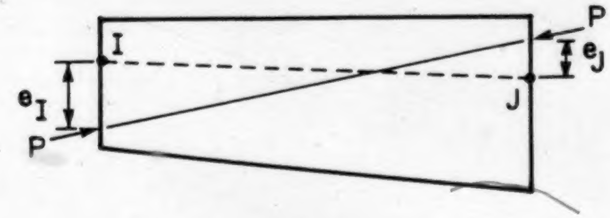

$N = P \cos \theta$

$V = P \sin \theta$

$M = P\,e$

(b) prestressing

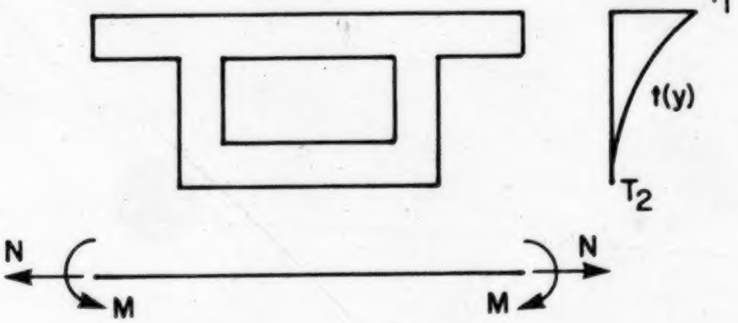
T1
t(y)
T2
N
N
M
M

(c) temperature

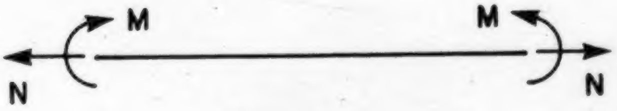

(d) time-dependent effects

Figure 3.12 Element load vectors

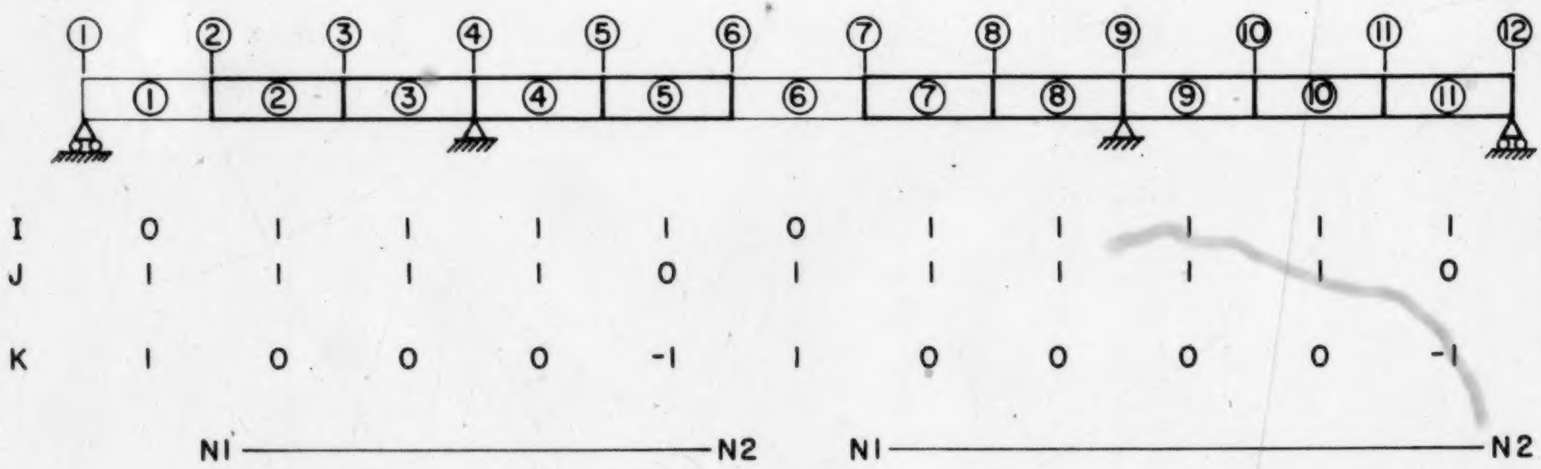
① ② ③ ④ ⑤ ⑥ ⑦ ⑧ ⑨ ⑩ ⑪ ⑫
① ② ③ ④ ⑤ ⑥ ⑦ ⑧ ⑨ ⑩ ⑪
I 0 1 1 1 1 0 1 1 1 1 1
J 1 1 1 1 0 1 1 1 1 1 0
K 1 0 0 0 -1 1 0 0 0 0 -1
N1
N2
N1
N2

Figure 3.13 Solution of equations

Let us propose the following method to find the first and last equation in a series of analyses. Define I for element i as being 0 if element i has not been assembled and 1 if it has been assembled at a particular stage of construction. Similarly, define J for element i as being 0 if element i+1 has not been assembled and 1 if it has been assembled at the same stage of construction. Let K=J-I for element i. If K is equal to 1, node i+1 is the first node N1 to be solved. Meanwhile, if K is equal to -1, node i+1 is the last node N2 to be solved. Figure 3.13 shows that equations corresponding to nodes 2 to 6 should be solved, followed by equations corresponding to nodes 7 to 12. Note that this method only works for a continuous beam type of structure; a different scheme must be used for a plane frame type of structure.

3.7 Computer program

Although a number of computer programs are currently available for the time-dependent analysis of segmental bridges, the decision was made to develop a new program rather than to modify an existing program. This new general purpose program would be coded in modular form so that additional features and future enhancements can easily be incorporated by others.

Before any programming could be undertaken, the philosophy of the program had to be developed. The purpose of the program was to simplify the task of the design engineer and provide him with access to more precise information. The program had to be able to perform a time-dependent analysis at each stage of construction for a segmental bridge. The analysis had to include self weight, prestress, construction loads, and temperature. Temperature is an important consideration, which was all but ignored in the past.

On this basis, the program TIMEDEP was developed. This program was written in the FORTRAN IV language for the Amdahl 5860 computer at the University of Alberta. Generally accepted programming procedures have been used so that the program can easily be converted to operate on other systems. Dynamic storage allocation is not included in the present version of the program but could easily be implemented. The program is based on the theory previously outlined.

The program is quite versatile and can be applied to a wide range of segmental structures. The program can handle precast and/or cast-in-place bridges built by balanced cantilever construction, progressive placing, and span-by-span construction (precast). Note that the present version of the program cannot handle span-by-span construction (cast-in-place) or incremental launching, since they require the incorporation of layered elements. In addition, the program can handle any prestressed concrete frame subjected to time-dependent effects.

The input data and output information are discussed in detail in Appendix A. Briefly, the input data is divided into two parts. The first part defines the structure; it consists of material information, section properties, node coordinates, element incidences, and prestressing tendon data. The second part describes the loading and support conditions at each stage of construction. The loading information can include self weight, prestress, construction loads, and temperature. Any consistent set of units may be used for the input. Output information provided by the program includes an echo of the input data, as well as the node displacements, element forces, element stresses, and support reactions at each stage of construction. Appendix B gives a source listing for the program. Sample input data is given in Appendix C while some selected output is included in Appendix D.

The program consists of the following set of subroutines. A flow chart is given in Figure 3.14.

1. Program MAIN - calls other subroutines

2. Subroutine READ - reads input data for overall structure
3. Subroutine STAG - reads input data for each stage
4. Subroutine SELF - adds self weight to structure load vector
5. Subroutine PRES - adds prestressing to structure load vector
6. Subroutine TEMP - adds temperature to structure load vector
7. Subroutine TYME - adds time dependent effects to structure load vector
8. Subroutine STIF - adds element stiffness matrix to structure stiffness matrix
9. Subroutine ELMK - forms element stiffness matrix
10. Subroutine TRAN - forms element transformation matrix
11. Subroutine FORC - finds node displacements and element forces
12. Subroutine RITE - writes node displacements and element forces
13. Subroutine SOLV - banded equation solver

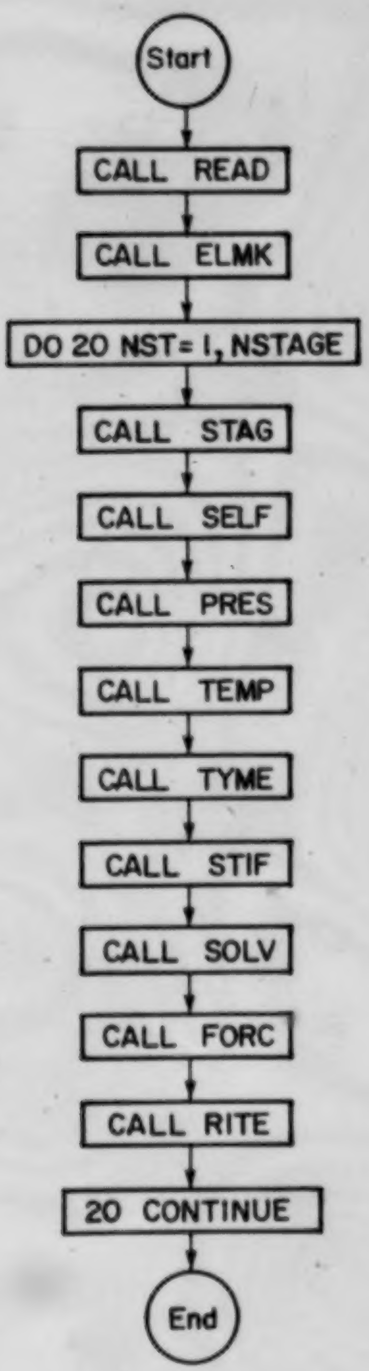
Start
CALL READ
CALL ELMK
DO 20 NST= I, NSTAGE
CALL STAG
CALL SELF
CALL PRES
CALL TEMP
CALL TYME
CALL STIF
CALL SOLV
CALL FORC
CALL RITE
20 CONTINUE
End

Figure 3.14 Flow chart for the computer program TIMEDEP

3.8 Numerical examples

3.8.1 Example 1 - Creep test

This example compares the results given by the computer program with those of experimental creep tests conducted by Ross (81). The two creep tests considered are shown in Figures 3.15 and 3.16. In the first creep test, a compressive stress of 2.180 ksi is applied to a concrete cylinder at 14 days and removed at 60 days whereas in the second creep test, a compressive stress of 2.180 ksi is applied to a concrete cylinder at 28 days and one-quarter is removed at 60, 91, 120 and 154 days respectively. The compressive strength of the concrete cylinders is 9600 psi while the modulus of elasticity is 5585 ksi. Note that a rapid hardening portland cement is used and that the cylinders are stored at 93% relative humidity.

Results from both the experiments and computer program are plotted in Figure 3.15 and 3.16. The computer program used the ACI 209 model. Steam-cured type III cement was assumed and the standard creep coefficient of 2.35 was multiplied by 0.647 corresponding to the 93% relative humidity.

From these creep tests, it appears that the ACI 209 model overestimates both the amount of creep deformation and

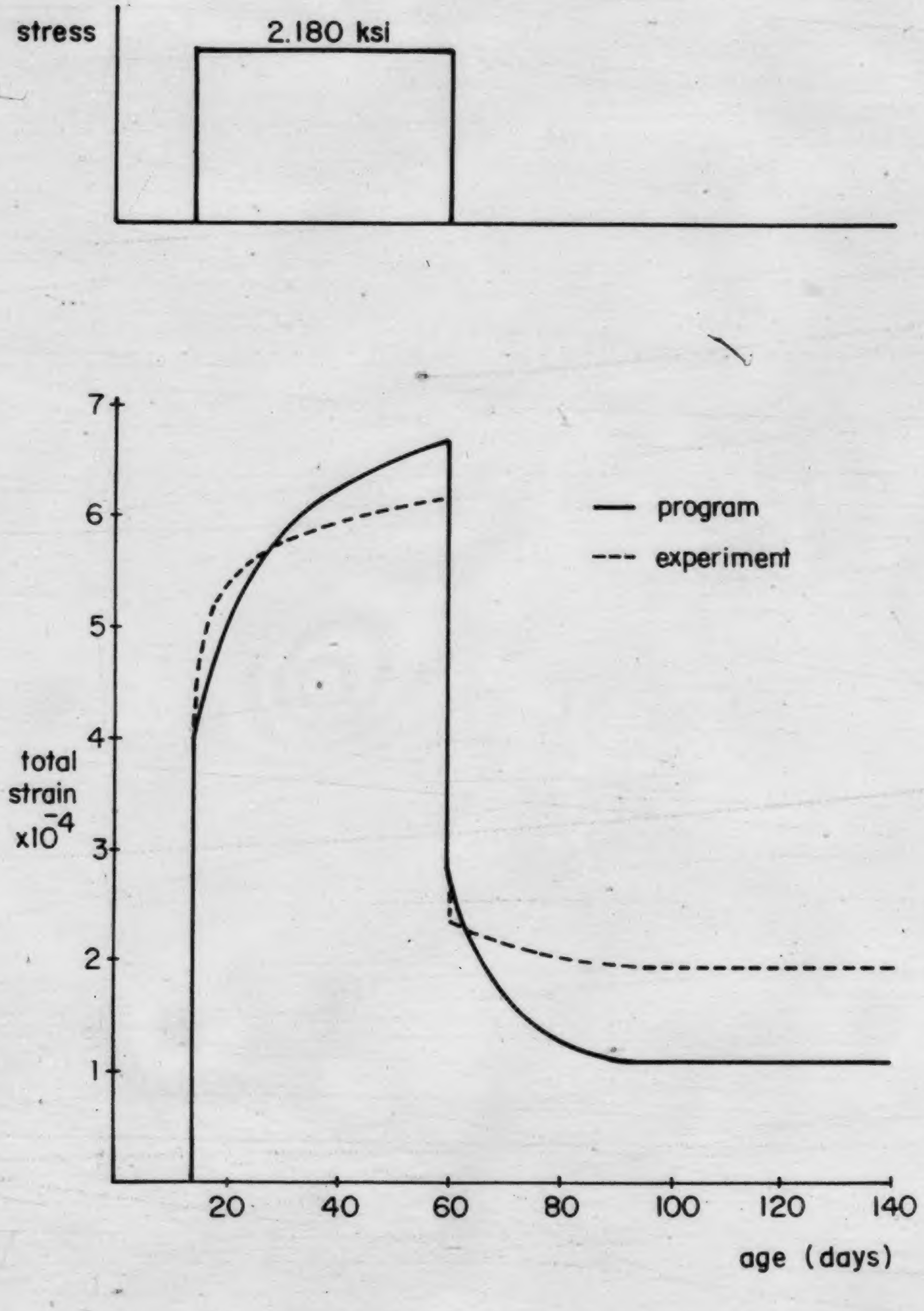

Figure 3.15 Creep test no. 1

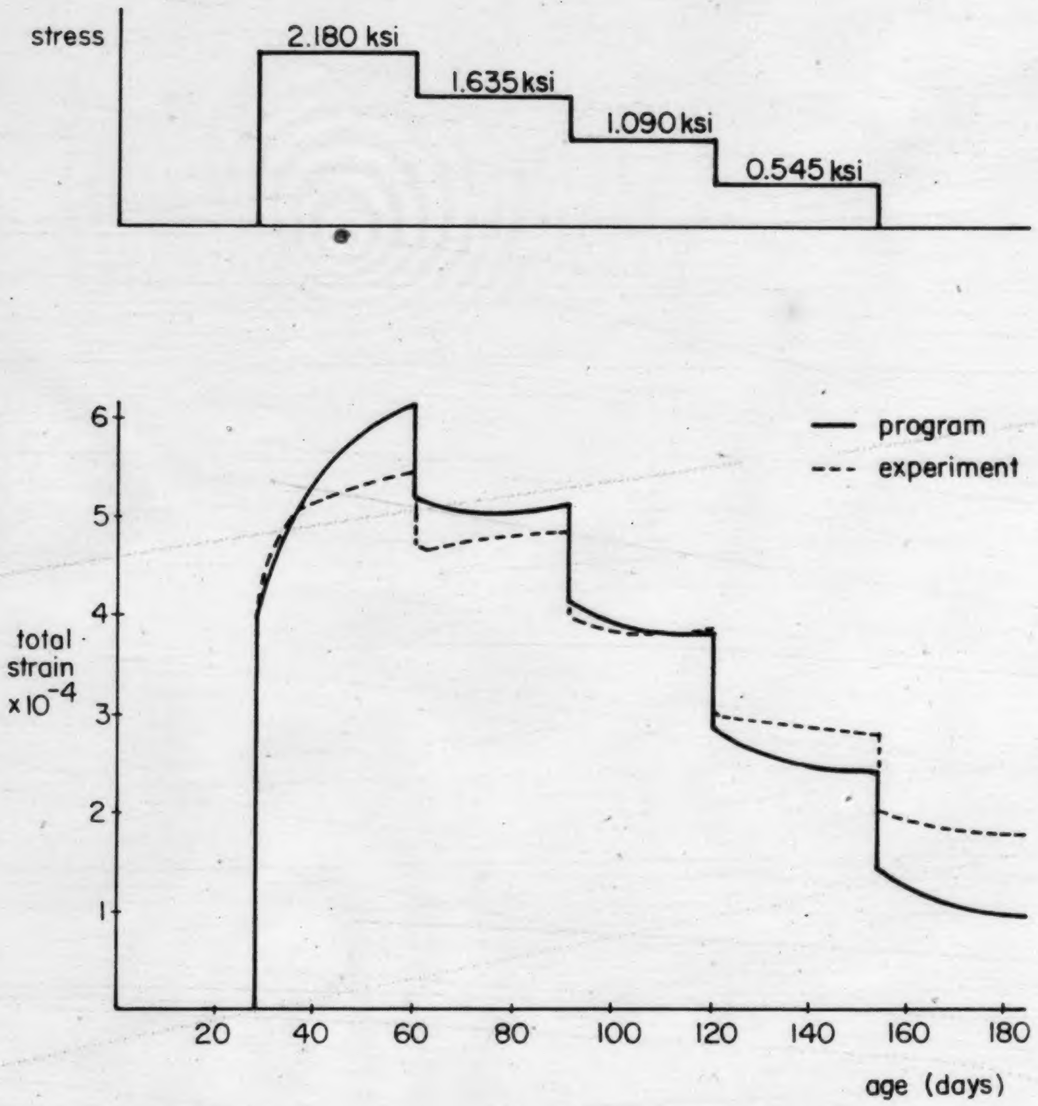

Figure 3.16 Creep test no. 2

creep recovery. Out of interest, the CEB 1978 model was also checked (but not plotted). This model underestimates both the amount of creep deformation and creep recovery. It should be noted that both models were found to be extremely sensitive to the determination of the creep factors.

The method of superposition without Dirichlet series was also used and compared to the method of superposition with Dirichlet series. The results were found to fall well within 5%. Sub-dividing the time-step for both methods had a neglible effect on the strains.

3.8.2 Example 2 - Precast segmental bridge

The purpose of this example is to show how the computer program TIMEDEP can be applied to the analysis of a precast concrete segmental bridge and to compare the results from the program with a previous analysis conducted by Tadros, Ghali, and Dilger (59,61).

The three span bridge is discretized as shown in Figure 3.17. There are 24 nodes, 23 elements, 3 sections, 17 prestressing tendons, and 29 construction stages. Cross section properties are given in Table 3.2 while prestressing tendon data is given in Table 3.3. The construction stages are defined in Table 3.4. Note that

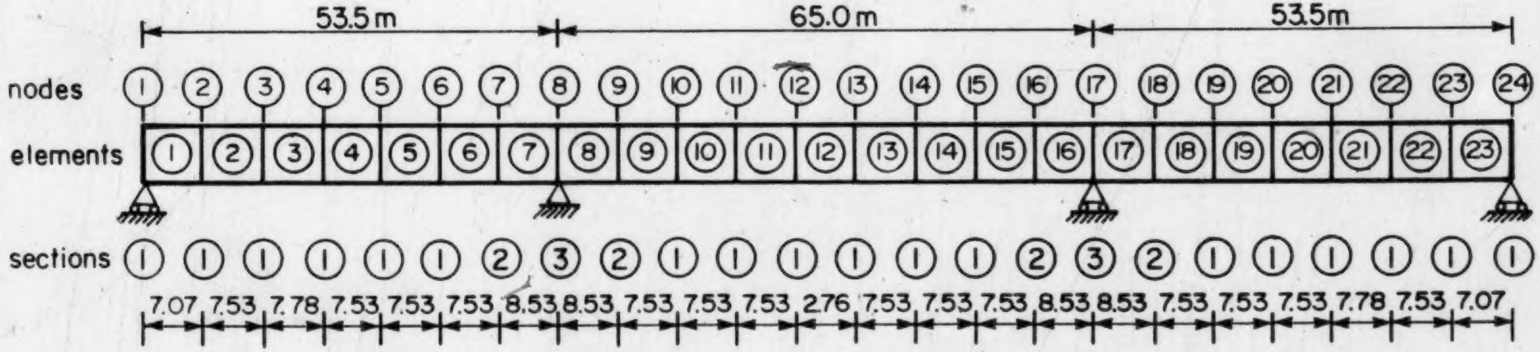
53.5 m
65.0 m
53.5 m
nodes
1 2 3 4 5 6 7 8 9 10 11 12 13 14 15 16 17 18 19 20 21 22 23 24
elements
1 2 3 4 5 6 7 8 9 10 11 12 13 14 15 16 17 18 19 20 21 22 23
sections
1 1 1 1 1 1 2 3 2 1 1 1 1 1 1 2 3 2 1 1 1 1 1 1
7.07 7.53 7.78 7.53 7.53 7.53 8.53 8.53 7.53 7.53 7.53 2.76 7.53 7.53 7.53 8.53 8.53 7.53 7.53 7.53 7.78 7.53 7.07

Figure 3.17 Precast concrete segmental bridge

Section	Area (m**2)	Inertia (m**4)	Centroid (m)	Depth (m)
1	10.035	10.058	0.974	2.80
2	11.055	12.027	1.093	2.80
3	12.075	14.942	1.340	2.80

Table 3.2 - Cross section properties

Tendon	Elmt-I	Elmt-J	Area (m**2)	Eccentricity (m)
1	7	8	0.012600	0.20
2	6	9	0.011970	0.20
3	5	10	0.011970	0.20
4	4	11	0.007980	0.20
5	16	17	0.012600	0.20
6	15	18	0.011970	0.20
7	14	19	0.011970	0.20
8	13	20	0.007980	0.20
9	3	4	0.005379	0.20
10	2	5	0.008150	2.65
11	1	6	0.007335	2.65
12	20	21	0.005379	2.65
13	19	22	0.008150	2.65
14	18	23	0.007335	2.65
15	11	13	0.005379	2.65
16	10	14	0.007335	2.65
17	9	15	0.003912	2.65

Table 3.3 - Prestressing tendon data

Stage	Phase	Date	Segments Assembled	Tendons Stressed	Support Nodes
1	1	2	7 , 8	1	8
2	1	5			
3	2	5	6 , 9	2	
4	2	8			
5	3	8	5 ,10	3	
6	3	11			
7	4	11	4 ,11	4	
8	4	15			
9	5	15	1,2,3	9,10,11	1,8
10	5	19			
11	6	19	16,17	5	17
12	6	22			
13	7	22	15,18	6	
14	7	25			
15	8	25	14,19	7	
16	8	28			
17	9	28	13,20	8	
18	9	32			
19	10	32	21,22,23	12,13,14	17,24
20	10	35			
21	11	35	12	15,16,17	17
22	11	45			
23	11	45	superimposed dead load = 45 kN/m		
24	11	60			
25	11	100			
26	11	200			
27	11	500			
28	11	1000			
29	11	2000			

Table 3.4 - Construction stages

straight tendons are used in this analysis whereas in the actual structure the tendons have a slight curvature in the immediate vicinity of the anchorages.

The concrete has a modulus of elasticity at 28 days of 35 GPa and a self weight force of 20.0 kN/m^3. The segments are cured for 3 days and erected at 28 days. The creep coefficient is 2.0 while the shrinkage coefficient is -0.0003. The computer program TIMEDEP uses the recommendations of ACI Committee 209 while Tadros, Ghali, and Dilger used the CEB 1970 recommendations.

The prestressing steel has a modulus of elasticity of 190 GPa and an ultimate tensile strength of 1.80 GPa. The tendons are stressed to 0.8 fpu and anchored at 0.7 fpu. The relaxation coefficient is 45.0 while the yield stress is 1.50 GPa. The nonprestressed steel has a modulus of elasticity of 200 GPa with an area of 0.022200 m^2 and an eccentricity of 1.0 m.

The geometry of the structure was selected to correspond to the example problem given by Tadros, Ghali, and Dilger so that the results could be compared directly. However, discrepancies between the results using TIMEDEP and the reported results were found. Subsequent correspondence with the authors revealed that the results presented in the paper did not conform entirely with the problem

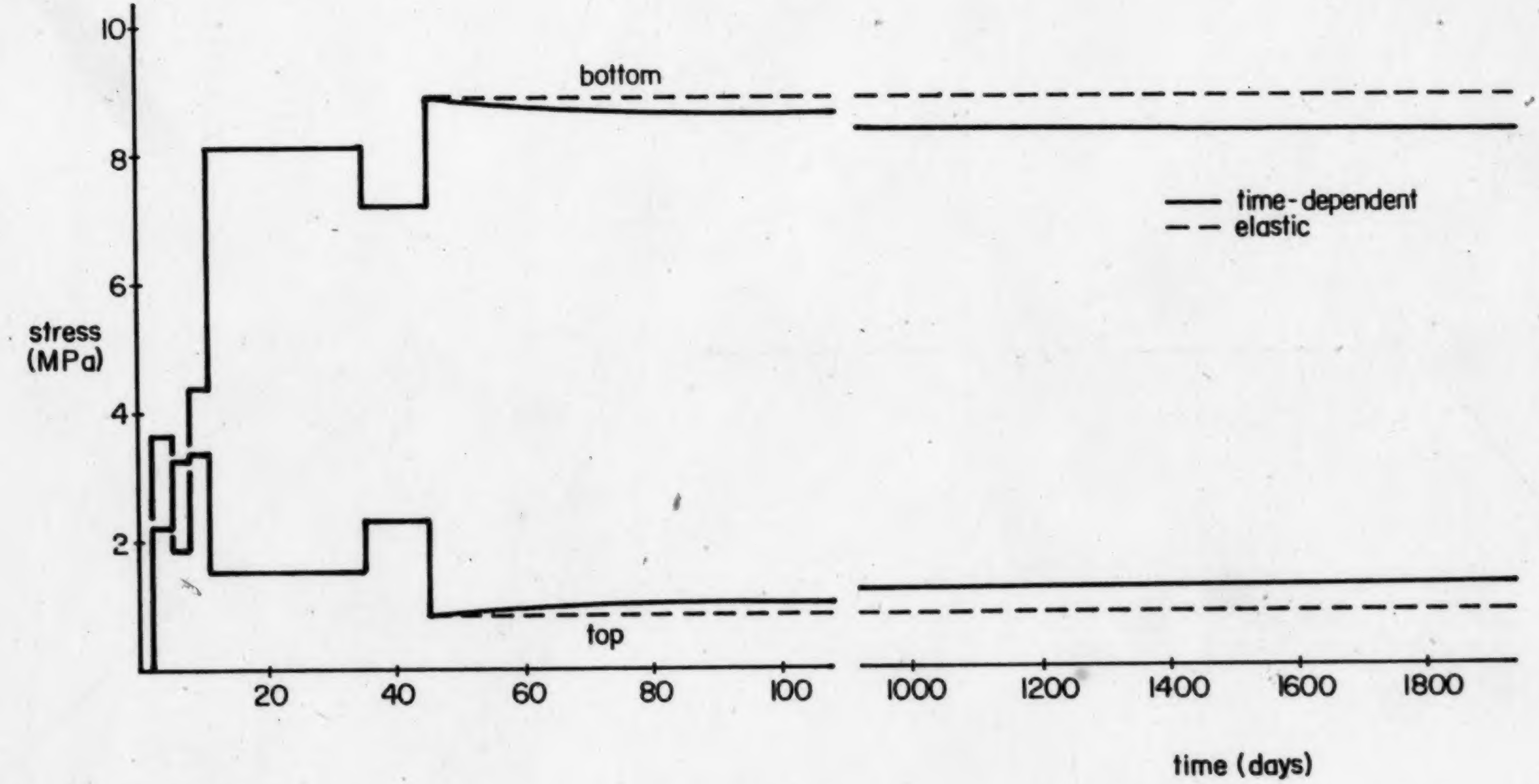

Figure 3.18 Stresses at left pier

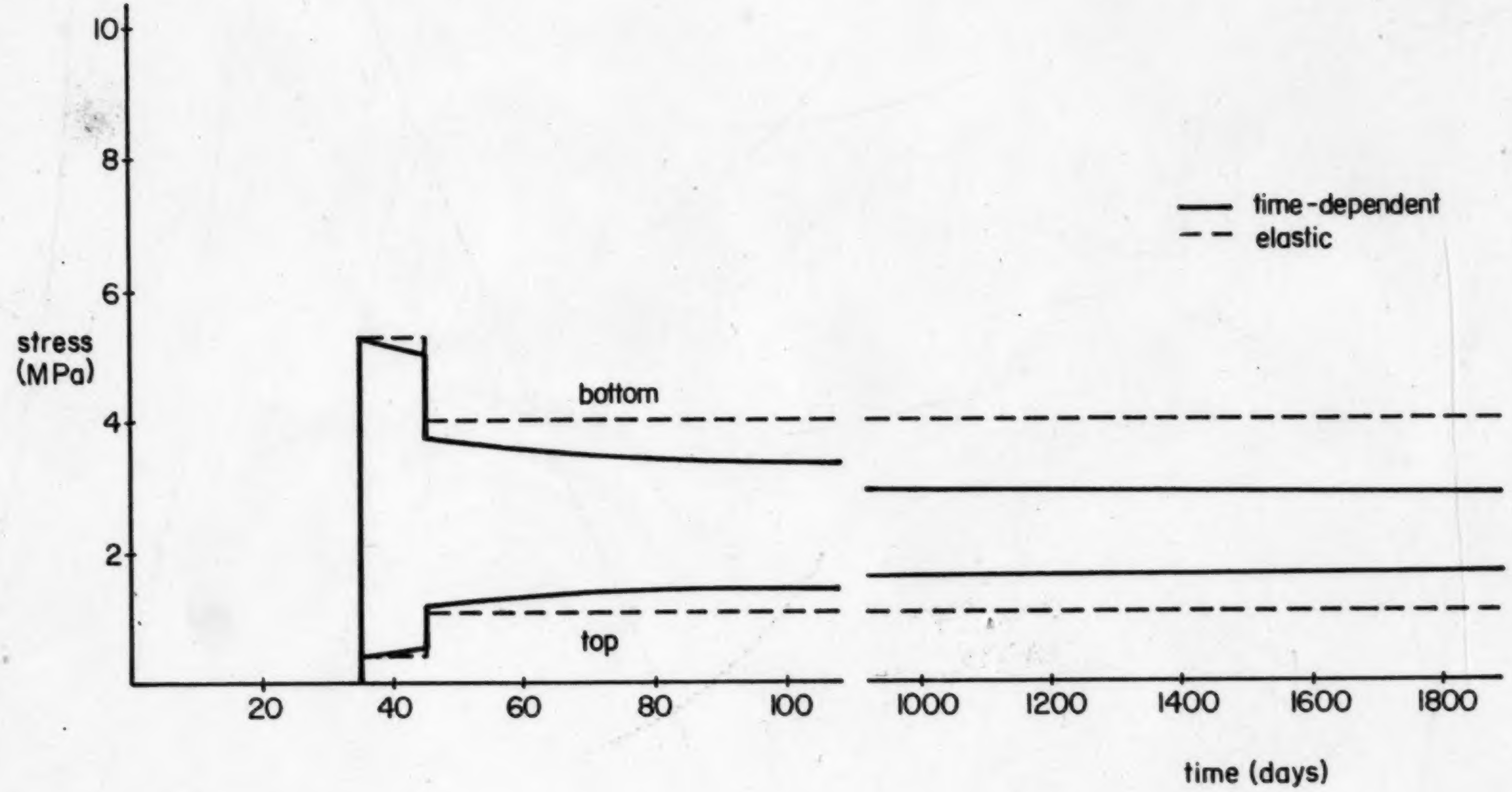

Figure 3.19 Stresses at midspan of interior span

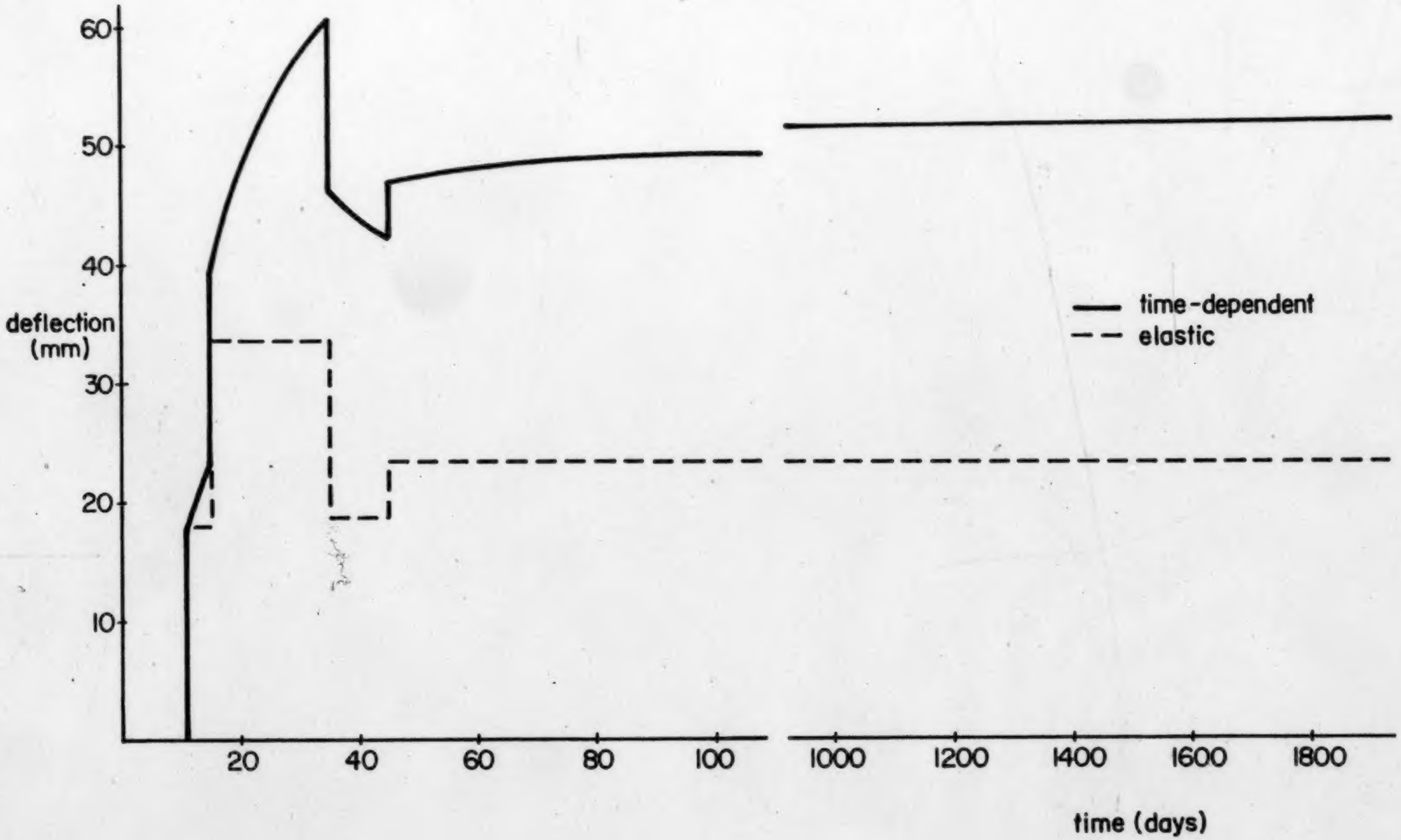

Figure 3.20 Deflections at midspan of interior span

described. For this reason, a direct comparison of the results is not meaningful.

Stresses at the pier (element 7 node 8) and at midspan (element 12 node 12) are plotted in Figures 3.18 and 3.19 respectively as a function of time. Furthermore, deflections at midspan (node 12) are plotted in Figure 3.20 as a function of time. Note that both the results with and without time-dependent effects have been plotted. The results by the method of superposition without Dirichlet series have been found to agree quite closely with the results by the method of superposition with Dirichlet series.

3.9 Conclusions

This chapter has developed the computer program TIMEDEP for the time-dependent analysis of segmental bridges. This program simplifies the task of the design engineer and provides him with access to more precise information. Numerical examples have illustrated the versatility and accuracy of the program.

4. THREE-DIMENSIONAL ANALYSIS

4.1 Introduction

This chapter discusses the three-dimensional analysis without time-dependent effects of box girder bridges in general and segmental bridges in particular. A three-dimensional analysis is necessary in order that reinforcing be proportioned for transverse flexure and stirrups be proportioned for longitudinal shear and torsion. In addition, an analysis of this type gives an idea as to the importance of shear lag effects. The loads considered must include self weight, superimposed dead load, truck loads, lane loads, temperature, and transverse prestressing.

The types of structural action occurring in a box girder bridge are reviewed, after which, a number of methods of analysis are summarized. Careful examination of the advantages and disadvantages of all the methods resulted in the folded plate method being chosen for this study. Since the method has been well documented in the past, only a summary as it pertains to the present work is included. A new efficient computer program is developed. The accuracy of any new features as well as the versatility of the program are illustrated by a series of numerical examples.

4.2 Types of structural action

4.2.1 Introduction

The types of structural action considered here are (1) longitudinal bending, (2) St Venant torsion, (3) warping torsion, (4) shear lag, and (5) local effects.

4.2.2 Longitudinal bending

Simple beam theory (where plane sections remain plane) gives the following well known expressions for the longitudinal normal stress (f) and shear stress (v).

$$f = \frac{Mx\ y}{Ix} \qquad (4.1), \qquad v = \frac{Vy\ Qx}{Ix\ t} \qquad (4.2)$$

Here Mx is the bending moment, Vy is the shear force, Ix is the moment of inertia, Qx is the statical moment, y is the distance from the neutral axis to the point under consideration, and t is the wall thickness.

4.2.3 St Venant torsion

The theory of St Venant torsion assumes that warping is unrestrained. Consequently, the longitudinal normal stress will be zero and only St Venant torsion shear stresses (vt) will exist. The following expression is given for thin-walled closed sections.

$$vt = \frac{Mt}{2\,A\,t} \qquad (4.3)$$

Here Mt is the torsional moment due to St Venant torsion, A is the area enclosed by the mid-line of the wall of the closed portion of the cross-section, and t is the wall thickness.

4.2.4 Warping torsion

Sections will, in general, be subjected to both St. Venant torsion and warping torsion. Warping torsion is that which is restrained by symmetry at midspan or the boundary conditions. Warping torsion creates longitudinal normal stresses and shear stresses.

4.2.5 Shear lag

The compression and tension forces are injected into the top and bottom flanges of a girder by longitudinal shear forces. Under the action of axial compression or tension and edge shear flows, the flanges distort in shear, and do not compress or extend the amount assumed by simple beam theory (i.e. plane sections remain plane). The amount of distortion depends on both the span/width ratio and on the distribution of the shear flow along the edge. Narrow flanges distort very little and their behaviour approximates that assumed by simple beam theory. Wider flanges distort considerably and much of the flange becomes ineffective. The effective width concept has been devised to allow simple beam theory to be used for all analyses.

The effects of shear lag have been found to be the greatest at a support but drop off quite rapidly away from the support (10). Fortunately, the shear lag effects of prestressing oppose those due to dead and live load to minimize the problem (10). Shear lag has not been found to be a serious problem for the span/width ratios of segmental bridges currently being constructed (10).

4.2.6 Local effects

Local effects due to concentrated loads may be evaluated by the influence surfaces of Pucher (109) and Homberg (107, 108) independent of the overall analysis. Statically equivalent forces and moments can then be applied at the webs to determine the effect of concentrated loads on the global behaviour.

4.2.7 Summary

An eccentric load on a box girder may be broken down into symmetric and anti-symmetric components causing bending and torsion respectively (Figure 4.1(a)). Under the bending

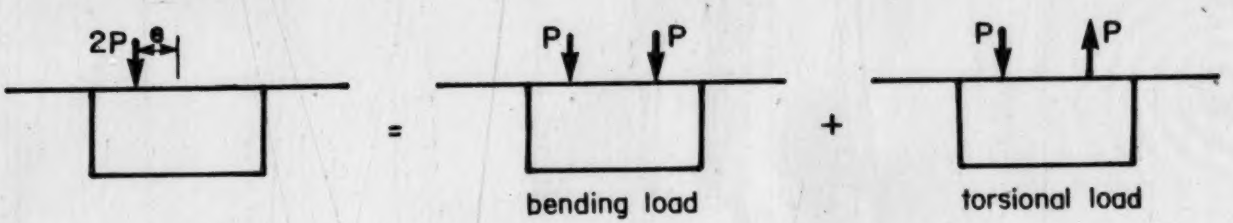
2P
e
=
P
P
+
P
P
bending load
torsional load

(a) loading components

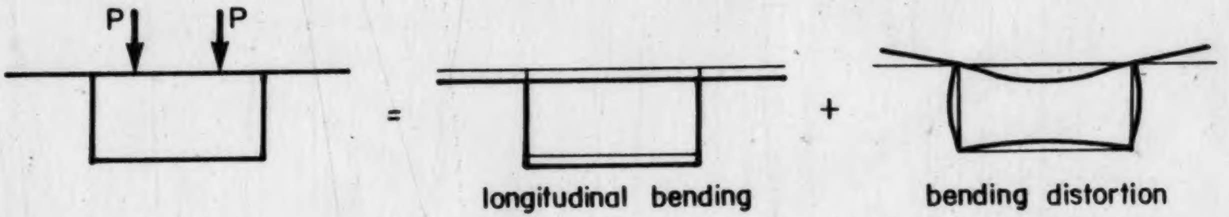
P
P
=
+
longitudinal bending
bending distortion

(b) bending load actions

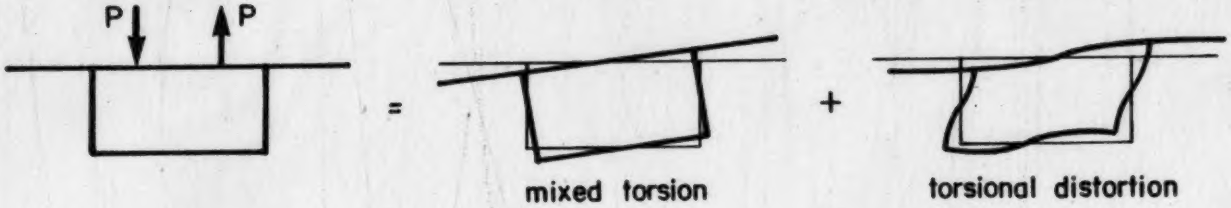
P
P
=
+
mixed torsion
torsional distortion

(c) torsional load actions

Figure 4.1 Decomposition of an eccentric load on a box girder

load, the section deflects rigidly (longitudinal bending) and deforms (bending distortion) (Figure 4.1(b)). Under the torsional load, the section rotates rigidly (mixed torsion) and deforms (torsional distortion) (Figure 4.1(c)).

Longitudinal bending occurs when the box girder is subjected to transverse loads whose resultant acts through the shear centre (Figure 4.2(a)). Assuming that plane sections remain plane under bending, bending normal stresses arise in the section (Figure 4.2(b)). From the equilibrium of a portion of the box girder, the bending shear stresses can be computed (Figure 4.2(c)). If the effects of shear lag are included, the bending normal stresses are as shown in Figure 4.2(d) rather than Figure 4.2(b). Bending distortion occurs due to the deformation of the cross section under bending loads (Figure 4.1(b)) and creates transverse bending stresses.

Consider the simply supported box girder loaded eccentrically at midspan (Figure 4.3(a) and 4.3(b)). Under uniform torsion (when warping and distortion are not restrained), only St Venant shear stresses are present. With warping prevented, warping torsion normal and shear stresses are introduced. In this example, symmetry at midspan prevents the cross section from warping, whereas warping is unrestrained at the supports. Therefore, the behaviour is predominantly that of St Venant torsion at the

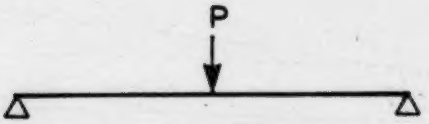

(a) beam elevation

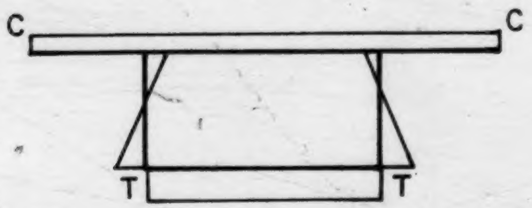

(b) bending normal stress distribution

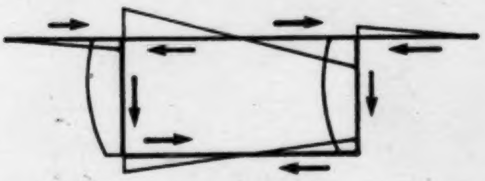

(c) bending shear stress distribution

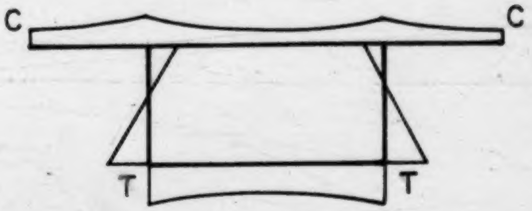

(d) bending normal stress distribution including shear lag effects

Figure 4.2 Stresses in a box girder due to bending

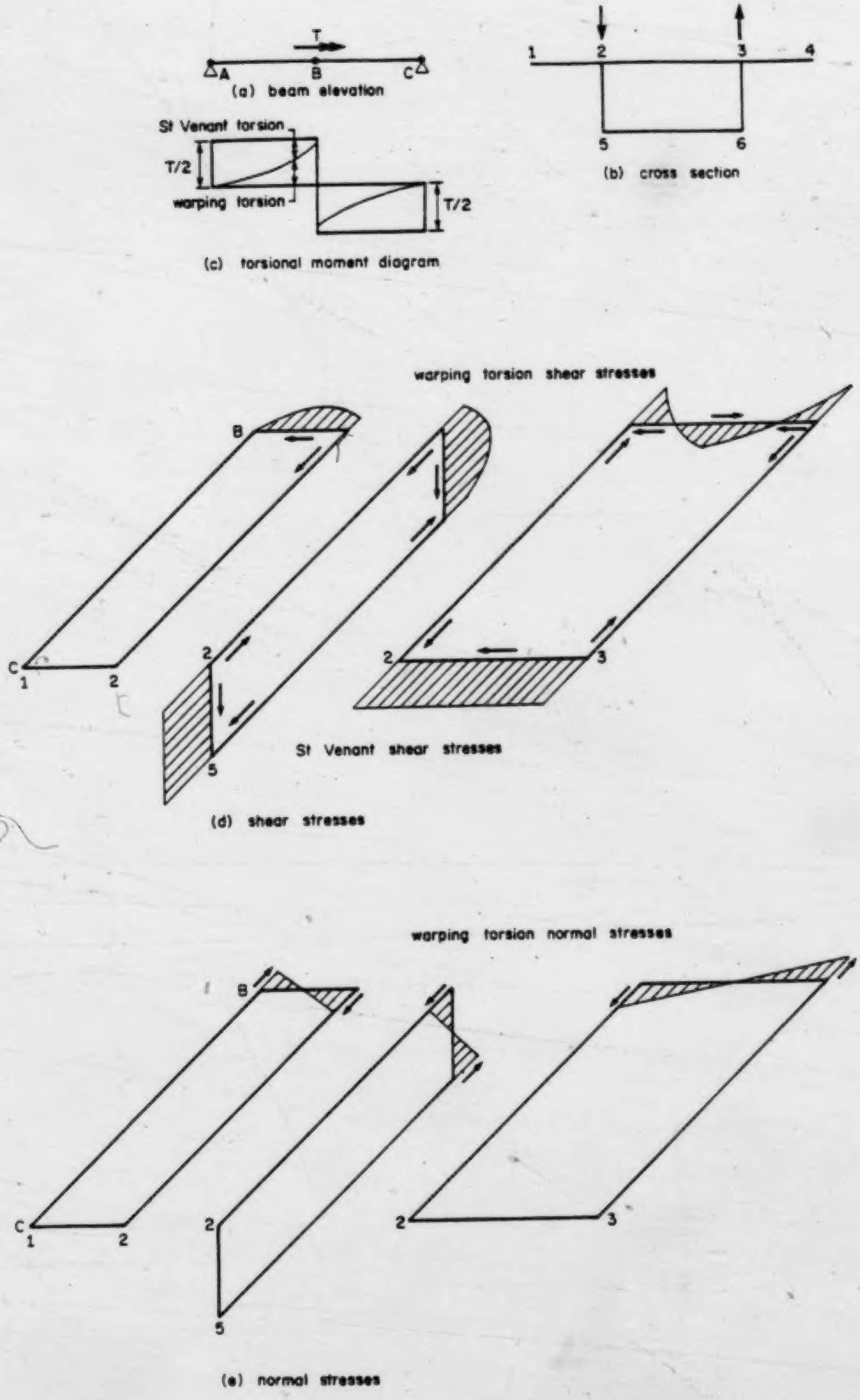
T
A
B
C
1
2
3
4
5
6
St Venant torsion
T/2
warping torsion
T/2
warping torsion shear stresses
B
C
1
2
2
5
2
3
St Venant shear stresses
warping torsion normal stresses
B
C
1
2
2
5
2
3

(a) beam elevation

(b) cross section

(c) torsional moment diagram

(d) shear stresses

(e) normal stresses

Figure 4.3 - Stresses in a box girder due to torsion

supports and warping torsion at midspan with a combination of the two in between (Figure 4.3(c)). The shear and normal stresses acting at the support and midspan for the cantilever, web, and interior plate are shown in Figure 4.3(d) and 4.3(e).

Let us take a brief look at warping torsion. Under a torsional load, the box girder (without the cantilevers) has a tendency to warp. In order to maintain compatibility with the warped box, the cantilevers tend to undergo a rigid body translation. The normal stresses shown on the box are necessary to bring the warped section back into the undeformed position if warping is restrained. The normal stresses shown on the cantilever are those required to rotate the restrained end back into the undeformed configuration. The shear stresses shown are a direct result of the normal stresses. Additional information on warping torsion of box girder bridges can be obtained from from Reference 196.

Torsional distortion occurs due to the deformation of the cross section under torsional loads (Figure 4.1(c)). This distortion results in transverse bending stresses.

4.3 Review of analysis methods

4.3.1 Introduction

Many methods have been developed for the analysis of box girder bridges. Cusens and Pama (95) and Hambly (96) discuss a number of these. Some of the more common ones will be mentioned here.

4.3.2 Hand methods

Maisel and Roll (90) have summarized and discussed at great length a number of methods which are suitable for hand calculation. Most of these methods, which are based on thin-wall beam theory, are labour intensive and strictly limited to single-celled sections, often with vertical webs. Consequently, they will not be considered in detail.

The beam on elastic foundation analogy is, however, worthy of mention. Wright, Abdel-Samad, and Robinson (93) and Tung (94) have investigated this procedure which considers the effects of transverse bending and distortional warping while ignoring torsional warping and shear lag. The procedure is based on the analogy between the distortional behaviour of a rectangular single cell box girder bridge and a beam on elastic foundation. Physically, the basis of the analogy is the fact that the transverse bending stiffnesses of the top and bottom slabs of the box girder provide a continuous elastic support for the webs, which therefore behave as beams on elastic foundation.

More recently, Maisel has proposed a method which he states is suitable for small capacity computers. He claims that this procedure can consider torsional and distortional effects as well as shear lag in multi-celled continous structures. Few details are available at this time (91,92).

4.3.3 Finite difference method

The bridge deck is divided into a grid of arbitrary mesh size and the deflections of the grid points or nodes are treated as the primary unknowns. The governing differential equation and boundary conditions are written in terms of the unknown nodal displacements, resulting in a large set of simultaneous equations. Once the nodal displacements have been found, the bending moments and shear forces can be found.

The accuracy of the solution is dependant on the fineness of the mesh. The method is generally quite versatile and has been applied to skewed and curved decks. The major problem with this technique is the application of the boundary conditions which can become quite cumbersome.

Westergaard (105) used this method, before the advent of more sophisticated techniques, to determine the stress distribution in bridge slabs subjected to concentrated loads.

4.3.4 Plane grid and space frame methods

The plane grid and space frame methods are based on the direct stiffness assembly procedure. The plane grid method is a two-dimensional discretization in the horizontal plane while the space frame method is a three-dimensional discretization. In the plane grid method or grillage method, the bridge deck is approximated by a gridwork of beam type elements connected to nodes possessing three degrees of freedom (a vertical displacement and two rotations). These elements are assigned axial, flexural, and torsional stiffnesses to approximate the two-way plate behaviour. In the space frame method, the bridge deck is approximated in much the same way, but here the nodes possess six degrees of freedom. Both of these methods require the solution of a large set of simultaneous equations.

The accuracy of the solution is dependant on the fineness of the mesh. The method is completely general and has been applied to a variety of skewed and curved decks with arbitrary boundary conditions. The major disadvantage with this scheme is the difficulty in assigning flexural and torsional properties to individual elements.

From this discussion, it might appear that the finite difference and plane grid methods are similar; they are not. The finite difference method is based on evaluating the governing differential equation and boundary equations at a series of nodes and solving for the nodal displacements. The finite element method (of which the plane grid method is a subset) is based on assembling element stiffnesses and load vectors into a global stiffness matrix and load vector and solving for the nodal displacements.

4.3.5 Folded plate method

The folded plate method is essentially the direct stiffness method coupled with a Fourier series harmonic analysis. The method allows two-dimensional folded plate type structures to be analysed with one-dimensional elements. The one-dimensional elements possess both plate bending and membrane stiffness and are connected to nodes having four degrees of freedom per node (three translations and a rotation). The method is based on the elasticity equations derived by Goldberg and Leve (101) and implemented in a direct stiffness solution by DeFries-Skene and Scordelis (37).

This is the most accurate of all methods presently available. It is often used as a basis of comparison for other less rigorous techniques, being denoted as the "exact" solution. Since one-dimensional elements are used to solve a two-dimensional problem, substantial savings in computational effort and computer storage are realized. As with any direct stiffness solution, the method results in a set of simultaneous equations. Although the equations must be solved for each Fourier series harmonic, the total effort is still much less than for a two-dimensional analysis. The method is limited to structures being simply supported at the extreme ends. Furthermore, it is limited to straight prismatic structures having isotropic plate properties. The folded plate method has been combined with the force method, allowing continuous structures, having intermediate diaphragms and supports, to be considered.

Scordelis has developed a series of programs for the analysis of box girder bridges using the folded plate method. MULTPL (25) considers single span structures while MUPDI (25) considers structures simply supported at the extreme ends, but having intermediate diaphragms and supports. MUPDI3 (34) is essentially the same program extended further to consider a larger number of diaphragms and supports.

4.3.6 Finite element method

The finite element method is based on the direct stiffness assemblage of two-dimensional triangular or quadrilateral elements connected at nodes possessing six degrees of freedom. It results in a large set of simultaneous equations which requires a large amount of computer time and storage to solve. Stresses found by the finite element method do not automatically satisfy equilibrium; however, it is approached as the mesh size is refined. The finite element method is usually reserved for those problems which cannot be handled by other methods.

This is the most versatile of all the methods presently available. It can handle sections having variable depth and width as well as plates having variable thickness in both the transverse and longitudinal directions. Material properties, boundary conditions, and loading are completely general. Skewed, curved, and bifurcated decks can easily be handled.

Scordelis has developed a series of programs for the finite element analysis of box girder bridges. FINPLA (26) analyses structures of constant depth and right planform while CELL (31) considers structures of constant depth and arbitrary planform. FINPLA2 (33) is further extended to handle nonprismatic box girders having variable depth and width.

4.3.7 Finite strip method

This hybrid method combines the harmonic analysis of the folded plate method in the longitudinal direction with the shape functions of the finite element method in the transverse direction. The net result is a method which is more versatile than the folded plate method and much cheaper to use than the finite element method. The method was originally proposed by Cheung (39).

Box girder bridges having orthotropic plate properties (including stiffening elements) can be handled. Structures which have a circular curve in plan can also be considered. The procedure has been applied to stability and dynamics problems. The method still has some of the limitations of the folded plate method; only prismatic sections being simply supported at the extreme ends can be considered. In addition, the method is still approximate in the context of the finite element method.

Scordelis has again developed a series of programs for the analysis of box girder bridges using the finite strip method. MULSTR (28) analyses prismatic structures having orthotropic material properties. CURSTR (30) considers structures curved in plan while CURDI (36) is essentially the same program extended further to consider a greater number of diaphragms and supports. A similar set of programs have been developed by Loo and Cusens. Cheung (97) and Loo and Cusens (98) have written texts on the finite strip method.

4.3.8 Conclusions

After careful examination of the advantages and disadvantages of all the procedures discussed, the folded plate method has been chosen for the remainder of this study. The decision is based on the combined simplicity and accuracy of the method. The folded plate method is chosen over the finite strip method since it is more accurate for coarse discretizations. In addition, the folded plate method is chosen over the finite element method since the preparation of input and interpretation of output is greatly reduced. In fact, using a folded plate program is no more difficult than running a plane frame program. The only negative feature in using the folded plate method is that sections having variable depth and variable bottom slab thickness can only be handled in an approximate way. This will be discussed in detail later.

4.4 Folded plate method

4.4.1 Introduction

The folded plate method is essentially the coupling of the direct stiffness method with a Fourier Series harmonic solution in a manner such that two-dimensional folded plate type structures may be analysed with one-dimensional elements. The use of one-dimensional elements based on the theory of elasticity represents a significant saving in computer time and storage and gives an "exact" solution.

The method is limited to straight prismatic structures which are simply supported at the extreme ends and have isotropic material properties. The end diaphragms are assumed to be infinitely rigid parallel to their own plane, but perfectly flexible perpendicular to their plane. Classical thin plate theory is used to determine the stresses and displacements due to normal loads while the elasticity equations defining the plane stress problem are used for the in-plane loads.

Goldberg and Leve (101) derived the elasticity equations which were implemented by DeFries-Skene and Scordelis (37) into a direct stiffness solution for folded plate roofs. Chu and Pinjarkar (103) extended the procedure to consider cellular structures while Lo (102) used the force method to consider both intermediate diaphragms and supports. Chu and Dudnik (104) developed fixed end moments due to uniform and concentrated loads. Since the development of the method has been well documented, it will only be briefly summarized in the following sections.

4.4.2 Coordinate systems

As with any direct stiffness assemblage procedure, two right handed Cartesian coordinate systems are defined.

(1) Global system (X,Y,Z) - An arbitrary point is chosen as the origin so that the structure spans in the X direction and its cross-section lies in the Y-Z plane. Nodal loads (Rx,Ry,Rz) and displacements (rx,ry,rz) are expressed in the global system (see Figure 4.4(a)).

(2) Local system (x,y,z) - Each element has a local coordinate system whose y axis is directed along the centroidal axis of the element from node I to node J. The global X axis and local x axis have the same direction. The local x and y directions define the direction of the local z axis. Element forces (M,Q,P,T) and deformations (θ,w,v,u) are expressed in the local system (see Figure 4.4(c)).

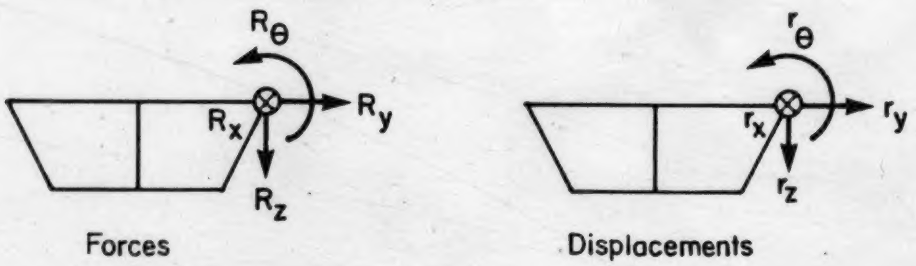
R_θ
R_x
R_y
R_z
Forces
r_θ
r_x
r_y
r_z
Displacements

(a) positive node forces and displacements in the global coordinate system

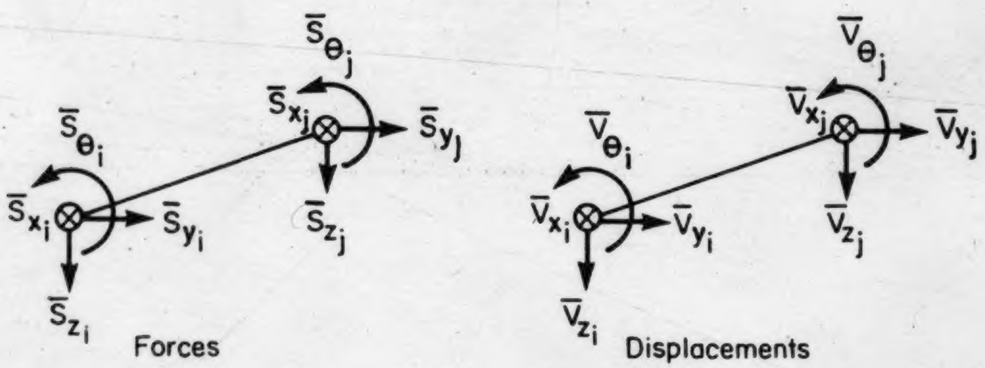
$\bar{S}_{\theta_j}$
$\bar{S}_{x_j}$
$\bar{S}_{y_j}$
$\bar{S}_{z_j}$
$\bar{S}_{\theta_i}$
$\bar{S}_{x_i}$
$\bar{S}_{y_i}$
$\bar{S}_{z_i}$
Forces
$\bar{V}_{\theta_j}$
$\bar{V}_{x_j}$
$\bar{V}_{y_j}$
$\bar{V}_{z_j}$
$\bar{V}_{\theta_i}$
$\bar{V}_{x_i}$
$\bar{V}_{y_i}$
$\bar{V}_{z_i}$
Displacements

(b) positive element forces and displacements in the global coordinate system

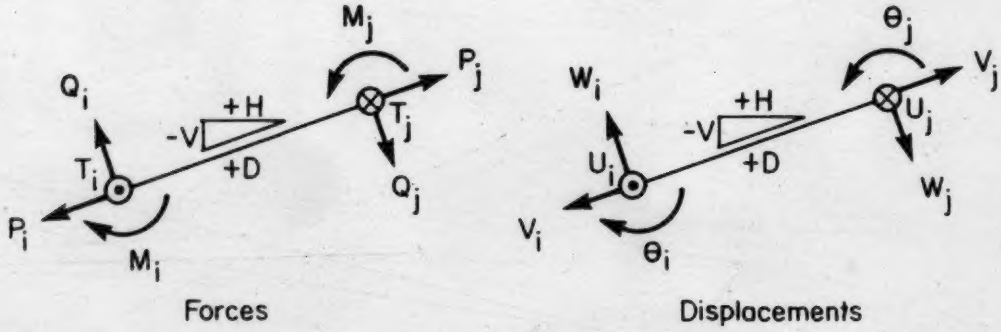
M_j
P_j
Q_i
+H
-V
T_j
T_i
+D
Q_j
P_i
M_i
Forces
θ_j
V_j
W_i
+H
-V
U_j
U_i
+D
W_j
V_i
θ_i
Displacements

(c) positive element forces and displacements in the local coordinate system

Figure 4.4 Node and element forces and displacements

The element forces and deformations are defined as follows:

(a) transverse bending moment M per unit length and rotation θ

(b) transverse normal shear force Q per unit length and displacement w

(c) transverse membrane force P per unit length and displacement v

(d) membrane shear force T per unit length and displacement u

Note that for the remainder of this discussion, H is the horizontal projection of the plate, V is the vertical projection of the plate, D is the width of the plate, B is the thickness of the plate, and L is the length of the plate (see Figure 4.4(c)).

4.4.3 Direct stiffness method

The direct stiffness method consists of the following sequence of matrix operations:

(1) Form element stiffness matrix in local coordinate system

$$[s] = [k]\,[v] \tag{4.4}$$

(2) Form element transformation matrix

$$[v] = [a]\,[\bar{v}] \tag{4.5a}$$

$$[\bar{s}] = [a]^{T}\,[s] \tag{4.5b}$$

(3) Form element stiffness matrix in global coordinate system

$$[s] = [k]\,[a]\,[\bar{v}] = [b]\,[\bar{v}] \tag{4.6a}$$

$$[\bar{s}] = [a]^{T}\,[k]\,[a]\,[\bar{v}] \tag{4.6b}$$

$$[\bar{s}] = [\bar{k}]\,[\bar{v}] \tag{4.6c}$$

(4) Add element stiffness matrix to structure stiffness matrix keeping in mind that a banded equation solver is being used. Form load vector using Fourier series.

$$[R] = [K]\,[r] \tag{4.7}$$

(5) Solve for node displacements

$$[r] = [K]^{-1}\,[R] \tag{4.8}$$

(6) Find element forces

$$[s] = [b]\,[\bar{v}] \quad \text{where} \quad [\bar{v}] = [r] \tag{4.9}$$

4.4.4 Element stiffness matrix

The element stiffness matrix in the local coordinate system has the following form

$$\begin{bmatrix} Mi \\ Mj \\ Qi \\ Qj \\ Pi \\ Pj \\ Ti \\ Tj \end{bmatrix} = \begin{bmatrix} K11 & K12 & K13 & K14 & 0 & 0 & 0 & 0 \\ K21 & K22 & K23 & K24 & 0 & 0 & 0 & 0 \\ K31 & K32 & K33 & K34 & 0 & 0 & 0 & 0 \\ K41 & K42 & K43 & K44 & 0 & 0 & 0 & 0 \\ 0 & 0 & 0 & 0 & K55 & K56 & K57 & K58 \\ 0 & 0 & 0 & 0 & K65 & K66 & K67 & K68 \\ 0 & 0 & 0 & 0 & K75 & K76 & K77 & K78 \\ 0 & 0 & 0 & 0 & K85 & K86 & K87 & K88 \end{bmatrix} \begin{bmatrix} ei \\ ej \\ wi \\ wj \\ vi \\ vj \\ ui \\ uj \end{bmatrix} \tag{4.10}$$

Expressions for the nonzero coefficients will be given in the next section. The plate bending problem is uncoupled from the in-plane or membrane problem as is illustrated by the large block of zero coefficients on the off-diagonal.

The element displacement transformation matrix is given as follows

$$\begin{bmatrix} ei \\ ej \\ wi \\ wj \\ vi \\ vj \\ ui \\ uj \end{bmatrix} = \begin{bmatrix} 0 & 0 & -1 & 0 & 0 & 0 & 0 & 0 \\ 0 & 0 & 0 & 0 & 0 & 0 & +1 & 0 \\ -V/D & -H/D & 0 & 0 & 0 & 0 & 0 & 0 \\ 0 & 0 & 0 & 0 & +V/D & +H/D & 0 & 0 \\ -H/D & +V/D & 0 & 0 & 0 & 0 & 0 & 0 \\ 0 & 0 & 0 & 0 & +H/D & -V/D & 0 & 0 \\ 0 & 0 & 0 & -1 & 0 & 0 & 0 & 0 \\ 0 & 0 & 0 & 0 & 0 & 0 & 0 & +1 \end{bmatrix} \begin{bmatrix} \nabla yi \\ \nabla zi \\ \nabla ei \\ \nabla xi \\ \nabla yj \\ \nabla zj \\ \nabla ej \\ \nabla xj \end{bmatrix} \tag{4.11}$$

The element stiffness matrix in the global coordinate system is obtained by multiplying $[a]^T[K][a]$ as discussed previously.

4.4.5 Stiffness influence coefficients

Two sets of stiffness influence coefficients are given in this section. The first set (Figure 4.5) are the folded plate coefficients based on the theory of elasticity as given by Goldberg and Leve (101). The second set (Figure 4.6) are for a plane frame having the cross-section of the structure and a unit length. It should be noted that the folded plate coefficients must be redetermined for each Fourier series harmonic in the analysis, since they are a function of the harmonic number n. The plane frame coefficients are included so that the results of the folded plate analysis can be compared to those given by the plane frame analysis. Note that the plane frame analysis requires the specification of some additional boundary conditions.

4.4.6 Element load vectors

Six different element load vectors are considered in this study. They are self weight, surcharge, truck load, lane load, temperature, and prestressing. The transverse distribution of each of these loads is shown in Figure 4.7. All loads are distributed uniformly in the longitudinal

Plate stiffness coefficients:

$$K11 = K22 = +D1\,w\left[\frac{\cosh a}{a\,\mathrm{sech}\,a + \sinh a} - \frac{\sinh a}{a\,\mathrm{csch}\,a - \cosh a}\right]$$

$$K12 = +D1\,w\left[\frac{\cosh a}{a\,\mathrm{sech}\,a + \sinh a} + \frac{\sinh a}{a\,\mathrm{csch}\,a - \cosh a}\right]$$

$$K13 = -K24 = -D1\,w^2\left[\frac{\cosh a}{a\,\mathrm{csch}\,a + \cosh a} - \frac{\sinh a}{a\,\mathrm{sech}\,a - \sinh a} - (1-v)\right]$$

$$K14 = -K23 = +D1\,w^2\left[\frac{\cosh a}{a\,\mathrm{csch}\,a + \cosh a} + \frac{\sinh a}{a\,\mathrm{sech}\,a - \sinh a}\right]$$

$$K33 = K44 = +D1\,w^3\left[\frac{\sinh a}{a\,\mathrm{csch}\,a + \cosh a} - \frac{\cosh a}{a\,\mathrm{sech}\,a - \sinh a}\right]$$

$$K34 = -D1\,w^3\left[\frac{\sinh a}{a\,\mathrm{csch}\,a + \cosh a} + \frac{\cosh a}{a\,\mathrm{sech}\,a - \sinh a}\right]$$

Membrane stiffness coefficients:

$$K55 = K66 = +D2\,w\left[\frac{\sinh a}{a\,\mathrm{csch}\,a + b\cosh a} - \frac{\cosh a}{a\,\mathrm{sech}\,a - b\sinh a}\right]$$

$$K56 = -D2\,w\left[\frac{\sinh a}{a\,\mathrm{csch}\,a + b\cosh a} + \frac{\cosh a}{a\,\mathrm{sech}\,a - b\sinh a}\right]$$

$$K57 = -K68 = -D2\,w\left[\frac{\sinh a}{a\,\mathrm{sech}\,a + b\sinh a} - \frac{\cosh a}{a\,\mathrm{csch}\,a - b\cosh a} - (1+v)\right]$$

$$K58 = -K67 = -D2\,w\left[\frac{\sinh a}{a\,\mathrm{sech}\,a + b\sinh a} + \frac{\cosh a}{a\,\mathrm{csch}\,a - b\cosh a}\right]$$

$$K77 = K88 = +D2\,w\left[\frac{\cosh a}{a\,\mathrm{sech}\,a + b\sinh a} - \frac{\sinh a}{a\,\mathrm{csch}\,a - b\cosh a}\right]$$

$$K78 = +D2\,w\left[\frac{\cosh a}{a\,\mathrm{sech}\,a + b\sinh a} + \frac{\sinh a}{a\,\mathrm{csch}\,a - b\cosh a}\right]$$

where $D1 = \dfrac{E\,B^3}{12(1-v^2)}$, $D2 = \dfrac{E\,B}{(1+v)^2}$

and $w = \dfrac{n\,\pi}{L}$, $a = w\,\dfrac{D}{2}$, $b = \dfrac{3-v}{1+v}$

Figure 4.5 - Stiffness influence coefficients using folded plate theory

Plate stiffness coefficients:

$$K11 = K22 = +4\frac{EI}{D}$$

$$K12 = -2\frac{EI}{D}$$

$$K13 = -K24 = -6\frac{EI}{D^2}$$

$$K14 = -K23 = -6\frac{EI}{D^2}$$

$$K33 = K44 = +12\frac{EI}{D^3}$$

$$K34 = \; = +12\frac{EI}{D^3}$$

Membrane stiffness coefficients:

$$K55 = K66 = +\frac{EA}{D}$$

$$K56 = +\frac{EA}{D}$$

$$K57 = -K68 = 0$$

$$K58 = -K67 = 0$$

$$K77 = K88 = 0$$

$$K78 = 0$$

Figure 4.6 - Stiffness influence coefficients using plane frame theory

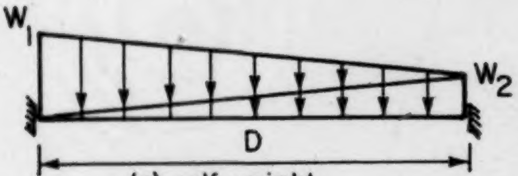

(a) self weight

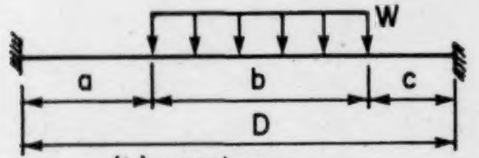

(b) surcharge

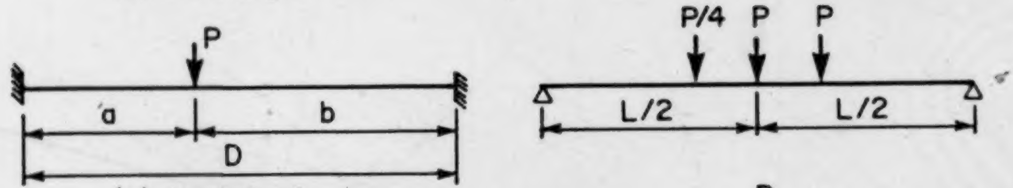
P
a
b
D
P/4
P
P
L/2
L/2

(c) truck load

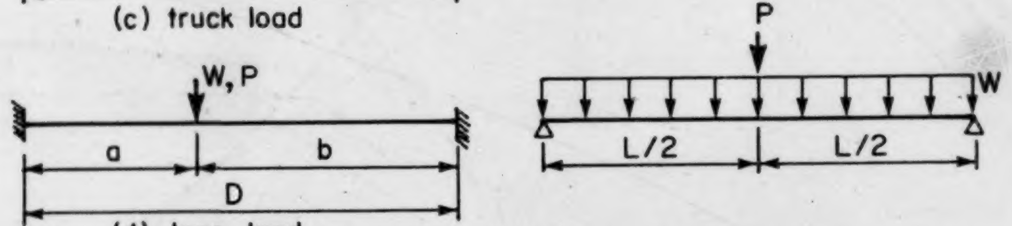
W, P
a
b
D
P
W
L/2
L/2

(d) lane load

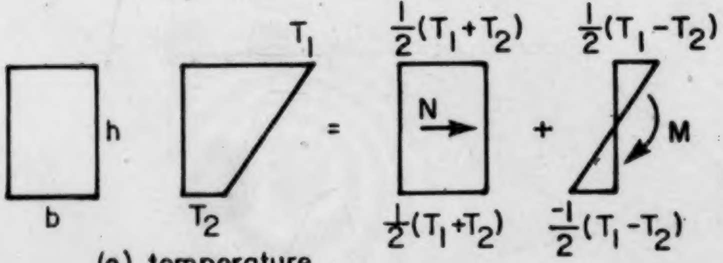
h
b
T1
T2
=
+
N
M
1/2(T1+T2)
1/2(T1+T2)
1/2(T1-T2)
-1/2(T1-T2)

$N = E\alpha(T_1+T_2)\frac{bh}{2}$

$M = E\alpha(T_1-T_2)\frac{bh^2}{12}$

(e) temperature

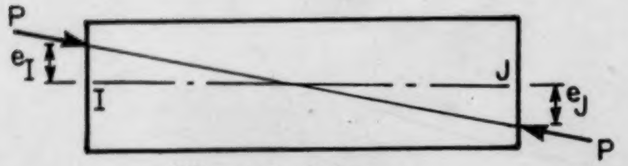

$N = P\cos\theta$

$V = P\sin\theta$

$M = -Pe$

(f) prestressing

Figure 4.7 Element load vectors

direction with the exception of truck loads and lane loads which are distributed as shown. The analysis procedure is to represent the loading as fixed end forces in the transverse direction and as Fourier series in the longitudinal direction. The truck load is an exception to this and will be considered separately.

The fixed end forces are found in the local coordinate system and transformed into the global coordinate system, after which they are added to the structure load vector. When the displacements have been found, the fixed end forces are subtracted from the forces calculated to give the actual forces. The standard fixed end forces for a beam are used rather than those for a plate. Experience has shown that for a uniformly distributed load, the solution is more sensitive to variations in Poisson's ratio than to whether beam theory or plate theory is used to find the fixed end moments.

The fixed end forces are expressed as a Fourier series in the longitudinal direction. The structure is analysed for the loading components of each harmonic separately and combined through the principle of superposition.

The Fourier series expressions for some common loading distributions in the longitudinal direction are

(1) uniform load of intensity po

$$p(x) = \sum_{n=1,3,5,\ldots} \frac{4}{n\pi} po \sin \frac{n\pi x}{L} \qquad (4.14)$$

(2) concentrated load po at midspan

$$p(x) = \sum_{n=1,3,5,\ldots} \frac{2}{L} po (-1)^{\frac{n+3}{2}} \sin \frac{n\pi x}{L} \qquad (4.15)$$

Although an infinite number of terms are theoretically required for convergence, experience has shown that 9 terms are sufficient for uniform loads while 99 terms are required for concentrated loads. It should be pointed out that the 99 terms required for concentrated loads are required near the point of application of the load, and that some distance away from the load only a few terms are necessary. Node displacements will, in general, converge much faster than element forces.

Hambly (96) points out that significant errors are obtained near discontinuities. An example of a discontinuity is the shear force on either side of a concentrated load. The shear force oscillates violently in the vicinity of the concentrated load. Increasing the number of harmonics moves the oscillation closer to the discontinuity, but does not eliminate it. Consequently, it is recommended that results be ignored within two or three wavelengths of the highest harmonic.

As mentioned earlier, the truck load is an exception to the above discussion. For this case, the equations of Chu and Dudnik (104) shown in Figure 4.8 are used. The derivation of these equations is given by Newmark (106).

4.4.7 Element forces

The element forces are evaluated by multiplying [k][a][v] as discussed previously. However, an additional term must be included since the Kirchhoff boundary shear force Vy must be evaluated along the plate edges rather than Qy and Myx.

$$Vy = Qy + \frac{dMyx}{dx} \qquad (4.12)$$

Also, the relationship $\epsilon xx = 1/E\ (\sigma xx - \nu\, \sigma yy)$ can be used to find the longitudinal membrane force (Nxx) per unit length.

$$Nxx = E\ B\ \frac{du}{dx} + \nu\ P \qquad (4.13)$$

The longitudinal membrane force gives an indication as to the severity of shear lag effects.

$$Mi = + \frac{2\ P}{n\ \pi\ A}\ (y1 \sinh a \sinh y2 - a\ y2 \sinh y1) \sinh x1$$

$$Mj = + \frac{2\ P}{n\ \pi\ A}\ (y2 \sinh a \sinh y1 - a\ y1 \sinh y2) \sinh x1$$

$$Qi = - \frac{2\ P}{L\ A}\ (U1 \sinh a - a\ U2) \sinh x1$$

$$Qj = + \frac{2\ P}{L\ A}\ (U2 \sinh a - a\ U1) \sinh x1$$

where

$$a = \frac{n\ \pi\ D}{L}$$

$$y1 = \frac{n\ \pi\ Y1}{L}$$

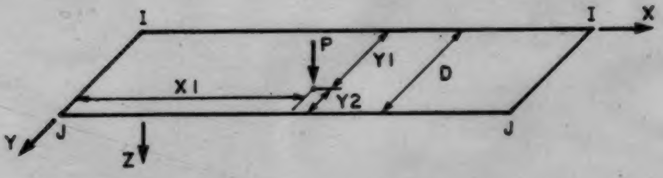

$$y2 = \frac{n\ \pi\ (D-Y1)}{L}$$

$$x1 = \frac{n\ \pi\ X1}{L}$$

$$A = \sinh^2 a - a^2$$

$$U1 = \sinh y2 + y1 \cosh y2$$

$$U2 = \sinh y1 + y2 \cosh y1$$

Figure 4.8 - Fixed end forces for concentrated loads

4.5 Computer program

Although a number of folded plate computer programs are currently available (MULTPL, MUPDI, MUPDI3), the decision was made to develop a new program rather than to modify an existing program. The basis of this decision was that substantial reorganization of an existing program would be required to render it suitable for the type of analyses envisioned.

Before any programming could be undertaken, the philosophy of the program had to be developed. The purpose of the program was to simplify the task of the design engineer and provide him with access to more precise information. The program had to be able to perform a transverse analysis for flexure as well as a longitudinal analysis for shear and torsion. The analysis had to include self weight, superimposed dead load, truck loads, lane loads, temperature, and transverse prestressing. Two of these loading cases in particular were quite time consuming by hand. The standard procedure for calculating the effects of truck loads was to plot the loads on the influence surfaces of Pucher (109) or Homberg (107,108). This was a slow operation at best. The normal method of considering prestressing was to calculate the equivalent loads or find the secondary moment using the moment-area theorem. Again, this was a slow procedure. Temperature is an important consideration, which was all but ignored in the past. Since plane frame theory was commonly used for the transverse flexural analysis, it would be interesting to include a plane frame analysis as a basis of comparison for the more precise folded plate analysis. It was also desirable to combine these load cases and summarize them in such a manner that the enveloping design values could easily be determined.

On this basis, the program BOXGIRD was developed. This program was written in the FORTRAN IV language for the Amdahl 5860 computer at the University of Alberta. Generally accepted programming procedures have been used so that the program can easily be converted to operate on other systems. Dynamic storage allocation is not included in the present version of the program but could easily be implemented. The program is based on the theory previously outlined.

The program is quite versatile and can be applied to a wide range of structures. Figure 4.9 shows some of the applications. The program can, of course, be used for single box girders, multiple box girders, and multicell box girders, as long as they are simply supported. In addition, single or multiple folded plate and cylindrical shell roofs can be considered, as well as various types of storage bunkers. Finally, the program can be used to

(a) single box girder

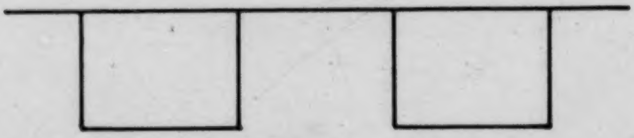

(b) multiple box girder

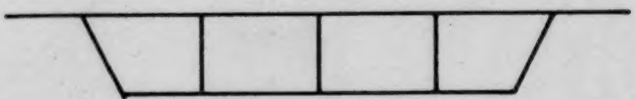

(c) multicell box girder

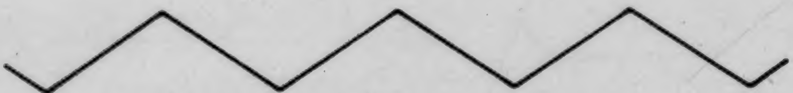

(d) folded plate roof

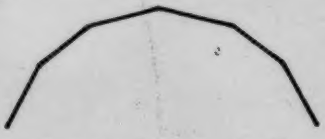

(e) cylindrical shell

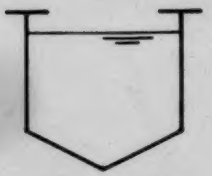

(f) coal bunker

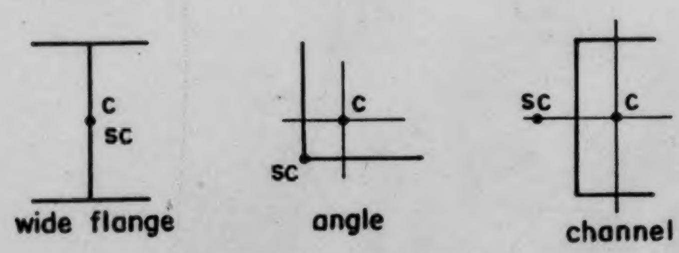

wide flange angle channel

(g) steel sections

Figure 4.9 Some applications for the folded plate method

analyse standard and built-up steel sections subjected to arbitrary flexural and torsional loads. Kristek (99) has even outlined a procedure whereby the folded plate method can be used to analyse the shear walls in multi-story buildings.

Although the program is limited to simply supported spans, it can handle continuous structures in an approximate way. With respect to flexure, the distance between the dead load inflection points of the continuous structure can be taken as the span length for the simply supported structure. With regard to shear and torsion, the actual span length of the interior span in the continuous structure can be used for the simply supported structure. Significant savings in computational effort (100 to 1000 times) can be realized by limiting the program to simply supported structures with only a 5% to 10% reduction in accuracy. This is discussed further in Example 4.

The input data and output information are discussed in detail in Appendix E. Briefly, the input data required is the node coordinates, element incidences, and loading information. The loading information can include self weight, surcharge, truck loads, lane loads, temperature, and prestress. Any consistent set of units may be used for the input. Output information provided by the program includes an echo of the input data, as well as the node displacements and element forces. Appendix F gives a source listing for the program. Input data for example 5 is given in Appendix G while some selected output is included in Appendix H.

The program consists of the following set of subroutines. A flow chart is given in Figure 4.10.

1. Program MAIN - calls other subroutines
2. Subroutine READ - reads input data
3. Subroutine CASE - reads load data
4. Subroutine STIF - sets up stiffness matrix for each harmonic
5. Subroutine LOAD - sets up load vector for each harmonic
6. Subroutine SOLV - banded equation solver
7. Subroutine FORC - updates node displacements and element forces
8. Subroutine RITE - writes node displacements and element forces

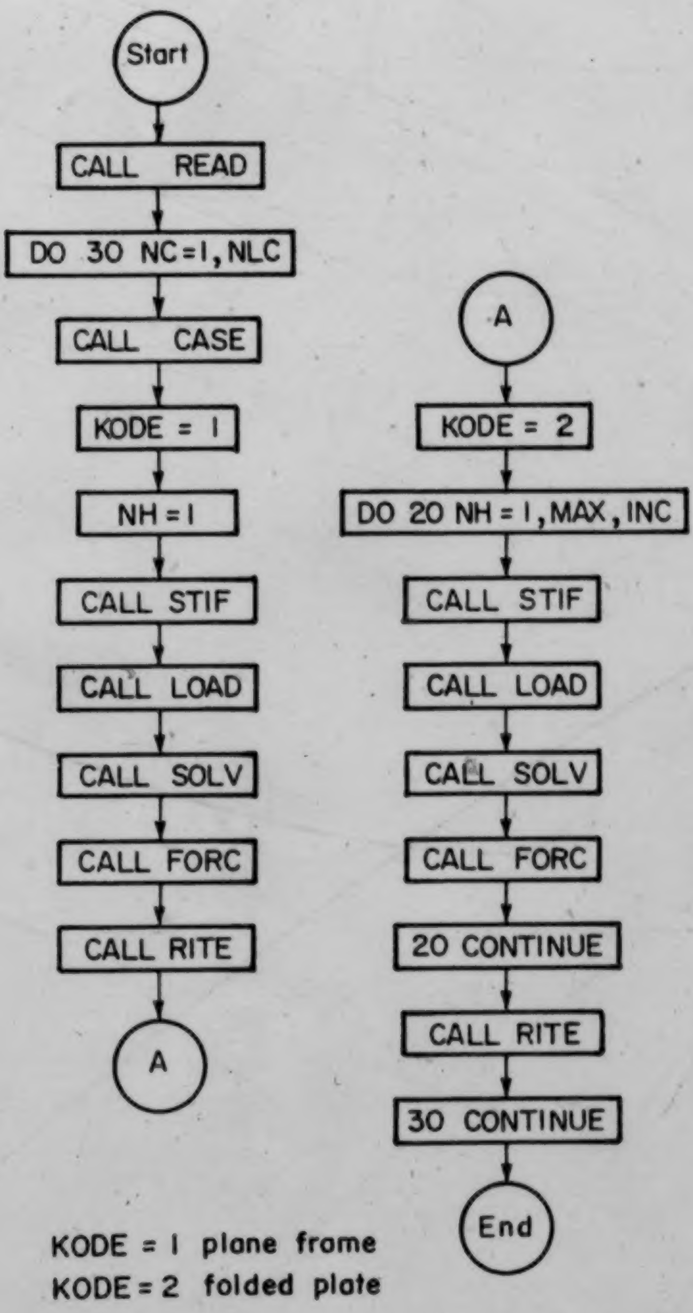
Start
CALL READ
DO 30 NC=1,NLC
CALL CASE
KODE = 1
NH=1
CALL STIF
CALL LOAD
CALL SOLV
CALL FORC
CALL RITE
A
A
KODE = 2
DO 20 NH = 1, MAX, INC
CALL STIF
CALL LOAD
CALL SOLV
CALL FORC
20 CONTINUE
CALL RITE
30 CONTINUE
End
KODE = 1 plane frame
KODE = 2 folded plate

Figure 4.10 Flow chart for the computer program BOXGIRD

4.6 Numerical examples

4.6.1 Introduction

There are two reasons for including numerical examples in this study. One is to illustrate the versatility of the method and the other is to show the accuracy of any new features or approximations to the method. Since the method has been discussed in great detail in the past, it is not necessary to prove that the method works.

Example 1 shows how the program can be applied to the analysis of a single box girder. Since the implementation of concentrated loads in the program is a new feature, Example 2 compares the results from the program with the influence surfaces of Pucher (109). Example 3 considers the approximate treatment of transverse prestressing in the program. Since the program replaces a continuous structure with an equivalent simply supported span, Example 4 compares the results from the program with an exact analysis using the program MUPDI (25) for the Corpus Christi bridge. Example 5 includes a complete analysis for the Islington Avenue extension. This example considers the effect of various loads on the transverse bending and longitudinal shear and torsion. The effects of shear lag are discussed.

Note that the various actions and their sign conventions are defined in detail in Appendix E. Briefly, we are concerned with the longitudinal membrane force (Nxx), the transverse membrane force (Nyy), the transverse bending moment (Myy), and the membrane shear force (Nxy). The sign convention is tension positive for the membrane forces and the bending moments are plotted on the tension side. Units are k/ft for the membrane forces and ft-k/ft for the bending moments.

4.6.2 Example 1 - Box girder bridge

The box girder shown in Figure 4.11 has a span length of 40 m and is subjected to a line load of 10 t/m. Identical results are found for the coarse and fine discretizations. This is an important generalization; the program is not sensitive to the discretization. Obviously, if a plate having variable thickness were approximated by a number of plates having constant thickness, a fine mesh would yield better results than a coarse mesh.

An approximate hand solution to this problem is given in the "Precast Segmental Box Girder Bridge Manual" (10). Figure 4.12 shows that the transverse bending moments and axial forces from the computer program and hand calculations are comparable, with the results from the program being more accurate. It should be evident that running the program is substantially easier than doing the hand calculations.

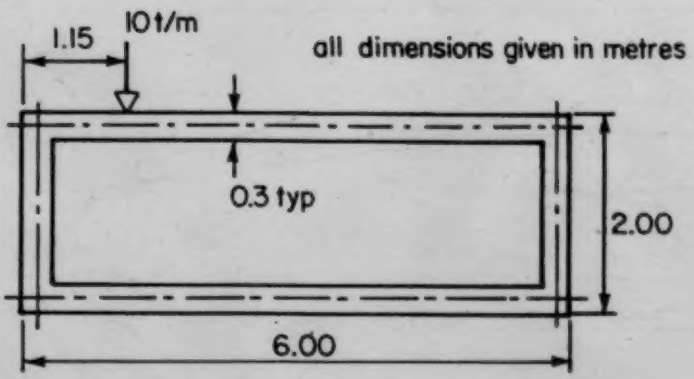
1.15
10 t/m
all dimensions given in metres
0.3 typ
2.00
6.00

(a) cross section

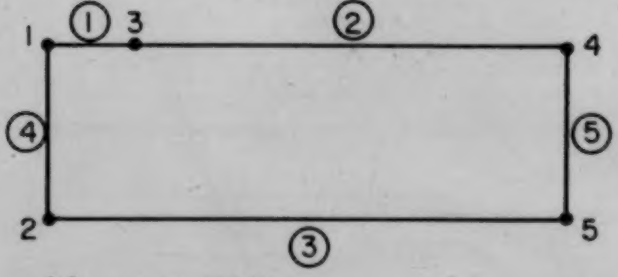
1
①
3
②
4
④
⑤
2
5
③

(b) coarse mesh

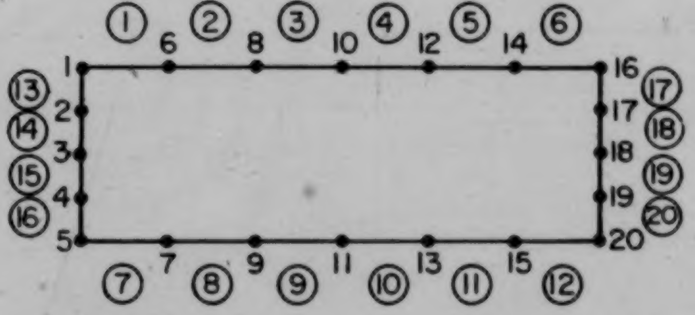
①
②
③
④
⑤
⑥
1
6
8
10
12
14
16
⑬
2
⑭
3
⑮
4
⑯
5
17
18
19
20
⑰
⑱
⑲
⑳
7
9
11
13
15
⑦
⑧
⑨
⑩
⑪
⑫

(c) fine mesh

Figure 4.11 Box girder bridge

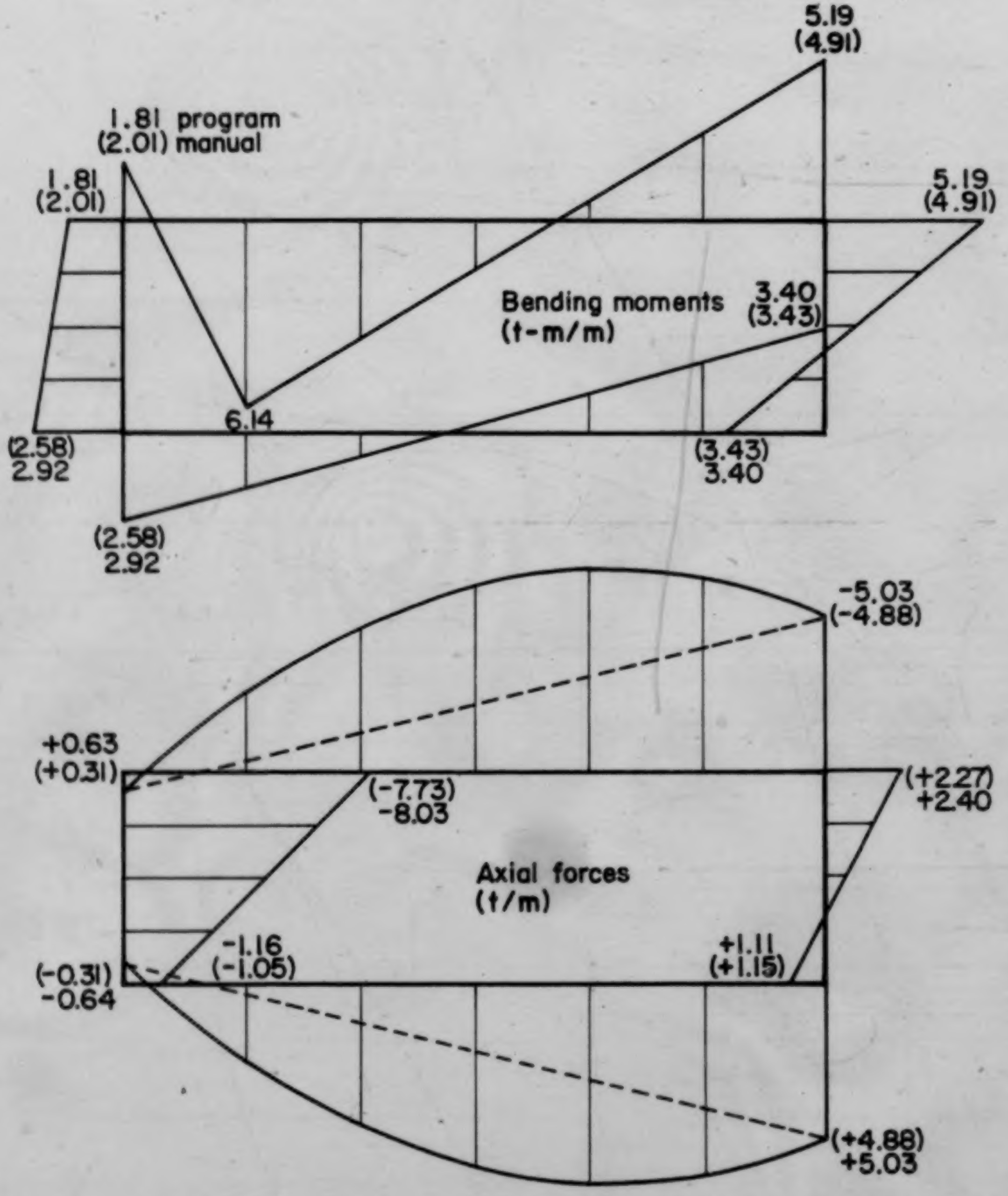
5.19
(4.91)
1.81 program
(2.01) manual
1.81
(2.01)
5.19
(4.91)
Bending moments
(t-m/m)
3.40
(3.43)
6.14
(2.58)
2.92
(3.43)
3.40
(2.58)
2.92
-5.03
(-4.88)
+0.63
(+0.31)
(-7.73)
-8.03
(+2.27)
+2.40
Axial forces
(t/m)
-1.16
(-1.05)
+1.11
(+1.15)
(-0.31)
-0.64
(+4.88)
+5.03

Figure 4.12 Bending moments and axial forces

4.6.3 Example 2 - Concentrated loads

This example compares the moments due to concentrated loads as given by the folded plate method and the influence surfaces of Pucher (109). Influence surfaces (Figures 4.13 to 4.16) are simply influence lines in two directions and physically resemble contour lines. Loaded areas are plotted on the influence surface and the volumes are calculated by Simpson's rule to give the resulting moment. For all intents and purposes, influence surfaces can be considered to be exact.

All influence surfaces discussed here are infinitely long and subjected to a variety of boundary conditions along their width. The influence surfaces shown in Figure 4.13 to 4.15 give the transverse and longitudinal moments at midspan for concentrated loads applied at various locations. Figure 4.13 is simply supported on both sides while Figure 4.14 is simply supported on one side and fixed on the other. Figure 4.15 is fixed on both sides. The influence surfaces shown in Figure 4.16 give the transverse moments at the support for the fixed-fixed case and fixed-free case.

The results given by the folded plate method at the grid points are shown. One can easily observe that the results given by the folded plate method are satisfactory. It

Tafel 1. m_x-Einflußfeld für die Feldmitte eines Plattenstreifens mit zwei frei aufliegenden Rändern (8 n-fach)
Chart 1. m_x-Influence surface for the center of a plate-strip with two supported edges (8 n-times)

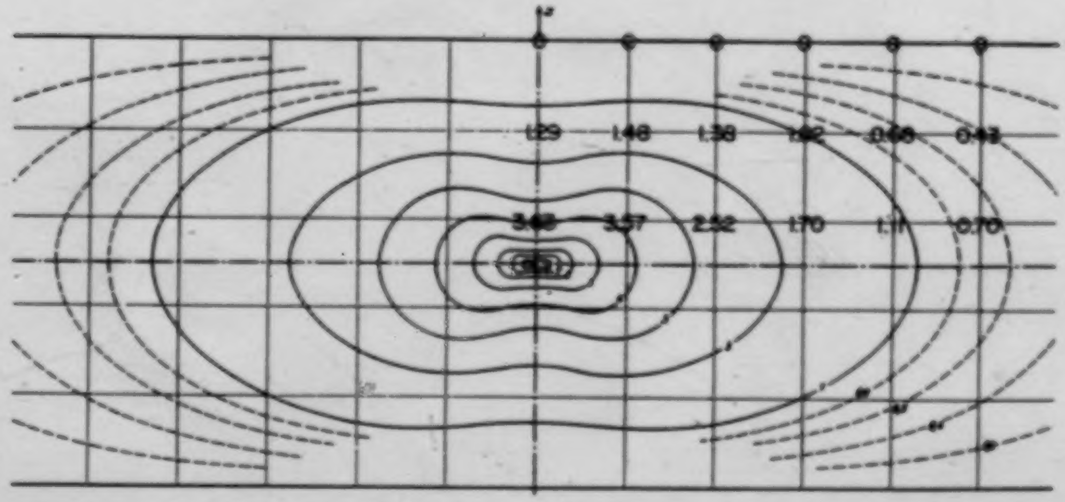

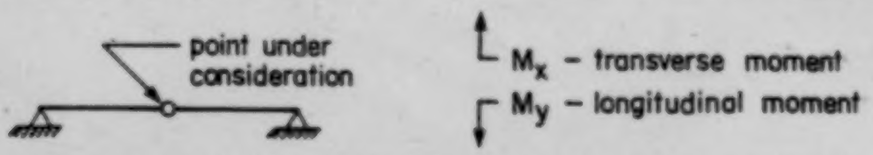
point under consideration
M_x - transverse moment
M_y - longitudinal moment

Tafel 2. m_y-Einflußfeld für die Feldmitte eines Plattenstreifens mit zwei frei aufliegenden Rändern (8 n-fach)
Chart 2. m_y-Influence surface for the center of a plate-strip with two supported edges (8 n-times)

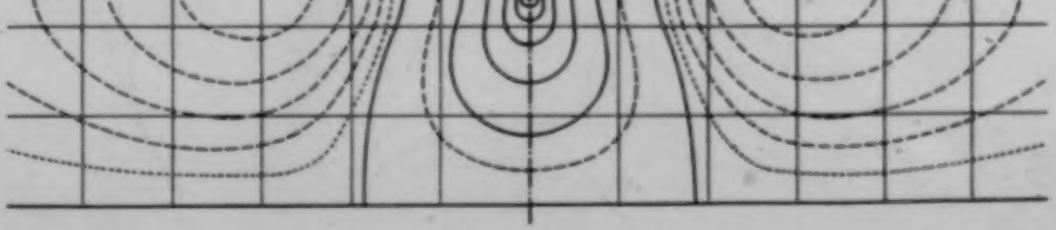

Figure 4.13 Mx and My at midspan for pinned-pinned case

Tafel 5. m_x-Einflußfeld für die Feldmitte eines Plattenstreifens mit einem eingespannten und einem frei aufliegenden Rand (8 π-fach)
Chart 5. m_x-Influence surface for the center of a plate-strip with a restrained and a supported edge (8 π-times)

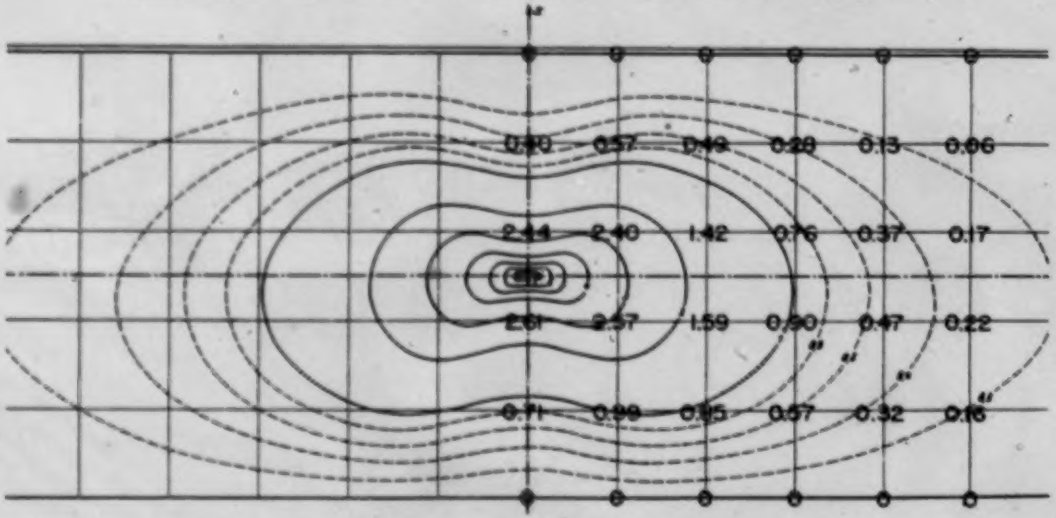

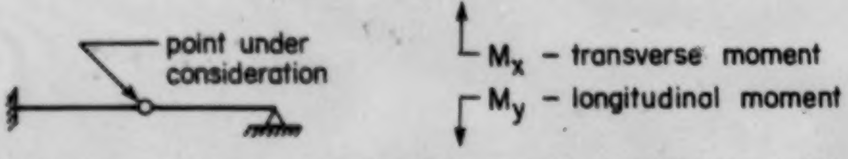
point under consideration
M_x – transverse moment
M_y – longitudinal moment

Tafel 6. m_y-Einflußfeld für die Feldmitte eines Plattenstreifens mit einem eingespannten und einem frei aufliegenden Rand (8 π-fach)
Chart 6. m_y-Influence surface for the center of a plate-strip with a restrained and a supported edge (8 π-times).

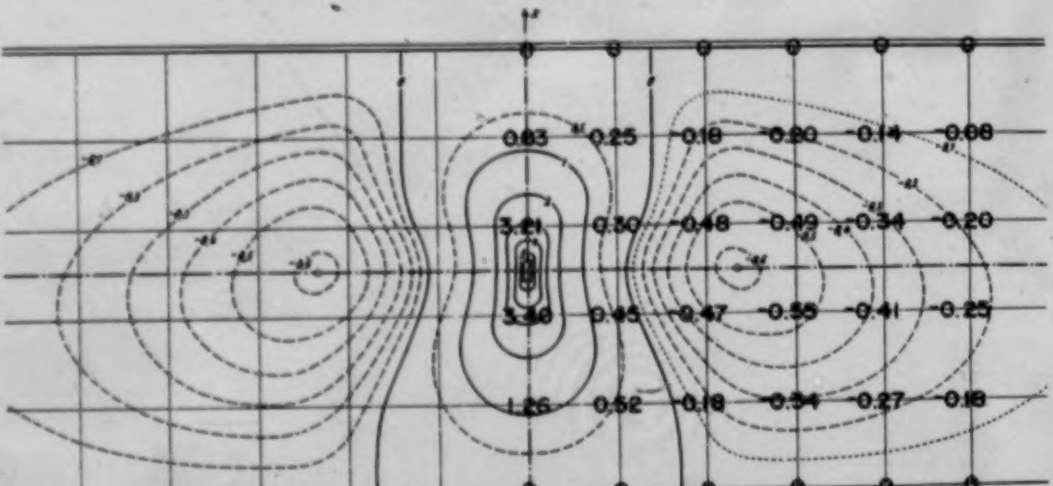

Figure 4.14 Mx and My at midspan for pinned-fixed case

Tafel 12. m_x-Einflußfeld für die Feldmitte eines Plattenstreifens mit zwei eingespannten Rändern (8 π-fach)
Chart 12. m_x-Influence surface for the center of a plate-strip with two restrained edges (8 π-times)

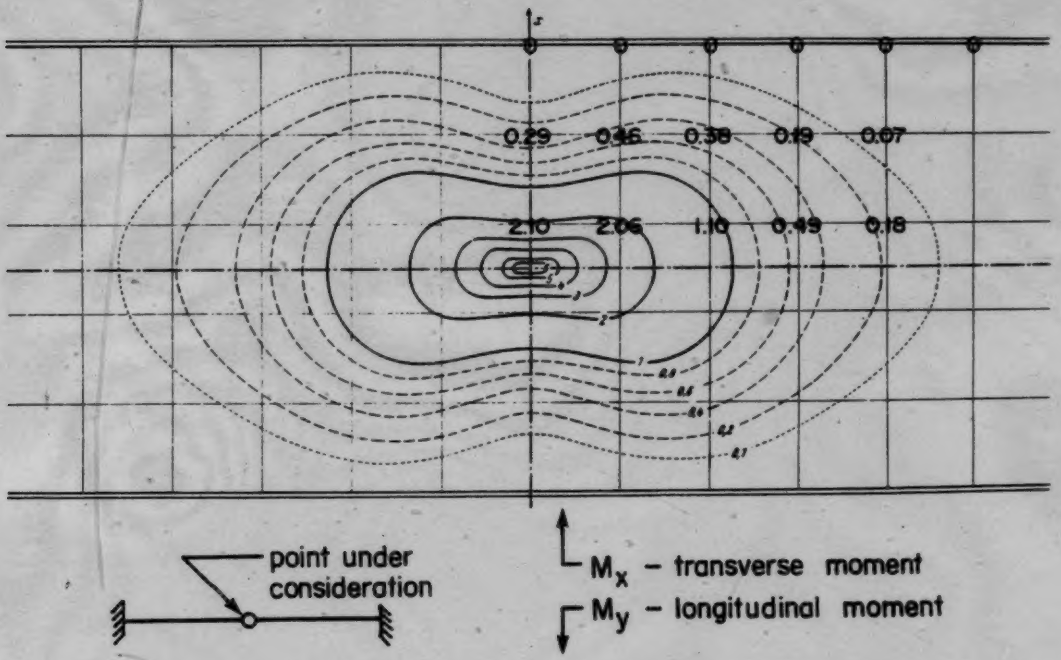

Tafel 13. m_y-Einflußfeld für die Feldmitte eines Plattenstreifens mit zwei eingespannten Rändern (8 π-fach)
Chart 13. m_y-Influence surface for the center of a plate-strip with two restrained edges (8 π-times)

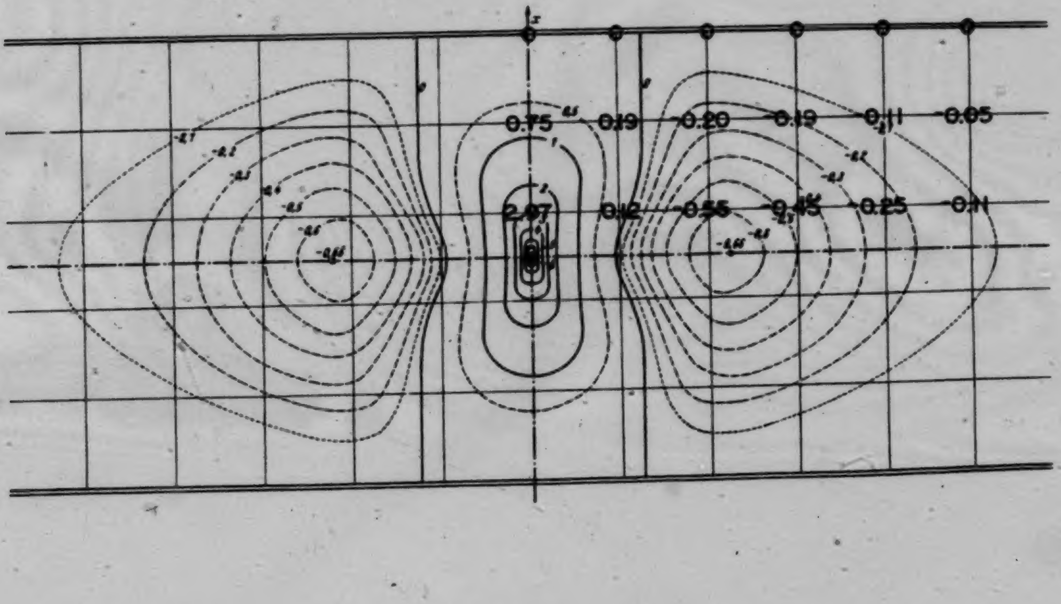

Figure 4.15 Mx and My at midspan for fixed-fixed case

Tafel 16. m_x-Stützmoment-Einflußfeld für den Rand eines Plattenstreifens mit zwei eingespannten Rändern (8 π-fach)
(Chart 16. m_x-Support-moment influence surface for the edge of a plate-strip with two restrained edges (8 π-times)

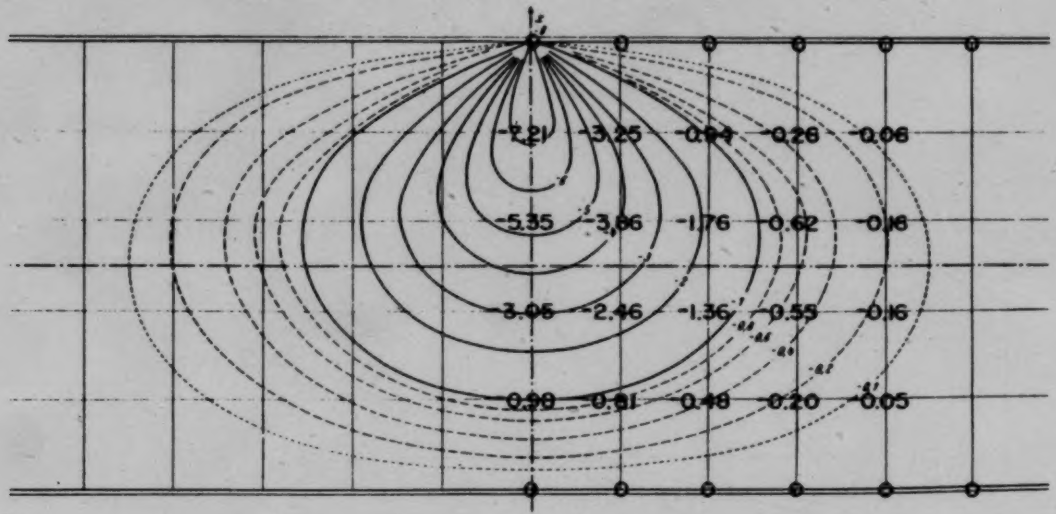

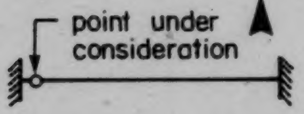

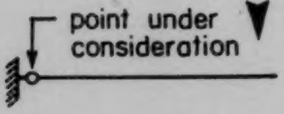

Tafel 17. m_x-Stützmoment-Einflußfeld für den eingespannten Rand eines auskragenden Plattenstreifens (Bereich $-1{,}31 < y < +1{,}31$, 8 π-fach)
Chart 17. m_x-Support-moment influence surface for the restrained edge of a cantilever plate-strip (range $-1.31 < y < +1.31$, 8 π-times)

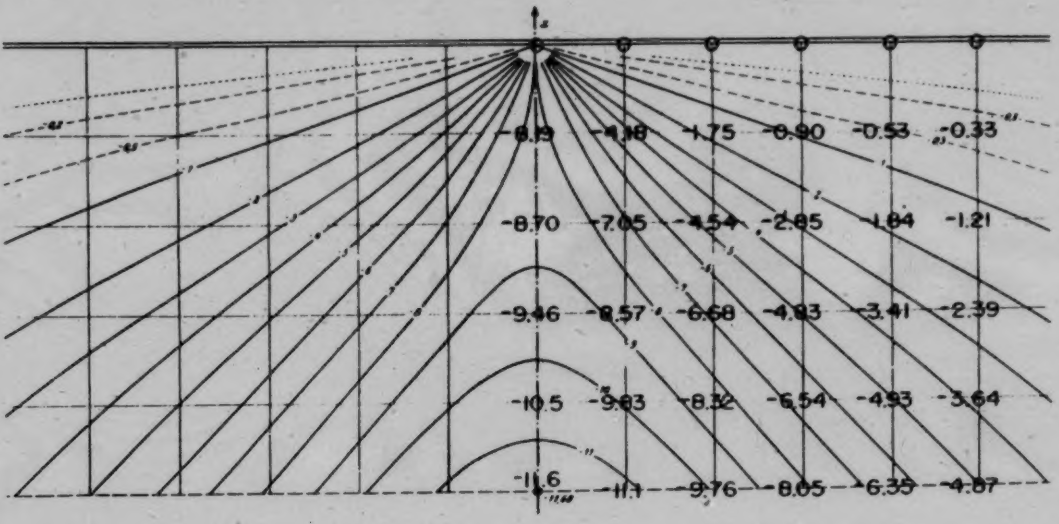

Figure 4.16 Mx at support for fixed-fixed case and fixed-free case

should be noted that plotting concentrated wheel loads on influence surfaces is a very time consuming exercise and having a program which will automatically give these results is a very welcome alternative.

4.6.4 Example 3 - Prestressing analysis

This example compares the accuracy of approximating a curved prestressing tendon as a series of straight line segments. Plane frame theory is used to analyse the two span continuous beam shown in Figure 4.17(a) and discretized in Figure 4.17(b). The results of the straight line treatment of prestressing are compared to those for an exact analysis using equivalent loads as shown in Figure 4.17(c).

The results for this analysis are given in Table 4.1. The bending moments are essentially the same while the shear forces calculated by the two methods vary somewhat. The only noteworthy difference in bending moments occurs near the support where the straight line estimation has trouble approximating the large curvature. The discrepancy in the shear forces is due to the fact that the straight line approximation averages the shears at the two ends of the element. One can thus conclude that prestressing can be treated as a series of straight line segments for the transverse analysis of box girder bridges where the

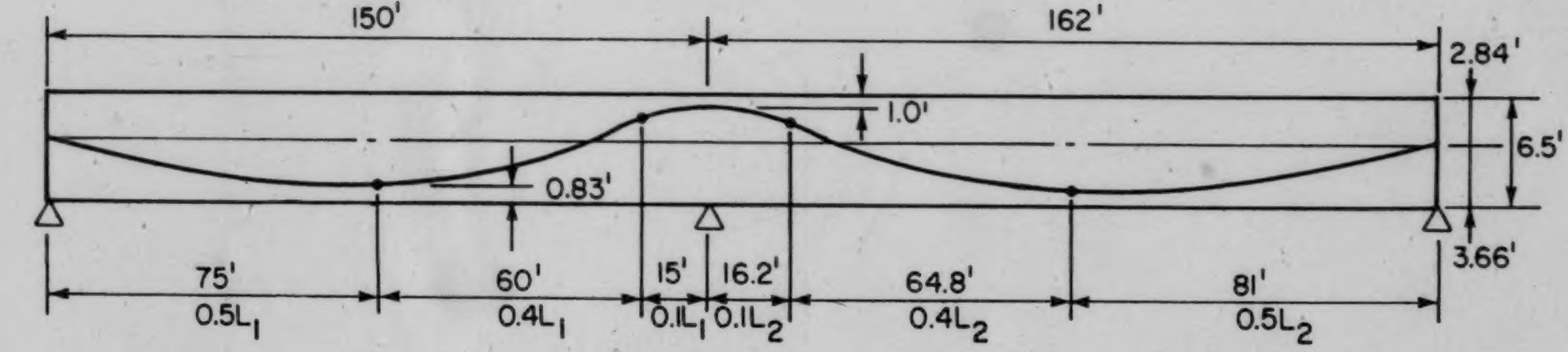
150'
162'
2.84'
1.0'
6.5'
0.83'
3.66'
75'
0.5L1
60'
0.4L1
15'
0.1L1
16.2'
0.1L2
64.8'
0.4L2
81'
0.5L2

(a) beam elevation

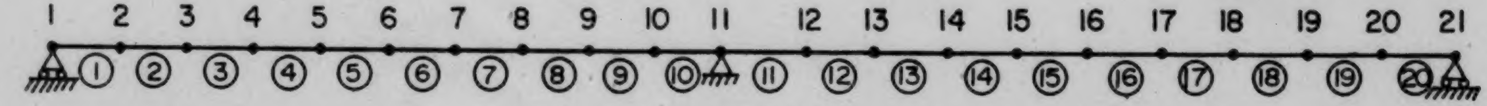
1 2 3 4 5 6 7 8 9 10 11 12 13 14 15 16 17 18 19 20 21
① ② ③ ④ ⑤ ⑥ ⑦ ⑧ ⑨ ⑩ ⑪ ⑫ ⑬ ⑭ ⑮ ⑯ ⑰ ⑱ ⑲ ⑳

(b) discretization

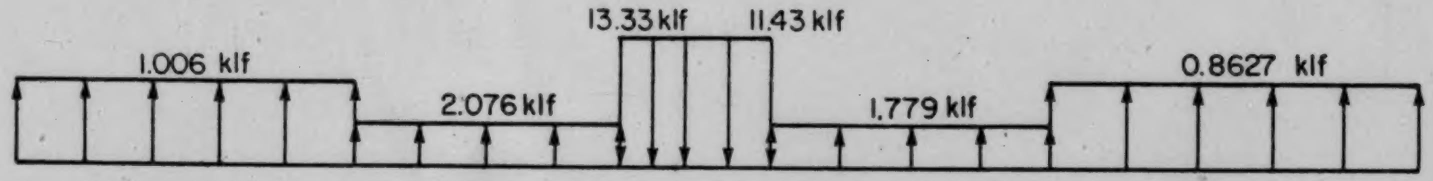
1.006 klf
2.076 klf
13.33 klf
11.43 klf
1.779 klf
0.8627 klf

(c) equivalent loads

Figure 4.17 Prestressing analysis

Table 4.1 - Equivalent loads vs direct treatment of prestressing

		Shear forces (k)		Bending moments (ft-k)		
Elmt	Node	EL	PS	EL	PS	Ratio
1	1	-64.24	-56.97	0.0	0.0	
1	2	-49.15	-56.97	-850.4	-854.3	1.00
2	2	-49.16	-41.71	-850.4	-854.3	
2	3	-34.06	-41.71	-1475.0	-1480.0	1.00
3	3	-34.06	-27.09	-1475.0	-1480.0	
3	4	-18.96	-27.09	-1872.0	-1886.0	1.01
4	4	-18.97	-11.11	-1872.0	-1886.0	
4	5	-3.87	-11.11	-2043.0	-2053.0	1.00
5	5	-3.87	2.88	-2043.0	-2053.0	
5	6	11.22	2.88	-1988.0	-2010.0	1.01
6	6	11.22	26.21	-1988.0	-2010.0	
6	7	42.35	26.21	-1587.0	-1616.0	1.02
7	7	42.35	58.16	-1587.0	-1616.0	
7	8	73.49	58.16	-717.8	-743.9	1.04
8	8	73.48	87.98	-717.8	-743.9	
8	9	104.60	87.98	618.0	575.9	0.93
9	9	104.60	119.60	618.0	575.9	
9	10	135.70	119.60	2421.0	2369.0	0.98
10	10	135.80	72.77	2421.0	2369.0	
10	11	64.25	72.77	2957.0	3461.0	1.17
11	11	-59.47	-67.38	2957.0	3461.0	
11	12	-125.70	-67.38	2421.0	2369.0	0.98
12	12	-125.70	-110.80	2421.0	2369.0	
12	13	-96.87	-110.80	618.1	574.7	0.93
13	13	-96.87	-81.48	618.1	574.7	
13	14	-68.04	-81.48	-717.6	-745.4	1.04
14	14	-68.04	-53.85	-717.7	-745.4	
14	15	-39.21	-53.85	-1586.0	-1618.0	1.02
15	15	-39.22	-24.27	-1586.0	-1618.0	
15	16	-10.39	-24.27	-1988.0	-2011.0	1.01
16	16	-10.39	-2.66	-1988.0	-2011.0	
16	17	3.59	-2.66	-2043.0	-2054.0	1.00
17	17	3.59	10.30	-2043.0	-2054.0	
17	18	17.56	10.30	-1872.0	-1887.0	1.01
18	18	17.56	25.09	-1872.0	-1887.0	
18	19	31.53	25.09	-1475.0	-1481.0	1.00
19	19	31.53	38.64	-1474.0	-1481.0	
19	20	45.51	38.64	-850.4	-854.8	1.00
20	20	45.51	52.76	-850.4	-854.8	
20	21	59.48	52.76	0.0	0.0	

EL - equivalent loads
PS - prestressing

Ratio = PS / EL

curvatures are generally quite small and shear is not of primary importance.

4.6.5 Example 4 - Corpus Christi bridge

The purpose of this example is to compare the results given by BOXGIRD with the more exact analysis of MUPDI (25). Although both programs are based on the folded plate method, MUPDI allows continuous structures having intermediate supports and diaphragms to be considered, while BOXGIRD is limited to simply supported structures.

MUPDI uses the force method to determine the interaction forces for the supports and diaphragms. Redundants corresponding to each degree of freedom for each diaphragm are defined. The structure is analysed for each redundant separately as well as for the external loading. Since the interaction forces are distributed over very small widths, they are essentially concentrated loads, and require a large number of Fourier series terms for convergence. The combination of a large number of separate analyses corresponding to each redundant and a large number of Fourier series terms for convergence renders MUPDI 100 to 1000 times as expensive to use as BOXGIRD. Consequently, the use of BOXGIRD can be justified if the results fall within reasonable limits, say 5% to 10%.

The Corpus Christi bridge in Texas (Figure 4.18) is used as the basis of comparison for BOXGIRD and MUPDI. This structure has span lengths of 100'-200'-100' and is comprised of two boxes which are joined after cantilever erection by a cast-in-place strip. The depth of the 26'-8" wide box remains constant at 8'-0" while the bottom slab thickness varies from 6" at midspan to 10" at the support. Two loading cases are considered. A line load is applied at midspan of the top slab as one case while a line load is applied at the tip of the cantilever as the other case.

This structure is chosen because a span ratio of 0.5 on a three span bridge makes it an extreme example. If the results for this example are satisfactory, the results for a multispan structure having a span ratio of 0.65 to 0.80 should also be acceptable.

Tables 4.2 to 4.5 illustrate that the results from BOXGIRD and MUPDI compare favourably. The membrane shear force (diagonal tension) Nxy at 10 ft inside of the interior support appears to be within 7% for the non-eccentric load and 12% for the eccentric load. It should be pointed out that the results are compared at a distance of 10 ft (0.05L) because of the problem of getting accurate results near a support with MUPDI. Recall that Fourier series will not converge within

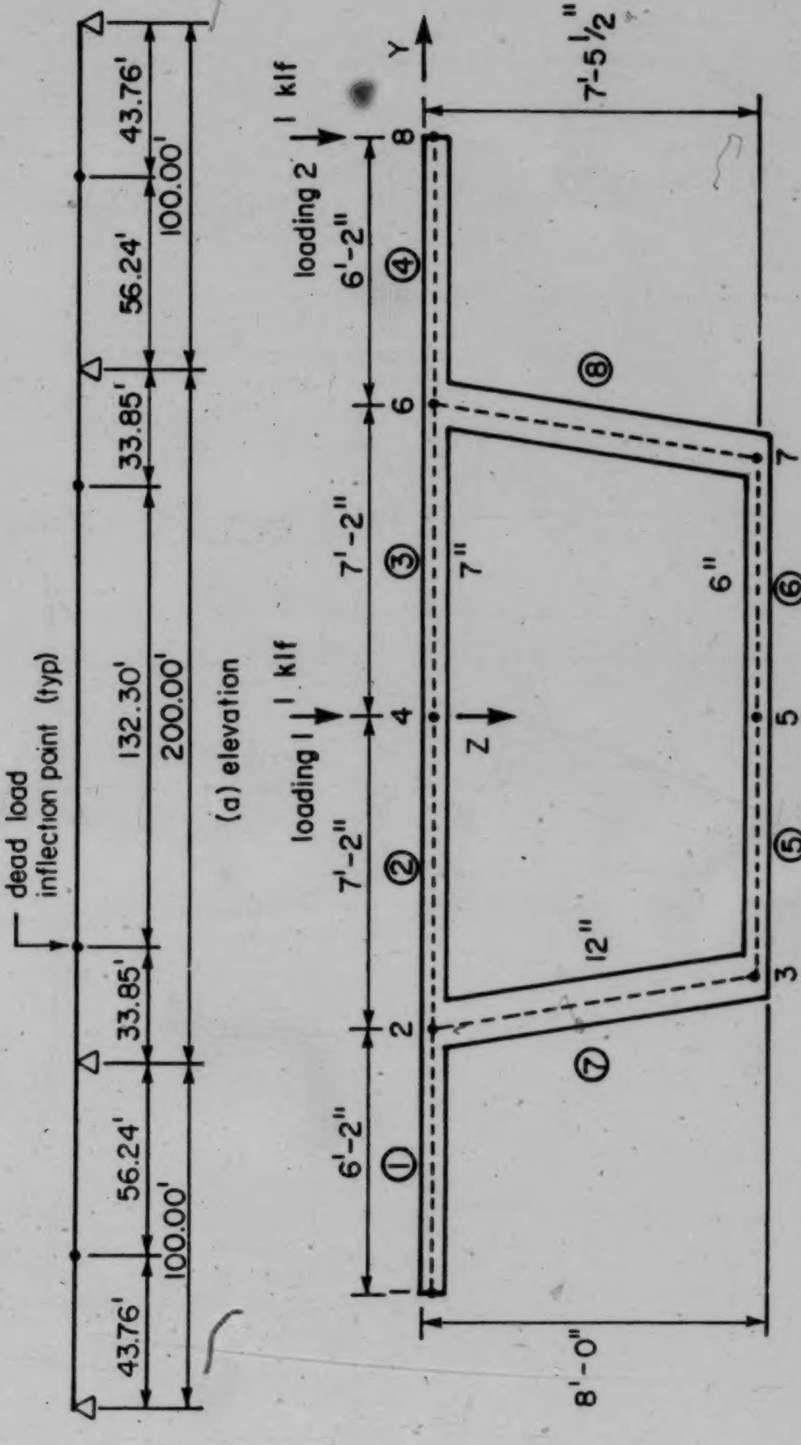
dead load
inflection point (typ)
43.76'
56.24'
33.85'
132.30'
33.85'
56.24'
43.76'
100.00'
200.00'
100.00'
(a) elevation
loading 1
1 klf
loading 2
1 klf
6'-2"
7'-2"
7'-2"
6'-2"
1
2
4
6
8
3
5
7
Y
Z
①
②
③
④
⑤
⑥
⑦
⑧
7"
12"
6"
6'-0"
6'-0"
8'-0"
7'-5 1/2"
(b) cross section

Figure 4.18 Corpus Christi bridge

Table 4.2 - Nxy (K/ft) at 10 ft inside of interior support

		Load case 1			Load case 2		
Elmt	Node	BOXGIRD	MUPDI	Ratio	BOXGIRD	MUPDI	Ratio
1	1	0.0	0.0	-	0.0	0.0	-
1	2	-2.683	-2.648	1.01	-2.653	-2.719	0.98
2	2	3.115	2.921	1.07	-2.966	-3.009	0.99
2	4	0.0	0.0	-	-6.013	-5.389	1.12
3	4	0.0	0.0	-	-6.013	-5.389	1.12
3	6	-3.115	-2.921	1.07	-9.201	-8.905	1.03
4	6	2.683	2.648	1.01	2.723	2.520	1.08
4	8	0.0	0.0	-	0.0	0.0	-
5	3	-3.823	-3.685	1.04	2.231	2.232	1.00
5	5	0.0	0.0	-	5.973	5.550	1.08
6	5	0.0	0.0	-	5.973	5.550	1.08
6	7	3.823	3.685	1.04	9.884	9.626	1.03
7	2	-5.798	-5.570	1.04	0.3133	0.2902	1.08
7	3	-3.823	-3.680	1.04	2.231	2.232	1.00
8	6	-5.798	-5.570	1.04	-11.92	-11.42	1.04
8	7	-3.823	-3.680	1.04	-9.884	-9.626	1.03

Table 4.3 - Nxx (K/ft) at midspan of interior span

		Load case 1			Load case 2		
Elmt	Node	BOXGIRD	MUPDI	Ratio	BOXGIRD	MUPDI	Ratio
1	1	-10.35	-10.41	0.99	-10.70	-10.67	1.00
1	2	-10.60	-10.65	1.00	-10.30	-10.28	1.00
2	2	-10.62	-10.68	0.99	-10.30	-10.28	1.00
2	4	-10.36	-10.43	0.99	-10.34	-10.34	1.00
3	4	-10.36	-10.43	0.99	-10.34	-10.34	1.00
3	6	-10.62	-10.68	0.99	-10.87	-10.88	1.00
4	6	-10.60	-10.65	1.00	-11.02	-11.03	1.00
4	8	-10.35	-10.41	0.99	-10.10	-10.16	0.99
5	3	15.48	15.57	0.99	15.12	15.15	1.00
5	5	15.22	15.32	0.99	15.22	15.22	1.00
6	5	15.22	15.32	0.99	15.22	15.22	1.00
6	7	15.48	15.57	0.99	15.83	15.80	1.00
7	2	-18.27	-18.37	0.99	-17.68	-17.76	1.00
7	3	30.89	31.08	0.99	30.24	30.31	1.00
8	6	-18.29	-18.37	0.99	-19.12	-19.12	1.00
8	7	30.89	31.08	0.99	31.89	31.82	1.00

Table 4.4 - Nyy (k/ft) at midspan of interior span

		Load case 1			Load case 2		
Elmt	Node	BOXGIRD	MUPDI	Ratio	BOXGIRD	MUPDI	Ratio
1	1	0.0	0.0	-	0.0	0.0	-
1	2	0.09482	0.09144	1.04	0.09421	0.09301	1.01
2	2	-0.06219	-0.06105	1.02	0.08319	0.08271	1.01
2	4	-0.1874	-0.1844	1.02	0.4469	0.4413	1.01
3	4	-0.1874	-0.1844	1.02	0.4469	0.4413	1.01
3	6	-0.06219	-0.06105	1.02	1.071	1.046	1.02
4	6	0.09482	0.09144	1.04	0.08413	0.08996	0.94
4	8	0.0	0.0	-	0.0	0.0	-
5	3	0.2359	0.2297	1.03	0.1128	0.09814	1.15
5	5	0.3640	0.3561	1.02	-0.2721	-0.2696	1.01
6	5	0.3640	0.3561	1.02	-0.2721	-0.2696	1.01
6	7	0.2359	0.2297	1.03	-0.8168	-0.8018	1.02
7	2	-0.4940	-0.4692	1.05	0.05203	0.05158	1.01
7	3	0.03639	0.03494	1.04	0.05453	0.05309	1.03
8	6	-0.4940	-0.4692	1.05	-1.242	-1.183	1.05
8	7	0.03639	0.03494	1.04	-0.1798	-0.1767	1.02

Table 4.5 - Myy (ft-k/ft) at midspan of interior span

		Load case 1			Load case 2		
Elmt	Node	BOXGIRD	MUPDI	Ratio	BOXGIRD	MUPDI	Ratio
1	1	0.0	0.0	-	0.0	0.0	-
1	2	0.0	0.0	-	0.0	0.0	-
2	2	-1.730	-1.673	1.03	0.1664	0.1671	1.00
2	4	1.985	1.906	1.04	-0.2019	-0.2009	1.00
3	4	1.985	1.906	1.04	-0.2019	-0.2009	1.00
3	6	-1.730	-1.673	1.03	-0.5847	-0.5670	1.03
4	6	0.0	0.0	-	-6.300	-6.156	1.02
4	8	0.0	0.0	-	0.0	0.0	-
5	3	-0.04124	-0.03986	1.03	-0.2444	-0.2404	1.02
5	5	-0.04059	-0.04030	1.01	0.07012	0.06980	1.00
6	5	-0.04059	-0.04030	1.01	0.07012	0.06980	1.00
6	7	-0.04124	-0.03986	1.03	0.3885	0.3808	1.02
7	2	1.725	1.673	1.03	-0.1728	-0.1739	0.99
7	3	-0.04124	-0.03986	1.03	-0.2444	-0.2404	1.02
8	6	-1.725	-1.673	1.03	5.715	5.589	1.02
8	7	0.04124	0.03986	1.03	-0.3885	-0.3809	1.02

two or three wavelengths of the highest harmonic near a concentrated load.

The results are compared at midspan for the interior span. The longitudinal membrane force Nxx is within 1% for both load cases. The transverse membrane force Nyy and transverse bending moment Myy are within 5% for both load cases (with one small exception). The maximum results have also been tabulated (but not included) for the end span. The longitudinal membrane force Nxx is within 8% for the non-eccentric load and 14% for the eccentric load.

In summary, these results are encouraging enough to justify the use of BOXGIRD for continuous structures.

4.6.6 Example 5 - Islington Avenue extension

The purpose of this example is to show how the computer program BOXGIRD can be used in a typical design. In general, the design of a segmental bridge requires that prestressed and/or non-prestressed reinforcement be proportioned for (1) longitudinal flexure, (2) transverse flexure, (3) longitudinal shear and torsion, and (4) local effects (ie shear keys, prestressing anchorages, etc.). The longitudinal flexural requirements can be obtained at various stages of erection and for the completed structure from the program TIMEDEP. The transverse flexural and longitudinal shear and torsional requirements can be obtained for the completed structure from the program BOXGIRD. Since the program is limited to simply supported spans, it cannot analyse the structure during balanced cantilever construction. This seldom governs the design anyway.

The structure considered here is the Islington Avenue extension in Toronto (Figure 4.19). This seven span bridge is comprised of two 45'-0" wide boxes separated by a 1" gap. The spans are 161'-200'-272'-272'-272'-272'-161'. The boxes vary in depth from 7'-6" at midspan to 11'-0" at the piers. The bottom slab thickness ranges from 9" at midspan to 27" at the piers while all other dimensions remain constant.

The program BOXGIRD has been written for constant depth sections having constant bottom slab thicknesses. Consequently, it can only be applied to this bridge in an approximate way. Two idealized constant depth structures having constant bottom slab thicknesses are considered; one has the minimum section while the other has the maximum section. Each section is analysed for transverse flexure as well as longitudinal shear and torsion. This gives a total of four approximate

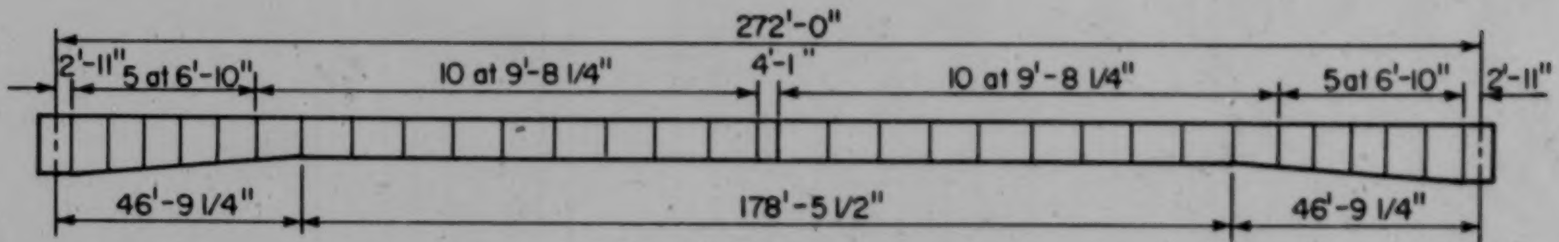
272'-0"
2'-11"
5 at 6'-10"
10 at 9'-8 1/4"
4'-1"
10 at 9'-8 1/4"
5 at 6'-10"
2'-11"
46'-9 1/4"
178'-5 1/2"
46'-9 1/4"

(a) elevation

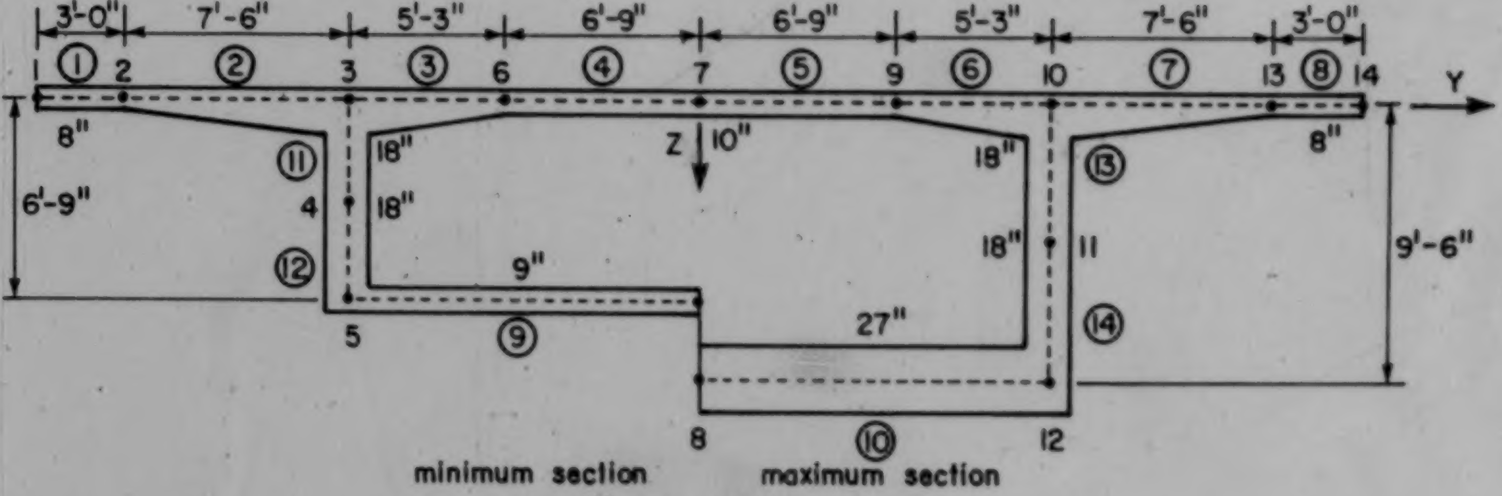
3'-0"
7'-6"
5'-3"
6'-9"
6'-9"
5'-3"
7'-6"
3'-0"
1
①
2
②
3
③
6
④
7
⑤
9
⑥
10
⑦
13
⑧
14
Y
8"
⑪
18"
Z
10"
18"
⑬
8"
6'-9"
4
18"
18"
11
9'-6"
⑫
9"
27"
⑭
5
⑨
8
⑩
12
minimum section
maximum section

(b) cross section

Figure 4.19 Islington Avenue extension

analyses:

(1) Transverse flexure of the minimum section

The span length is assumed to be the distance between the dead load inflection points or 158'-0" for a 272'-0" span. The minimum section is taken and the results are considered at midspan (79'-0").

(2) Transverse flexure of the maximum section

A suggestion is to use the above recommendations but replace the minimum section by the maximum section.

(3) Longitudinal shear and torsion of the minimum section

The span length is assumed to be the distance between piers. This is reasonable with respect to shear if one considers an interior span of a multispan structure and the loads are more or less uniformly distributed. This is also reasonable with respect to torsion since the pier diaphragms are very rigid in their plane. The minimum section is used and the results are found at the point where the depth starts to increase (46'-9 1/4").

(4) Longitudinal shear and torsion of the maximum section

The span length is again assumed to be the distance between piers but this time the maximum section is used and the results are found at the pier (0'-0").

The analysis for transverse flexure (minimum section) is considered first. The structure is subjected to nine different loading cases (Figure 4.20). They include self weight, superimposed dead load, sidewalk live load, three variations of truck load, two variations of temperature, and transverse prestress. The superimposed dead load includes the asphalt overlay (0.038 ksf), the sidewalk and curb (0.125 ksf), and the railing (0.675 klf). The three variations of AASHTO HS25 truck load relate to locations causing negative cantilever moment, negative interior moment, and positive interior moment. Note that 16 k is the wheel load for an HS20 truck load, 1.25 converts an HS20 load to an HS25 load, and 1.30 is the impact factor. The two thermal loads correspond to the heating of the deck during the day and the cooling of the box at night. Transverse prestressing is employed as shown to reduce the amount of conventional reinforcement. Both folded plate and plane frame theory are used. Input data is given in Appendix G while some selected output is included in Appendix H.

The longitudinal membrane stresses for self weight are given in Figure 4.21 as Nxx/t where t is the thickness. Note that tension is positive and that the units are ksf. The values along the top and bottom flanges are reasonably uniform, indicating that the effects of shear lag are minimal.

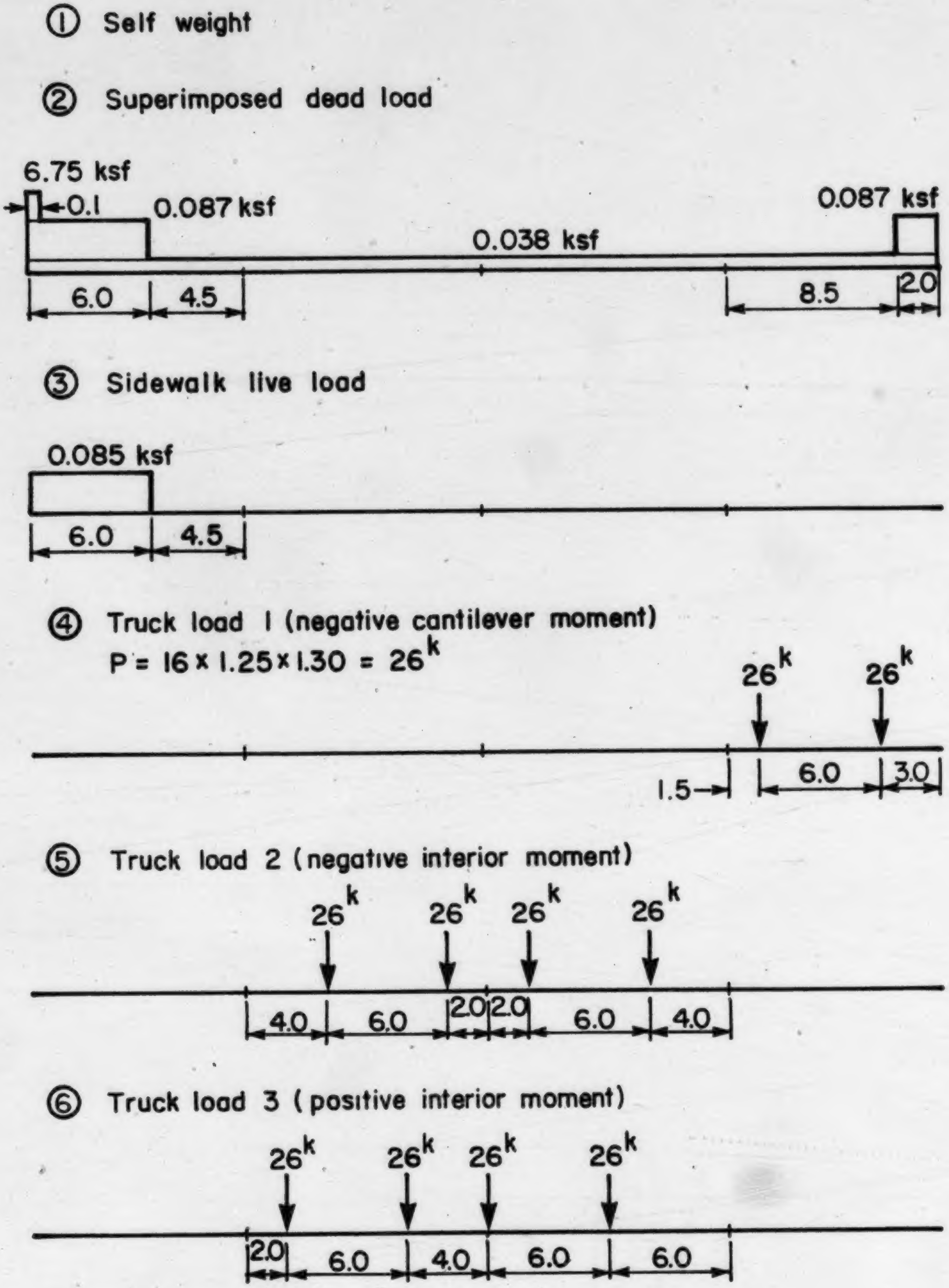
① Self weight
② Superimposed dead load
6.75 ksf
0.1
0.087 ksf
0.038 ksf
0.087 ksf
6.0
4.5
8.5
2.0
③ Sidewalk live load
0.085 ksf
6.0
4.5
④ Truck load 1 (negative cantilever moment)
P = 16 × 1.25 × 1.30 = 26k
26k
26k
1.5
6.0
3.0
⑤ Truck load 2 (negative interior moment)
26k
26k
26k
26k
4.0
6.0
2.0
2.0
6.0
4.0
⑥ Truck load 3 (positive interior moment)
26k
26k
26k
26k
2.0
6.0
4.0
6.0
6.0

Figure 4.20 Loading cases for transverse flexure

⑦ Temperature 1 (top surface 40°F above datum)

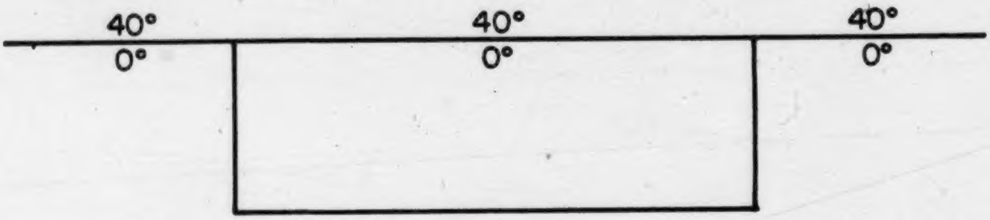

⑧ Temperature 2 (interior surface 20°F above datum)

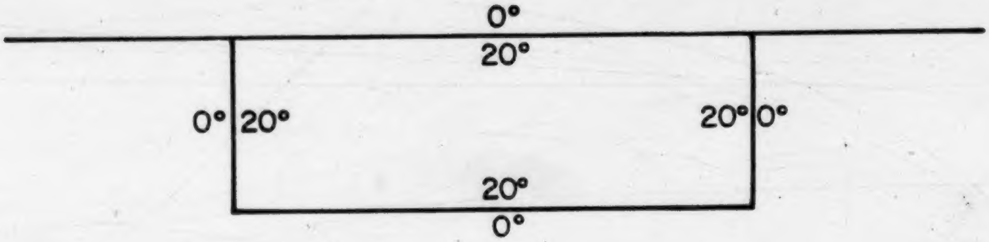
0°
20°
0°
20°
20°
0°
20°
0°

⑨ Transverse prestress

distance of prestress from top

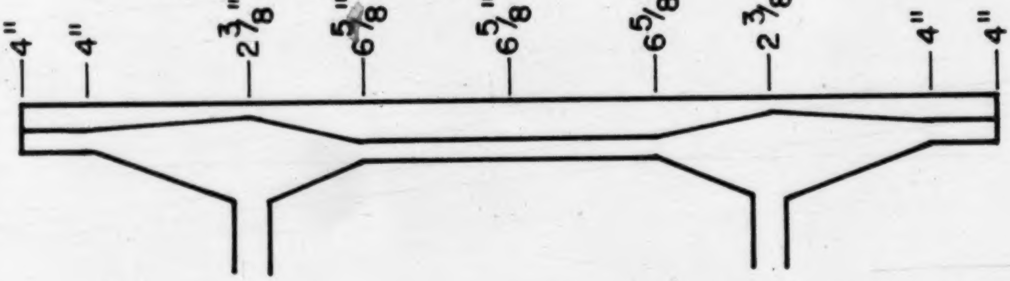
4"
4"
2 3/8"
6 5/8"
6 5/8"
6 5/8"
2 3/8"
4"
4"

$P = 0.7 \times 60 \times \frac{4}{9.69} = 17.34^{\text{klf}}$ (4 cables distributed over 9'-8 1/4")

Figure 4.20 Loading cases for transverse flexure con't

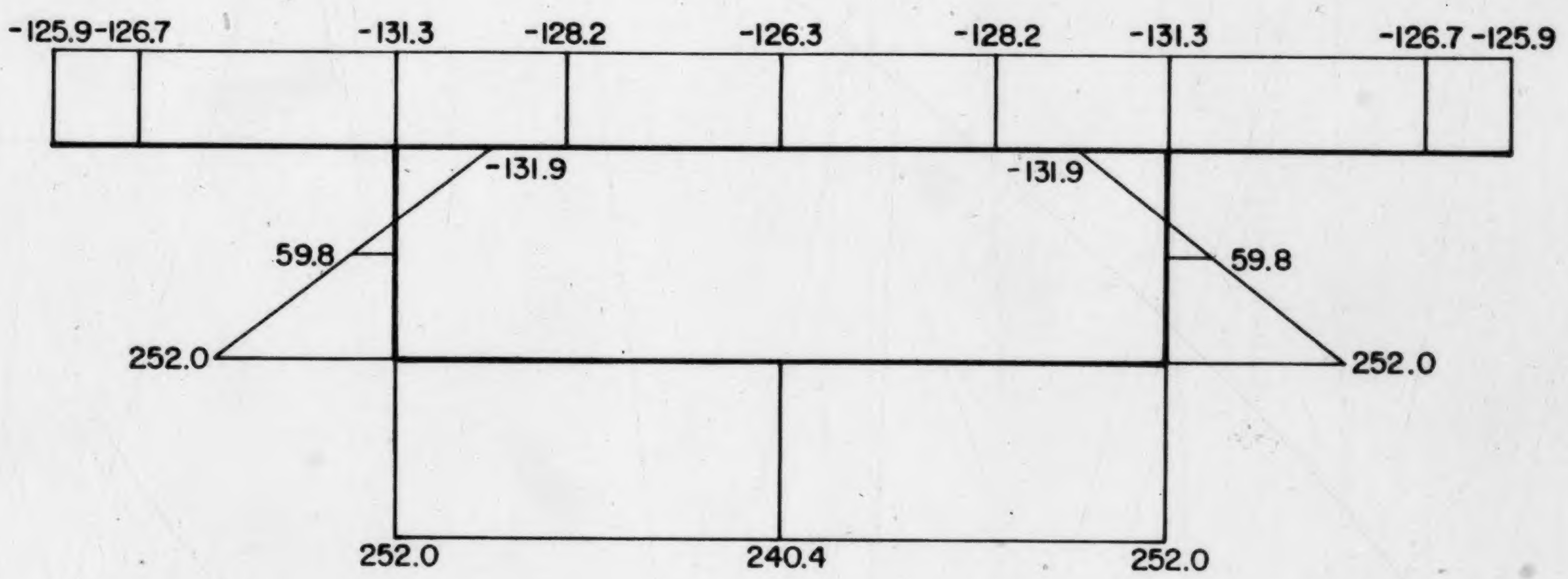
-125.9-126.7
-131.3
-128.2
-126.3
-128.2
-131.3
-126.7 -125.9
-131.9
-131.9
59.8
59.8
252.0
252.0
252.0
240.4
252.0

Figure 4.21 - Nxx/t for self weight

Figures 4.22 to 4.30 show the transverse bending moment diagram (Myy) and the transverse membrane force (axial force) diagram (Nyy) for each loading case. Note that tension is positive for the membrane forces and that the bending moments are plotted on the tension side. Units are k/ft for the membrane forces and ft-k/ft for the bending moments. In general, both the folded plate and plane frame results are plotted. Of course only the folded plate results are plotted for the truck load cases, since the plane frame results are unnecessarily conservative.

With regard to axial force, the folded plate and plane frame results have significant differences for all load cases. For example, the axial force at midspan of the bottom slab under self weight is given as 0.903 klf by plane frame theory and 5.223 klf by folded plate theory. This is a dramatic difference. Furthermore, plane frame theory gives zero axial force in the cantilevers while folded plate theory predicts significant axial force in the cantilevers for all loading cases. Appendix L shows that the significant differences between the folded plate and plane frame results are due to the fact that plane frame theory neglects the interaction of the membrane forces.

With respect to bending moment, the results for folded plate and plane frame theory are extremely close for self weight, temperature, and prestressing, while there are significant

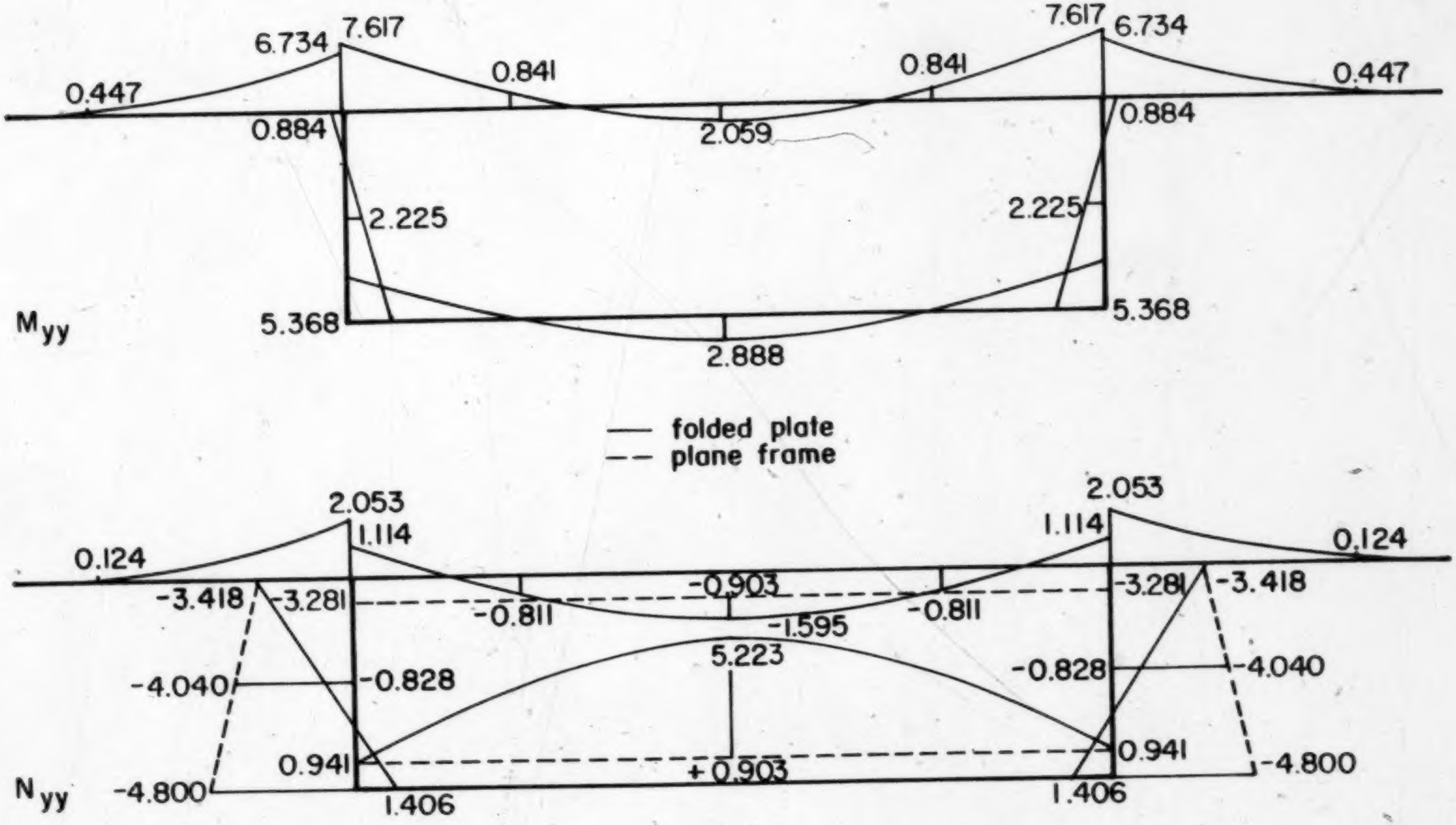
6.734
7.617
7.617
6.734
0.447
0.841
0.841
0.447
0.884
2.059
0.884
2.225
2.225
M_yy
5.368
5.368
2.888
— folded plate
– – plane frame
2.053
2.053
1.114
1.114
0.124
0.124
-3.418
-3.281
-0.903
-3.281
-3.418
-0.811
-1.595
-0.811
5.223
-4.040
-0.828
-0.828
-4.040
0.941
0.941
N_yy
-4.800
+0.903
-4.800
1.406
1.406

Figure 4.22 Myy and Nyy for self weight

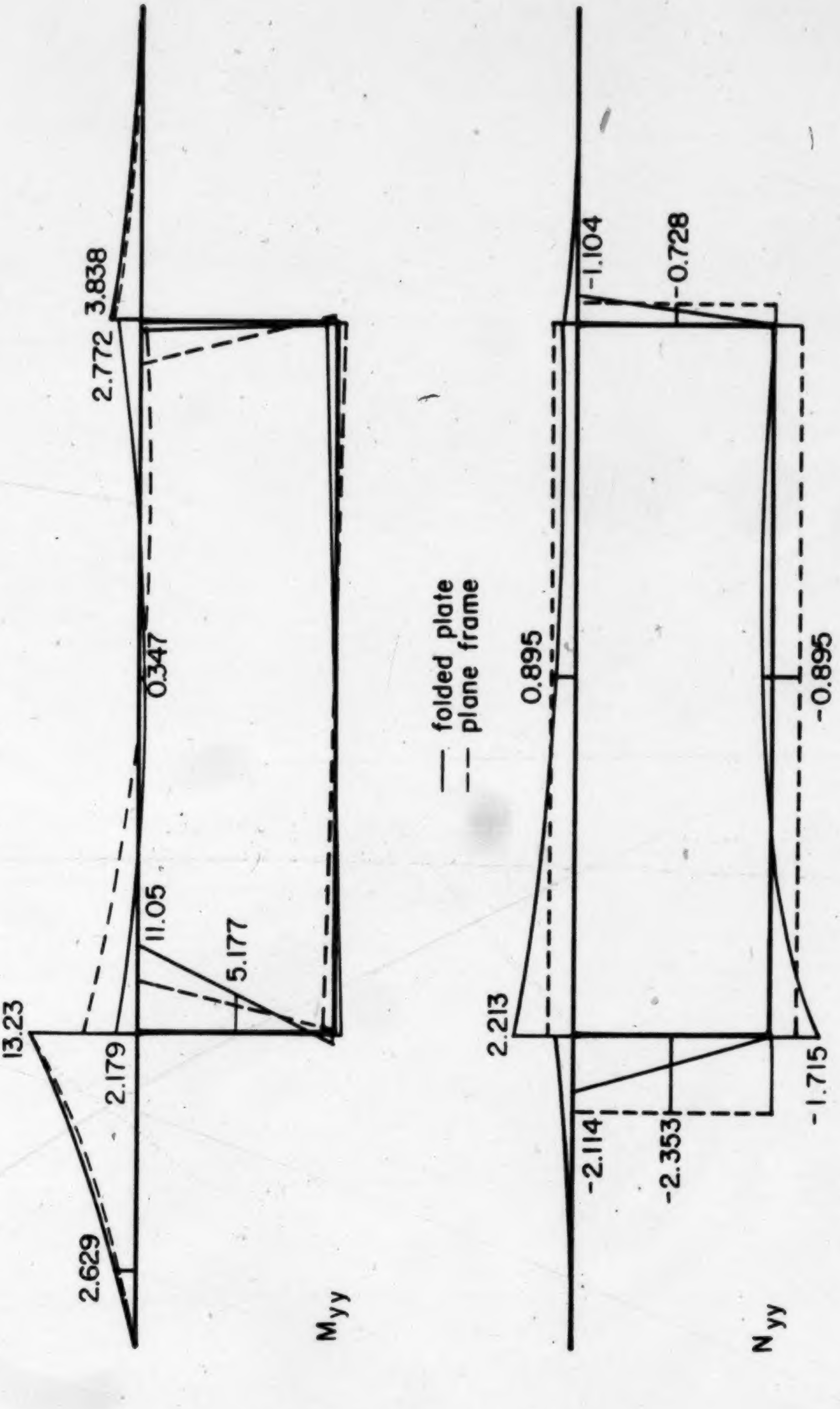

Figure 4.23 Myy and Nyy for superimposed dead load

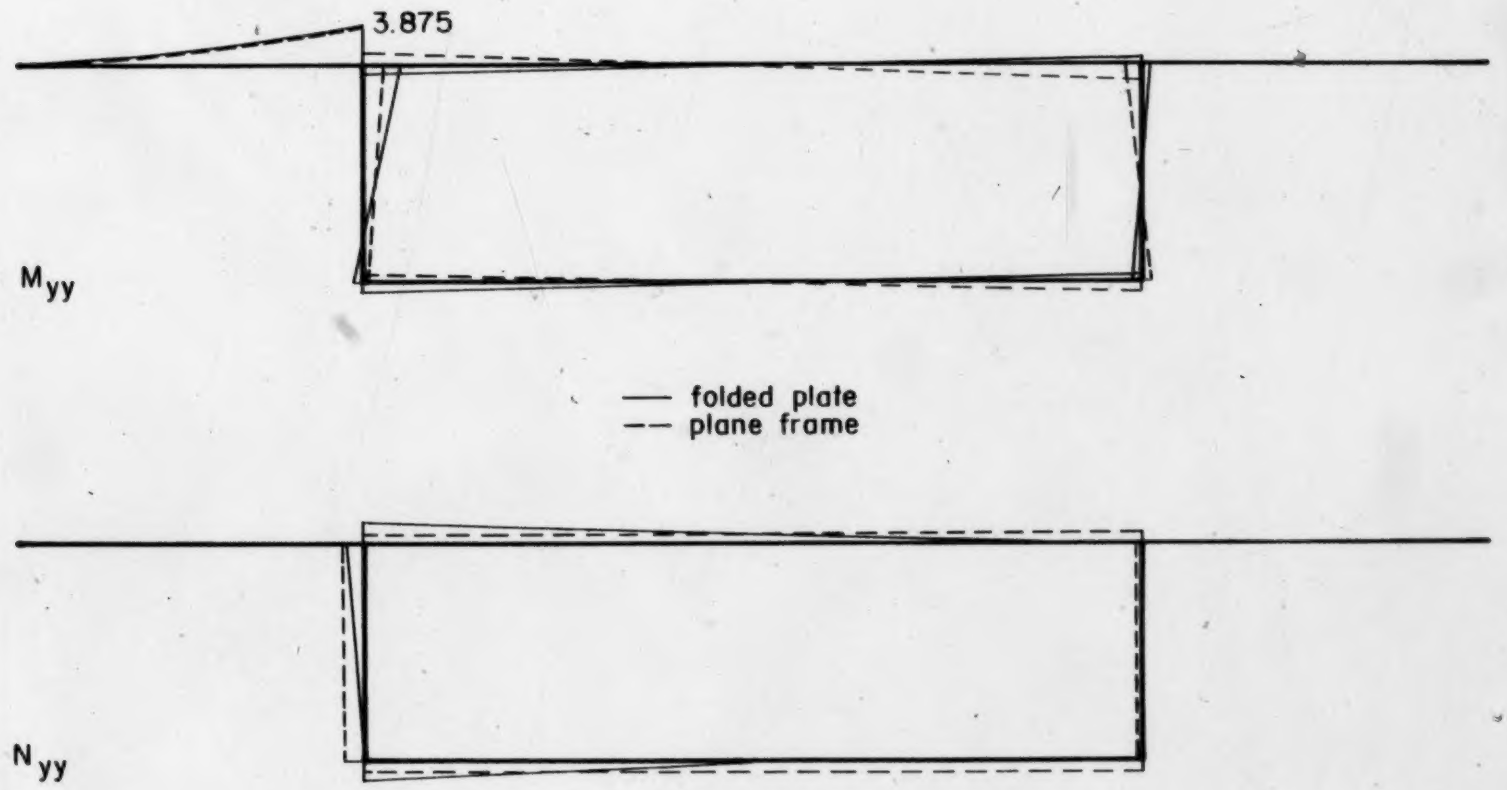

Figure 4.24 Myy and Nyy for sidewalk live load

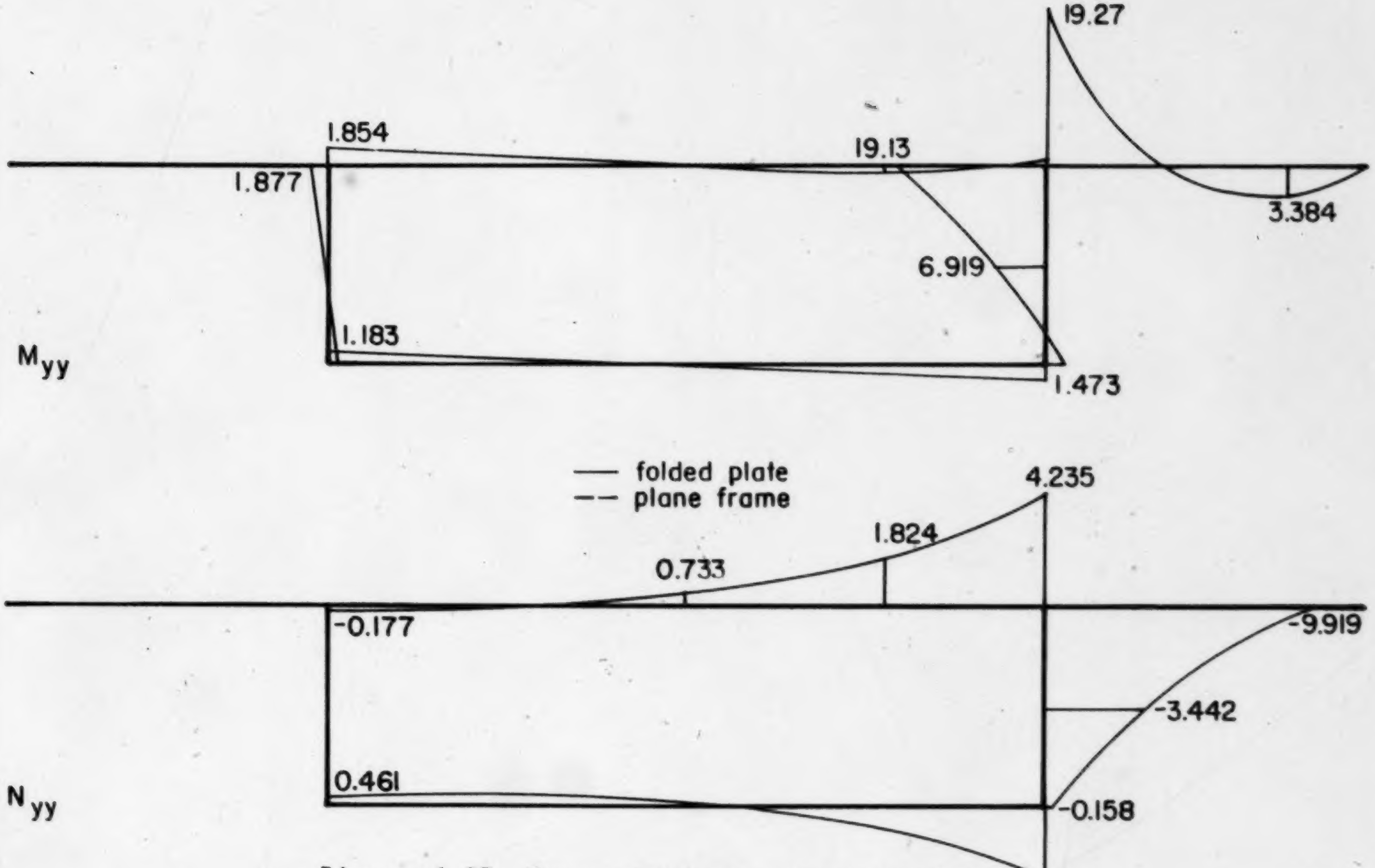

Figure 4.25 Myy and Nyy for truck load 1 (negative cantilever moment)

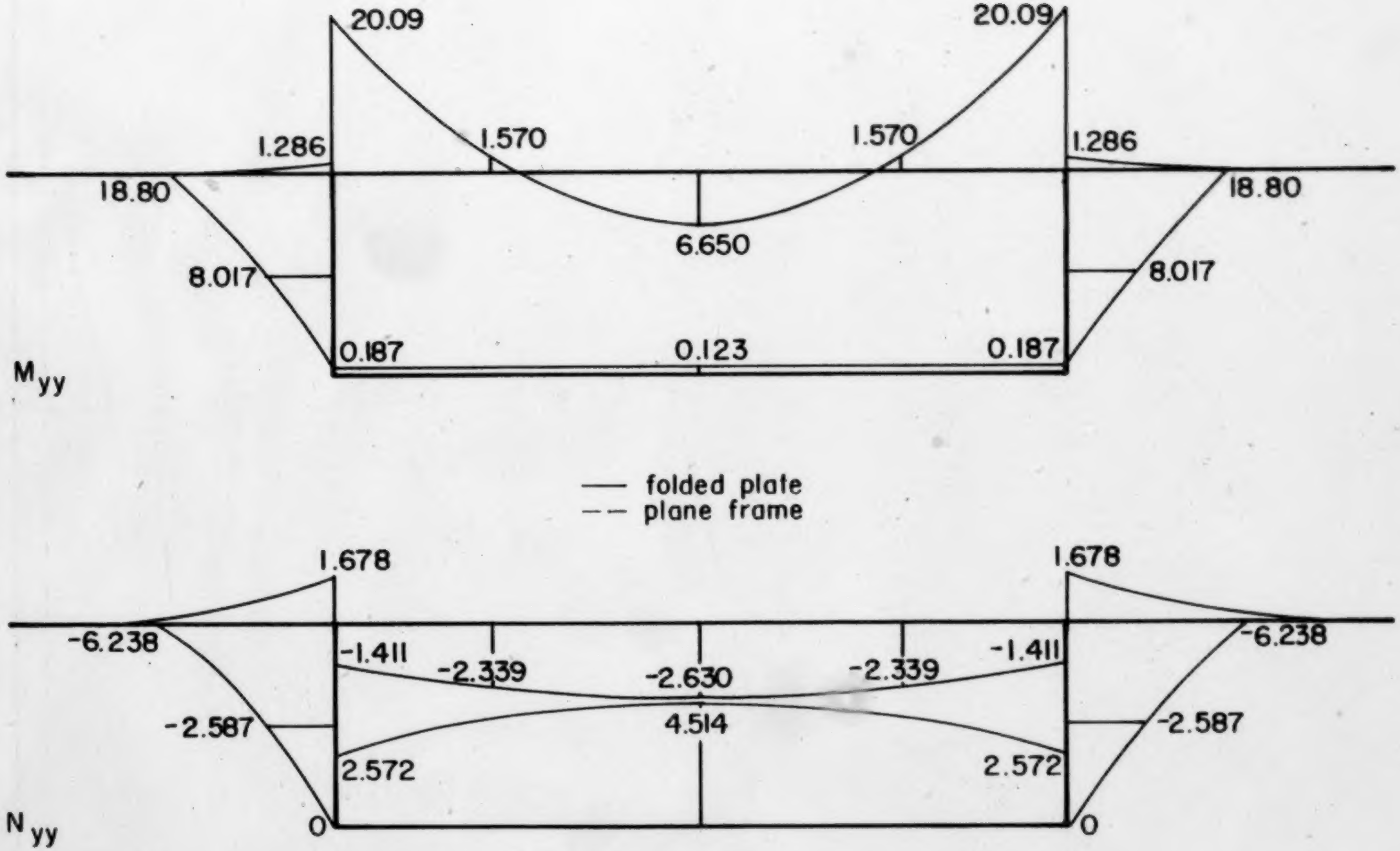
20.09
20.09
1.286
1.570
1.570
1.286
18.80
18.80
6.650
8.017
8.017
0.187
0.123
0.187
M_yy
— folded plate
-- plane frame
1.678
1.678
-6.238
-6.238
-1.411
-2.339
-2.630
-2.339
-1.411
-2.587
4.514
-2.587
2.572
2.572
0
0
N_yy

Figure 4.26 Myy and Nyy for truck load 2 (negative interior moment)

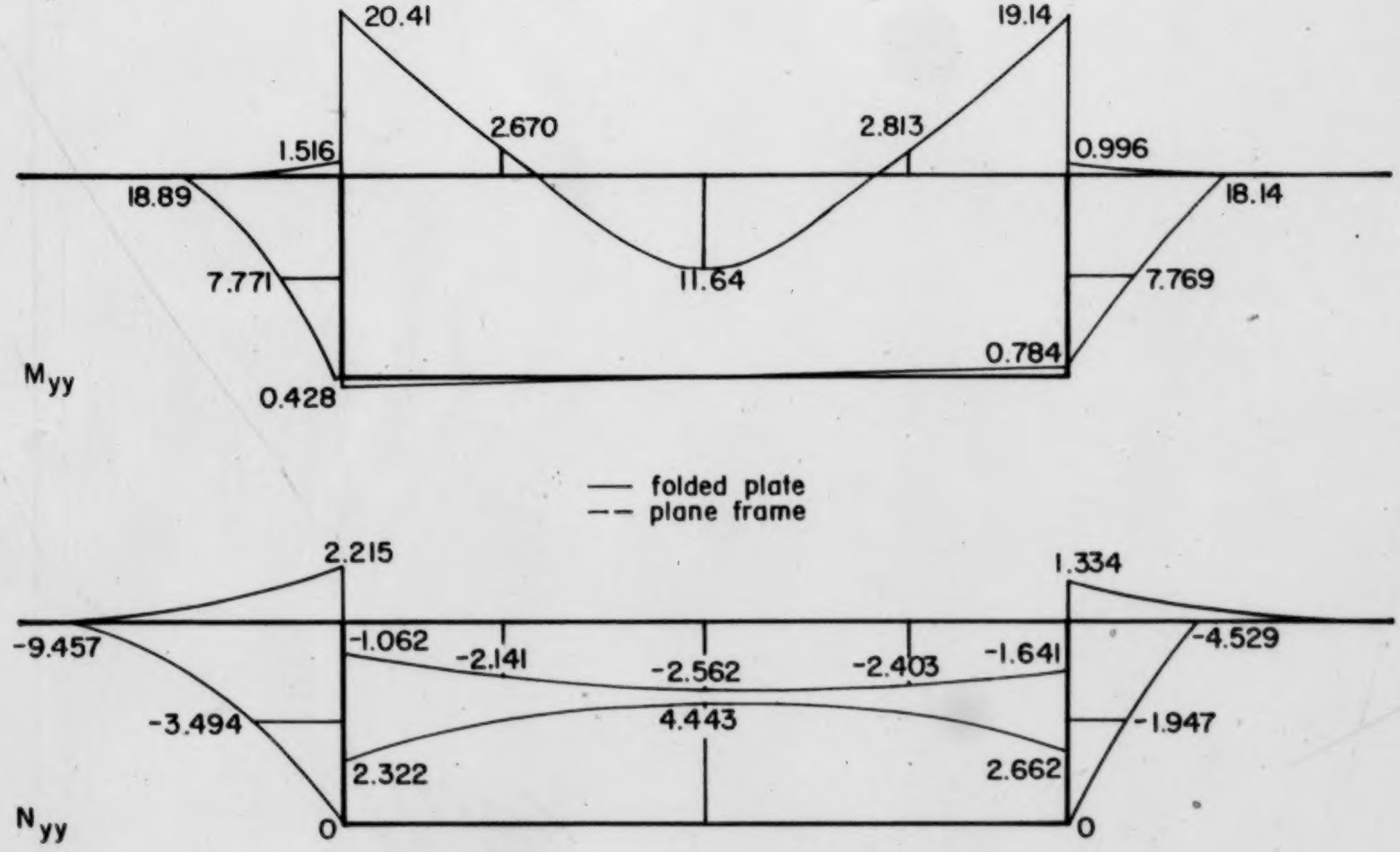

Figure 4.27 Myy and Nyy for truck load 3
(positive interior moment)

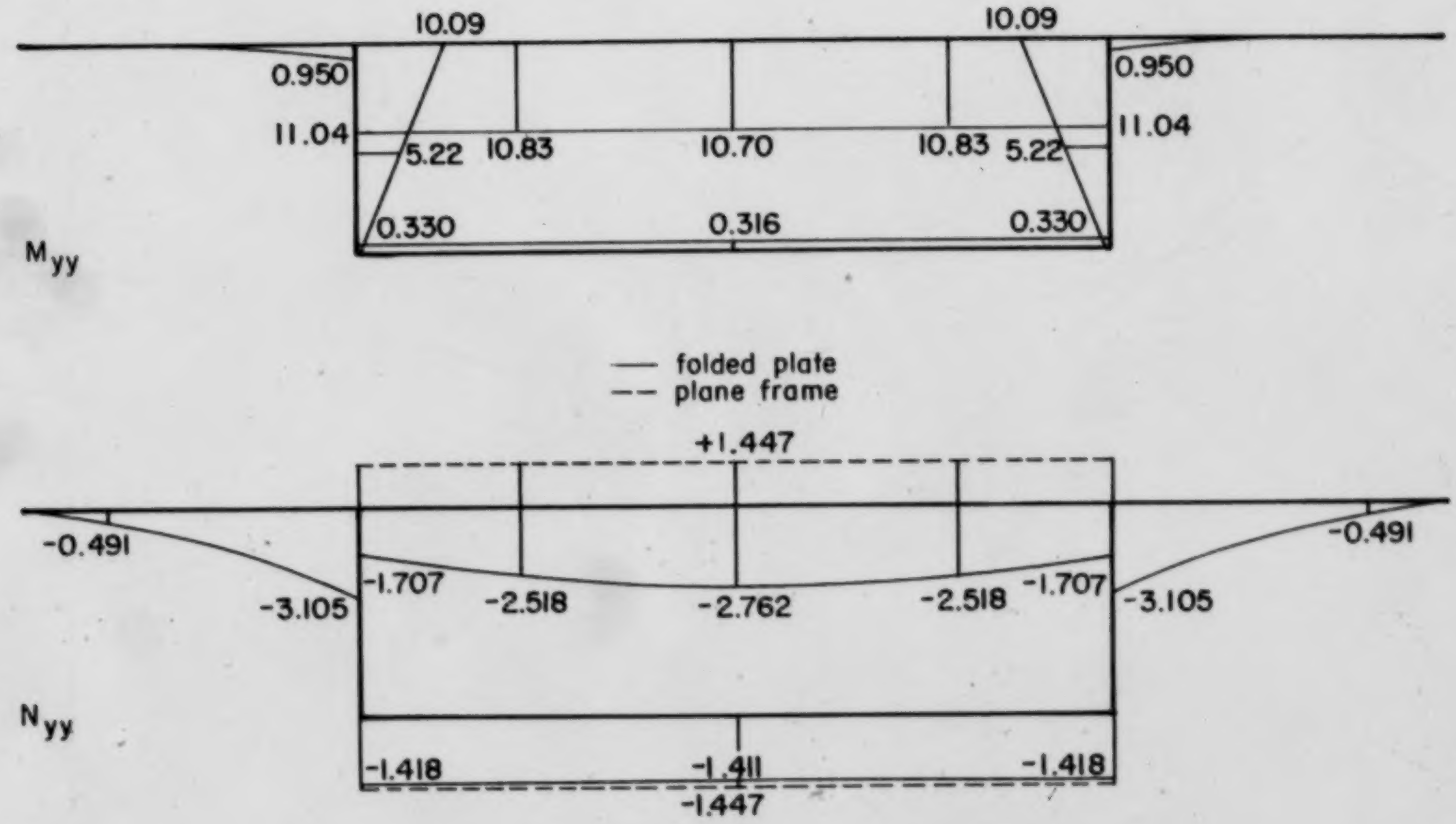

Figure 4.28 Myy and Nyy for temperature 1
(top surface 40 F above datum)

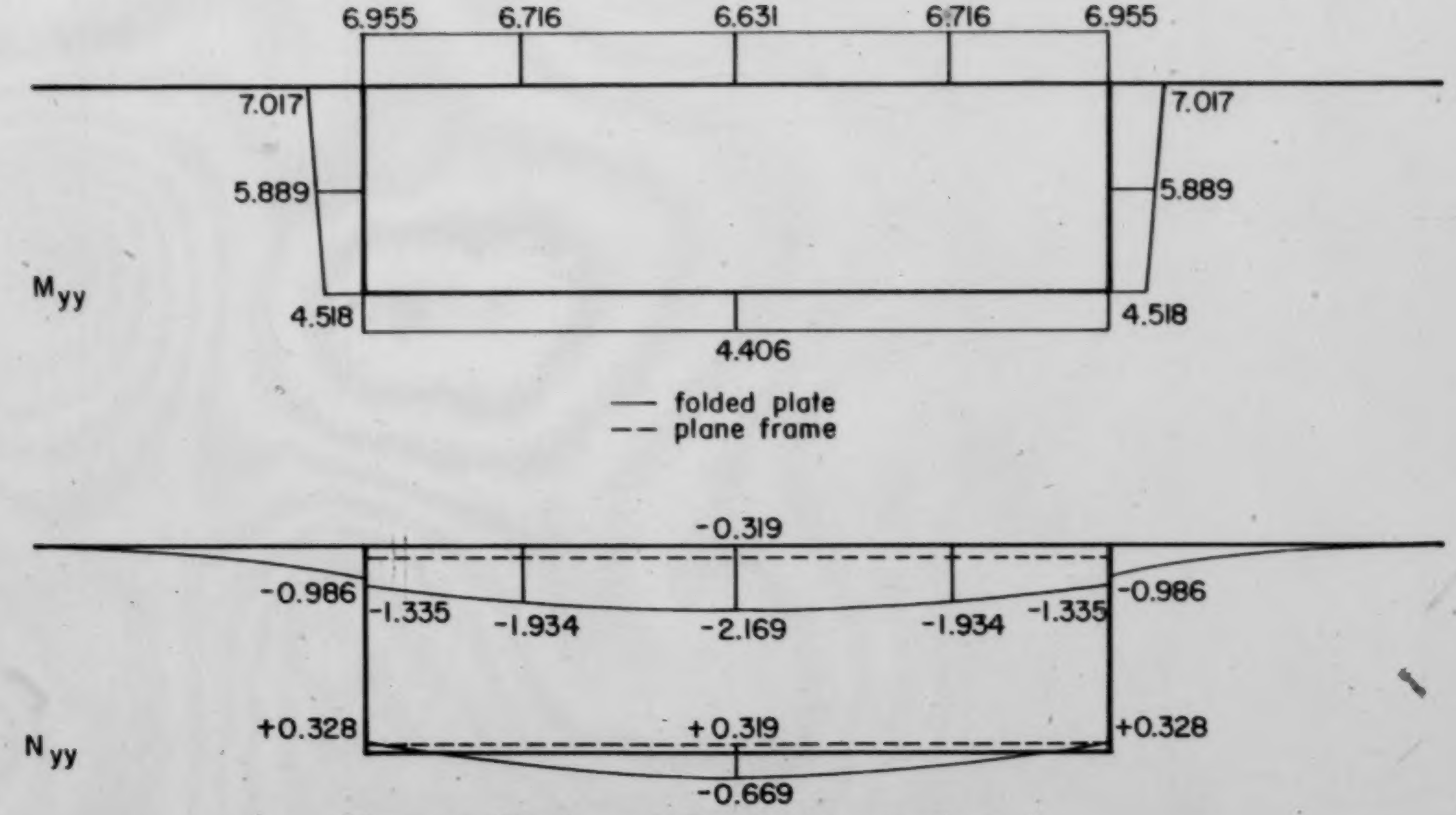
6.955
6.716
6.631
6:716
6.955
7.017
7.017
5.889
5.889
M_{yy}
4.518
4.518
4.406
— folded plate
-- plane frame
-0.319
-0.986
-1.335
-1.934
-2.169
-1.934
-1.335
-0.986
+0.328
+0.319
+0.328
N_{yy}
-0.669

Figure 4.29 Myy and Nyy for temperature 2 (interior surface 20 F above datum)

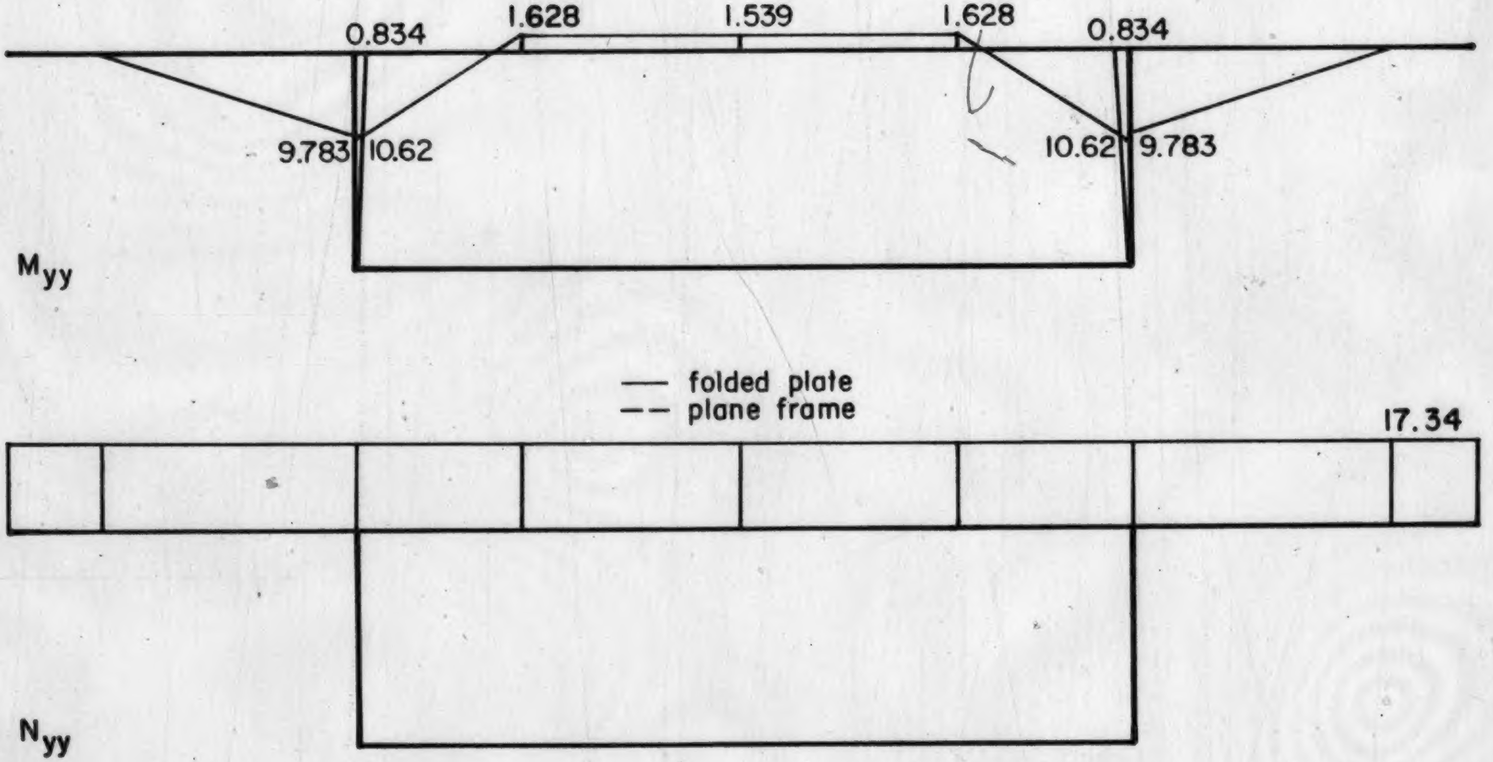
0.834
1.628
1.539
1.628
0.834
9.783
10.62
10.62
9.783
M_{yy}
— folded plate
-- plane frame
17.34
N_{yy}

Figure 4.30 Myy and Nyy for transverse prestress

differences for superimposed dead load and sidewalk live load. One can observe that for self weight, temperature, and prestressing, the loads are distributed across the deck while they are predominantly on the cantilevers for superimposed dead load and sidewalk live load.

Through the study of Figure 4.23, an interesting phenomena has been discovered. Note that the left interior moment given by folded plate theory is less than the right interior moment (2.179 vs 2.772) despite the fact that the left cantilever has a greater load than the right cantilever and the structure is symmetrical. In order to understand this, the superimposed dead load was separated into three components. Component 1 corresponded to a uniform load on the entire top surface. Component 2 consisted of the sidewalk and railing on the left cantilever while component 3 consisted of the curb on the right cantilever. It was found that for the load on the left cantilever, the moment in the web was greater than that in the cantilever. In fact, the sum of the moments in the cantilever and top slab equalled the moment in the web. This contradicts our intuition which tells us that the moment in the cantilever should equal the sum of the moments in the top slab and web for a load applied on the cantilever.

To understand this phenomena, the model of Figure 4.19 was simplified and an investigation was carried out. All elements were assumed to have constant thickness. The element loads were replaced by nodal loads. Poisson's ratio was set to zero. Four loading cases were considered. Loading 1 consisted of a uniform load at node 1 (tip of the cantilever) while loading 2 consisted of a uniform load at node 2 (interior portion of the cantilever). Loadings 3 and 4 consisted of concentrated midspan loads at nodes 1 and 2 respectively. The cantilever moment was found to be greater than the web moment for all loading cases except loading 2. For this case, the web moment was found to be greater than the cantilever moment. As an independent check, program MUPDI (25) was also run and the results were found to be identical to those given by program BOXGIRD. No explanation has been found for this anomaly of having the web moment greater than the cantilever moment for a uniform load applied on the interior portion on the cantilever.

The analysis for longitudinal shear and torsion (minimum section) is now considered. Six different loading cases are applied to the structure (Figure 4.31). These include self weight, superimposed dead load, sidewalk live load, and three variations of lane load. The variations of AASHTO HS25 lane load correspond to no eccentricity, left eccentricity, and right eccentricity. Note that 26 k and 0.64 klf are the concentrated load for shear and uniform load respectively for an HS20 load, 1.25 converts an HS20 load to an HS25 load, 1.126 is the impact

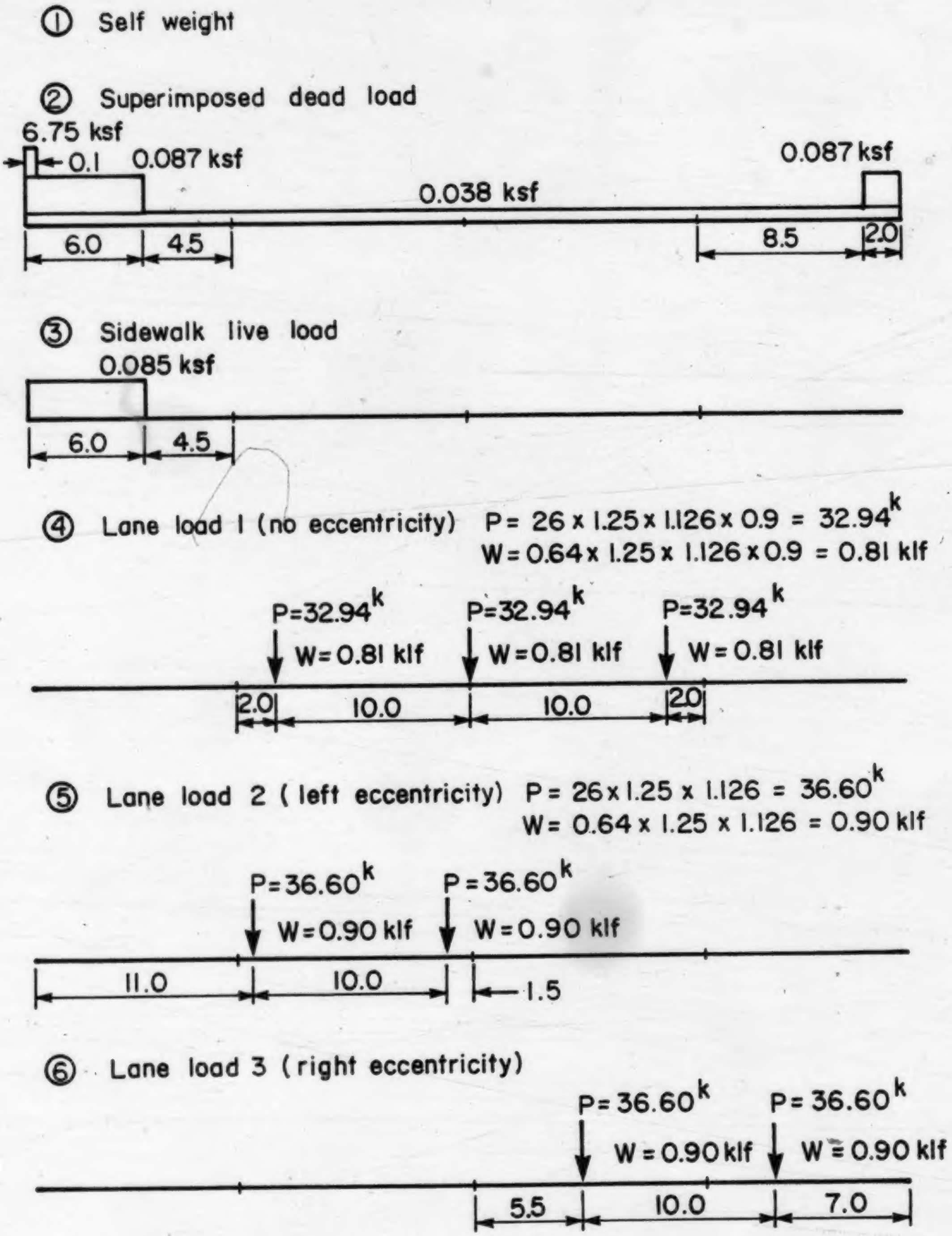
① Self weight
② Superimposed dead load
6.75 ksf
0.1
0.087 ksf
0.087 ksf
0.038 ksf
6.0
4.5
8.5
2.0
③ Sidewalk live load
0.085 ksf
6.0
4.5
④ Lane load 1 (no eccentricity)
P = 26 x 1.25 x 1.126 x 0.9 = 32.94^k
W = 0.64 x 1.25 x 1.126 x 0.9 = 0.81 klf
P=32.94^k
W=0.81 klf
P=32.94^k
W=0.81 klf
P=32.94^k
W=0.81 klf
2.0
10.0
10.0
2.0
⑤ Lane load 2 (left eccentricity)
P = 26 x 1.25 x 1.126 = 36.60^k
W = 0.64 x 1.25 x 1.126 = 0.90 klf
P=36.60^k
W=0.90 klf
P=36.60^k
W=0.90 klf
11.0
10.0
1.5
⑥ Lane load 3 (right eccentricity)
P=36.60^k
W=0.90 klf
P=36.60^k
W=0.90 klf
5.5
10.0
7.0

Figure 4.31 Loading cases for longitudinal shear and torsion

factor for a 272′ span, and 0.9 is the load reduction factor for 3 lanes.

Figures 4.32 to 4.37 show the membrane shear force diagram (Nxy) for each loading case. Note again that tension is positive and the units are k/ft. It should be observed that all diagrams have the same general shape, but the results shift towards one web or the other depending on the eccentricity. It should also be noted that the scale for self weight is one third the scale for the other five diagrams. This indicates that most of the diagonal tension in the web is due to self weight. One may notice that the longitudinal prestress, which counteracts the effects of self weight, has not been included in this analysis. This is because the compressive stress and vertical component of the prestressing are included in the ACI design equations. These values would be obtained from the program TIMEDEP.

4.7 Conclusions

This chapter has developed the computer program BOXGIRD, based on the folded plate method, for the three-dimensional analysis of box girder bridges. This program simplifies the task of the design engineer and provides him with more precise information. Numerical examples have illustrated the versatility and accuracy of the program.

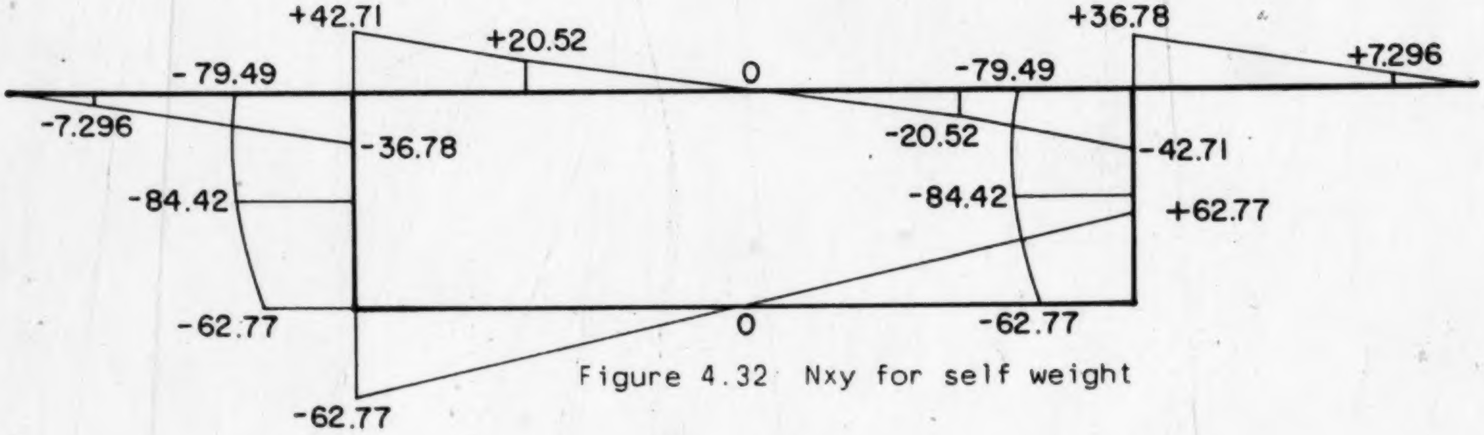
+42.71
+20.52
0
+36.78
+7.296
-79.49
-79.49
-7.296
-36.78
-20.52
-42.71
-84.42
-84.42
+62.77
-62.77
0
-62.77
-62.77

Figure 4.32 Nxy for self weight

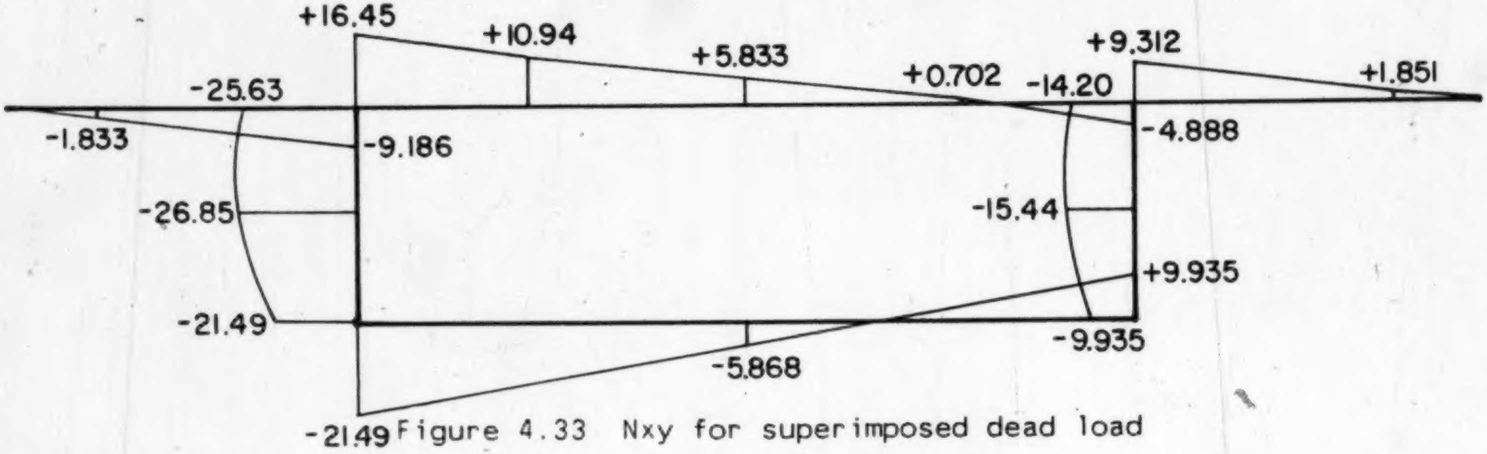
+16.45
+10.94
+5.833
+0.702
+9.312
+1.851
-25.63
-14.20
-1.833
-9.186
-4.888
-26.85
-15.44
+9.935
-21.49
-9.935
-5.868
-21.49

Figure 4.33 Nxy for superimposed dead load

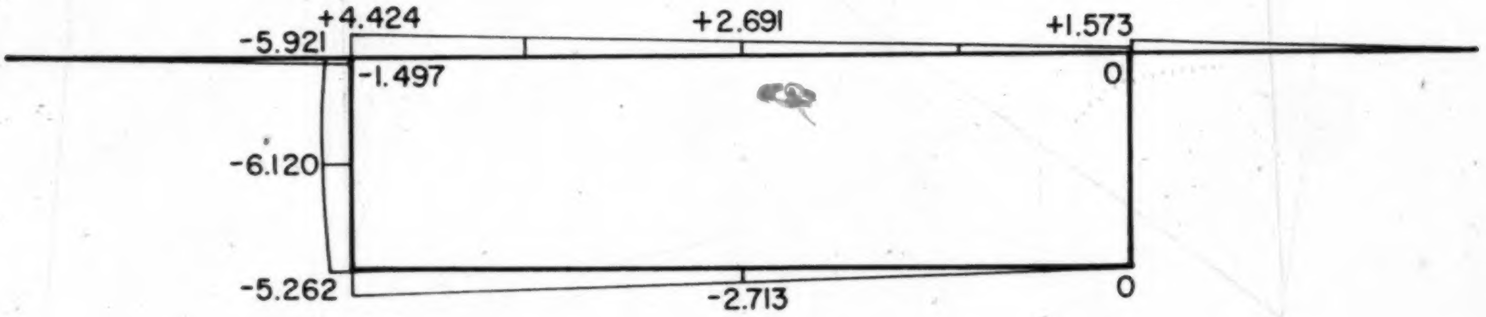
+4.424
+2.691
+1.573
-5.921
-1.497
0
-6.120
-5.262
-2.713
0

Figure 4.34 Nxy for sidewalk live load

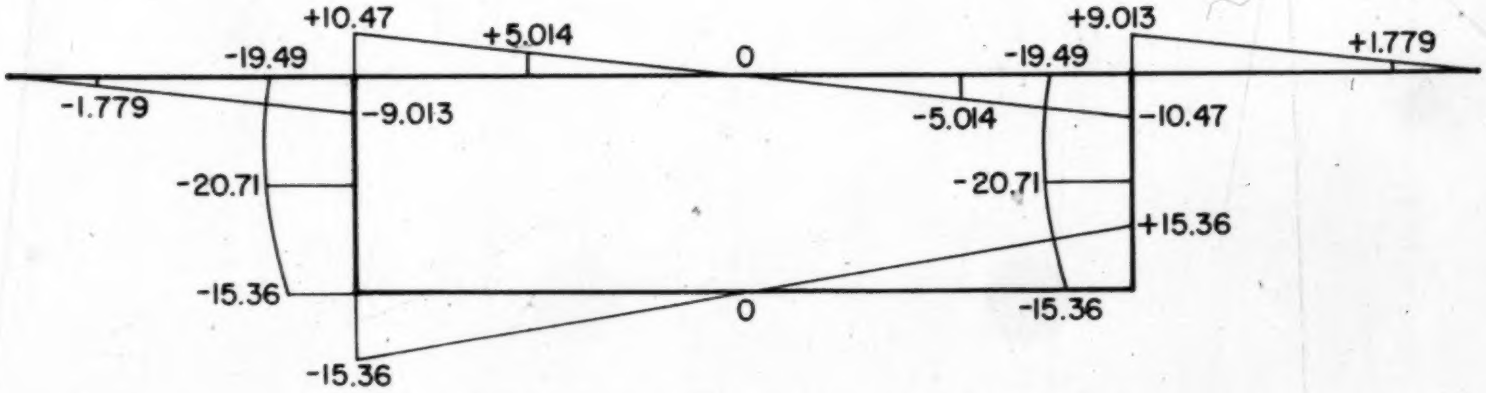
+10.47
+5.014
-19.49
0
+9.013
-19.49
+1.779
-1.779
-9.013
-5.014
-10.47
-20.71
-20.71
+15.36
-15.36
0
-15.36
-15.36

Figure 4.35 Nxy for lane load 1 (no eccentricity)

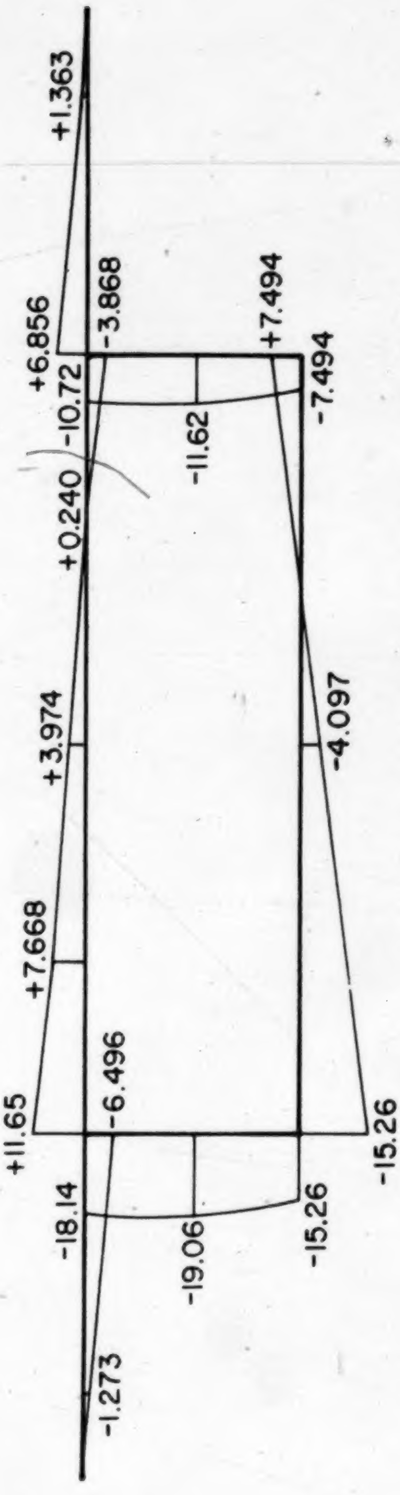
+1.363
+6.856
-3.868
+7.494
-7.494
-10.72
-11.62
+0.240
+3.974
-4.097
+7.668
+11.65
-6.496
-15.26
-18.14
-19.06
-15.26
-1.273

Figure 4.36 Nxy for lane load 2 (left eccentricity)

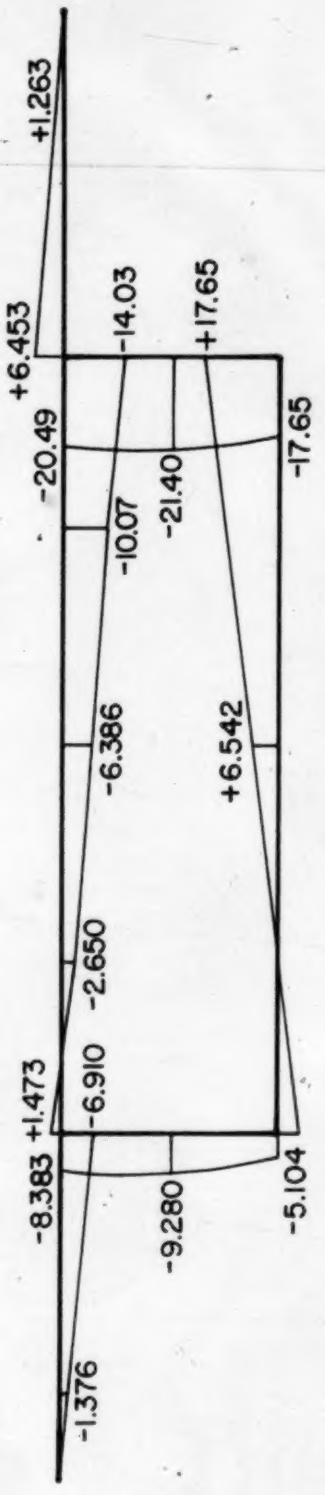
+1.263
+6.453
-14.03
+17.65
-20.49
-17.65
-10.07
-21.40
-6.386
+6.542
-2.650
+1.473
-6.910
-8.383
-9.280
-5.104
-1.376

Figure 4.37 Nxy for lane load 3 (right eccentricity)

5. PARTIAL PRESTRESSING

5.1 Introduction

This chapter discusses the application of partial prestressing to the design of segmental bridges and offers some new computational techniques for the analysis of partially prestressed concrete sections. Although the concept of partial prestressing was introduced by Abeles as early as 1945, it is only in recent years that it has become a widely discussed topic. Consequently, the motivation behind the use of partial prestressing will be reviewed. Then the load-deflection response of partially prestressed concrete beams will be discussed. From this discussion, it will be apparent that three types of analysis are required to completely describe the behaviour of a partially prestressed concrete beam: (1) uncracked section analysis, (2) cracked section analysis, and (3) ultimate strength analysis. Each of these types of analysis will be considered in detail. Some serviceability aspects of partial prestressing will then be studied. These include cracking, fatigue, and deformation. Finally, numerical examples will show how the analysis procedures can be applied.

5.2 Why partial prestressing?

By virtue of their historical developments, reinforced concrete and prestressed concrete have been treated differently. On one hand, reinforced concrete members have been analysed on the basis of the cracked section, and pseudo tensile stresses in the order of 2000 to 3000 psi would be obtained if one divides the moment by the section modulus. On the other hand, prestressed concrete members have been analysed on the basis of the uncracked section. Tensile stresses have been limited to zero or a small value.

Abeles (149) coined the term "partially prestressed concrete" to consider the general case whose extremes are conventional reinforced concrete and fully prestressed concrete. In the general case, partial prestressing can be achieved by having prestressing tendons stressed to lower levels, or by combining fully prestressed tendons with nonprestressed reinforcement (either nonstressed prestressing or conventional bars).

Partial prestressing can be used to improve the economy and serviceability of the design while maintaining the same ultimate strength. It possesses some advantages of each of its limiting cases. When compared to reinforced concrete, partially prestressed concrete offers better cracking and deflection control (short and long term). When compared to fully prestressed concrete, partially prestressed concrete offers better camber control (short and long term) as well as higher ductility and energy absorption to failure.

It should be noted that tensile stresses in prestressed concrete are not necessarily objectionable by themselves. Rather, it is their effect on cracking, fatigue, and deformation that is of concern:

(1) cracking - the maximum crack width under full service load must be limited to a specified value to prevent corrosion of the reinforcement and to ensure water-tightness of bridge decks and reservoirs.

(2) fatigue - the maximum stress range in the reinforcing and prestressing due to the application of live load must be less than a specified value in order to guarantee the required fatigue life.

(3) deformation - the short and long-term deflections under service load must be within specified limits.

5.3 Load deflection response

The behaviour of partially prestressed concrete can best be understood by first considering the load-deflection response of a simply supported fully prestressed concrete beam subjected to a monotonically increasing load (Figure 5.1). Note that the curve shown is for an under-reinforced beam having bonded tendons. A number of points on this curve should be mentioned. Points 1 and 2 correspond to the camber of a theoretically weightless beam under initial and effective prestress respectively. The stress diagram of the section under combined self weight and prestressing is given at point 3. Point 4 represents the balanced state (prestressing exactly balances the load) while point 5 shows decompression at the bottom fiber. Point 6 corresponds to cracking (at first loading) as the modulus of rupture is reached. Upon subsequent loading, points 5 and 6 coincide. Point 7 represents the level at which either the steel or concrete becomes inelastic while point 8 corresponds to the onset of yielding in the steel. Finally, point 9 corresponds to the maximum or ultimate load.

To fully predict the load-deflection response of a prestressed concrete beam, three distinct types of analysis must be performed:

(1) uncracked section analysis - an elastic analysis using the uncracked section must be carried out at load levels below that of cracking (for first loading) and decompression (for subsequent loading).

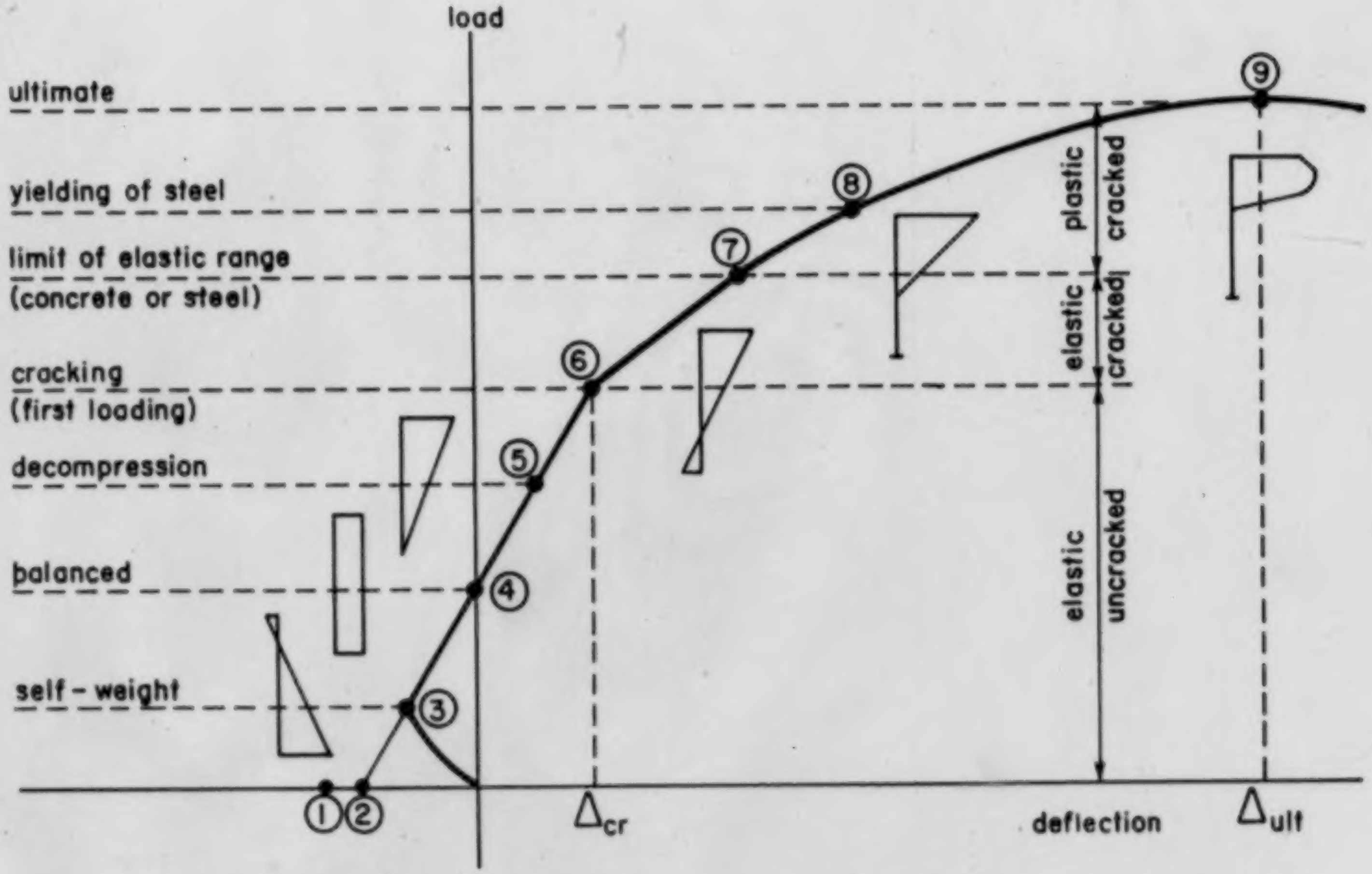

Figure 5.1 Typical load-deflection response of a prestressed concrete beam

(2) cracked section analysis - after cracking has occurred but before the steel or concrete has reached the inelastic range, an elastic analysis using the cracked section must be conducted.

(3) inelastic analysis - an inelastic analysis using the cracked section (such as a strain compatibility analysis) must be performed after the onset of inelastic behaviour.

The first two analyses give the response of the section to service loads while the last analysis gives the ultimate strength of the section. Each of these types of analysis will be discussed in detail in subsequent sections.

It is interesting to observe how the load-deflection response of a partially prestressed concrete beam differs from that of a fully prestressed concrete beam or a reinforced concrete beam (Figure 5.2). The diagram shows the magnitude of the dead load, live load, and ultimate (factored) load as well as the cracking load for each type of beam. A reinforced concrete beam is cracked under the effect of dead load while a fully prestressed concrete beam is uncracked under the effect of service load (dead load and live load). A partially prestressed beam falls anywhere between these two limits.

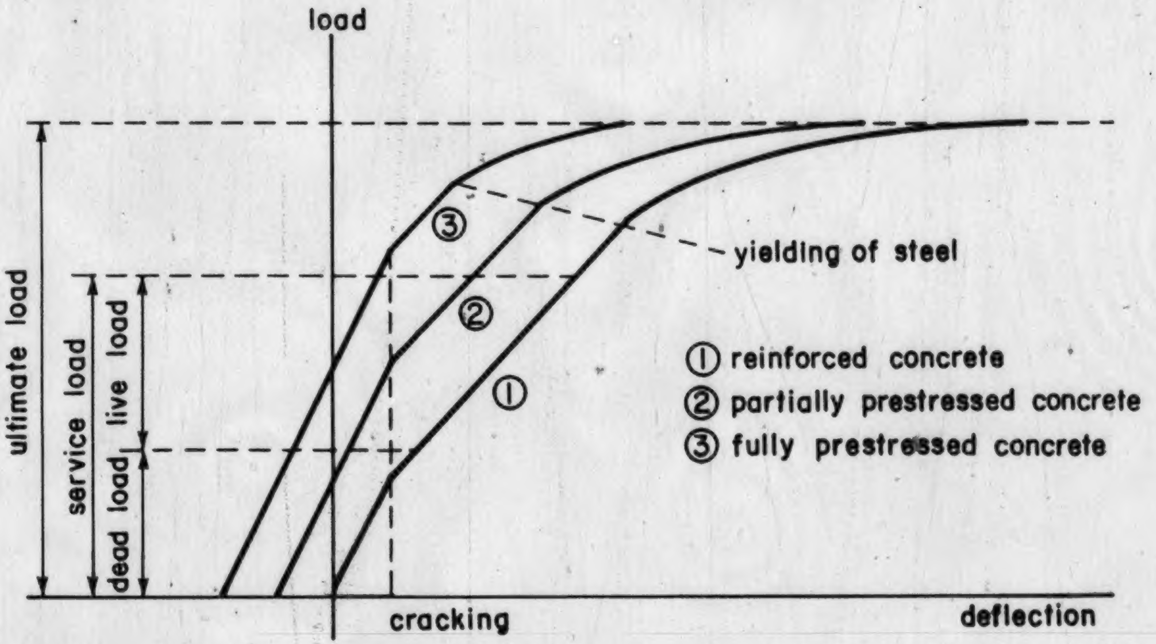
load
ultimate load
service load
live load
dead load
③
②
①
yielding of steel
① reinforced concrete
② partially prestressed concrete
③ fully prestressed concrete
cracking
deflection

Figure 5.2 Typical load-deflection response of various concrete beams

5.4 Analysis procedures

5.4.1 Introduction

A segmental bridge must be proportioned such that the combination of prestressed and/or nonprestressed reinforcement be adequate for both longitudinal and transverse flexure (Figure 5.3). The longitudinal flexural requirements can be obtained at various stages of erection and for the completed structure with the computer program TIMEDEP. Meanwhile, the transverse flexural requirements can be obtained for the completed structure with the computer program BOXGIRD. Once the flexural requirements have been determined, the steel can be proportioned by some method, and the design can be evaluated by the procedures outlined in the following sections. The service load response is given by either an uncracked or cracked section analysis while an inelastic analysis gives the ultimate strength.

The types of sections commonly considered in a segmental bridge (Figure 5.3) can conveniently be transformed into the case of a general I-girder (Figure 5.4) having both compressive and tensile conventional reinforcing in addition to prestressing. This section is subjected to both a normal force N′ and a bending moment M′ at the centroid of the uncracked section. The effective force

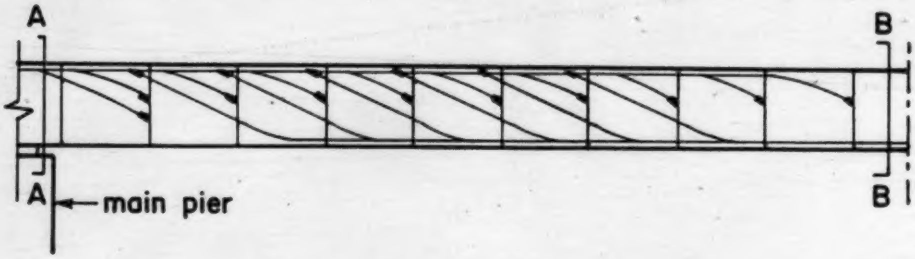
A
B
A
main pier
B

(a)elevation

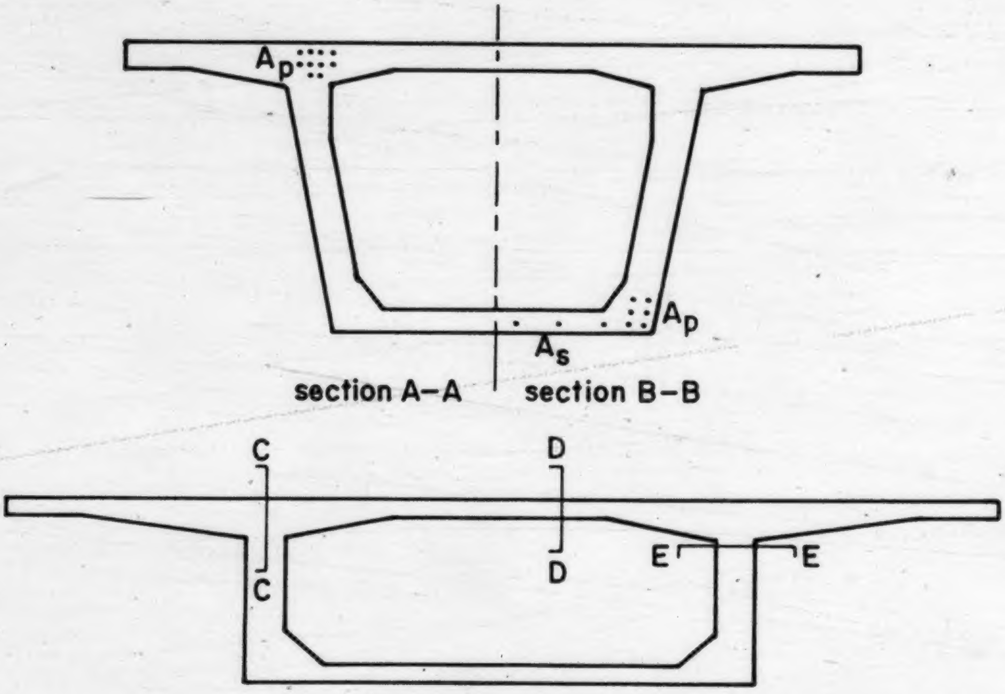
A_p
A_p
A_s
section A–A
section B–B
C
D
C
D
E
E

(b) cross section

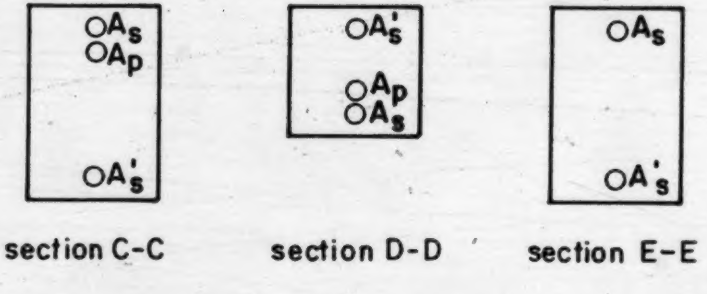
A_s
A_p
A'_s
A'_s
A_p
A_s
A_s
A'_s
section C-C
section D-D
section E-E

Figure 5.3 Segmental bridge analysis

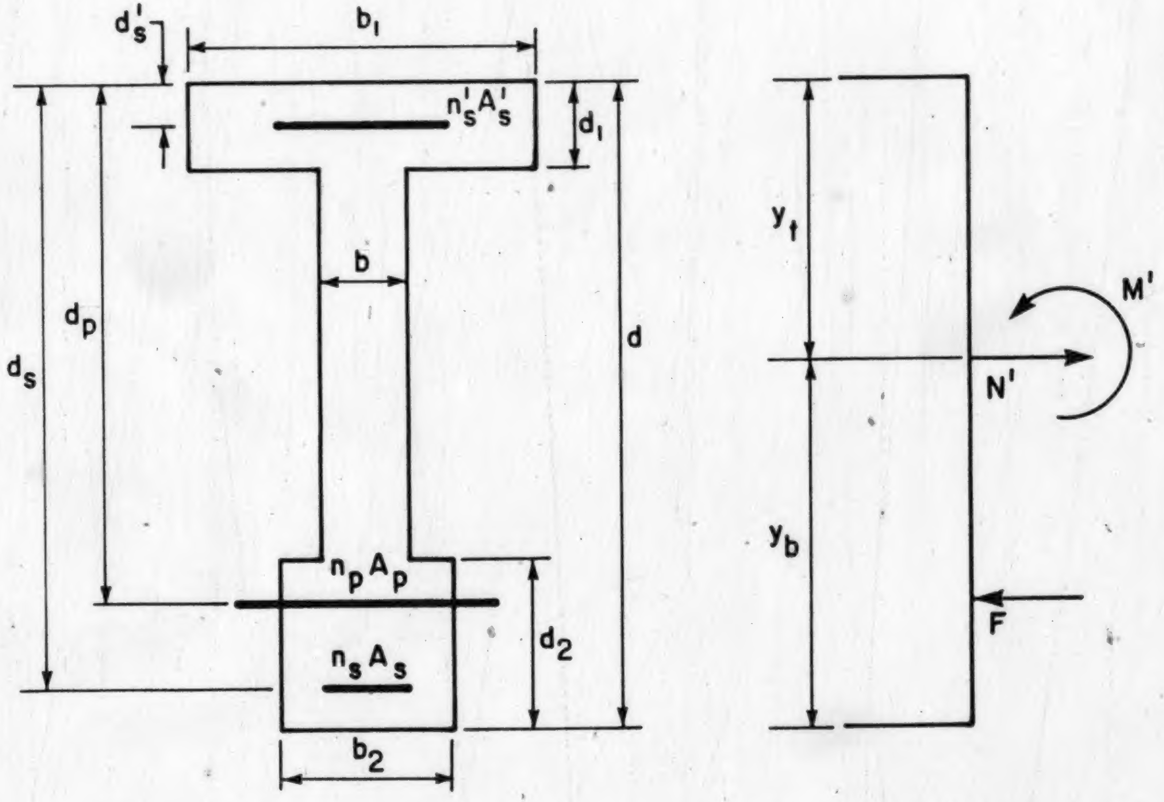
d_s'
b_1
$n_s' A_s'$
d_1
b
d_p
d_s
d
$n_p A_p$
$n_s A_s$
d_2
b_2
y_t
y_b
M'
N'
F

(a) cross section

(b) resultant forces

Figure 5.4 General I-girder analysis

of prestressing is given as F.

Let b be the stem width, b1 be the width of the top flange, and b2 be the width of the bottom flange. Also, let d be the section depth, d1 be the thickness of the top flange, and d2 be the thickness of the bottom flange. Furthermore, let As', As, and Ap be the areas of the compressive reinforcing, tensile reinforcing, and prestressing respectively having modular ratios ns', ns, and np and distances from the top of the section of ds', ds, and dp.

5.4.2 Uncracked section analysis

Consider the case of an uncracked I-girder having both compressive and tensile conventional reinforcing in addition to prestressing (Figure 5.5). Pertinent dimensions and actions have been defined previously.

The section properties of the uncracked section can conveniently be calculated by using a set of factors Auc, Quc, and Iuc'. These factors are respectively the area, first moment of area, and second moment of area about the top of the section. Note the similarity between these factors and the factors α, β, and γ which are used in conjunction with the cracked section analysis.

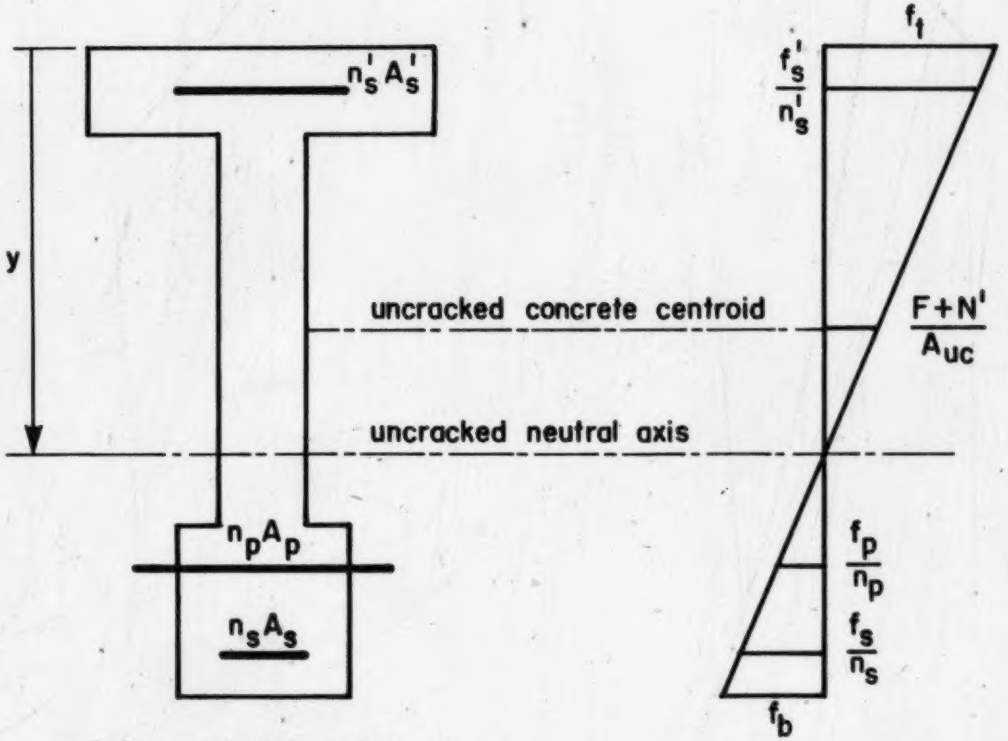
y
$n_s' A_s'$
$n_p A_p$
$n_s A_s$
uncracked concrete centroid
uncracked neutral axis
f_t
$\frac{f_s'}{n_s'}$
$\frac{F+N'}{A_{uc}}$
$\frac{f_p}{n_p}$
$\frac{f_s}{n_s}$
f_b

(a)uncracked transformed cross section

(b)concrete stresses

Figure 5.5 Uncracked section analysis

The following factors are used to determine the gross or uncracked untransformed section properties:

$$Auc = b\,d + (b1-b)d1 + (b2-b)d2 \tag{5.1a}$$

$$Quc = 1/2\,b\,d^{2} + 1/2(b1-b)d1^{2} - 1/2(b2-b)d2^{2} + (b2-b)d2\,d \tag{5.1b}$$

$$Iuc' = 1/3\,b\,d^{3} + 1/3(b1-b)d1^{3} + 1/3(b2-b)d2^{3} + (b2-b)d2\,d(d-d2) \tag{5.1c}$$

The second term is omitted for sections which do not have a top flange, while the third and fourth terms are neglected for sections which do not have a bottom flange. In other words, a rectangular beam requires only the first term, a T beam requires the first two terms, and an I beam requires all the terms.

The following additional terms must be added to those given previously to determine the uncracked transformed section properties:

$$Auc = Auc + (ns'-1)\,As' + (ns-1)\,As + (np-1)\,Ap \tag{5.2a}$$

$$Quc = Quc + (ns'-1)\,As'\,ds' + (ns-1)\,As\,ds + (np-1)\,Ap\,dp \tag{5.2b}$$

$$Iuc' = Iuc' + (ns'-1)\,As'\,ds'^{2} + (ns-1)\,As\,ds^{2} + (np-1)\,Ap\,dp^{2} \tag{5.2c}$$

Again these are general equations and only the necessary terms are required.

The remaining section properties can now be calculated as follows:

$$yt = Quc/Auc \tag{5.3}$$

$$yb = d - yt \tag{5.4}$$

$$Iuc = Iuc' - Auc\ yt^2 \tag{5.5}$$

$$St = Iuc/yt \tag{5.6}$$

$$Sb = Iuc/yb \tag{5.7}$$

Here yt and yb are the distances from the centroid to the top and bottom of the section, while St and Sb are the section moduli at the top and bottom. Of course, Auc and Iuc are the area and moment of inertia about the centroid.

The cracking moment can be determined (assuming that the modulus of rupture is equal to zero) with the following equation:

$$Mcr = F\ (Sb/Auc + dp - yt) - N'\ (Sb/Auc) \tag{5.8}$$

If the service moment M' exceeds the cracking moment Mcr, a cracked section analysis is required. The section properties calculated here are necessary for the cracked section analysis and thus have not been calculated in vain.

If the section has not cracked, the concrete stresses at the top and bottom of the section can be found.

$$ft = - \frac{F}{Auc} + \frac{F\ (dp - yt)}{St} + \frac{N'}{Auc} - \frac{M'}{St} \qquad (5.9)$$

$$fb = - \frac{F}{Auc} - \frac{F\ (dp - yt)}{Sb} + \frac{N'}{Auc} + \frac{M'}{Sb} \qquad (5.10)$$

Once the stresses at the top and bottom of the section have been found, the location of the neutral axis can be determined with the equation

$$y = \frac{ft}{ft - fb}\, d \qquad (5.11)$$

The steel stresses in the compressive reinforcement, tensile reinforcement, and prestressing are respectively found by proportion.

$$fs' = -ns' \frac{ds' - y}{y}\ ft \qquad (5.12a)$$

$$fs = -ns \frac{ds - y}{y}\ ft \qquad (5.12b)$$

$$fp = -np \frac{dp - y}{y}\ ft \qquad (5.12c)$$

The sign convention for the stresses is such that tension is positive and compression is negative.

5.4.3 Cracked section analysis

Consider the case of a cracked I-girder having both compressive and tensile conventional reinforcing in addition to prestressing (Figure 5.6). Pertinent dimensions and actions have been defined previously.

Nilson (152,189) has proposed that the effective prestressing force F be replaced by a fictitious external force R which causes decompression. In this way, the analysis can be simplified to that of a conventionally reinforced concrete section under the combined effects of axial force and bending moment.

$$R = F \left\{ 1 + \frac{Ep\ Ap}{Ec\ Auc} \left[1 + \frac{(dp - yt)^2}{Iuc/Auc} \right] \right\} \tag{5.13}$$

It is convenient to relate all forces and dimensions to the top of the section. Consequently, the resultant forces N and M at the top of the section are given by the equations

$$N = R - N' \tag{5.14}$$

$$M = M' + N'\ yt - R\ dp \tag{5.15}$$

The location of the neutral axis y of the cracked transformed section is given by the following cubic equation.

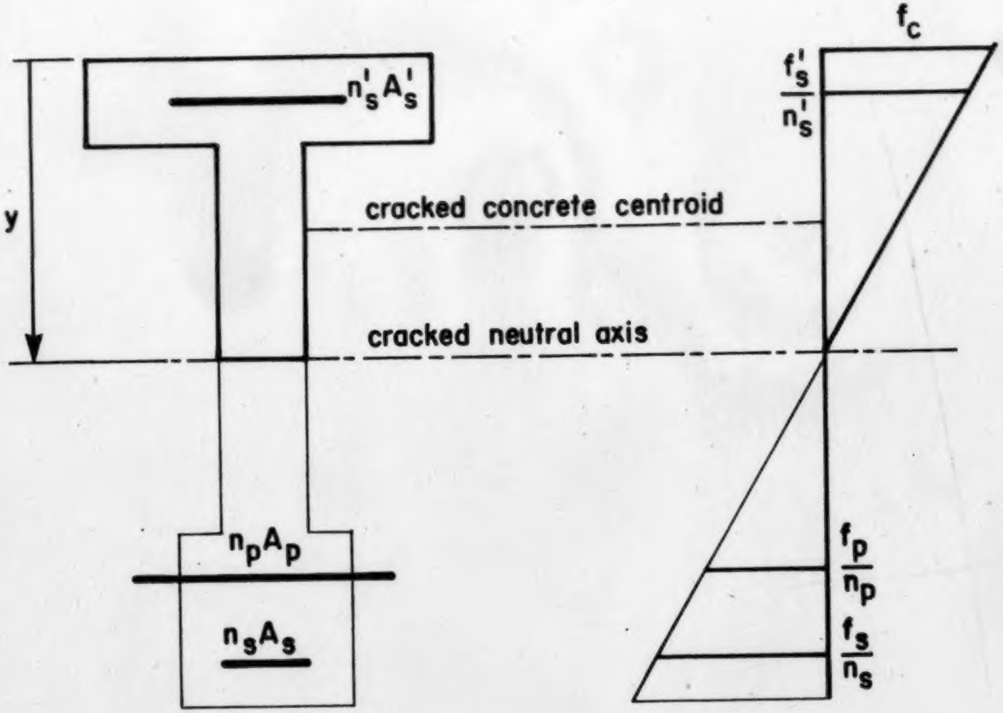
y
$n_s' A_s'$
cracked concrete centroid
cracked neutral axis
$n_p A_p$
$n_s A_s$
f_c
$\frac{f_s'}{n_s'}$
$\frac{f_p}{n_p}$
$\frac{f_s}{n_s}$

(a) cracked transformed cross section

(b) concrete stresses

Figure 5.6 Cracked section analysis

$$1/6\ b\ N\ y^3 + 1/2\ b\ M\ y^2 + (\beta N + \alpha M)\ y - (\gamma N + \beta M) = 0 \tag{5.16}$$

where

$$\alpha = (b1-b)\ d1 + (ns'-1)\ As' + ns\ As + np\ Ap \tag{5.17a}$$

$$\beta = 1/2\ (b1-b)\ d1^2 + (ns'-1)\ As'\ ds' + ns\ As\ ds + np\ Ap\ dp \tag{5.17b}$$

$$\gamma = 1/3\ (b1-b)\ d1^3 + (ns'-1)\ As'\ ds'^2 + ns\ As\ ds^2 + np\ Ap\ dp^2 \tag{5.17c}$$

One advantage of the method is that the form of the cubic equation always remains the same. By including various terms in the factors α, β, and γ a wide range of problems may be solved. For instance, only the third term would be required for a singly reinforced beam while the second and third terms would be included for a doubly reinforced beam. A T beam would have the first and third terms. The fourth term would be included for prestressing steel and so on.

The Newton-Raphson method (with a starting value of y=0) is suggested for solving the cubic equation. It has been found by experience that 3 to 4 iterations are usually sufficient to achieve an accuracy of 0.1%.

Once the neutral axis has been found the concrete stress can be determined with the equation

$$fc = \frac{M\,y}{1/6\;b\;y^3 + \beta y - \gamma} \qquad (5.18)$$

The steel stresses in the compressive reinforcement, tensile reinforcement, and prestressing are respectively found by proportion.

$$fs' = -ns' \; \frac{ds' - y}{y} \; fc \qquad (5.19a)$$

$$fs = -ns \; \frac{ds - y}{y} \; fc \qquad (5.19b)$$

$$fp = -np \; \frac{dp - y}{y} \; fc + \frac{R}{Ap} \qquad (5.19c)$$

The sign convention for the stresses is such that tension is positive and compression is negative.

A second advantage of the method is that the stresses can be determined directly without the intermediate calculation of the section properties. Should the section properties be required (ie for the calculation of deflections), they can be found with the following equations.

$$Acr = b\;y + \alpha \qquad (5.20)$$

$$Qcr = 1/2\;b\;y^2 + \beta \qquad (5.21)$$

$$Icr' = 1/3\;b\;y^3 + \gamma \qquad (5.22)$$

$$ycr = Qcr/Acr \quad (5.23)$$

$$Icr = Icr' - Acr\ ycr^2 \quad (5.24)$$

Here ycr is the distance from the centroid of the cracked transformed section to the top of the section while Acr, Qcr, and Icr are the area, first moment of area, and second moment of area (ie moment of inertia) of the cracked transformed section respectively.

Derivation of the preceding equations are discussed by Shushkewich (180). Simplified equations (requiring the solution of a quadratic instead of a cubic) are also given for the special case of no axial force or prestressing.

It is interesting to note the similarities and differences in the analysis of the uncracked and cracked sections (Table 5.1). The analysis of the uncracked section requires the calculation of the section properties, concrete stresses, and neutral axis whereas the analysis of the cracked section requires the calculation of the neutral axis, concrete stress, and section properties (which are optional). In other words, the order of the operations are exactly the opposite for the two analyses. The steel stresses are determined by the same equations for both analyses. As well, there is a similarity between the factors Auc, Quc, and Iuc' of the uncracked section analysis and the factors α, β, and γ of the cracked section analysis.

uncracked section analysis	cracked section analysis
1. factors	1. factors
2. section properties	2. neutral axis
3. concrete stresses	3. concrete stress
4. neutral axis	4. section properties
5. steel stresses	5. steel stresses

Table 5.1 - Order of operations for the analysis of uncracked and cracked sections

5.4.4 Ultimate strength analysis

The ultimate strength of an I-girder having both compressive and tensile reinforcing in addition to prestressing (Figure 5.7) can be found with the equations of ACI 318-77 (195) or by performing a strain-compatibility analysis. The equations in the code are approximate, and a conservative estimate is made for the level of stress in the prestressing. Various equations must be used depending on whether the section is rectangular or flanged, and also on whether the reinforcement index is less than or greater than a certain value. Consequently, the strain-compatibility approach is an attractive alternative. This iterative technique invokes the compatibility of strains across the section as well as the equations of equilibrium. Although only a few iterations are usually necessary, the use of a programmable calculator or micro-computer is still recommended.

The primary requirement for a strain-compatibility analysis is a mathematical relationship for the stress-strain curve of the prestressing. Although many investigators have proposed expressions for this curve, the equation of Mattock (157), as given below, is both concise and accurate.

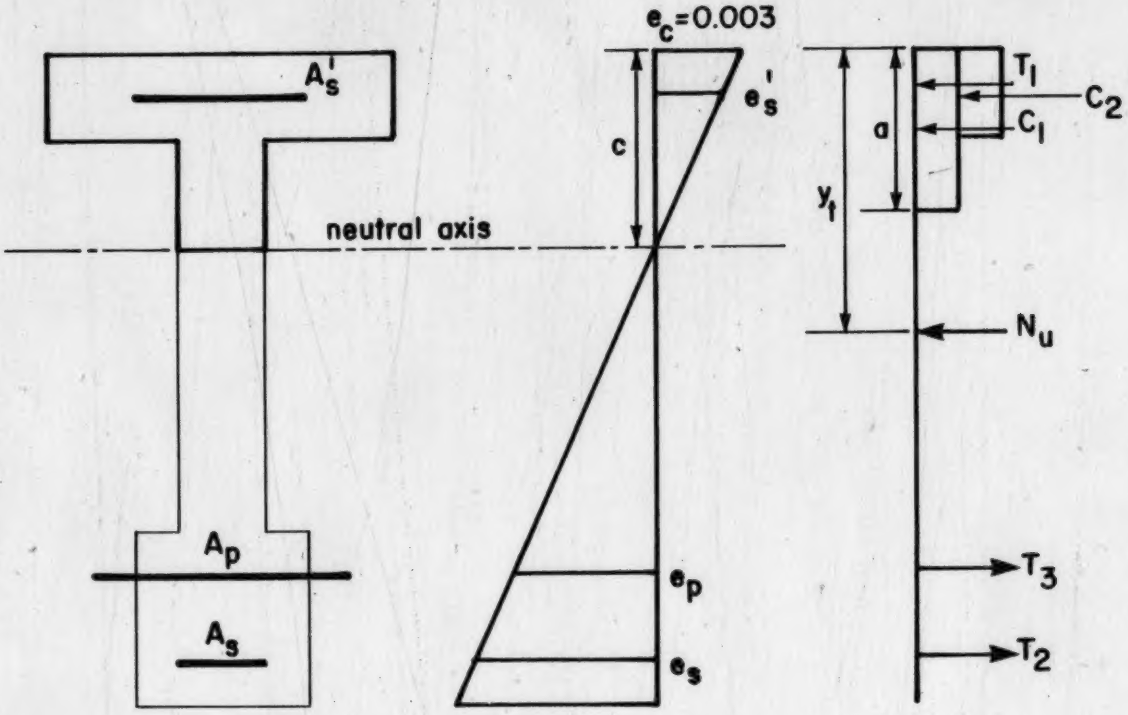
A_s'
neutral axis
A_p
A_s
$e_c=0.003$
e_s'
c
e_p
e_s
T_1
C_2
C_1
a
y_t
N_u
T_3
T_2

(a) cross section (b) strains (c) forces

Figure 5.7 Ultimate strength analysis

$$fp = Ep\, ep \left\{ Q + \frac{1 - Q}{\left[1 + \left(\frac{Ep\, ep}{K\, fpy} \right)^{R} \right]^{(1/R)}} \right\} \qquad (5.25)$$

The variables used in this equation are defined in Figure 5.8. Before this expression can be used for a particular type of steel, the constants K, Q, and R must be evaluated. The value of K is determined by extrapolating the two linear parts of the curve so that they meet at a stress of K fpy. Since fpy is known, K can be determined. The coefficient Q is evaluated by using the following equation:

$$Q = \frac{fpu - K\, fpy}{Ep\, epu - K\, fpy} \qquad (5.26)$$

Finally, the value of R is found by solving the nonlinear Mattock equation for the case fp=fpy when ep=0.010.

The coefficients have been determined by Mattock for the following two cases:

(1) seven wire strand (fpu=274.0 ksi fpy=239.2 ksi)
K=1.06 Q=0.0105 R=7.447

(2) alloy steel bar (fpu=156.6 ksi fpy=148.0 ksi)
K=1.02 Q=0.0043 R=4.190

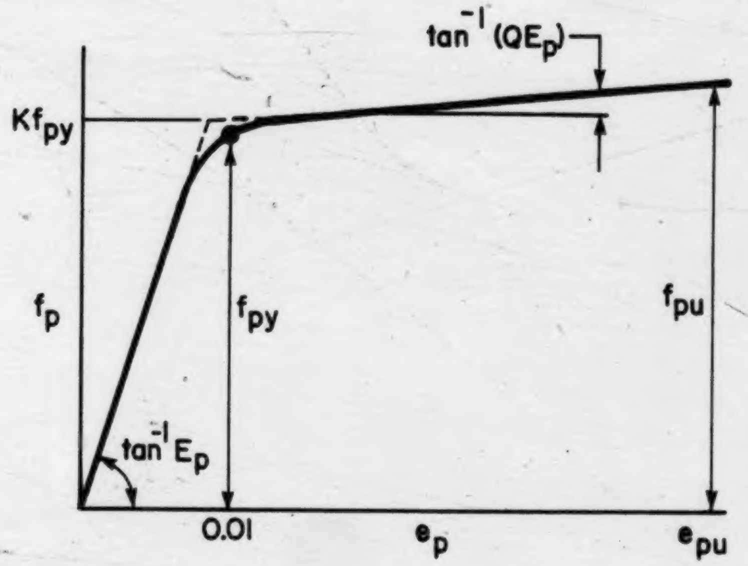

Figure 5.8 Typical stress-strain curve for prestressing steel

Let us first describe strain-compatibility in general terms and then take a detailed look at a step-by-step procedure. The depth of the equivalent rectangular stress block is arbitrarily assumed and the distance from the neutral axis to the top of the section is calculated. Since the distribution of strains across the section is linear and the ultimate strain in the concrete is known, strains in the compressive reinforcing, tensile reinforcing, and prestressing can be determined. It is important to note that the strain in the prestressing must be added to the strain due to the effective prestress force as well as the strain causing decompression (see Nilson (189)). Once the strains have been found, the stresses can be calculated. A bilinear stress-strain curve is used to determine the stress in the reinforcing, whereas the stress in the prestressing is based on the equation previously outlined. Forces in the steel and concrete can be found, and the equations of equilibrium are used to find a new value for the depth of the stress block. A slight complication results in determining whether the depth of the stress block falls within the flange or web of a T beam. The procedure is repeated until the difference between the old value and new value becomes sufficiently small. The ultimate moment capacity is determined by taking moments about the top of the section.

The strain-compatibility method consists of the following sequence of operations:

(1) Assume $a=d/10$

(2) Find location of neutral axis $c=a/\beta_1$

(3) Find strains

$$es' = 0.003\ \frac{ds' - c}{c}$$

$$es = 0.003\ \frac{ds - c}{c}$$

$$ep = 0.003\ \frac{dp - c}{c} + \frac{R}{Ep\ Ap}$$

(4) Find stresses

$fs' = Es'es' \qquad -fy < fs' < fy$

$fs = Es\ es \qquad -fy < fs < fy$

fp : see Mattock equation

(5) Find forces (C1 and C2 are not yet complete forces)

$T1 = As'fs'$

$T2 = As\ fs$

$T3 = Ap\ fp$

$C1 = -0.85\ fc'\ b$

$C2 = -0.85\ fc'\ (b1 - b)$

(6) Find a'

if $a < d1$ $\quad a' = -(T1 + T2 + T3 - Nu)/(C1 + C2)$

$\qquad\qquad d' = a'$

if $a > d1$ $\quad a' = -(T1 + T2 + T3 + C2\ d1 - Nu)/C1$

$\qquad\qquad d' = d1$

(7) Check tolerance

if $\left|\frac{a' - a}{a'}\right| > 0.001$ set $a = a'$ and go to (2)

(8) Determine ultimate axial force and bending moment

$$Nu = \phi\,(T1 + T2 + T3 + C1\,a + C2\,d')$$

$$Mu = \phi\,(T1\,ds' + T2\,ds + T3\,dp + C1\,a^2/2 + C2\,d'^2/2) - Nu\,yt$$

5.5 Serviceability considerations

When tensile stresses are allowed in concrete structures, the serviceability criteria of cracking, fatigue, and deformation must be respected. This requires that one be able to predict crack widths, fatigue stress ranges, and deflections and compare these values to maximum permissable limits.

Several formulas exist for the prediction of crack widths at the tension face of concrete members. The expression of Gergely and Lutz has been adopted by the ACI (195) and is used extensively in the design of reinforced concrete members in North America. It should be noted that this formula is not directly applicable to partially prestressed concrete elements. In Europe, the formulas of CEB/FIP 1970 (73) and CEB/FIP 1978 (74) have commonly been used. Nawy and Huang (156) and Nawy and Chiang (161) have recommended expressions for the crack width and mean stabilized crack spacing of pretensioned and post-tensioned beams. These expressions will be used here.

The maximum crack width Wmax in inches at the outer face of the concrete is given by the expression

$$W_{max} = Z\ R_i\ \frac{A_t}{\Sigma O}\ (\Delta f_s) \qquad (5.27)$$

where

$Z = 5.85 \times 10^{-6}$ for pretensioned beams

$= 6.51 \times 10^{-6}$ for post-tensioned beams

R_i = ratio of the distances to the neutral axis from the extreme tension fiber and from the centroid of the reinforcement

A_t = area of the concrete tensile zone (in^2)

ΣO = sum of the prestressed and nonprestressed reinforcement perimeters (in)

Δf_s = net stress change in the prestressed reinforcement after decompression or tensile stress in the nonprestressed reinforcement (ksi)

The fatigue stress range in the concrete, nonprestressed steel, and prestressed steel can be found by using the previous methods for the analysis of uncracked and cracked sections.

The I-effective method commonly used to compute deflections of reinforced concrete members has been extended by Branson and Trost (167,168) to consider partially prestressed concrete members. Recall that the effective moment of inertia Ie is given by the expression

$$Ie = \left(\frac{Mcr}{Ma}\right)^3 Ig + \left[1 - \left(\frac{Mcr}{Ma}\right)^3\right] Icr < Ig \qquad (5.28)$$

where

Ig = moment of inertia of the gross (uncracked transformed) section

Icr = moment of inertia of the cracked transformed section

Mcr = moment at first cracking

Ma = moment at the stage at which the deflection is being computed

The previous methods for the analysis of uncracked and cracked sections may be used to compute Ig, Icr, and Mcr. Note that Icr changes as Ma changes for the general case of combined axial force and bending moment.

Figure 5.9 shows the similarities and differences in the application of the I-effective method to reinforced concrete members and partially prestressed concrete members.

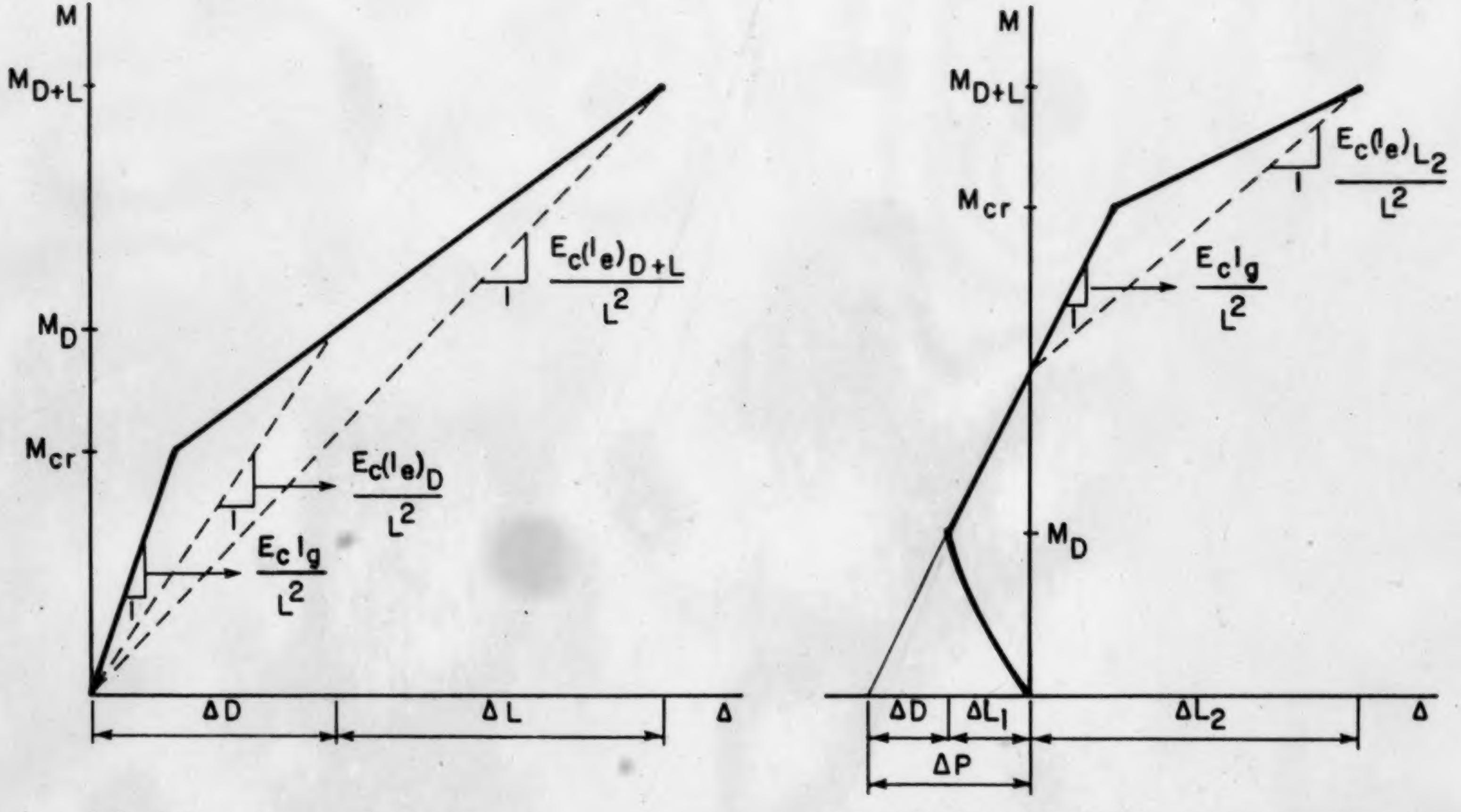
M
M_{D+L}
M_D
M_{cr}
$\frac{E_c I_g}{L^2}$
$\frac{E_c (I_e)_D}{L^2}$
$\frac{E_c (I_e)_{D+L}}{L^2}$
1
ΔD
ΔL
Δ
M
M_{D+L}
M_{cr}
M_D
$\frac{E_c I_g}{L^2}$
$\frac{E_c (I_e)_{L_2}}{L^2}$
ΔD
ΔL_1
ΔL_2
ΔP
Δ

(a) reinforced concrete member

(b) partially prestressed concrete member

Figure 5.9 Idealized moment-deflection diagrams for concrete members

A reinforced concrete member is already cracked under the application of the dead load whereas a partially prestressed concrete member normally cracks only after a portion of the live load has been applied. Consequently, the live load deflection of a reinforced concrete member is the difference between the total load deflection and the dead load deflection. Effective moments of inertia are used for both calculations. On the other hand, the live load deflection of a partially prestressed concrete member is equal to the deflection due to live load 2 only. Again, the effective moment of inertia is used.

Table 5.2 gives important serviceability limit states for segmental bridges and their specified values. The maximum crack widths are based on the recommendations of ACI Committee 224. The value of 0.007 in (0.18 mm) applies to the top surface of the bridge deck when deicing chemicals are used. This value can be increased to 0.013 in (0.33 mm) for other surfaces. The fatigue stress ranges for concrete, nonprestressed steel, and prestressed steel are taken from the recommendations of ACI Committee 215. Note that fmin is the stress in the concrete due to dead load and prestressing only. The live load deflection has been taken from AASHTO.

Description	Symbol	Limitation
Maximum crack width (bridge deck)	Wmax	0.007 in
Maximum crack width (other)	Wmax	0.013 in
Concrete fatigue stress range	fcr	0.4 fc' - fmin/2
Nonprestressed steel fatigue stress range	fsr	20.0 ksi
Prestressed steel fatigue stress range	fpr	0.1 fpu
Live load deflection	ΔL	L/800

Table 5.2 - Serviceability limit states

(Note: 1 in = 25.4 mm; 1 ksi = 6.9 MPa)

5.6 Computer program

The computer program PREBEAM has been developed for the analysis of partially prestressed concrete beams. This program is based on the theory described in this chapter. A FORTRAN listing of the program is given in Appendix I while the output information for the numerical example considered in the following section is included in Appendix J.

Note that the program could easily be modified to run in a conversational mode. Also, the calculations could well fit into the memory of a programmable calculator or small micro-computer.

5.7 Numerical examples

5.7.1 Example 1 - Partially prestressed T beam

A partially prestressed T beam (Figure 5.10) is subjected to a service moment of 3744 in-k and has an effective prestressing force of 123 kips. The stresses in the concrete, reinforcing, and prestressing are to be determined. In addition, the ultimate moment capacity is to be found. This example is given on pp. 100-104 of Nilson (189). Note that discrepancies between this solution and that given by Nilson are due to the approximate calculation of R by Nilson.

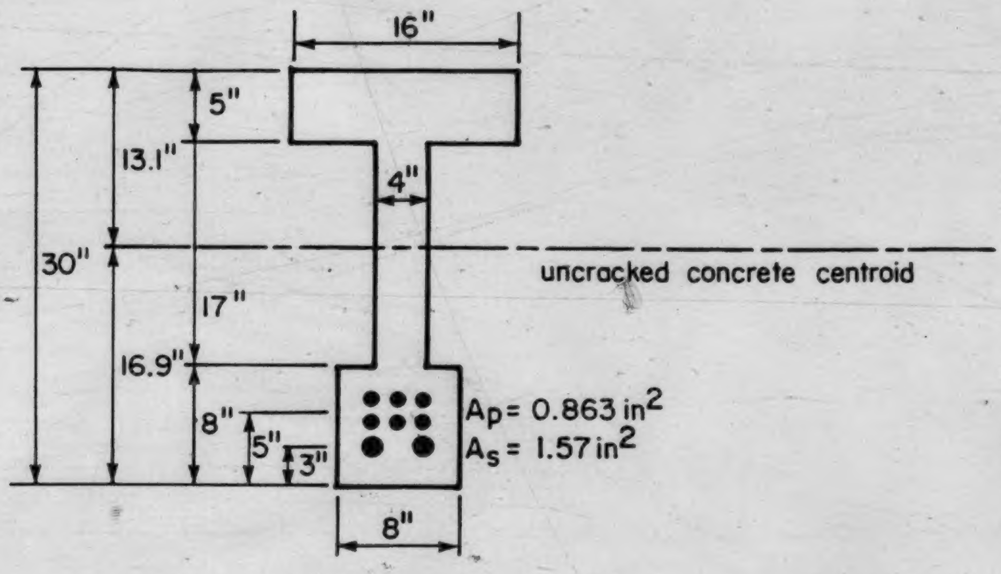
16"
5"
13.1"
4"
30"
uncracked concrete centroid
17"
16.9"
8"
5"
3"
$A_p = 0.863\ in^2$
$A_s = 1.57\ in^2$
8"

(a) uncracked cross section

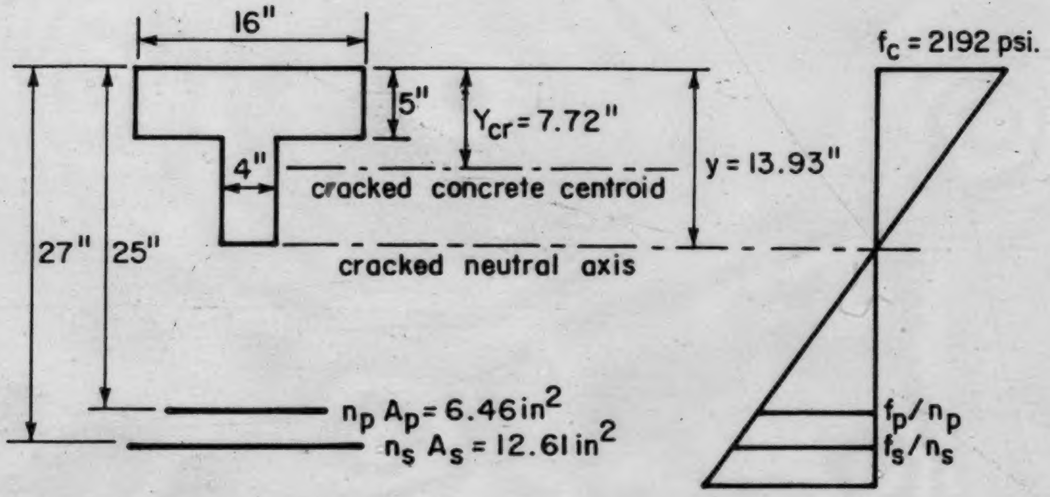
16"
5"
$Y_{cr} = 7.72"$
$y = 13.93"$
4"
cracked concrete centroid
27"
25"
cracked neutral axis
$n_p A_p = 6.46\ in^2$
$n_s A_s = 12.61\ in^2$
$f_c = 2192$ psi.
f_p/n_p
f_s/n_s

(b) cracked transformed cross section

(c) concrete stresses

Figure 5.10 Partially prestressed T beam

F = 123 k

N′ = 0 k

M′ = 3744 in-k

b = 4 in   b1 = 16 in   b2 = 8 in

d = 30 in   d1 = 5 in   d2 = 8 in

Es′ = 0 ksi   As′ = 0 sq in   ds′ = 0 in

Es = 29000 ksi   As = 1.57 sq in   ds = 27 in

Ep = 27000 ksi   Ap = 0.863 sq in   dp = 25 in

Ec = 3641 ksi

fc′ = 4 ksi   fy = 60 ksi   fpu = 274 ksi

Uncracked section analysis

Determine modular ratios:

$$\text{ns} = \frac{\text{Es}}{\text{Ec}} = \frac{29000}{3641} = 8.03$$

$$\text{np} = \frac{\text{Ep}}{\text{Ec}} = \frac{27000}{3641} = 7.48$$

Determine factors (gross section):

Auc = b d + (b1-b) d1 + (b2-b) d2

Auc = 4 x 30 + 12 x 5 + 4 x 8

$\text{Auc} = 212\ \text{in}^2$

$Quc = 1/2\ b\ d^2 + 1/2\ (b1-b)\ d1^2 - 1/2\ (b2-b)\ d2^2 + (b2-b)\ d2\ d$

$Quc = 1/2 \times 4 \times 30^2 + 1/2 \times 12 \times 5^2 - 1/2 \times 4 \times 8^2 + 4 \times 8 \times 30$

$Quc = 2782\ in^3$

$Iuc' = 1/3\ b\ d^3 + 1/3\ (b1-b)\ d1^3 + 1/3\ (b2-b)\ d2^3$

$+ (b2-b)\ d2\ d\ (d-d2)$

$Iuc' = 1/3 \times 4 \times 30^3 + 1/3 \times 12 \times 5^3 + 1/3 \times 4 \times 8^3$

$+ 4 \times 8 \times 30 \times 22$

$Iuc' = 58303\ in^4$

Determine section properties:

$yt = \frac{Quc}{Auc} = \frac{2782}{212} = 13.12\ in$

$yb = d - yt = 30 - 13.12 = 16.88\ in$

$Auc = 212\ in^2$

$Iuc = Iuc' - Auc\ yt^2 = 58303 - 212 \times 13.12^2 = 21795\ in^4$

$St = \frac{Iuc}{yt} = \frac{21795}{13.12} = 1661\ in^3$

$Sb = \frac{Iuc}{yb} = \frac{21795}{16.88} = 1291\ in^3$

Determine cracking moment:

$Mcr = F\ (Sb/Auc + dp - yt) + N'\ (Sb/Auc)$

$Mcr = 123\ (1291/212 + 25 - 13.12) + 0 = 2210\ in\text{-}k < 3744\ in\text{-}k$

The section has cracked since the service moment exceeds the cracking moment.

Cracked section analysis

Determine fictitious external force:

$$R = F \left\{ 1 + \frac{Ep\ Ap}{Ec\ Auc} \left[1 + \frac{(dp - yt)^2}{Iuc/Auc} \right] \right\}$$

$$R = 123 \left\{ 1 + \frac{27000 \times 0.863}{3610 \times 212} \left[1 + \frac{(25-13.12)^2}{21795/212} \right] \right\} = 131.9 \text{ k}$$

Determine resultant forces:

$$N = N' + F = 0 + 131.9 = 131.9 \text{ k}$$

$$M = M' - N'\ yt - F\ dp = 3744 - 0 - 131.9 \times 25 = 446.9 \text{ in-k}$$

Determine neutral axis of cracked section:

$$\alpha = (b'-b)\ d' + (ns'-1)\ As' + ns\ As + np\ Ap$$

$$\alpha = 12 \times 5 + 0 + 12.61 + 6.46 = 79.06$$

$$\beta = 1/2\ (b'-b)\ d'^2 + (ns'-1)\ As'\ ds' + ns\ As\ ds + np\ Ap\ dp$$

$$\beta = 1/2 \times 12 \times 5^2 + 0 + 12.61 \times 27 + 6.46 \times 25 = 651.8$$

$$\gamma = 1/3\ (b'-b)\ d'^3 + (ns'-1)\ As'\ ds'^2 + ns\ As\ ds^2 + np\ Ap\ dp^2$$

$$\gamma = 1/3 \times 12 \times 5^3 + 0 + 12.61 \times 27^2 + 6.46 \times 25^2 = 13730$$

$$1/6\ b\ N\ y^3 + 1/2\ b\ M\ y^2 + (\beta N + \alpha M)\ y - (\gamma N + \beta M) = 0$$

$$1/6 \times 4 \times 131.9 \times y^3 + 1/2 \times 4 \times 446.9 \times y^2$$
$$+ (651.8 \times 131.9 + 79.06 \times 446.9)\ y$$
$$- (13730 \times 131.9 + 651.8 \times 446.9) = 0$$

$$87.92\ y^3 + 893.8\ y^2 + 121300\ y - 2102000 = 0$$

$y = 13.93$ in (Four cycles of Newton-Raphson iteration yield a value of y which is accurate to 0.1%)

Determine stresses:

$$fc = \frac{M\ y}{1/6\ b\ y^3 + \beta y - \gamma}$$

$$fc = \frac{446.9 \times 13.93}{1/6 \times 4 \times 13.93^3 + 651.8 \times 13.93 - 13730} = -2.192 \text{ ksi}$$

$$fs = -ns\ \frac{ds - y}{y}\ fc = -8.03 \times \frac{27 - 13.93}{13.93} \times -2.192 = 16.510 \text{ ksi}$$

$$fp = -np\ \frac{dp - y}{y}\ fc + \frac{R}{Ap}$$

$$fp = -7.48 \times \frac{25 - 13.93}{13.93} \times -2.192 + \frac{131.9}{0.863}$$

$$fp = 13.000 + 152.800 = 165.800 \text{ ksi}$$

Ultimate strength analysis

(1) Assume $a = d/10 = 30/10 = 3.0$ in

after 8 iterations $a = 7.522$ in

(2) Find location of neutral axis

$c = a/\beta_1 = 7.522/0.85 = 8.850$ in

(3) Find strains

$$es = 0.003\ \frac{ds - c}{c}$$

$$es = 0.003\ \frac{27 - 8.850}{8.850} = 0.0062$$

$$ep = 0.003 \; \frac{dp - c}{c} + \frac{R}{Ep\ Ap}$$

$$ep = 0.003 \; \frac{25 - 8.850}{8.850} + \frac{131.9}{27000\ 0.863}$$

$$ep = 0.0054 + 0.0057 = 0.0111$$

(4) Find stresses

$fs = Es\ es = 29000 \times 0.0062 = 179.8 > 60.0$ ksi

$fp = 245.8$ ksi (from Mattock equation)

(5) Find forces

$T2 = As\ fs = 1.57 \times 60.0 = 94.2$ k

$T3 = Ap\ fp = 0.863 \times 245.8 = 212.2$ k

$C1 = -0.85\ fc'\ b = 0.85 \times 4 \times 4 = -13.6$ k/in

$C2 = -0.85\ fc'\ (b1 - b) = 0.85 \times 4 \times 12 = -40.8$ k/in

(6) Find a'

since $a > d1$

$a' = -(T1 + T2 + T3 + C2 \times d1)/C1$

$a' = -(0 + 94.2 + 212.2 - 20.4 \times 5)/-13.6 = 7.526$ in

$d' = d1 = 5$ in

(7) Check tolerance

$$\left| \frac{a' - a}{a'} \right| = \left| \frac{7.526 - 7.522}{7.526} \right| = 0.0005 < 0.001$$

$a = 7.526$ in

(8) Determine ultimate moment capacity

$$Mu = \phi\ (T1\ ds' + T2\ ds + T3\ dp + C1\ a^2/2 + C2\ d'^2/2)$$

$$Mu = 0.9\ (0 + 94.2 \times 27 + 212.2 \times 25 - 13.6 \times 7.526^2/2 - 40.8 \times 5^2/2) = 6257 \text{ in-k}$$

5.7.2 Example 2 - Islington Avenue extension

The purpose of this example is to show how the procedures discussed in this chapter can be applied to a typical design. The structure considered here is the Islington Avenue extension in Toronto (Figure 4.19). It is necessary to check the completed structure in the longitudinal direction for the combined effects of self weight, superimposed dead load, live load, temperature, and prestress. Normally, one would consider the critical sections at the support and at midspan. Since the structure is built by the method of balanced cantilever, the loads occurring at the supports (piers) during construction are much more severe than those acting on the completed structure. Therefore, only the section at midspan has to be considered.

For the purpose of analysis, the box girder can be transformed into a general I-girder as shown in Figure 5.11. The following pertinent dimensions can be defined:

$b = 3.0$ ft $b1 = 45.00$ ft $b2 = 25.50$ ft

$d = 7.5$ ft $d1 = 0.973$ ft $d2 = 0.823$ ft

The prestressing consists of 18 - 12/.6 tendons having an area of 0.345 ft^2 and a distance from the top of 6.951 ft.

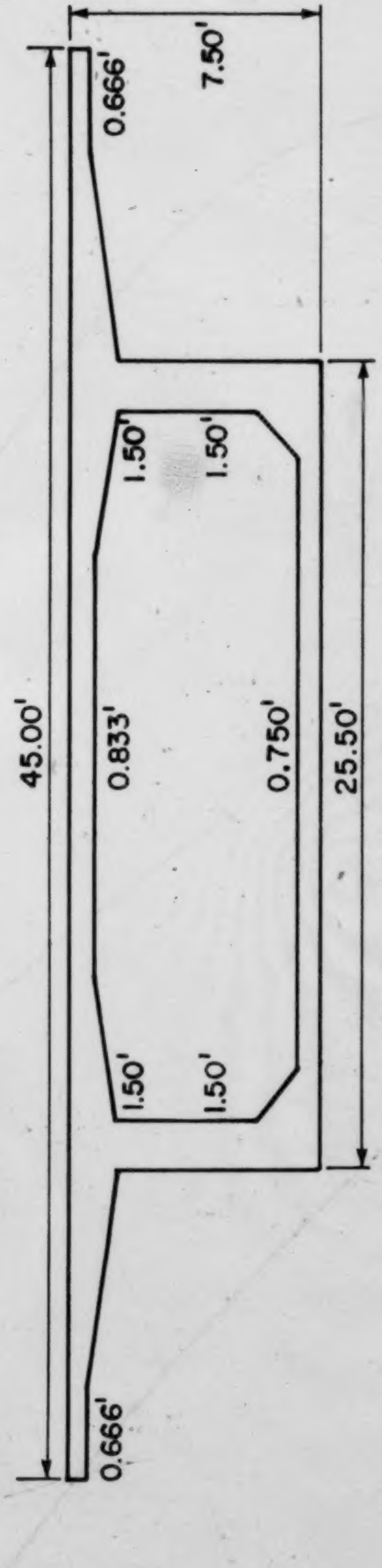
45.00'
7.50'
0.666'
0.666'
1.50'
1.50'
1.50'
1.50'
0.833'
0.750'
25.50'

(a) box girder

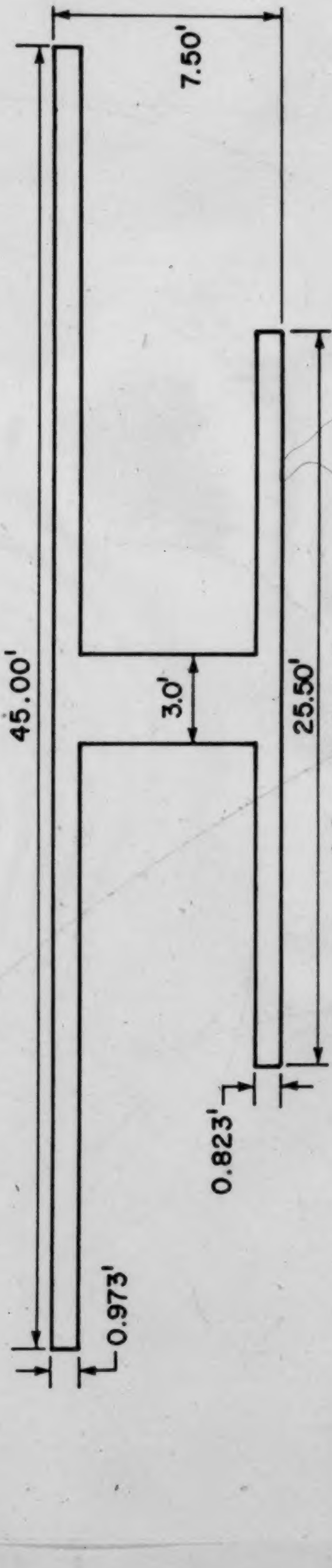
45.00'
7.50'
3.0'
25.50'
0.823'
0.973'

(b) equivalent I - girder

Figure 5.11 Discretization of a box girder as an equivalent I-girder

The material properties are as follows:

fc' = 6 ksi = 864 ksf
fpu = 270 ksi = 38880 ksf
Ec = 4696 ksi = 676200 ksf
Ep = 28000 ksi = 4032000 ksf

The loadings considered are self weight, superimposed dead load, live load, temperature, and prestress. The effects of self weight, prestress, and temperature come from the computer program TIMEDEP while the effects of the superimposed dead load and live load can be obtained from any one of a number of existing programs.

The temperature load corresponds to a linear gradient over the top slab with a temperature differential of 72°F. Figure 5.12(a) shows how the thermal stress distribution acting on the section can be broken down into its component form.

A complete analysis of this section requires the consideration of both the working stresses (and their effect on serviceability) and the ultimate strength. With respect to working stresses, two load combinations must be considered, depending on whether or not temperature is included. With regard to ultimate strength, temperature is usually unimportant (137), and only one load combination must be considered. The loading information is summarized

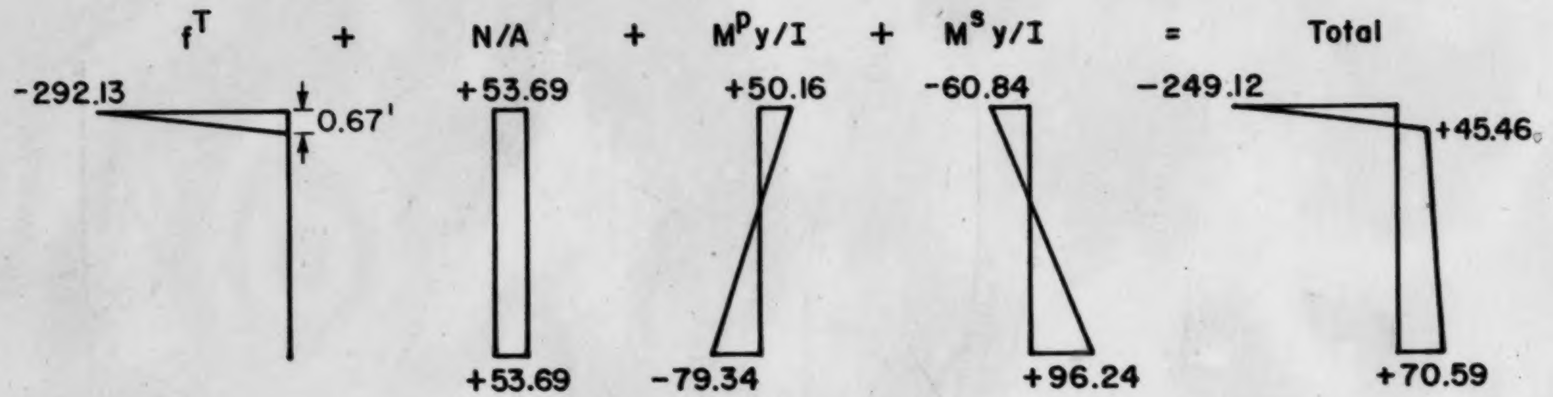
f^T
+
N/A
+
M^p y/I
+
M^s y/I
=
Total
-292.13
0.67'
+53.69
+53.69
+50.16
-79.34
-60.84
+96.24
-249.12
+45.46
+70.59

(a) thermal stresses

(all stresses in ksf)

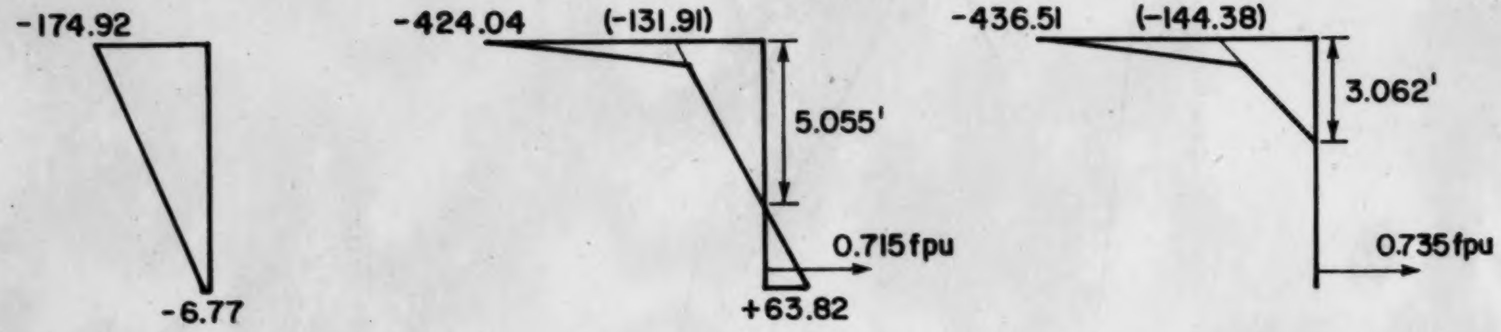
-174.92
-6.77
-424.04
(-131.91)
5.055'
0.715 fpu
+63.82
-436.51
(-144.38)
3.062'
0.735 fpu

(b) uncracked section stresses AASHTO load case I

(c) uncracked section stresses AASHTO load case IV

(d) cracked section stresses AASHTO load case IV

Figure 5.12 Stress results for the Islington Avenue extension

as follows:

Working stress

(1) AASHTO load case I (D + L @ 100%)

Self weight	27060
Superimposed dead load	7961
Live load	16496
M =	51517 ft-k

(2) AASHTO load case IV (D + L + T @ 125%)

Self weight	27060
Superimposed dead load	7961
Live load	16496
Temperature	2504
M =	54021 ft-k
Temperature N =	4382 k

Ultimate strength

(1) AASHTO load case I 1.3 (D + 1.67 L)

Self weight	27060 x 1.30 =	35178
Superimposed dead load	7961 x 1.30 =	10349
Live load	16496 x 2.17 =	35796
	Mu =	81324 ft-k

Let us explain how the bending moment and axial force due to temperature have been determined. The bending moment (2504 ft-k) is the sum of the primary and secondary bending moments. The axial force (4382 k) is that acting at the centroid of the section and which is counteracted by an equal and opposite force in the top slab. This equal and opposite force produces a triangular stress distribution which is added in by hand to the stresses acting on the section (Figure 5.12).

Note that the secondary moment of prestressing is normally multiplied by a load factor of 1.0 and included here. However, the secondary moment of prestressing is not available for this case and consequently cannot be included.

With respect to the working stresses, the section is uncracked under AASHTO load case I (Figure 5.12(b)) and cracked under AASHTO load case IV (Figure 5.12(d)). The compressive stress in the concrete is within the acceptable range for load case I. However, the compressive stress of 436.5 ksf for load case IV is slightly over the allowable limit of 864 x 0.4 x 1.25 = 432.0 ksf. As a matter of interest, Figure 5.12(c) is included to show the incorrect stress distribution that is obtained when the uncracked section is used for load case IV. Note how much the neutral axis moves up when the section cracks!

With regard to the ultimate strength, a moment capacity of 79600 ft-k is calculated while the moment required is 81324 ft-k. Since this is a little low, some bonded auxiliary reinforcement (unstressed tendons) could be added to make up the difference.

The cracking, fatigue, and deformation should also be checked to complete this example. A crack width of

0.011 in is calculated, while the acceptable value is 0.013 in. Fatigue is not a problem since the section is uncracked under live load. Only in the uncommon case of maximum live load and temperature acting together is there cracking. Since the cracking occurs over a very limited length, the effect on the deformation of the overall structure is minimal.

5.8 Conclusions

This chapter has developed the computer program PREBEAM for the analysis of partially prestressed concrete beams, subjected to axial force as well as bending moment. Both service load and ultimate strength behaviour have been considered. Numerical examples have illustrated the versatility and accuracy of the program.

6. CONCLUSIONS AND RECOMMENDATIONS

6.1 Conclusions

This research has provided a methodology for the analysis of prestressed concrete segmental bridges. To maximize the design efficiency, the analysis of the bridge is uncoupled into two parts; the first part considers the time-dependent analysis of a segmental bridge under construction while the second part deals with the approximate three-dimensional analysis of a completed segmental bridge. The time-dependent analysis gives the longitudinal flexural requirements at each stage of construction, while the three-dimensional analysis gives the requirements for transverse flexure as well as longitudinal shear and torsion in the completed structure. The computer programs TIMEDEP and BOXGIRD have been developed to handle the time-dependent and three-dimensional analyses respectively.

TIMEDEP gives the time-dependent effects of creep and shrinkage in the concrete as well as relaxation of the prestressing. The loadings considered are self weight, prestress, construction loads, and temperature. The program is based on the direct stiffness method. The method of superposition is used to determine time-dependent effects. In the present version of the program, creep and shrinkage are based on the recommendation of ACI Committee 209 while relaxation is given by the expression of Magura, Sozen, and Siess. The program can easily be modified to handle other material and analytical models.

The program is easier to use and computationally more efficient than other similar programs. The amount of input required for an analysis has been greatly reduced and simplified. By using untransformed section properties in the analysis, the number of operations required has been substantially reduced. The computational efficiency has also been vastly increased by using Dirichlet series for the estimation of the effects of creep. The analysis for thermal effects is greatly simplified by introducing the integrals S1 and S2 as section properties. The number of operations is also reduced substantially by modifying the existing equation solver rather than by modifying the analysis to suit the existing equation solver.

BOXGIRD gives a three-dimensional analysis of a box girder bridge. The loadings considered are self weight, superimposed dead load, truck loads, lane loads, temperature, and prestressing. The program utilizes folded plate theory and is based on the direct stiffness method. Element stiffnesses are evaluated by the equations of Goldberg-Leve while the loads are given by an appropriate number of Fourier series terms. For comparison purposes, a unit length of structure is also analysed with plane frame theory.

Although simply supported structures can be handled exactly, it is computationally efficient to treat continuous structures in an approximate manner. With respect to transverse flexure, the distance between the dead load inflection points of the continuous structure can be taken as the span length for the simply supported structure and the results can be found at midspan. With regard to longitudinal shear and torsion, the actual span length of the continuous structure can be taken as the span length for the simply supported structure and the results can be found at the point under consideration. Significant savings in computational effort (100 to 1000 times) can be realized with only a 5% to 10% loss in accuracy by limiting the program to simply supported structures.

This research has also provided a methodology for the analysis of partially prestressed concrete sections. Since partial prestressing can be defined as the general case whose extremes are conventional reinforced concrete and fully prestressed concrete, the development of simple analysis procedures has a wide range of application. These include (but are not limited to) the longitudinal and transverse analysis of segmental bridges having prestressed and/or conventional reinforcing.

New computational techniques have been developed for the (1) uncracked section analysis, (2) cracked section analysis, and (3) ultimate strength analysis. The serviceability criteria of cracking, fatigue, and deformation have been examined. The computer program PREBEAM has been developed for the analysis of partially prestressed concrete sections.

6.2 Recommendations for further study

The following topics related to time-dependent behaviour are worthy of some additional consideration:

(1) It is necessary to correlate experimental and analytical results for creep, shrinkage, and relaxation of real structures.

(2) It may be desirable to implement different material and/or analytical models in the computer program.

(3) It is necessary to refine the treatment of prestressing in the computer program as discussed in Section 3.6.4.

(4) Span-by-span construction for cast-in-place structures and incremental launching could be considered by including concrete layers in the computer program. However, if concrete layers are included, the overall numerical efficiency of the program will be reduced.

The computer program TIMEDEP has been specifically written in modular form so that enhancements and modifications can easily be made.

Bibliography

1. Muller, J., "Ten Years of Experience in Precast Segmental Construction," Journal of the Prestressed Concrete Institute, Vol. 20, No. 1, January/February 1975, pp. 28-61.

2. PCI Committee on Segmental Construction, "Recommended Practice for Segmental Construction in Prestressed Concrete," Journal of the Prestressed Concrete Institute, Vol. 20, No. 2, March/April 1975, pp. 22-41.

3. PCI Bridge Committee, "Tentative Design and Construction Specifications for Precast Segmental Box Girder Bridges," Journal of the Prestressed Concrete Institute, Vol. 20, No. 3, July/August 1975, pp. 34-42.

4. Podolny, W. Jr., "An Overview of Precast Prestressed Segmental Bridges," Journal of the Prestressed Concrete Institute, Vol. 24, No. 1, January/February 1979, pp. 56-87.

5. Joint PCI - PTI Committee on Segmental Construction, "Recommended Practice for Precast Post-Tensioned Segmental Construction," Journal of the Prestressed Concrete Institute, Vol. 27, No. 1, January/February 1982, pp. 14-61.

6. Kulka, F., and Thoman, S. J., "Feasibility Study of Standard Sections for Segmental Prestressed Concrete Bridges," Journal of the Prestressed Concrete Institute, Vol. 28, No. 5, September/October 1983, pp. 54-77.

7. Chadha, G., and Ketchek, K., "Computerized Structural Design and Analysis of Continuous Prestressed Concrete Box-Girder Bridges Built by Cantilever Method of Construction," Computers and Structures, Vol. 2, 1972, pp. 915-932.

8. O'Conner, H., "Design of Bridge Superstructures," John Wiley & Sons, New York, 1971.

9. Libby, J. R., and Perkins, N. D., "Modern Prestressed Concrete Highway Bridge Superstructures - Design Principles and Construction Methods," Grantville Publishing Company, San Diego, California, 1976.

10. PCI and PTI, "Precast Segmental Box Girder Manual," published jointly by the Prestressed Concrete Institute (Chicago, Illinois) and the Post-Tensioning Institute (Phoenix, Arizona), 1978.

11. PTI, "Post-Tensioned Box Girder Bridge Manual," Post-Tensioning Institute, Phoenix, Arizona, 1978.

12. Ballinger, C. A., Podolny, W. Jr., and Abrahams, M. J., "A Report on the Design and Construction of Segmental Prestressed Concrete Bridges in Western Europe - 1977," International Road Federation, Washington, DC, June 1978.

13. FHWA, "Cable-Stayed Bridges," Structural Engineering Series Report No. 4, Federal Highway Administration, Washington, DC, June 1978.

14. FHWA, "Prestressed Concrete Segmental Bridges," Structural Engineering Series Report No. 6, Federal Highway Administration, Washington, DC, August 1979.

15. Mathivat, J., "Construction par Encorbellement des Ponts en Beton Precontrainte," Editions Eyrolles, Paris, France, 1979 (in French).

16. Podolny, W. Jr., and Muller, J. M., "Construction and Design of Prestressed Concrete Segmental Bridges," John Wiley & Sons, New York, 1982.

17. Lacey, G. C., and Breen, J. E., "State-of-the-Art - Long Span Prestressed Concrete Bridges of Segmental Construction," Research Report No. 121-1, Center for Highway Research, The University of Texas at Austin, May 1969.

18. Kashima, S., and Breen, J. E., "Epoxy Resins for Jointing Segmentally Constructed Prestressed Concrete Bridges," Center for Highway Research, Research Report No. 121-2, The University of Texas at Austin, August 1974.

19. Lacey, G. C., and Breen, J. E., "The Design and Optimization of Segmentally Precast Prestressed Box Girder Bridges," Research Report No. 121-3, Center for Highway Research, The University of Texas at Austin, July 1975.

20. Brown, R. C., Burns, N. H., and Breen, J. E., "Computer Analysis of Segmentally Erected Precast Prestressed Box Girder Bridges," Research Report No. 121-4, Center for Highway Research, The University of Texas at Austin, November 1974.

21. Kashima, S., and Breen, J. E., "Construction and Load Tests of a Segmental Precast Box Girder Bridge Model," Research Report No. 121-5, Center for Highway Research, The University of Texas at Austin, February 1975.

22. Breen, J. E., Cooper, R. L., and Gallaway, T. M., "Minimizing Construction Problems in Segmentally Precast Box Girder Bridges," Research Report No. 121-6F, Center for Highway Research, The University of Texas at Austin, August 1975.

23. Lacey, G. C., Breen, J. E., and Burns, N. H., "State of the Art for Long Span Prestressed Concrete Bridges of Segmental Construction," Journal of the Prestressed Concrete Institute, Vol. 16, No. 5, September/October 1971, pp. 53-77.

24. Brown, R. C. Jr., and Burns, N. H., "Computer Analysis of Segmentally Erected Bridges," Journal of the Structural Division, Proceedings of American Society of Civil Engineers, Vol. 101, No. ST4, April 1975, pp. 761-778.

25. Scordelis, A.C., "Analysis of Simply Supported Box Girder Bridges," Structural Engineering and Structural Mechanics Report No. SESM 66-17, University of California, Berkeley, October 1966.

26. Scordelis, A. C., "Analysis of Continuous Box Girder Bridges," Structural Engineering and Structural Mechanics Report No. SESM 67-25, University of California, Berkeley, November 1967.

27. Scordelis, A. C., and Meyer, C., "Wheel Load Distribution in Concrete Box Girder Bridges," Structural Engineering and Structural Mechanics Report No. SESM 69-1, University of California, Berkeley, January 1969.

28. Willam, K. J., and Scordelis, A. C., "Analysis of Orthotropic Folded Plates with Eccentric Stiffeners," Structural Engineering and Structural Mechanics Report No. SESM 70-2, University of California, Berkeley, February 1970.

29. Meyer, C., and Scordelis, A. C., "Computer Program for Prismatic Folded Plates with Plate and Beam Elements," Structural Engineering and Structural Mechanics Report No. SESM 70-3, University of California, Berkeley, February 1970.

30. Meyer, C., and Scordelis, A. C., "Analysis of Curved Folded Plate Structures," Structural Engineering and Structural Mechanics Report No. UC SESM 70-8, University of California, Berkeley, June 1970.

31. Willam, K. J., and Scordelis, A. C., "Computer Program for Cellular Structures of Arbitrary Plan Geometry," Structural Engineering and Structural Mechanics Report No. UC SESM 70-10, University of California, Berkeley, September 1970.

32. Meyer, C., "Analysis and Design of Curved Box Girder Bridges," Structural Engineering and Structural Mechanics Report No. UC SESM 70-22, University of California, Berkeley, December 1970.

33. Meyer, C., and Scordelis, A. C., "Computer Program for Non-Prismatic Folded Plates with Plate and Beam Elements," Structural Engineering and Structural Mechanics Report No. UC SESM 71-23, University of California, Berkeley, December 1971.

34. Lin, C. S., and Scordelis, A. C., "Computer Program for Bridges on Flexible Bents," Structural Engineering and Structural Mechanics Report No. UC SESM 71-24, University of California, Berkeley, December 1971.

35. Comartin, C. D., and Scordelis, A. C., "Analysis and Design of Skew Box Girder Bridges," Structural Engineering and Structural Mechanics Report No. UC SESM 72-14, University of California, Berkeley, December 1972.

36. Kabir, A. F., and Scordelis, A. C., "Computer Programs for Curved Bridges on Flexible Bents," Structural Engineering and Structural Mechanics Report No. UC SESM 74-10, University of California, Berkeley, September 1974.

37. DeFries-Skene, A., and Scordelis, A. C., "Direct Stiffness Solution for Folded Plates," Journal of the Structural Division, Proceedings of American Society of Civil Engineers, Volume 90, No. ST4, August 1964, pp. 15-47.

38. Lo, K. S., and Scordelis, A. C., "Finite Segment Analysis of Folded Plates," Journal of the Structural Division, Proceedings of American Society of Civil Engineers, Volume 95, No. ST5, May 1969, pp. 831-852.

39. Cheung, Y. K., "Folded Plate Structures by Finite Strip Method," Journal of the Structural Division, Proceedings of American Society of Civil Engineers, Volume 95, No. ST12, December 1969, pp. 2963-2979.

40. Willam, K. J., and Scordelis, A. C., "Analysis of Eccentrically Stiffened Folded Plates," Proceedings of IASS Symposium on Folded Plates and Prismatic Structures, Vienna, September 1970.

41. Meyer, C., and Scordelis, A. C., "Analysis of Curved Folded Plate Structures," Journal of the Structural Division, Proceedings of American Society of Civil Engineers, Volume 97, No. ST10, October 1971, pp. 2459-2480.

42. William, K. J., and Scordelis, A. C., "Cellular Structures of Arbitrary Plan Geometry," Journal of the Structural Division, Proceedings of American Society of Civil Engineers, Volume 98, No. ST7, July 1972, pp. 1377-1394.

43. Lin, C. S., "Nonlinear Analysis of Reinforced Concrete Slabs and Shells," Structural Engineering and Structural Mechanics Report No. UC SESM 73-7, University of California, Berkeley, April 1973.

44. Kabir, A. F., "Nonlinear Analysis of Reinforced Concrete Panels, Slabs and Shells for Time Dependent Effects," Structural Engineering and Structural Mechanics Report No. UC SESM 76-6, University of California, Berkeley, December 1976.

45. Kang, Y. J., "Nonlinear Geometric, Material and Time Dependent Analysis of Reinforced and Prestressed Concrete Frames," Structural Engineering and Structural Mechanics Report No. UC SESM 77-1, University of California, Berkeley, January 1977.

46. Van Zyl, S. F., "Analysis of Curved Segmentally Erected Prestressed Concrete Box Girder Bridges," Structural Engineering and Structural Mechanics Report No. UC SESM 78-2, University of California, Berkeley, January 1978.

47. Van Greunen, J., "Nonlinear Geometric, Material and Time Dependent Analysis of Reinforced and Prestressed Concrete Slabs and Panels," Structural Engineering and Structural Mechanics Report No. UC SESM 79-3, University of California, Berkeley, October 1979.

48. Van Zyl, S. F., and Scordelis, A. C., "Analysis of Curved Prestressed Segmental Bridges," Journal of the Structural Division, Proceedings of American Society of Civil Engineers, Vol. 105, No. ST11, November 1979, pp. 2399-2417.

49. Kang, Y. J., and Scordelis, A. C., "Nonlinear Analysis of Prestressed Concrete Frames," Journal of the Structural Division, Proceedings of American Society of Civil Engineers, Vol. 106, No. ST2, February 1980, pp. 445-462.

50. Van Greunen, J., and Scordelis, A. C., "Nonlinear Analysis of Prestressed Concrete Slabs," Journal of the Structural Division, Proceedings of American Society of Civil Engineers, Vol. 109, No. ST7, July 1983, pp. 1742-1760.

51. Scordelis, A. C., "Berkeley Computer Programs for the Analysis of Concrete Box Girder Bridges," Proceedings, NATO-Advanced Study Institute on Analysis and Design of Bridges, Cesme, Turkey, 1982.

52. Tadros, M. K., "Time-Dependent Deformations and Stresses in Prestressed Concrete Structures," Ph D Dissertation, University of Calgary, 1975.

53. Khalil, M. S. A., "Time-Dependent Non-Linear Analysis of Prestressed Concrete Cable-Stayed Girders and Other Concrete Structures," Ph D Dissertation, University of Calgary, 1979.

54. Rao, V. T., and Dilger, W. H., "Analysis of Composite Prestressed Concrete Beams," Journal of the Structural Division, Proceedings of American Society of Civil Engineers, Vol. 100, No. ST10, October 1974, pp. 2109-2121.

55. Ghali, A., Sisodiya, R. G., and Tadros, G. S., "Displacements and Losses in Multistage Prestressed Members," Journal of the Structural Division, Proceedings of American Society of Civil Engineers, Vol. 100, No. ST11, November 1974, pp. 2307-2322.

56. Tadros, M. K., Ghali, A., and Dilger, W. H., "Time-Dependent Prestress Loss and Deflection in Prestressed Concrete Members," Journal of the Prestressed Concrete Institute, Vol. 20, No. 3, May/June 1975, pp. 86-98.

57. Tadros, M. K., Ghali, A., and Dilger, W. H., "Effect of Non-Prestressed Steel on Prestress Loss and Deflection," Journal of the Prestressed Concrete Institute, Vol. 22, No. 2, March/April 1977, pp. 50-63.

58. Tadros, M. K., Ghali, A., and Dilger, W. H., "Time-Dependent Analysis of Composite Frames," Journal of the Structural Division, Proceedings of American Society of Civil Engineers, Vol. 103, No. ST4, April 1977, pp. 871-884.

59. Tadros, M. K., Ghali, A., and Dilger, W. H., "Long-Term Stresses and Deformation of Segmental Bridges," Journal of the Prestressed Concrete Institute, Vol. 24, No. 4, July/August 1979, pp. 66-87.

60. Dilger, W. H., "Creep Analysis of Prestressed Concrete Structures Using Creep-Transformed Section Properties," Journal of the Prestressed Concrete Institute, Vol. 27, No. 1, January/February 1982, pp. 98-118.

61. Tadros, M. K., Ghali, A., and Dilger, W. H., "Computer Program for Analysis of Stress and Deformation in Segmental Construction: A User's Manual," Research Report No. CE80-11, The University of Calgary and the University of Nebraska at Omaha, September 1980.

62. "Segmental Time Dependent System," Engineering Computer Corporation, Sacramento, California, 1982.

63. Khalil, M. S., Dilger, W. H., and Ghali, A., "Design Considerations Dictated by Creep and Shrinkage in Prestressed Concrete Frames," American Concrete Institute Publication SP-76, 1982.

64. Khalil, M. S., Dilger, W. H., and Ghali, A., "Time-Dependent Analysis of PC Cable-Stayed Bridges," Journal of the Structural Division, Proceedings of American Society of Civil Engineers, Vol. 109, No. ST8, August 1983, pp. 1980-1996.

65. Hernandez, H. D., and Gamble, W. L., "Time-Dependent Prestress Losses in Pretensioned Concrete Construction," Civil Engineering Studies, Structural Research Series No. 417, University of Illinois at Urbana-Champaign, Urbana, 1972.

66. Danon, J. R., and Gamble, W. L., "Time-Dependent Deformations and Losses in Concrete Bridges Built by the Cantilever Method," Civil Engineering Studies, Structural Research Series No. 437, University of Illinois at Urbana-Champaign, Urbana, 1977.

67. Marshall, V., and Gamble, W. L., "Time-Dependent Deformations in Segmental Prestressed Concrete Bridges," Civil Engineering Studies, Structural Research Series No. 495, University of Illinois at Urbana-Champaign, Urbana, 1981.

68. Potgieter, I., and Gamble, W. L., "Response of Highway Bridges to Nonlinear Temperature Distributions," Civil Engineering Studies, Structural Research Series No. 505, University of Illinois at Urbana-Champaign, Urbana, 1983.

69. Neville, A. M., and Dilger, W., "Creep of Concrete: Plain, Reinforced, and Prestressed," North-Holland Publishing Company, Amsterdam, 1970.

70. ACI Committee 209 Subcommittee 2, "Prediction of Creep, Shrinkage, and Temperature Effects in Concrete Structures," American Concrete Institute Publication SP-27, 1971, pp. 51-93.

71. Branson, D. E., and Christiason, M. L., "Time Dependent Concrete Properties Related to Design - Strength and Elastic Properties, Creep and Shrinkage," American Concrete Institute Publication SP-27, 1971, pp. 257-277.

72. Branson, D. E., "Deformation of Concrete Structures," McGraw-Hill, New York, 1977.

73. CEB/FIP, "International Recommendations for the Design and Construction of Concrete Structures," Comite Europeen du Beton/Federation Internationale de la Precontrainte, Paris, 1970. (English translation by Cement and Concrete Association, London, 1970).

74. CEB/FIP, "CEB-FIP Model Code for Concrete Structures," Bulletin D'Information No. 124/125-E," Comite Euro-International du Beton/Federation Internationale de la Precontrainte, Paris, 1978.

75. Kristek, V., and Smerda, Z., "Simplified Calculation of the Relaxation of Stress Respecting the Delayed Elasticity," Fundamental Research on Creep and Shrinkage of Concrete, Martinus Nijhoff Publishers, The Hague, 1982, pp. 425-438.

76. Bazant, Z. P., and Panula, L., "Creep and Shrinkage Characterization for Analyzing Prestressed Concrete Structures," Journal of the Prestressed Concrete Institute, Vol. 25, No. 3, May/June 1980, pp. 86-122.

77. Magura, D. D., Sozen, M. A., and Siess, C. P., "A Study of Stress Relaxation in Prestressing Reinforcement," Journal of the Prestressed Concrete Institute, Vol. 9, No. 2, April 1964, pp. 13-57.

78. PCI Committee on Prestress Losses, "Recommendations for Estimating Prestress Losses," Journal of the Prestressed Concrete Institute, Vol. 20, No. 4, July/August 1975, pp. 43-75.

79. Zia, P., Preston, H. K., Scott, N. L., and Workman, E. B., "Estimating Prestress Losses," Concrete International: Design and Construction, Vol. 1, No. 6, June 1979, pp. 33-38.

80. Browne, R., "Property of Concrete in Reactor Vessels," Proceedings of Conference on Prestressed Concrete Pressure Vessels, London, 1967.

81. Ross, A. D., "Creep of Concrete Under Variable Stress," Journal of the American Concrete Institute, Vol. 64, No. 9, March 1958, pp. 739-758.

82. "Finite Element Analysis of Reinforced Concrete," American Society of Civil Engineers, 1982.

83. "Designing for Creep & Shrinkage in Concrete Structures," American Concrete Institute Publication SP-76, 1982.

84. Bazant, Z. P., and Wittmann, F. H., "Creep and Shrinkage in Concrete Structures," John Wiley & Sons, New York, 1982.

85. Wittmann, F. H., "Fundamental Research on Creep and Shrinkage of Concrete," Martinus Nijhoff Publishers, The Hague, 1982.

86. CEB, "Structural Effects of Time Dependent Behaviour of Concrete," Bulletin D'Information No. 136, Comite Euro-International Du Beton, Paris, July 1982.

87. Popov, E. P., "Introduction to Mechanics of Solids," Prentice-Hall, Englewood Cliffs, New Jersey, 1968.

88. Heins, C. P., "Bending and Torsional Design in Structural Members," Lexington Books, Lexington, Massachusetts, 1975.

89. Viasov, V. Z., "Thin-Walled Elastic Beams," National Science Foundation, 1961.

90. Maisel, B. I., and Roll, F., "Methods of Analysis and Design of Concrete Boxbeams with Side Cantilevers," Technical Report 42.494, Cement and Concrete Association, London, November 1974.

91. Maisel, B. I., "Structural Analysis of Concrete Boxbeams using Small Computer Capacity," Proceedings of International Conference on Short and Medium Span Bridges, Toronto, August 1982.

92. Maisel, B. I., "Analysis of Concrete Boxbeams using Small Computer Capacity," Technical Report 44.005, Cement and Concrete Association, London, to be published.

93. Wright, R. N., Abdel-Samad, S. R., and Robinson, A. R., "BEF Analogy for Analysis of Box Girders," Journal of the Structural Division, Proceedings of American Society of Civil Engineers, Vol. 94, No. ST7, July 1968, pp. 1719-1743.

94. Tung, D. H. H., "Torsional Analysis of Single Thin-Walled Trapezoidal Concrete Box Girder Bridges," Concrete Bridge Design, ACI Publication SP.23, 1969, pp. 205-220.

95. Cusens, A. R., and Pama, R. P., "Bridge Deck Analysis," John Wiley & Sons, New York, 1975.

96. Hambly, E. C., "Bridge Deck Behaviour, " John Wiley & Sons, New York, 1976.

97. Cheung, Y. K., "The Finite Strip Method in Structural Analysis," Pergamon Press Ltd., Oxford, England, 1976.

98. Loo, Y. C., and Cusens, A. R., "The Finite-Strip Method in Bridge Engineering," Cement and Concrete Association, London, 1978.

99. Kristek, V., "Theory of Box Girders," John Wiley & Sons, 1979.

100. Iffland, J. S. B., "Folded Plate Structures," Journal of the Structural Division, Proceedings of American Society of Civil Engineers, Vol. 105, No. ST1, January 1979, pp. 111-123.

101. Goldberg, J. E., and Leve, H. L., "Theory of Prismatic Folded Plate Structures," International Association for Bridge and Structural Engineering Publications, Vol. 87, 1957, pp. 59-86.

102. Lo, K. S., "Analysis of Cellular Folded Plate Systems," Ph D Dissertation, University of California at Berkeley, 1967.

103. Chu, K. H., and Pinjarkar, S. G., "Multiple Folded Plate Structures," Journal of the Structural Division, Proceedings of American Society of Civil Engineers, Vol. 92, No. ST2, April 1966, pp. 297-321.

104. Chu, K. H., and Dudnik, E., "Concrete Box Girder Bridges Analysed as Folded Plates," Concrete Bridge Design, ACI Publication SP-23, 1969, pp. 221-246.

105. Westergaard, H. M., "Computation of Stresses in Bridge Slabs Due to Wheel Loads," Public Roads, Vol. 11, No. 1, March 1930, pp. 1-23.

106. Newmark, N. M., "A Distribution Procedure for the Analysis of Slabs Continuous over Flexible Beams," University of Illinois Engineering Experiment Station Bulletin No. 304, 1938, pp. 7-118.

107. Homberg, H., and Ropers, W., "Fahrbahnplatten mit Veranderlicher Dicke," Springer-Verlag, New York, 1965.

108. Homberg, H., "Fahrbahnplatten mit Veranderlicher Dicke," Springer-Verlag, New York, 1968.

109. Pucher, A., "Influence Surfaces of Elastic Plates," Springer-Verlag, New York, 1977.

110. CEB, "Trial and Comparison Calculations Based on the CEB/FIP Model Code for Concrete Structures," Bulletin D'Information No. 129, Comite Euro-International Du Beton, Paris, October 1978.

111. Darwin, D., "Shear Component of Prestress by Equivalent Loads," Journal of the Prestressed Concrete Institute, Vol. 22, No. 2, March/April 1977, pp. 64-77.

112. Leonhardt, F., Kolbe, G., and Peter, J., "Temperature Differences Endanger Precast Concrete Bridges," Beton und Stahlbetonbau, No. 7, July 1965, pp. 157-163, (in German).

113. Leonhardt, F., and Lippoth, W., "Lessons from Damage to Prestressed Concrete Bridges," Beton und Stahlbetonbau, No. 10, October 1970, pp. 231-244, (in German).

114. Berwanger, C., and Symko, Y., "Thermal Stresses in Steel-Concrete Composite Bridges," Canadian Journal of Civil Engineering, Vol. 2, No. 1, March 1975, pp. 66-84.

115. Radolli, M., and Green, R., "Thermal Stresses in Concrete Bridge Superstructures Under Summer Conditions," Transportation Research Board Report No. 547, 1975, pp. 23-36.

116. Radolli, M., and Green, R., "Thermal Stress Analysis of Concrete Bridge Superstructures", Transportation Research Board Report No. 607, 1976, pp. 7-13.

117. Emanuel, J. H., and Hulsey, J. L., "Thermal Stresses and Deformations in Nonprismatic Indeterminate Composite Bridges," Transportation Research Board Report No. 607, 1976, pp. 4-6.

118. White, I. G., "Non-Linear Differential Temperature Distributions in Concrete Bridge Structures: A Review of Current Literature," Technical Report No. 525, Cement and Concrete Association, London, 1979.

119. Lovell, J. A. B., "The Islington Avenue Bridge," Journal of the Prestressed Concrete Institute, Vol. 25, No. 3, May/June 1980, pp. 32-66.

120. Lin, T. Y., and Redfield, C., "Some Design Issues Facing American Bridge Contractors," Journal of the Prestressed Concrete Institute, Vol. 27, No. 4, July/August 1982, pp. 58-71.

121. Hoffman, P. E., McClure, R. M., and West, H. H., "Temperature Study of an Experimental Concrete Segmental Bridge," Journal of the Prestressed Concrete Institute, Vol. 28, No. 2, March/April 1983, pp. 78-97.

122. CEB, "Structural Analysis - Volume II - Theme 4: Thermal Effects," Bulletin D'Information No. 154, Comite Euro-International Du Beton, Paris, April 1982.

123. Reynolds, J. C., and Emanuel, J. H., "Thermal Stresses and Movements in Bridges," Journal of the Structural Division, Proceedings of American Society of Civil Engineers, Vol. 100, No. ST1, January 1974, pp. 63-78.

124. Hunt, B., and Cooke, N., "Thermal Calculations for Bridge Design," Journal of the Structural Division, Proceedings of American Society of Civil Engineers, Vol. 101, No. ST9, September 1975, pp. 1763-1781.

125. Vaidyanathan, H., "Calculation of Thermal Stresses in Bridge Structures," Journal of the Structural Division, Proceedings of American Society of Civil Engineers, Vol. 103, No. ST4, April 1977, pp. 907-911.

126. Emanuel, J. H., and Hulsey, J. L., "Temperature Distributions in Composite Bridges," Journal of the Structural Division, Proceedings of American Society of Civil Engineers, Vol. 104, No. ST1, January 1978, pp. 65-78.

127. Millman, P., Kilcup, R., and Cornell, C. A., "Design Temperature for Structural Elements," Journal of the Structural Division, Proceedings of American Society of Civil Engineers, Vol. 106, No. ST4, April 1980, pp. 877-895.

128. Churchward, A., and Sokal, Y. J., "Prediction of Temperatures in Concrete Bridges," Journal of the Structural Division, Proceedings of American Society of Civil Engineers, Vol. 107, No. ST11, November 1981, pp. 2163-2176.

129. Dilger, W. H., Ghali, A., Chan, M., Cheung, M. S., and Maes, M. A., "Temperature Stresses in Composite Box Girder Bridges," Journal of the Structural Division, Proceedings of the American Society of Civil Engineers, Vol. 109, No. 6, June 1983, pp. 1460-1478.

130. Berwanger, C., "Transient Thermal Behaviour of Composite Bridges," Journal of the Structural Division, Proceedings of American Society of Civil Engineers, Vol. 109, No. ST10, October 1983, pp. 2325-2339.

131. Elbadry, M. M., and Ghali, A., "Temperature Variations in Concrete Bridges," Journal of the Structural Division, Proceedings of American Society of Civil Engineers, Vol. 109, No. ST10, October 1983, pp. 2355-2374.

132. Priestley, M. J. N., "Thermal Gradients in Bridges - Some Design Considerations," New Zealand Engineering (Wellington), Vol. 27, No. 7, July 1972, pp. 228-233.

133. Priestley, M. J. N., "Design Thermal Gradients for Concrete Bridges," New Zealand Engineering (Wellington), Vol. 31, No. 9, September 1976, pp. 213-219.

134. Priestley, M. J. N., "Ambient Thermal Stresses in Circular Prestressed Concrete Tanks," Journal of the American Concrete Institute, Vol. 73, No. 10, October 1976, pp. 553-560.

135. Priestley, M. J. N., "Design of Concrete Bridges for Temperature Gradients," Journal of the American Concrete Institute, Vol. 75, No. 5, May 1978, pp. 209-217.

136. Thurston, S. J., Priestley, M. J. N., and Cooke, N., "Thermal Analysis of Thick Concrete Sections," Journal of the American Concrete Institute, Vol. 77, No. 5, September-October 1980, pp. 347-357.

137. Priestley, M. J. N., "Thermal Stresses in Concrete Structures," Proceedings of the Canadian Structural Concrete Conference, Toronto, 1981.

138. Emerson, M., "Bridge Temperatures and Movements in the British Isles," Transport and Road Research Laboratory Report No. LR228, Crowthorne, Berkshire, England, 1968.

139. Emerson, M., "The Calculation of the Distribution of Temperature in Bridges," Transport and Road Research Laboratory Report No. LR561, Crowthorne, Berkshire, England, 1973.

140. Mortlock, J. D., "The Instrumentation of Bridges for the Measurement of Temperature and Movement," Transport and Road Research Laboratory Report No. LR641, Crowthorne, Berkshire, England, 1974.

141. Emerson, M., "Bridge Temperatures Estimated from the Shade Temperature," Transport and Road Research Laboratory Report No. LR696, Crowthorne, Berkshire, England, 1976.

142. Jones, M. R., "Bridge Temperatures Calculated by a Computer Program," Transport and Road Research Laboratory Report No. LR702, Crowthorne, Berkshire, England, 1976.

143. Emerson, M., "Extreme Values of Bridge Temperatures for Design Purposes," Transport and Road Research Laboratory Report No. LR744, Crowthorne, Berkshire, England, 1976.

144. Black, W., Moss, D. S., and Emerson, M., "Bridge Temperatures Derived from Measurement of Movement," Transport and Road Research Laboratory Report No. LR748, Crowthorne, Berkshire, England, 1976.

145. Jones, M. R., "Calculated Deck Plate Temperatures for a Steel Box Bridge," Transport and Road Research Laboratory Report No. LR760, Crowthorne, Berkshire, England, 1977.

146. Emerson, M., "Temperature Differences in Bridges: Basis of Design Requirements," Transport and Road Research Laboratory Report No. LR765, Crowthorne, Berkshire, England, 1977.

147. Emerson, M., "Temperatures in Bridges During the Hot Summer of 1976," Transport and Road Research Laboratory Report No. LR783, Crowthorne, Berkshire, England, 1977.

148. Emerson, M., "Temperatures in Bridges During the Cold Winter of 1978-1979," Transport and Road Research Laboratory Report No. LR926, Crowthorne, Berkshire, England, 1980.

149. Abeles, P. W., "Design of Partially Prestressed Concrete Beams" Journal of the American Concrete Institute, Vol. 64, No. 10, October 1967, pp. 669-677.

150. Burns, N. H., "Moment Curvature Relationships for Partially Prestressed Concrete Beams," Journal of the Prestressed Concrete Institute, Vol. 9, No. 1, February 1964, pp. 52-63.

151. Leonhardt, F., "To New Frontiers for Prestressed Concrete Design and Construction," Journal of the Prestressed Concrete Institute, Vol. 19, No. 5, September/October 1974, pp. 54-69.

152. Nilson, A. H., "Flexural Stresses After Cracking in Partially Prestressed Beams," Journal of the Prestressed Concrete Institute, Vol. 21, No. 4, July/August 1976, pp. 72-81.

153. Naaman, A. E., "Ultimate Analysis of Prestressed and Partially Prestressed Sections by Strain Compatability," Journal of the Prestressed Concrete Institute, Vol. 22, No. 1, January/February 1977, pp. 32-51.

154. Bennett, E. W., and Joynes, H. W., "Fatigue Resistance of Reinforcement in Partially Prestressed Beams," Journal of the Prestressed Concrete Institute, Vol. 22, No. 2, March/April 1977, pp. 78-88.

155. Moustafa, S. E., "Design of Partially Prestressed Concrete Flexural Members," Journal of the Prestressed Concrete Institute, Vol. 22, No. 3, May/June 1977, pp. 12-29.

156. Nawy, E. G., and Huang, P. T., "Crack and Deflection Control of Pretensioned Prestressed Beams," Journal of the Prestressed Concrete Institute, Vol. 22, No. 3, May/June 1977, pp. 30-47.

157. Mattock, A. H., "Flexural Strength of Prestressed Concrete Sections by Programmable Calculator," Journal of the Prestressed Concrete Institute, Vol. 24, No. 1, January/February 1979, pp. 32-54.

158. Brondum-Nielsen, T., "Service Analysis of Concrete Sections Under Service Load," Journal of the American Concrete Institute, Vol. 76, No. 2, February 1979, pp. 195-211.

159. Naaman, A. E., and Siriaksorn, A., "Serviceability Based Design of Partially Prestressed Beams - Part 1: Analytic Formulation," Journal of the Prestressed Concrete Institute, Vol. 24, No. 2, March/April 1979, pp. 64-89.

160. Naaman, A. E., and Siriaksorn, A., "Serviceability Based Design of Partially Prestressed Beams - Part 2: Computerized Design and Evaluation of Major Parameters," Journal of the Prestressed Concrete Institute, Vol. 24, No. 3, May/June 1979, pp. 40-60.

161. Nawy, E. G., and Chiang, J. Y., "Serviceability Behaviour of Post-Tensioned Beams," Journal of the Prestressed Concrete Institute, Vol. 25, No. 1, January/February 1980, pp. 74-95.

162. Thompson, K. J., and Park, R., "Ductility of Prestressed and Partially Prestressed Concrete Beam Sections," Journal of the Prestressed Concrete Institute, Vol. 25, No. 2, March/April 1980, pp. 46-70.

163. Brondum-Nielsen, T., "Stress Analysis of Cracked Arbitrary Concrete Section Under Service Load," Journal of the American Concrete Institute, Vol. 77, No. 6, November/December 1980, pp. 458-468.

164. Naaman, A. E., "Summary Review of FIP Symposia in Bucharest, Romania," Journal of the Prestressed Concrete Institute, Vol. 25, No. 6, November/December 1980, pp. 24-27.

165. Naaman, A. E., "A Proposal to Extend Some Code Provisions on Reinforcement to Partial Prestressing," Journal of the Prestressed Concrete Institute, Vol. 26, No. 2, March/April 1981, pp. 74-91.

166. Balaguru, P. N., "Design of Partially Prestressed Post-Tensioned Beams with Unbonded Tendons," Concrete International: Design and Construction, Vol. 3, No. 11, November 1981, pp. 30-41.

167. Branson, D. E., and Trost, H., "Unified Procedures for Predicting the Deflection and Centroidal Axis Location of Partially Cracked Nonprestressed and Prestressed Concrete Members," Journal of the American Concrete Institute, Vol. 79, No. 2, March/April 1982, pp. 119-130.

168. Branson, D. E., and Trost, H., "Application of the I-Effective Method in Calculating Deflections of Partially Prestressed Members," Journal of the Prestressed Concrete Institute, Vol. 27, No. 5, September/October 1982, pp. 62-77.

169. Inomata, S., "A Design Procedure for Partially Prestressed Concrete Beams Based on Strength and Serviceability," Journal of the Prestressed Concrete Institute, Vol. 27, No. 5, September/October 1982, pp. 100-116.

170. Brondum-Nielsen, T., "Ultimate Limit States of Cracked Arbitrary Concrete Sections Under Axial Load and Biaxial Bending," Concrete International: Design & Construction, Vol. 4, No. 11, November 1982, pp. 51-55.

171. Naaman, A. E., and Siriaksorn, A., "Reliability of Partially Prestressed Beams at Serviceability Limit States," Journal of the Prestressed Concrete Institute, Vol. 27, No. 6, November/December 1982, pp. 66-85.

172. Tadros, M. K., "Expedient Serviceability Analysis of Cracked Prestressed Concrete Beams," Journal of the Prestressed Concrete Institute, Vol. 27, No. 6, November/December 1982, pp. 86-111.

173. Cohn, M. Z., and Bartlett, M., "Computer-Simulated Flexural Tests of Partially Prestressed Concrete Sections," Journal of the Structural Division, Proceedings the of American Society of Civil Engineers, Vol. 108, No. ST12, December 1982, pp. 2747-2765.

174. Brondum-Nielsen, T., "Ultimate Flexural Capacity of Partially or Fully Prestressed Cracked Arbitrary Concrete Sections Under Axial Load Combined with Biaxial Bending," Concrete International: Design & Construction, Vol. 5, No. 1, January 1983, pp. 75-78.

175. Naaman, A. E., "Time-Dependent Deflection of Prestressed Beams by the Pressure-Line Method," Journal of the Prestressed Concrete Institute, Vol. 28, No. 2, March/April 1983, pp. 98-119.

176. Menn, C., "Partial Prestressing from the Designer's Point of View," Concrete International: Design and Construction, Vol. 5, No. 3, March 1983, pp. 52-59.

177. Huber, A., "Practical Design of Partially Prestressed Concrete Beams," Concrete International: Design and Construction, Vol. 5, No. 4, April 1983, pp. 49-54.

178. Bachmann, H., "From Full to Partial Prestressing," Concrete International: Design and Construction, Vol. 5, No. 10, October 1983, pp. 36-39.

179. Cohn, M. Z., and Frostig, Y., "Inelastic Behaviour of Continuous Prestressed Concrete Beams," Journal of the Structural Division, Proceedings of American Society of Civil Engineers, Vol. 109, No. ST10, October 1983, pp. 2292-2309.

180. Shushkewich, K. W., "Simplified Cracked Section Analysis," Journal of the American Concrete Institute, Vol. 80, No. 6, November/December 1983, pp. 526-531.

181. Lin, T. Y., "Partial Prestressing Design - Philosophy and Approach," American Concrete Institute Publication SP-59, 1979, pp. 257-267.

182. Leonhardt, F., "Recommendations for the Degree of Prestressing in Prestressed Concrete Structures," American Concrete Institute Publication SP-59, 1979, pp. 269-286.

183. Abeles, P. W., "Philosophy of Design of Partial Prestressing," American Concrete Institute Publication SP-59, 1979, pp. 287-304.

184. Guyon, Y, "Limit-State Design of Prestressed Concrete - Volume 2: The Design of the Member," John Wiley & Sons, New York, 1974.

185. Leonhardt, F., "Prestressed Concrete - Design and Construction," Wilhelm Ernst, Berlin, Germany, 1964.

186. Lin, T. Y., "Design of Prestressed Concrete Structures," John Wiley & Sons, New York, 1963.

187. Khachaturian, N., and Gurfinkel, G., "Prestressed Concrete," McGraw-Hill, New York, 1969.

188. Libby, J. R., "Modern Prestressed Concrete - Design Principles and Construction Methods," Van Nostrand Reinhold Co., New York, 1971.

189. Nilson, A. H., "Design of Prestressed Concrete," John Wiley & Sons, New York, 1978.

190. Lin, T. Y., and Burns, N. H., "Design of Prestressed Concrete Structures," John Wiley & Sons, New York, 1981.

191. Naaman, A. E., "Prestressed Concrete Analysis and Design - Fundamentals," McGraw-Hill, New York, 1982.

192. American Association of State Highway and Transportation Officials," Standard Specification for Highway Bridges," Twelfth Edition, Washington, DC, 1977.

193. Canadian Standard Association, "Design of Highway Bridges (CAN3-S6-M78)," Rexdale, Ontario, August 1978.

194. Ontario Ministry of Transportation and Communications, "Ontario Highway Bridge Design Code," Downsview, Ontario, 1979.

195. ACI Committee 318, "Building Code Requirements for Reinforced Concrete (ACI 318-77)," American Concrete Institute, Detroit, 1977.

196. Kollbrunner, C.F., and Basler, K., "Torsion in Structures: An Engineering Approach," Springer-Verlag, New York, 1969.

Appendix A

TIMEDEP user's manual

IDENTIFICATION

TIMEDEP: Time Dependent Analysis of Segmental Bridges
Programmed by K W Shushkewich, Jan 1984.

PURPOSE

The program computes the node displacements, element forces, element stresses, and support reactions for two-dimensional segmentally erected structures of arbitrary shape subjected to the time dependent effects of creep, shrinkage, and relaxation. The loads considered at each stage of erection are self weight, prestressing, construction loads, and thermal effects.

RESTRICTIONS

Dimension statements limit the program to structures with no more than 200 nodes, 200 elements, 20 cross sections, and 300 prestressing tendons. In addition, the storage occupied by the structure stiffness matrix may not exceed 4000 locations. The capacity can easily be expanded.

DESCRIPTION

The program is based on the direct stiffness method. Dirichlet series are used with the method of superposition to determine time dependent effects. Creep and shrinkage are based on the recommendations of ACI Committee 209 while relaxation is given by the expression of Magura, Sozen, and Siess. The program can easily be modified to handle other creep and shrinkage models.

STRUCTURAL IDEALIZATION

The structure is defined by a series of nodes (joints) connected by one-dimensional elements (members) possessing both flexural and axial stiffness. The nodes must be numbered, and this numbering should be chosen to minimize the largest node number difference within the elements. The elements must also be numbered, but in any convenient manner.

Two right-handed orthogonal Cartesian coordinate systems are used:

(a) Global system (X,Y,Z) - An arbitrary point is chosen as the origin such that the structure lies in the X-Y plane. Node displacements and support reactions are expressed in the global system.

(b) Local system (x,y,z) - Each element has a local coordinate system whose x axis is directed along the centroidal axis of the element from node I to node J. The global Z and local z axes have the same direction. The local x and z axes define the direction of the local y axis. Element forces are expressed in the local system.

INPUT DATA

The following sequence of data numerically defines the problem. Consistent units must be used.

A. PROBLEM TITLE (20A4) - One card
Columns 1-80: Problem title to be printed with output

B. CONTROL INFORMATION (9I5) - One card
Columns 1- 5: Number of nodes (max. 200)
6-10: Number of elements (max. 200)
11-15: Number of sections (max. 20)
16-20: Number of prestressing tendons (max. 300)
21-25: Number of construction stages (no limit)
26-30: IFLAG 0=echo check 1=production run
31-35: JFLAG 0=elastic analysis 1=time dependent
36-40: KFLAG 0=continuous beam 1=plane frame
41-45: LFLAG 0=ignore stresses 1=print stresses

C. CONCRETE PROPERTIES (8E10.0) - One card
Columns 1-10: Compressive strength (at 28 days)
11-20: Modulus of elasticity (at 28 days)
21-30: Poisson's ratio
31-40: Mass density
41-50: Thermal coefficient
51-60: Creep coefficient
61-70: Shrinkage coefficient
71-80: Curing period (days)

D. PRESTRESSED STEEL PROPERTIES (7E10.0) - One card
Columns 1-10: Modulus of elasticity
11-20: Guaranteed ultimate tensile strength
21-30: Yield stress (at 1% extension)
31-40: Friction coefficent
41-50: Wobble coefficient
51-60: Anchor set
61-70: Relaxation coefficient

E. NONPRESTRESSED STEEL PROPERTIES (3E10.0) - One card
Columns 1-10: Modulus of elasticity
11-20: Area
21-30: Eccentricity

F. SECTION DATA (I5,5X,8E10.0) - One card for each section

Columns 1- 5: Section number
11-20: Section area
21-30: Moment of inertia
31-40: Distance to centroid from top
41-50: Section depth
51-60: Section width
61-70: Statical moment
71-80: Thermal integral S1
81-90: Thermal integral S2

continuous beam	KFLAG=0	use section G
plane frame	KFLAG=1	use section H and I

G. NODE & ELEMENT DATA (3I5,5X,2E10.0) - One for each node

Columns 1- 5: Node number
6-10: Section number (default=1)
11-15: Stage number
21-30: Segment length
31-40: Casting date

H. NODE DATA (I5,5X,2E10.0) - One card for each node

Columns 1- 5: Node number
11-20: X coordinate
21-30: Y coordinate

I. ELEMENT DATA (6I5,10X,E10.0) - One card for each element

Columns 1- 5: Element number
6-10: Node I
11-15: Node J
16-20: Section number at node I (default=1)
21-25: Section number at node J (blank taken as section no. at node I)
26-30: Stage number
41-50: Casting date

J. PRESTRESSING TENDON DATA (4I5,10X,2E10.0)

One card for each prestressing tendon
Columns 1- 5: Prestressing tendon number
6-10: Element I
11-15: Element J
16-20: Stage number
31-40: Area
41-50: Eccentricity

K. STAGE DATA - One set of cards for each stage

(a) CONTROL INFORMATION (I5,5X,3I0.0) - One card

Columns 1- 5: Stage number
11-20: Erection date
21-30: Temperature at top
31-40: Temperature at bottom

(b) SUPPORT CONDITIONS (4I5)
As many cards as necessary - use blank card to terminate
Columns 1- 5: Node number
6-10: Support code in X direction 0=no support
11-15: Support code in Y direction 1=support
16-20: Support code in R direction

(c) CONSTRUCTION LOADS (I5,5X,3E10.0)
As many cards as necessary - use blank card to terminate
Columns 1- 5: Node number
11-20: X load
21-30: Y load
31-40: Moment

L. NEXT PROBLEM

Any number of problems may be entered and the data is terminated by two blank cards.

OUTPUT INFORMATION

The following information is printed at each stage by the program.

A. Echo of the input data

B. Node displacements

C. Element forces

D. Element stresses (optional)

E. Support Reactions

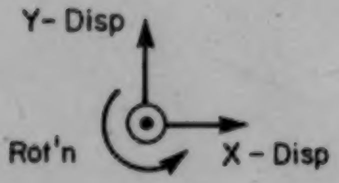
Y- Disp
Rot'n
X - Disp

(a) node displacements

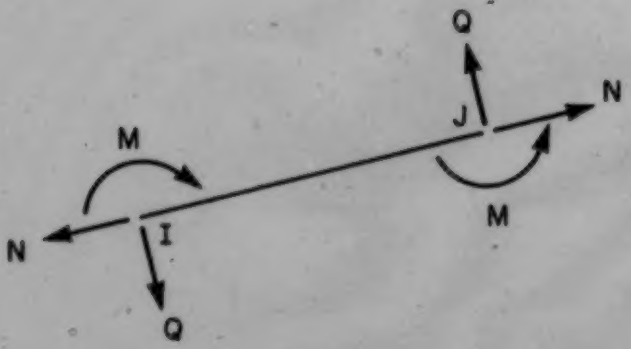

(b) element forces

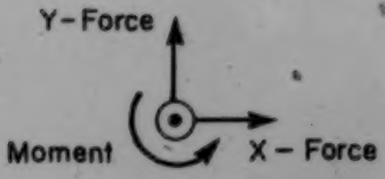
Y-Force
Moment
X - Force

(c) support reactions

Figure A.1 Sign conventions for node displacements and element forces

Appendix B

FORTRAN listing of TIMEDEP

```
C      PROGRAM TIMEDEP (INPUT,OUTPUT,TAPE5=INPUT,TAPE6=OUTPUT)
C
C      ****************************************************************
C      *                                                              *
C      *  TIMEDEP:  TIME DEPENDENT ANALYSIS OF SEGMENTAL BRIDGES      *
C      *            PROGRAMMED BY K W SHUSHKEWICH, JAN 1984.          *
C      *                                                              *
C      ****************************************************************
C
       COMMON /CNL/  DAT,TIM,HED(20),T1,T2,NSTAGE,NST,IFL,JFL,KFL,LFL
       COMMON /CON/  FC28,EC28,PR,RO,TC,CRP,SHR,TCUR,ENS,ANS,YNS
       COMMON /STL/  EPS,FPU,FPY,FPJ,FPI,FPE,FRIC,WOBL,SET,RLX
       COMMON /SEC/  SA(20),SI(20),SY(20),SD(20),SB(20),SO(20),
      1              S1(20),S2(20),NS
       COMMON /NOD/  X(200),Y(200),KSUP(200,3),INI(200),INJ(200),NN
       COMMON /EMT/  NODI(200),NODJ(200),NSECI(200),NSECJ(200),ECEF(200),
      1              EA(200),EI(200),EY(200),XL(200),COSA(200),SINA(200),
      2              NSTG(200),SEGL(200),CDAT(200),EDAT(50),KSTG(200),NE
       COMMON /PRS/  NELI(300),NELJ(300),MSTG(300),APS(300),YPS(300),NPT
       COMMON /TYM/  DNR(200),DMR(200),AN(200,3),AM(200,3)
       COMMON /STF/  AKA(200,6,6),EKA(200,6,6),RP(200,6),LM(200,6),SHP
       COMMON /FRC/  DN(200,3),FE(200,6),R(600),NEQ,MBAND,MAXL
C
       COMMON SK(4000)
       MAXL=4000
C
       CALL TIME(10,0,DAT)
       CALL TIME( 4,0,TIM)
    10 CALL READ
       CALL ELNK
       DO 20 NST=1,NSTAGE
       CALL STAG
       IF (IFL.EQ.0) GO TO 20
       CALL SELF
       CALL PRES
       CALL TEMP
       CALL TYME
       CALL STIF(SK,NEQ,MBAND)
       CALL SOLV(SK,R,NEQ,MBAND,1)
       CALL SOLV(SK,R,NEQ,MBAND,2)
       CALL FORC
       CALL RITE
    20 CONTINUE
       GO TO 10
C
       END
C      ****************************************************************
       SUBROUTINE READ
C
       COMMON /CNL/  DAT,TIM,HED(20),T1,T2,NSTAGE,NST,IFL,JFL,KFL,LFL
       COMMON /CON/  FC28,EC28,PR,RO,TC,CRP,SHR,TCUR,ENS,ANS,YNS
       COMMON /STL/  EPS,FPU,FPY,FPJ,FPI,FPE,FRIC,WOBL,SET,RLX
       COMMON /SEC/  SA(20),SI(20),SY(20),SD(20),SB(20),SO(20),
      1              S1(20),S2(20),NS
       COMMON /NOD/  X(200),Y(200),KSUP(200,3),INI(200),INJ(200),NN
       COMMON /EMT/  NODI(200),NODJ(200),NSECI(200),NSECJ(200),ECEF(200),
      1              EA(200),EI(200),EY(200),XL(200),COSA(200),SINA(200),
      2              NSTG(200),SEGL(200),CDAT(200),EDAT(50),KSTG(200),NE
       COMMON /PRS/  NELI(300),NELJ(300),MSTG(300),APS(300),YPS(300),NPT
       COMMON /TYM/  DNR(200),DMR(200),AN(200,3),AM(200,3)
       COMMON /STF/  AKA(200,6,6),EKA(200,6,6),RP(200,6),LM(200,6),SHP
       COMMON /FRC/  DN(200,3),FE(200,6),R(600),NEQ,MBAND,MAXL
C
C      READ & WRITE CONTROL INFORMATION
C
       READ  (5,10) HED,NN,NE,NS,NPT,NSTAGE,IFL,JFL,KFL,LFL
    10 FORMAT(20A4/9I5)
       IF (NN.EQ.0) CALL EXIT
       WRITE (6,20) DAT,TIM,HED,NN,NE,NS,NPT,NSTAGE
    20 FORMAT(45H1TIME DEPENDENT ANALYSIS OF SEGMENTAL BRIDGES/
      1        1H ,6HDATE: ,A8,4X,6HTIME: ,A8///1H ,20A4///
      2       31H NO. OF NODES                 =,I4/
      3       31H NO. OF ELEMENTS              =,I4/
      4       31H NO. OF SECTIONS              =,I4/
      5       31H NO. OF PRESTRESSING TENDONS  =,I4/
      6       31H NO. OF CONSTRUCTION STAGES   =,I4//)
C
C      READ & WRITE MATERIAL PROPERTIES
C
       READ  (5,30) FC28,EC28,PR,RO,TC,CRP,SHR,TCUR,
      1             EPS,FPU,FPY,FRIC,WOBL,SET,RLX,ENS,ANS,YNS
    30 FORMAT(8E10.0/7E10.0/3E10.0)
       FPJ=0.8*FPU
       FPI=0.7*FPU
       FPE=0.6*FPU
       WRITE (6,40) FC28,EC28,PR,RO,TC,CRP,SHR,TCUR
    40 FORMAT(21H CONCRETE PROPERTIES://
      1       45H COMPRESSIVE STRENGTH (AT 28 DAYS) . . . . . =,E12.4/
      2       45H MODULUS OF ELASTICITY (AT 28 DAYS)  . . . . =,E12.4/
      3       45H POISSON'S RATIO . . . . . . . . . . . . . . =,E12.4/
      4       45H MASS DENSITY  . . . . . . . . . . . . . . . =,E12.4/
      5       45H THERMAL COEFFICIENT . . . . . . . . . . . . =,E12.4/
      6       45H CREEP COEFFICIENT . . . . . . . . . . . . . =,E12.4/
      7       45H SHRINKAGE COEFFICIENT . . . . . . . . . . . =,E12.4/
      8       45H CURING PERIOD (DAYS)  . . . . . . . . . . . =,E12.4/)
       WRITE (6,50) EPS,FPU,FPY,FPJ,FPI,FPE,FRIC,WOBL,SET,RLX
    50 FORMAT(30H PRESTRESSED STEEL PROPERTIES://
      1       45H MODULUS OF ELASTICITY . . . . . . . . . . . =,E12.4/
      2       45H GUARANTEED ULTIMATE TENSILE STRENGTH  . . . =,E12.4/
      3       45H YIELD STRESS (AT 1% EXTENSION)  . . . . . . =,E12.4/
      4       45H JACKING STRESS (0.8*FPU)  . . . . . . . . . =,E12.4/
      5       45H INITIAL STRESS (0.7*FPU)  . . . . . . . . . =,E12.4/
      6       45H EFFECTIVE STRESS  . . . . . . . . . . . . . =,E12.4/
      7       45H FRICTION COEFFICIENT  . . . . . . . . . . . =,E12.4/
      8       45H WOBBLE COEFFICIENT  . . . . . . . . . . . . =,E12.4/
      9       45H ANCHOR SET  . . . . . . . . . . . . . . . . =,E12.4/
      1       45H RELAXATION COEFFICIENT  . . . . . . . . . . =,E12.4/)
       WRITE (6,60) ENS,ANS,YNS
    60 FORMAT(33H NONPRESTRESSED STEEL PROPERTIES://
      1       45H MODULUS OF ELASTICITY . . . . . . . . . . . =,E12.4/
      2       45H AREA OF REINFORCEMENT . . . . . . . . . . . =,E12.4/
      3       45H ECCENTRICITY OF REINFORCEMENT . . . . . . . =,E12.4)
C
```

```
C     READ & WRITE SECTION DATA
C
      READ  (5,70)
     1  (M,SA(M),SI(M),SY(M),SD(M),SB(M),SO(M),S1(M),S2(M),N=1,NS)
   70 FORMAT(I5,5X,8E10.0)
      WRITE (6,80)
     1  (N,SA(N),SI(N),SY(N),SD(N),SB(N),SO(N),S1(N),S2(N),N=1,NS)
   80 FORMAT(//13H SECTION DATA//
     1  5H SECT,14X,2HAC,14X,2HIC,14X,2HYC,14X,2HDC,
     2          14X,2HBC,14X,2HOC,14X,2HS1,14X,2HS2/
     3  (I5,8E16.4))
      DO 85 N=1,NS
      IF (SB(N).EQ.0.0) SB(N)=1.E+15
   85 CONTINUE
C
C     READ & WRITE NODE AND ELEMENT DATA
C
      IF (KFL.EQ.1) GO TO 130
      READ  (5,90) (M,NSECI(M),NSTG(M),SEGL(M),CDAT(M),N=1,NN)
   90 FORMAT(3I5,5X,2E10.0)
      X(1)=0.0
      DO 100 N=1,NE
  100 X(N+1)=X(N)+SEGL(N)
      DO 110 N=1,NN
  110 Y(N)=-SY(NSECI(N))
      DO 120 N=1,NE
      NODI(N)=N
      NODJ(N)=N+1
  120 NSECJ(N)=NSECI(N+1)
      GO TO 160
  130 READ  (5,140) (M,X(M),Y(M),N=1,NN)
  140 FORMAT(I5,5X,2E10.0)
      READ  (5,150)
     1  (M,NODI(M),NODJ(M),NSECI(M),NSECJ(M),NSTG(M),CDAT(M),N=1,NE)
  150 FORMAT(6I5,10X,E10.0)
  160 WRITE (6,170) (N,X(N),Y(N),N=1,NN)
  170 FORMAT(//10H NODE DATA//
     1  5H NODE,11X,5HX-ORD,11X,5HY-ORD/
     2  (I5,2E16.4))
      WRITE (6,180)
  180 FORMAT(//13H ELEMENT DATA/82X,7HCASTING/
     1  5H ELMT,3X,5HNOD-I,3X,5HNOD-J,3X,5HSEC-I,3X,5HSEC-J,3X,5HSTAGE,
     2              9X,7H LENGTH,9X,7H WEIGHT,5X,7H   DATE)
      DO 200 N=1,NE
      IF (NSECI(N).EQ.0) NSECI(N)=1
      IF (NSECJ(N).EQ.0) NSECJ(N)=NSECI(N)
      NI=NODI(N)
      NJ=NODJ(N)
      NSI=NSECI(N)
      NSJ=NSECJ(N)
      EA(N)=(SA(NSI)+SA(NSJ))/2.0
      EI(N)=(SI(NSI)+SI(NSJ))/2.0
      EY(N)=(SY(NSI)+SY(NSJ))/2.0
      DX=X(NJ)-X(NI)
      DY=Y(NJ)-Y(NI)
      SEGL(N)=SQRT(DX**2+DY**2)
      SEGW=RD*EA(N)*SEGL(N)
      WRITE (6,190) N,NI,NJ,NSI,NSJ,NSTG(N),SEGL(N),SEGW,CDAT(N)
  190 FORMAT(I5,5I8,2E16.4,F12.1)
  200 CONTINUE
C
C     READ & WRITE PRESTRESSING TENDON DATA
C
      IF (NPT.EQ.0) GO TO 230
      READ  (5,210) (M,NELI(M),NELJ(M),NSTG(M),APS(M),YPS(M),N=1,NPT)
  210 FORMAT(4I5,10X,2E10.0)
      WRITE (6,220) (N,NELI(N),NELJ(N),NSTG(N),APS(N),YPS(N),N=1,NPT)
  220 FORMAT(//25H PRESTRESSING TENDON DATA//
     1  5H TEND,3X,5HEMT-I,3X,5HEMT-J,3X,5HSTAGE,
     2  12X,4HAREA,4X,12HECCENTRICITY/
     3  (I5,3I8,2E16.4))
  230 CONTINUE
C
C     FIND LOCATION MATRIX
C
      DO 240 N=1,NE
      LM(N,1)=3*NODI(N)-2
      LM(N,2)=LM(N,1)+1
      LM(N,3)=LM(N,2)+1
      LM(N,4)=3*NODJ(N)-2
      LM(N,5)=LM(N,4)+1
  240 LM(N,6)=LM(N,5)+1
C
C     DETERMINE BANDWIDTH
C
      NEQ=3*NN
      MBAND=0
      DO 250 N=1,NE
      MM=IABS(NODI(N)-NODJ(N))
      IF (MBAND.LT.MM) MBAND=MM
  250 CONTINUE
      MBAND=3*(MBAND+1)
      WRITE (6,260) NEQ,MBAND
  260 FORMAT(//19H NO. OF EQUATIONS =,I4/
     1           19H BANDWIDTH        =,I4)
      L=NEQ*MBAND
      IF (L.LE.MAXL) GO TO 280
      WRITE (6,270)
  270 FORMAT(///27H STIFFNESS MATRIX TOO LARGE)
      CALL EXIT
  280 CONTINUE
C
C     INITIALIZE NODE DISPLACEMENTS, ELEMENT FORCES, & SUPPORT CONDITIONS
C
      DO 290 I=1,NN
      DO 290 J=1,3
      KSUP(I,J)=0.0
  290 DN(I,J)=0.0
      DO 300 I=1,NE
      ECEF(I)=EC28
      DO 300 J=1,6
  300 FE(I,J)=0.0
C
```

```
      RETURN
      END
C     ***************************************************************
      SUBROUTINE STAG
C
      COMMON /CNL/  DAT,TIM,HED(20),T1,T2,NSTAGE,NST,IFL,JFL,KFL,LFL
      COMMON /CON/  FC28,EC28,PR,RO,TC,CRP,SHR,TCUR,ENS,ANS,YNS
      COMMON /STL/  EPS,FPU,FPY,FPJ,FPI,FPE,FRIC,WOBL,SET,RLX
      COMMON /SEC/  SA(20),SI(20),SY(20),SD(20),SB(20),SO(20),
     1              S1(20),S2(20),NS
      COMMON /NOD/  X(200),Y(200),KSUP(200,3),INI(200),INJ(200),NN
      COMMON /EMT/  NODI(200),NODJ(200),NSECI(200),NSECJ(200),ECEF(200),
     1              EA(200),EI(200),EY(200),XL(200),COSA(200),SINA(200),
     2              NSTG(200),SEGL(200),CDAT(200),EDAT(50),KSTG(200),NE
      COMMON /PRS/  NELI(300),NELJ(300),MSTG(300),APS(300),YPS(300),NPT
      COMMON /TYM/  DNR(200),DMR(200),AN(200,3),AM(200,3)
      COMMON /STF/  AKA(200,6,6),EKA(200,6,6),RP(200,6),LM(200,6),SMP
      COMMON /FRC/  DN(200,3),FE(200,6),R(600),NEQ,MBAND,MAXL
      COMMON /ABC/  IJKSTG(200)
C
C     INITIALIZE STRUCTURE LOAD VECTOR
C
      DO 10 I=1,NEQ
   10 R(I)=0.0
C
C     INITIALIZE ELEMENT LOAD VECTOR
C
      DO 20 I=1,NE
      DO 20 J=1,6
   20 RP(I,J)=0.0
C
C     WRITE HEADING
C
      READ  (5,30) MST,EDAT(MST+1),T1,T2
   30 FORMAT(I5,5X,3E10.0)
      EDAT(1)=EDAT(2)
      IF (MST.EQ.NST) GO TO 50
      WRITE (6,40)
   40 FORMAT(45H1DATA OUT OF SEQUENCE - EXECUTION TERMINATED!)
      CALL EXIT
   50 WRITE (6,60) DAT,TIM,HED,NST,EDAT(NST+1),T1,T2
   60 FORMAT(45H1TIME DEPENDENT ANALYSIS OF SEGMENTAL BRIDGES/
     1        1H ,6HDATE: ,A6,4X,6HTIME: ,A6///1H ,20A4//
     2        8H STAGE =,I3,12X,15HERECTION DATE =,F7.1///
     3       24H TEMPERATURE AT TOP    =,F8.1/
     4       24H TEMPERATURE AT BOTTOM =,F8.1)
C
C     READ & WRITE SEGMENTS ASSEMBLED
C
      WRITE (6,70)
   70 FORMAT(//19H SEGMENTS ASSEMBLED/        28X,7HCASTING/
     1         5H ELMT,3X,6HNOD-I,3X,6HNOD-J,5X,7H   DATE)
      DO 90 N=1,NE
      IF (NSTG(N).NE.NST) GO TO 90
      WRITE (6,80) N,NODI(N),NODJ(N),CDAT(N)
   80 FORMAT(I5,2I8,F12.1)
   90 CONTINUE
C
C     READ & WRITE TENDONS STRESSED
C
      IF (NPT.EQ.0) GO TO 130
      WRITE (6,100)
  100 FORMAT(//17H TENDONS STRESSED//
     1         5H TEND,3X,6HEMT-I,3X,6HEMT-J)
      DO 120 N=1,NPT
      IF (MSTG(N).NE.NST) GO TO 120
      WRITE (6,110) N,NELI(N),NELJ(N)
  110 FORMAT(I5,2I8)
  120 CONTINUE
C
C     READ & WRITE SUPPORT CONDITIONS
C
  130 READ  (5,140) N,I,J,K
  140 FORMAT(4I5)
      IF (N.EQ.0) GO TO 150
      KSUP(N,1)=I
      KSUP(N,2)=J
      KSUP(N,3)=K
      GO TO 130
  150 CONTINUE
      WRITE (6,160)
  160 FORMAT(//19H SUPPORT CONDITIONS//
     1         5H NODE,3X,6HX-SUP,3X,6HY-SUP,3X,6HR-SUP)
      DO 180 N=1,NN
      I=KSUP(N,1)
      J=KSUP(N,2)
      K=KSUP(N,3)
      IF (I.EQ.0.AND.J.EQ.0.AND.K.EQ.0) GO TO 180
      WRITE (6,170) N,I,J,K
  170 FORMAT(I5,3I8)
  180 CONTINUE
C
C     READ & WRITE CONSTRUCTION LOADS
C
      WRITE (6,190)
  190 FORMAT(//19H CONSTRUCTION LOADS//
     1         5H NODE,10X,6HX-LOAD,10X,6HY-LOAD,10X,6HMOMENT)
  200 READ  (5,210) N,RX,RY,RM
  210 FORMAT(I5,5X,3E10.0)
      IF (N.EQ.0) GO TO 230
      WRITE (6,220) N,RX,RY,RM
  220 FORMAT(I5,3E16.4)
      K=3*(N-1)
      R(K+1)=R(K+1)+RX
      R(K+2)=R(K+2)+RY
      R(K+3)=R(K+3)+RM
      GO TO 200
  230 CONTINUE
C
C     FORM KSTG(N)
C
      IF (IFL.EQ.0) RETURN
      DO 240 N=1,NN
  240 KSTG(N)=0
      DO 250 N=1,NE
      IF (NSTG(N).GT.NST) GO TO 250
      KSTG(NODI(N))=1
      KSTG(NODJ(N))=1
  250 CONTINUE
C
C     FORM IJKSTG(N)
C
      DO 260 N=1,NE
      I=1
      J=1
      IF (NSTG(N  ).GT.NST) I=0
      IF (NSTG(N+1).GT.NST) J=0
      IF (N.EQ.NE) J=0
  260 IJKSTG(N)=J-I
C
      RETURN
      END
C     ******************************************************************
      SUBROUTINE SELF
C
      COMMON /CNL/  DAT,TIM,HED(20),T1,T2,NSTAGE,NST,IFL,JFL,KFL,LFL
      COMMON /CON/  FC28,EC28,PR,RO,TC,CRP,SHR,TCUR,ENS,ANS,YNS
      COMMON /STL/  EPS,FPU,FPY,FPJ,FPI,FPE,FRIC,WOBL,SET,RLX
      COMMON /SEC/  SA(20),SI(20),SY(20),SD(20),SB(20),SQ(20),
     1              S1(20),S2(20),NS
      COMMON /NOD/  X(200),Y(200),KSUP(200,3),IHI(200),IHJ(200),NN
      COMMON /EMT/  NODI(200),NODJ(200),NSECI(200),NSECJ(200),ECEF(200),
     1              EA(200),EI(200),EY(200),XL(200),COSA(200),SINA(200),
     2              NSTG(200),SEGL(200),CDAT(200),EDAT(50),KSTG(200),NE
      COMMON /PRS/  NELI(300),NELJ(300),MSTG(300),APS(300),YPS(300),NPT
      COMMON /TYM/  DNR(200),DMR(200),AN(200,3),AM(200,3)
      COMMON /STF/  AKA(200,6,6),EKA(200,6,6),RP(200,6),LM(200,6),SHP
      COMMON /FRC/  DN(200,3),FE(200,6),R(600),NEQ,MBAND,MAXL
C
C     ADD SELF WEIGHT TO STRUCTURE LOAD VECTOR
C
      DO 10 N=1,NE
      IF (NSTG(N).NE.NST) GO TO 10
      W1=RO*SA(NSECI(N))
      W2=RO*SA(NSECJ(N))
      WR1=-(7.0*W1+3.0*W2)*XL(N)/20.0
      WR2=-(3.0*W1+7.0*W2)*XL(N)/20.0
      WM1=-(6.0*W1+4.0*W2)*XL(N)**2/120.0*COSA(N)
      WM2=+(4.0*W1+6.0*W2)*XL(N)**2/120.0*COSA(N)
      RP(N,1)=+WR1*SINA(N)
      RP(N,2)=+WR1*COSA(N)
      RP(N,3)=+WM1
      RP(N,4)=+WR2*SINA(N)
      RP(N,5)=+WR2*COSA(N)
      RP(N,6)=+WM2
      K=3*(NODI(N)-1)
      R(K+2)=R(K+2)+WR1
      R(K+3)=R(K+3)+WM1
      K=3*(NODJ(N)-1)
      R(K+2)=R(K+2)+WR2
      R(K+3)=R(K+3)+WM2
   10 CONTINUE
C
      RETURN
      END
C     ******************************************************************
.     SUBROUTINE PRES
C
      COMMON /CNL/  DAT,TIM,HED(20),T1,T2,NSTAGE,NST,IFL,JFL,KFL,LFL
      COMMON /CON/  FC28,EC28,PR,RO,TC,CRP,SHR,TCUR,ENS,ANS,YNS
      COMMON /STL/  EPS,FPU,FPY,FPJ,FPI,FPE,FRIC,WOBL,SET,RLX
      COMMON /SEC/  SA(20),SI(20),SY(20),SD(20),SB(20),SQ(20),
     1              S1(20),S2(20),NS
      COMMON /NOD/  X(200),Y(200),KSUP(200,3),IHI(200),IHJ(200),NN
      COMMON /EMT/  NODI(200),NODJ(200),NSECI(200),NSECJ(200),ECEF(200),
     1              EA(200),EI(200),EY(200),XL(200),COSA(200),SINA(200),
     2              NSTG(200),SEGL(200),CDAT(200),EDAT(50),KSTG(200),NE
      COMMON /PRS/  NELI(300),NELJ(300),MSTG(300),APS(300),YPS(300),NPT
      COMMON /TYM/  DNR(200),DMR(200),AN(200,3),AM(200,3)
      COMMON /STF/  AKA(200,6,6),EKA(200,6,6),RP(200,6),LM(200,6),SHP
      COMMON /FRC/  DN(200,3),FE(200,6),R(600),NEQ,MBAND,MAXL
C
C     ADD PRESTRESS TO STRUCTURE LOAD VECTOR
C
      IF (NPT.EQ.0) RETURN
      DO 20 M=1,NPT
      IF (MSTG(M).NE.NST) GO TO 20
      N1=NELI(M)
      N2=NELJ(M)
      P=FPI*APS(M)
      DO 10 N=N1,N2
      K=3*(NODI(N)-1)
      R(K+1)=R(K+1)+P
      R(K+3)=R(K+3)+P*(YPS(M)-SY(NSECI(N)))
      K=3*(NODJ(N)-1)
      R(K+1)=R(K+1)-P
   10 R(K+3)=R(K+3)-P*(YPS(M)-SY(NSECJ(N)))
   20 CONTINUE
C
      RETURN
      END
C     ******************************************************************
      SUBROUTINE TEMP
C
      COMMON /CNL/  DAT,TIM,HED(20),T1,T2,NSTAGE,NST,IFL,JFL,KFL,LFL
      COMMON /CON/  FC28,EC28,PR,RO,TC,CRP,SHR,TCUR,ENS,ANS,YNS
      COMMON /STL/  EPS,FPU,FPY,FPJ,FPI,FPE,FRIC,WOBL,SET,RLX
      COMMON /SEC/  SA(20),SI(20),SY(20),SD(20),SB(20),SQ(20),
     1              S1(20),S2(20),NS
      COMMON /NOD/  X(200),Y(200),KSUP(200,3),IHI(200),IHJ(200),NN
      COMMON /EMT/  NODI(200),NODJ(200),NSECI(200),NSECJ(200),ECEF(200),
     1              EA(200),EI(200),EY(200),XL(200),COSA(200),SINA(200),
     2              NSTG(200),SEGL(200),CDAT(200),EDAT(50),KSTG(200),NE
      COMMON /PRS/  NELI(300),NELJ(300),MSTG(300),APS(300),YPS(300),NPT
      COMMON /TYM/  DNR(200),DMR(200),AN(200,3),AM(200,3)
      COMMON /STF/  AKA(200,6,6),EKA(200,6,6),RP(200,6),LM(200,6),SHP
      COMMON /FRC/  DN(200,3),FE(200,6),R(600),NEQ,MBAND,MAXL
C
C     ADD TEMPERATURE TO STRUCTURE LOAD VECTOR
C
      IF (T1.EQ.0.0.AND.T2.EQ.0.0) RETURN
      DO 10 N=1,NE
      IF (NSTG(N).GT.NST) GO TO 10
      NSI=NSECI(N)
      NSJ=NSECJ(N)
      TN=EC28*TC*(T1-T2)*(S1(NSI)+S1(NSJ))/2.0+EC28*TC*T2*EA(N)
      TM=EC28*TC*(T1-T2)*(S2(NSI)+S2(NSJ))/2.0
      RP(N,1)=RP(N,1)-TN
      RP(N,3)=RP(N,3)+TM
      RP(N,4)=RP(N,4)+TN
      RP(N,6)=RP(N,6)-TM
      K=3*(NODI(N)-1)
      R(K+1)=R(K+1)-TN*COSA(N)
      R(K+2)=R(K+2)-TN*SINA(N)
      R(K+3)=R(K+3)+TM
      K=3*(NODJ(N)-1)
      R(K+1)=R(K+1)+TN*COSA(N)
      R(K+2)=R(K+2)+TN*SINA(N)
      R(K+3)=R(K+3)-TM
   10 CONTINUE
C
      RETURN
      END
C     ****************************************************************
      SUBROUTINE TYME
C
      COMMON /CNL/  DAT,TIM,HED(20),T1,T2,NSTAGE,NST,IFL,JFL,KFL,LFL
      COMMON /CON/  FC28,EC28,PR,RO,TC,CRP,SHR,TCUR,ENS,ANS,YNS
      COMMON /STL/  EPS,FPU,FPY,FPJ,FPI,FPE,FRIC,WOBL,SET,RLX
      COMMON /SEC/  SA(20),SI(20),SY(20),SD(20),SB(20),SO(20),
     1              S1(20),S2(20),NS
      COMMON /NOD/  X(200),Y(200),KSUP(200,3),INI(200),INJ(200),NN
      COMMON /EMT/  NODI(200),NODJ(200),NSECI(200),NSECJ(200),ECEF(200),
     1              EA(200),EI(200),EY(200),XL(200),COSA(200),SINA(200),
     2              NSTG(200),SEGL(200),CDAT(200),EDAT(50),KSTG(200),NE
      COMMON /PRS/  NELI(300),NELJ(300),MSTG(300),APS(300),YPS(300),NPT
      COMMON /TYM/  DNR(200),DMR(200),AN(200,3),AM(200,3)
      COMMON /STF/  AKA(200,6,6),EKA(200,6,6),RP(200,6),LM(200,6),SNP
      COMMON /FRC/  DN(200,3),FE(200,6),R(600),NEQ,MBAND,MAXL
C
      DIMENSION A(3),Z(3)
      DATA A /0.721982,0.677982,0.486549/
      DATA Z /0.1     ,0.01    ,0.001   /
C
C     EC(T)=SQRT(T/(4.00+0.85*T))*EC28
      EC(T)=SQRT(T/(2.30+0.92*T))*EC28
C     EC(T)=SQRT(T/(1.00+0.95*T))*EC28
C     EC(T)=SQRT(T/(0.70+0.98*T))*EC28
      CU(T)=1.25*(T**(-0.118))
C     CU(T)=1.13*(T**(-0.095))
      CREEP(T,TO)=((T-TO)**0.6)/(10.0+((T-TO)**0.6))*CU(TO)*CRP
      SHRNK(T,TO)=(T-TO)/(35.0+(T-TO))*SHR
C     SHRNK(T,TO)=(T-TO)/(55.0+(T-TO))*SHR
      RELAX(T,TO,FSI)=FSI/RLX*(FSI/FPY-0.55)
     1      *(ALOG10(24.0*T)-ALOG10(24.0*TO))
C
C     ADD CREEP & SHRINKAGE EFFECTS TO STRUCTURE LOAD VECTOR
C
      IF (JFL.EQ.0) RETURN
      DO 30 N=1,NE
      IF (NSTG(N).GT.NST) GO TO 30
      TJ  =EDAT(NST  )-CDAT(N)
      TJP1=EDAT(NST+1)-CDAT(N)
      IF (TJ  .LE.0.01) TJ  =1.0
      IF (TJP1.LE.0.01) TJP1=1.0
      ECEF(N)=EC(TJ)/(1.0+CREEP(TJP1,TJ))
      IF (NST.EQ.1) GO TO 30
      DNC=ECEF(N)*EA(N)*(SHRNK(TJP1,TCUR)-SHRNK(TJ,TCUR))
      DMC=0.0
      AGE=1.0/EC(TJ)*CU(TJ)/CU(28.0)*CRP/2.35
      DO 20 I=1,3
      TAN=DNR(N)*A(I)*AGE
      TAM=DMR(N)*A(I)*AGE
      IF (NST.EQ.2) GO TO 10
      DTJM1=EDAT(NST)-EDAT(NST-1)
      FACT=EXP(-Z(I)*DTJM1)
      TAN=TAN+AN(N,I)*FACT
      TAM=TAM+AM(N,I)*FACT
   10 AN(N,I)=TAN
      AM(N,I)=TAM
      DTJ=EDAT(NST+1)-EDAT(NST)
      FACT=(1.0-EXP(-Z(I)*DTJ))
      DNC=DNC+ECEF(N)*AN(N,I)*FACT
   20 DMC=DMC+ECEF(N)*AM(N,I)*FACT
      RP(N,1)=RP(N,1)-DNC
      RP(N,3)=RP(N,3)-DMC
      RP(N,4)=RP(N,4)+DNC
      RP(N,6)=RP(N,6)+DMC
      K=3*(NODI(N)-1)
      R(K+1)=R(K+1)-DNC*COSA(N)
      R(K+2)=R(K+2)-DNC*SINA(N)
      R(K+3)=R(K+3)-DMC
      K=3*(NODJ(N)-1)
      R(K+1)=R(K+1)+DNC*COSA(N)
      R(K+2)=R(K+2)+DNC*SINA(N)
      R(K+3)=R(K+3)+DMC
   30 CONTINUE
C
C     ADD RELAXATION EFFECTS TO STRUCTURE LOAD VECTOR
C
      IF (NPT.EQ.0) RETURN
      DO 50 M=1,NPT
      IF (MSTG(M).GT.NST) GO TO 50
      N1=NELI(M)
      N2=NELJ(M)
      DO 40 N=N1,N2
      TJ  =EDAT(NST  )-CDAT(N)
      TJP1=EDAT(NST+1)-CDAT(N)
      IF (TJ  .LE.0.01) TJ  =1.0
      IF (TJP1.LE.0.01) TJP1=1.0
      PSI=FPI/FPY
      IF (PSI.LT.0.55) GO TO 50
      DMP=RELAX(TJP1,TJ,FPI)*APS(M)
      DMP=DMP*(YPS(M)-EY(N))
      K=3*(NODI(N)-1)
      R(K+1)=R(K+1)-DMP*COSA(N)
      R(K+2)=R(K+2)-DMP*SINA(N)
      R(K+3)=R(K+3)-DMP
      K=3*(NODJ(N)-1)
      R(K+1)=R(K+1)+DMP*COSA(N)
      R(K+2)=R(K+2)+DMP*SINA(N)
   40 R(K+3)=R(K+3)+DMP
   50 CONTINUE
C
      RETURN
      END
C     ******************************************************************
      SUBROUTINE STIF(SK,NNN,MMM)
C
      COMMON /CNL/  DAT,TIM,HED(20),T1,T2,NSTAGE,NST,IFL,JFL,KFL,LFL
      COMMON /CON/  FC28,EC28,PR,RO,TC,CRP,SHR,TCUR,ENS,ANS,YNS
      COMMON /STL/  EPS,FPU,FPY,FPJ,FPI,FPE,FRIC,WOBL,SET,RLX
      COMMON /SEC/  SA(20),SI(20),SY(20),SD(20),SB(20),SQ(20),
     1              S1(20),S2(20),NS
      COMMON /NOD/  X(200),Y(200),KSUP(200,3),INI(200),INJ(200),NN
      COMMON /EMT/  NODI(200),NODJ(200),NSECI(200),NSECJ(200),ECEF(200),
     1              EA(200),EI(200),EY(200),XL(200),COSA(200),SINA(200),
     2              NSTG(200),SEGL(200),CDAT(200),EDAT(50),KSTG(200),NE
      COMMON /PRS/  NELI(300),NELJ(300),MSTG(300),APS(300),YPS(300),NPT
      COMMON /TYM/  DNR(200),DMR(200),AN(200,3),AM(200,3)
      COMMON /STF/  AKA(200,6,6),EKA(200,6,6),RP(200,6),LM(200,6),SHP
      COMMON /FRC/  DN(200,3),FE(200,6),R(600),NEQ,MBAND,MAXL
C
      DIMENSION SK(NNN,MMM)
C
C     INITIALIZE STRUCTURE STIFFNESS MATRIX
C
      DO 10 I=1,NEQ
      DO 10 J=1,MBAND
   10 SK(I,J)=0.0
C
C     ADD ELEMENT STIFFNESS TO STRUCTURE STIFFNESS MATRIX
C     -
      DO 30 N=1,NE
      IF (NSTG(N).GT.NST) GO TO 30
      DO 20 I=1,6
      II=LM(N,I)
      DO 20 J=1,6
      JJ=LM(N,J)-II+1
      IF (JJ.LE.0) GO TO 20
      SK(II,JJ)=SK(II,JJ)+ECEF(N)*AKA(N,I,J)
   20 CONTINUE
   30 CONTINUE
C
C     ADD SUPPORT STIFFNESS TO STRUCTURE STIFFNESS MATRIX
C
      DO 40 N=1,NN
      K=3*(N-1)
      DO 40 L=1,3
      IF (KSUP(N,L).EQ.1) SK(K+L,1)=SK(K+L,1)+1.E+15
   40 CONTINUE
C
      RETURN
      END
C     ******************************************************************
      SUBROUTINE ELMK
C
      COMMON /CNL/  DAT,TIM,HED(20),T1,T2,NSTAGE,NST,IFL,JFL,KFL,LFL
      COMMON /CON/  FC28,EC28,PR,RO,TC,CRP,SHR,TCUR,ENS,ANS,YNS
      COMMON /STL/  EPS,FPU,FPY,FPJ,FPI,FPE,FRIC,WOBL,SET,RLX
      COMMON /SEC/  SA(20),SI(20),SY(20),SD(20),SB(20),SQ(20),
     1              S1(20),S2(20),NS
      COMMON /NOD/  X(200),Y(200),KSUP(200,3),INI(200),INJ(200),NN
      COMMON /EMT/  NODI(200),NODJ(200),NSECI(200),NSECJ(200),ECEF(200),
     1              EA(200),EI(200),EY(200),XL(200),COSA(200),SINA(200),
     2              NSTG(200),SEGL(200),CDAT(200),EDAT(50),KSTG(200),NE
      COMMON /PRS/  NELI(300),NELJ(300),MSTG(300),APS(300),YPS(300),NPT
      COMMON /TYM/  DNR(200),DMR(200),AN(200,3),AM(200,3)
      COMMON /STF/  AKA(200,6,6),EKA(200,6,6),RP(200,6),LM(200,6),SHP
      COMMON /FRC/  DN(200,3),FE(200,6),R(600),NEQ,MBAND,MAXL
C
      DIMENSION EK(3,3),A(3,6),EKAA(6,6)
C
C     FORM ELEMENT STIFFNESS MATRIX IN LOCAL COORDINATES
C
      IF (IFL.EQ.0) RETURN
      DO 60 N=1,NE
      NI=NODI(N)
      NJ=NODJ(N)
      DX=X(NJ)-X(NI)
      DY=Y(NJ)-Y(NI)
      XL(N)=SQRT(DX**2+DY**2)
      COSA(N)=DX/XL(N)
      SINA(N)=DY/XL(N)
      E=1.0
      G=1.0/(2.0*(1.0+PR))
      SHP=0.0
      EAL=E*EA(N)/XL(N)
      EIL=E*EI(N)/XL(N)
      GAL=G*EA(N)*XL(N)*SHP
      SHF=0.0
      IF (GAL.NE.0.0) SHF=6.0*EIL/GAL
C
      EK(1,1)=EAL
      EK(1,2)=0.0
      EK(1,3)=0.0
      EK(2,2)=4.0*EIL*(1.0+SHF/2.0)/(1.0+2.0*SHF)
      EK(2,3)=2.0*EIL*(1.0-SHF    )/(1.0+2.0*SHF)
      EK(3,3)=EK(2,2)
C
      DO 10 I=1,3
      DO 10 J=1,3
   10 EK(J,I)=EK(I,J)
C
C     FORM ELEMENT STIFFNESS MATRIX IN GLOBAL COORDINATES
C
      CALL TRAN(A,0,0,COSA(N),SINA(N),XL(N))
      DO 30 I=1,3
      DO 30 J=1,6
      TEMP=0.0
      DO 20 K=1,3
   20 TEMP=TEMP+EK(I,K)*A(K,J)
   30 EKAA(I,J)=TEMP
C
      DO 50 I=1,6
      DO 50 J=1,6
      TEMP=0.0
      DO 40 K=1,3
   40 TEMP=TEMP+A(K,I)*EKAA(K,J)
   50 AKA(N,I,J)=TEMP
C
C     FORM ELEMENT STRESS MATRIX
C
      CALL TRAN(A,0,0,1.0,0.0,XL(N))
      DO 70 I=1,6
      DO 70 J=1,6
      TEMP=0.0
      DO 60 K=1,3
   60 TEMP=TEMP+A(K,I)*EKAA(K,J)
   70 EKA(N,I,J)=TEMP
   80 CONTINUE
C
      RETURN
      END
C     ******************************************************************
      SUBROUTINE TRAN(A,IHI,IHJ,COSA,SINA,XL)
C
      DIMENSION A(3,6)
C
C     FORM TRANSFORMATION MATRIX A
C
C     NO HINGES
C
      A(1,1)=-COSA
      A(1,2)=-SINA
      A(1,3)=0.0
      A(1,4)=+COSA
      A(1,5)=+SINA
      A(1,6)=0.0
      A(2,1)=-SINA/XL
      A(2,2)=+COSA/XL
      A(2,3)=1.0
      A(2,4)=+SINA/XL
      A(2,5)=-COSA/XL
      A(2,6)=0.0
      A(3,1)=-SINA/XL
      A(3,2)=+COSA/XL
      A(3,3)=0.0
      A(3,4)=+SINA/XL
      A(3,5)=-COSA/XL
      A(3,6)=1.0
C
      IF (IHI.EQ.0.AND.IHJ.EQ.0) GO TO 60
      IF (IHI.NE.0.AND.IHJ.EQ.0) GO TO 20
      IF (IHI.EQ.0.AND.IHJ.NE.0) GO TO 40
C
C     HINGES AT I AND J ENDS
C
      DO 10 I=2,3
      DO 10 J=1,6
   10 A(I,J)=0.0
      GO TO 60
C
C     HINGE AT I END ONLY
C
   20 DO 30 J=1,6
   30 A(2,J)=-A(3,J)/2.
      GO TO 60
C
C     HINGE AT J END ONLY
C
   40 DO 50 J=1,6
   50 A(3,J)=-A(2,J)/2.
C
   60 RETURN
      END
C     ******************************************************************
      SUBROUTINE FORC
C
      COMMON /CNL/  DAT,TIM,HED(20),T1,T2,NSTAGE,NST,IFL,JFL,KFL,LFL
      COMMON /CON/  FC28,EC28,PR,RO,TC,CRP,SHR,TCUR,ENS,ANS,YNS
      COMMON /STL/  EPS,FPU,FPY,FPJ,FPI,FPE,FRIC,WOBL,SET,RLX
      COMMON /SEC/  SA(20),SI(20),SY(20),SD(20),SB(20),SQ(20),
     1              S1(20),S2(20),NS
      COMMON /NOD/  X(200),Y(200),KSUP(200,3),IHI(200),IHJ(200),NN
      COMMON /EMT/  NODI(200),NODJ(200),NSECI(200),NSECJ(200),ECEF(200),
     1              EA(200),EI(200),EY(200),XL(200),COSA(200),SINA(200),
     2              NSTG(200),SEGL(200),CDAT(200),EDAT(50),KSTG(200),NE
      COMMON /PRS/  NELI(300),NELJ(300),MSTG(300),APS(300),YPS(300),NPT
      COMMON /TYM/  DNR(200),DMR(200),AN(200,3),AM(200,3)
      COMMON /STF/  AKA(200,6,6),EKA(200,6,6),RP(200,6),LM(200,6),SHP
      COMMON /FRC/  DN(200,3),FE(200,6),R(600),NEQ,MBAND,MAXL
C
      DIMENSION DFE(6)
C
C     FIND NODE DISPLACEMENTS
C
      DO 20 N=1,NN
      IF (KSTG(N).EQ.0) GO TO 20
      K=3*(N-1)
      DO 10 M=1,3
   10 DN(N,M)=DN(N,M)+R(K+M)
   20 CONTINUE
C
C     FIND ELEMENT FORCES
```

```
C
      DO 50 N=1,NE
      IF (NSTG(N).GT.NST) GO TO 50
      DO 40 I=1,6
      TEMP=0.0
      DO 30 J=1,6
      JJ=LM(N,J)
   30 TEMP=TEMP+ECEF(N)*EKA(N,I,J)*R(JJ)
      DFE(I)=TEMP-RP(N,I)
   40 FE(N,I)=FE(N,I)+DFE(I)
      DNR(N)=(DFE(4)-DFE(1))/2.0
      DMR(N)=(DFE(6)-DFE(3))/2.0
   50 CONTINUE
C
      RETURN
      END
C     ****************************************************************
      SUBROUTINE RITE
C
      COMMON /CNL/  DAT,TIM,HED(20),T1,T2,NSTAGE,NST,IFL,JFL,KFL,LFL
      COMMON /CON/  FC28,EC28,PR,RO,TC,CRP,SHR,TCUR,ENS,ANS,YNS
      COMMON /STL/  EPS,FPU,FPY,FPJ,FPI,FPE,FRIC,WOBL,SET,RLX
      COMMON /SEC/  SA(20),SI(20),SY(20),SD(20),SB(20),SO(20),
     1              S1(20),S2(20),NS
      COMMON /NOD/  X(200),Y(200),KSUP(200,3),INI(200),INJ(200),NN
      COMMON /EMT/  NODI(200),NODJ(200),NSECI(200),NSECJ(200),ECEF(200),
     1              EA(200),EI(200),EY(200),XL(200),COSA(200),SINA(200),
     2              NSTG(200),SEGL(200),CDAT(200),EDAT(50),KSTG(200),NE
      COMMON /PRS/  NELI(300),NELJ(300),NSTG(300),APS(300),YPS(300),NPT
      COMMON /TYM/  DNR(200),DMR(200),AN(200,3),AM(200,3)
      COMMON /STF/  AKA(200,6,6),EKA(200,6,6),RP(200,6),LM(200,6),SHP
      COMMON /FRC/  DN(200,3),FE(200,6),R(600),NEQ,MBAND,MAXL
C
      DIMENSION SE(6),RS(3)
C
C     WRITE HEADING
C
      WRITE (6,10) DAT,TIM,HED,NST,EDAT(NST+1)
   10 FORMAT(45H1TIME DEPENDENT ANALYSIS OF SEGMENTAL BRIDGES/
     1         1H ,6HDATE: ,A8,4X,6HTIME: ,A8///1H ,20A4//
     2         8H STAGE =,I3,12X,15HERECTION DATE =,F7.1)
      IF (JFL.EQ.0) WRITE (6,15)
   15 FORMAT(//17H ELASTIC ANALYSIS)
C
C     WRITE NODE DISPLACEMENTS
C
      WRITE (6,20)
   20 FORMAT(//19H NODE DISPLACEMENTS//
     1         5H NODE,16X,6HX-DISP,10X,6HY-DISP,11X,5HROT'N)
      DO 40 N=1,NN
      IF (KSTG(N).EQ.0) GO TO 40
      WRITE (6,30) N,(DN(N,M),M=1,3)
   30 FORMAT(I5,6X,3E16.4)
   40 CONTINUE
C
C     WRITE ELEMENT FORCES
C
      WRITE (6,50)
   50 FORMAT(//15H ELEMENT FORCES/
     1         11H          ,11X,5HAXIAL,11X,5HSHEAR,8X,7HBENDING/
     2         11H ELMT  NODE,11X,5HFORCE,11X,5HFORCE,8X,7H MOMENT)
      DO 80 N=1,NE
      IF (NSTG(N).GT.NST) GO TO 80
      DO 60 M=1,3
      SE(M  )=-FE(N,M  )
   60 SE(M+3)=+FE(N,M+3)
      WRITE (6,70) N,NODI(N),(SE(M),M=1,3),N,NODJ(N),(SE(M),M=4,6)
   70 FORMAT(I5,I6,3E16.4)
   80 CONTINUE
C
C     WRITE ELEMENT STRESSES
C
      IF (LFL.EQ.0) GO TO 120
      WRITE (6,90)
   90 FORMAT(//17H ELEMENT STRESSES/
     1         11H          ,10X,6HSTRESS,10X,6HSTRESS,10X,6H SHEAR/
     2         11H ELMT  NODE,10X,6HAT TOP,10X,6HAT BOT,10X,6HSTRESS)
      DO 110 N=1,NE
      IF (NSTG(N).GT.NST) GO TO 110
      NSI=NSECI(N)
      NSJ=NSECJ(N)
      SE(1)=-FE(N,1)/SA(NSI)+FE(N,3)*SY(NSI)/SI(NSI)
      SE(4)=+FE(N,4)/SA(NSJ)-FE(N,6)*SY(NSJ)/SI(NSJ)
      SE(2)=-FE(N,1)/SA(NSI)-FE(N,3)*(SD(NSI)-SY(NSI))/SI(NSI)
      SE(5)=+FE(N,4)/SA(NSJ)+FE(N,6)*(SD(NSJ)-SY(NSJ))/SI(NSJ)
      SE(3)=-FE(N,2)*SO(NSI)/(SI(NSI)*SB(NSI))
      SE(6)=+FE(N,5)*SO(NSJ)/(SI(NSJ)*SB(NSJ))
      WRITE (6,100) N,NODI(N),(SE(M),M=1,3),N,NODJ(N),(SE(M),M=4,6)
  100 FORMAT(I5,I6,3E16.4)
  110 CONTINUE
  120 CONTINUE
C
C     WRITE SUPPORT REACTIONS
C
      WRITE (6,130)
  130 FORMAT(//18H SUPPORT REACTIONS//
     1         5H NODE,15X,7HX-FORCE,9X,7HY-FORCE,10X,6HMOMENT)
      DO 160 N=1,NN
      I=KSUP(N,1)
      J=KSUP(N,2)
      K=KSUP(N,3)
      IF (I.EQ.0.AND.J.EQ.0.AND.K.EQ.0) GO TO 160
      DO 140 M=1,3
  140 RS(M)=-KSUP(N,M)*DN(N,M)*1.E+15
      WRITE (6,150) N,(RS(M),M=1,3)
  150 FORMAT(I5,6X,3E16.4)
  160 CONTINUE
C
      RETURN
      END
C     ****************************************************************
      SUBROUTINE SOLV(A,B,NEQ,MM,KKK)
C
```

```
      DIMENSION A(NEQ,MM),B(NEQ)
      COMMON /ABC/  IJKSTG(200)
C
C     DETERMINE FIRST AND LAST EQUATION TO BE SOLVED
C
      N1=1
      NE=NEQ/3-1
      DO 140 L=1,NE
      IF (IJKSTG(L)) 20,140,10
   10 N1=3*L+1
      GO TO 140
   20 NN=3*L+3
      GO TO (30,90), KKK
C
C     REDUCE STIFFNESS MATRIX
C
   30 DO 80 N=N1,NN
      IF (A(N,1).GT.0.001) GO TO 50
      WRITE (6,40) N
   40 FORMAT(///30H ZERO ON DIAGONAL FOR EQUATION,I4)
      CALL EXIT
   50 DO 70 M=2,MM
      FACT=A(N,M)/A(N,1)
      I=N+M-1
      IF (I.GT.NN) GO TO 70
      J=0
      DO 60 K=M,MM
      J=J+1
   60 A(I,J)=A(I,J)-FACT*A(N,K)
   70 A(N,M)=FACT
   80 CONTINUE
      GO TO 140
C
C     REDUCE LOAD VECTOR
C
   90 DO 110 N=N1,NN
      DO 100 M=2,MM
      I=N+M-1
      IF (I.GT.NN) GO TO 110
  100 B(I)=B(I)-A(N,M)*B(N)
  110 B(N)=B(N)/A(N,1)
C
C     BACK SUBSTITUTE
C
      N=NN
  120 N=N-1
      IF (N+1.EQ.N1) GO TO 140
      DO 130 M=2,MM
      I=N+M-1
      IF (I.GT.NN) GO TO 130
      B(N)=B(N)-A(N,M)*B(I)
  130 CONTINUE
      GO TO 120
  140 CONTINUE
C
      RETURN
      END
End of file
```

Appendix C

Listing of input data for TIMEDEP

```
GHALI EXAMPLE
   24   23    3   17   20     1     0     0    1
6400.      3800000.   0.0      2.00        0.0         2.0         -0.0003    3.0
18000000.  180000.    180000.  0.0         0.0         0.0         45.0
20000000.  0.022200   1.00
        1  10.035     10.086   0.974       2.6         0.0
        2  11.055     13.027   1.083       2.6         0.0
        3  12.075     14.943   1.360       3.6         0.0
        1     1    8     7.07      -28.0
        2     1    8     7.53      -28.0
        3     1    9     7.78      -28.0
        4     1    7     7.53      -28.0
        5     1    5     7.53      -28.0
        6     1    3     7.53      -28.0
        7     2    1     8.53      -28.0
        8     2    1     8.53      -28.0
        9     2    3     7.53      -28.0
       10     1    5     7.53      -28.0
       11     1    7     7.53      -28.0
       12     1   21     2.78      -28.0
       13     1   17     7.53      -28.0
       14     1   15     7.53      -28.0
       15     1   13     7.53      -28.0
       16     2   11     8.53      -28.0
       17     3   11     8.53      -28.0
       18     2   12     7.53      -28.0
       19     1   15     7.53      -28.0
       20     1   17     7.53      -28.0
       21     1   19     7.78      -28.0
       22     1   19     7.53      -28.0
       23     1   19     7.07      -28.0
       24     1
        1     7    8     1             0.012800  0.2
        2     6    8     3             0.011970  0.2
        3     5   10     5             0.011970  0.2
        4     4   11     7             0.007880  0.2
        5    16   17    11             0.012800  0.2
        6    15   16    13             0.011970  0.2
        7    14   18    15             0.011970  0.2
        8    13   20    17             0.007880  0.2
        9     3    4     8             0.005378  2.65
       10     2    5     9             0.006155  2.65
       11     1    6     9             0.007335  2.65
       12    20   21    19             0.005378  2.65
       13    19   22    19             0.006155  2.65
       14    18   23    19             0.007335  2.65
       15    11   12    21             0.005378  2.65
       16    10   14    21             0.007335  2.65
       17     9   15    21             0.003812  2.65
        1      2.0
        8     1    1     1
        0
        0
        2      5.0
        0
        0
        3      5.0
        0
        0
        4      8.0
        0
        0
        5      8.0
        0
        0
        6     11.0
        0
        0
        7     11.0
        0
        0
        8     15.0
        0
        0
        9     15.0
        1     0    1     0
        8     1    1     0
        0
        0
       10     18.0
        0
        0
       11     18.0
       17     1    1     1
        0
        0
       12     22.0
        0
        0
       13     22.0
        0
        0
       14     25.0
        0
        0
       15     25.0
        0
        0
       16     28.0
        0
        0
       17     28.0
        0
        0
       18     32.0
        0
        0
       19     32.0
       17     1    1     0
       24     0    1     0
        0
        0
       20     35.0
```

```
     114            0
     115            0
     116           21     30.0
     117           17   5      1      0
     118            0
     119            0
     120           22     45.0
     121            0
     122            0
     123           23     45.0
     124            0
     125            1                -15.000
     126            2                -32.000
     127            3                -34.444
     128            4                -34.444
     129            5                -33.666
     130            6                -33.666
     131            7                -36.136
     132            8                -36.266
     133            9                -36.136
     134           10                -33.666
     135           11                -33.666
     136           12                -33.153
     137           13                -33.153
     138           14                -33.666
     139           15                -33.666
     140           16                -36.136
     141           17                -36.266
     142           18                -36.136
     143           19                -33.666
     144           20                -33.666
     145           21                -34.444
     146           22                -34.444
     147           23                -32.000
     148           24                -15.000
     149            0
     150           24     50.0
     151            0
     152            0
     153           25     100.0
     154            0
     155            0
     156           26     200.0
     157            0
     158            0
     159           27     500.0
     160            0
     161            0
     162           28     1000.0
     163            0
     164            0
     165           29     2000.0
     166            0
     167            0
     168
     169
End of file
```

Appendix D

Listing of output information for TIMEDEP

```
1TIME DEPENDENT ANALYSIS OF SEGMENTAL BRIDGES
 DATE: 03-26-84     TIME: 22:03:14


 GHALI EXAMPLE


 NO. OF NODES                   =  24
 NO. OF ELEMENTS                =  23
 NO. OF SECTIONS                =   3
 NO. OF PRESTRESSING TENDONS    =  17
 NO. OF CONSTRUCTION STAGES     =  28


 CONCRETE PROPERTIES:

 COMPRESSIVE STRENGTH (AT 28 DAYS) . . . . . =  0.5400E+04
 MODULUS OF ELASTICITY (AT 28 DAYS) . . . . =  0.3500E+07
 POISSON'S RATIO . . . . . . . . . . . . . =  0.0
 MASS DENSITY . . . . . . . . . . . . . . . =  0.2000E+01
 THERMAL COEFFICIENT . . . . . . . . . . . =  0.0
 CREEP COEFFICIENT . . . . . . . . . . . . =  0.2000E+01
 SHRINKAGE COEFFICIENT . . . . . . . . . . = -0.3000E-03
 CURING PERIOD (DAYS) . . . . . . . . . . . =  0.3000E+01

 PRESTRESSED STEEL PROPERTIES:

 MODULUS OF ELASTICITY . . . . . . . . . . =  0.1900E+08
 GUARANTEED ULTIMATE TENSILE STRENGTH . . . =  0.1800E+06
 YIELD STRESS (AT 1% EXTENSION) . . . . . . =  0.1500E+06
 JACKING STRESS (0.8*FPU) . . . . . . . . . =  0.1440E+06
 INITIAL STRESS (0.7*FPU) . . . . . . . . . =  0.1260E+06
 EFFECTIVE STRESS . . . . . . . . . . . . . =  0.1080E+06
 FRICTION COEFFICIENT . . . . . . . . . . . =  0.0
 WOBBLE COEFFICIENT . . . . . . . . . . . . =  0.0
 ANCHOR SET . . . . . . . . . . . . . . . . =  0.0
 RELAXATION COEFFICIENT . . . . . . . . . . =  0.4500E+02

 NONPRESTRESSED STEEL PROPERTIES:

 MODULUS OF ELASTICITY . . . . . . . . . . =  0.2000E+08
 AREA OF REINFORCEMENT . . . . . . . . . . =  0.2220E-01
 ECCENTRICITY OF REINFORCEMENT . . . . . . =  0.1000E+01


 SECTION DATA

 SECT             AC             IC             YC             DC            BC
    1     0.1003E+02     0.1008E+02     0.8740E+00     0.2800E+01     0.0
    2     0.1105E+02     0.1203E+02     0.1083E+01     0.2800E+01     0.0
    3     0.1207E+02     0.1484E+02     0.1340E+01     0.2800E+01     0.0


 NODE DATA

 NODE          X-ORD          Y-ORD
    1     0.0            -0.8740E+00
    2     0.7070E+01     -0.8740E+00
    3     0.1460E+02     -0.8740E+00
    4     0.2238E+02     -0.8740E+00
    5     0.2991E+02     -0.8740E+00
    6     0.3744E+02     -0.8740E+00
    7     0.4497E+02     -0.1083E+01
    8     0.5350E+02     -0.1340E+01
    9     0.6203E+02     -0.1083E+01
   10     0.6956E+02     -0.8740E+00
   11     0.7709E+02     -0.8740E+00
   12     0.8462E+02     -0.8740E+00
   13     0.8738E+02     -0.8740E+00
   14     0.9491E+02     -0.8740E+00
   15     0.1024E+03     -0.8740E+00
   16     0.1100E+03     -0.1083E+01
   17     0.1185E+03     -0.1340E+01
   18     0.1270E+03     -0.1083E+01
   19     0.1346E+03     -0.8740E+00
   20     0.1421E+03     -0.8740E+00
   21     0.1496E+03     -0.8740E+00
   22     0.1574E+03     -0.8740E+00
   23     0.1649E+03     -0.8740E+00
   24     0.1720E+03     -0.8740E+00


 ELEMENT DATA
                                                                                      CASTING
 ELMT   NOD-I   NOD-J   SEC-I   SEC-J   STAGE          LENGTH          WEIGHT         DATE
    1       1       2       1       1       9      0.7070E+01      0.1418E+03        -28.0
    2       2       3       1       1       9      0.7530E+01      0.1511E+03        -28.0
    3       3       4       1       1       9      0.7780E+01      0.1561E+03        -28.0
    4       4       5       1       1       7      0.7530E+01      0.1511E+03        -28.0
    5       5       6       1       1       5      0.7530E+01      0.1511E+03        -28.0
    6       6       7       1       2       3      0.7531E+01      0.1588E+03        -28.0
    7       7       8       2       3       1      0.8534E+01      0.1974E+03        -28.0
    8       8       9       3       2       1      0.8534E+01      0.1974E+03        -28.0
    9       9      10       2       1       3      0.7531E+01      0.1588E+03        -28.0
   10      10      11       1       1       5      0.7530E+01      0.1511E+03        -28.0
   11      11      12       1       1       7      0.7530E+01      0.1511E+03        -28.0
   12      12      13       1       1      21      0.2760E+01      0.5538E+02        -28.0
   13      13      14       1       1      17      0.7530E+01      0.1511E+03        -28.0
   14      14      15       1       1      15      0.7530E+01      0.1511E+03        -28.0
   15      15      16       1       2      13      0.7531E+01      0.1588E+03        -28.0
   16      16      17       2       3      11      0.8534E+01      0.1974E+03        -28.0
   17      17      18       3       2      11      0.8534E+01      0.1974E+03        -28.0
   18      18      19       2       1      13      0.7531E+01      0.1588E+03        -28.0
   19      19      20       1       1      15      0.7530E+01      0.1511E+03        -28.0
   20      20      21       1       1      17      0.7530E+01      0.1511E+03        -28.0
   21      21      22       1       1      19      0.7780E+01      0.1561E+03        -28.0
   22      22      23       1       1      19      0.7530E+01      0.1511E+03        -28.0
   23      23      24       1       1      19      0.7070E+01      0.1418E+03        -28.0


 PRESTRESSING TENDON DATA

 TEND   EMT-I   EMT-J   STAGE          AREA    ECCENTRICITY
```

```
   1         7         8         1       0.1260E-01       0.2000E+00
   2         6         9         3       0.1197E-01       0.2000E+00
   3         5        10         5       0.1197E-01       0.2000E+00
   4         4        11         7       0.7980E-02       0.2000E+00
   5        16        17        11       0.1260E-01       0.2000E+00
   6        15        18        13       0.1197E-01       0.2000E+00
   7        14        19        15       0.1197E-01       0.2000E+00
   8        13        20        17       0.7980E-02       0.2000E+00
   9         3         4         9       0.5379E-02       0.2650E+01
  10         2         5         9       0.6150E-02       0.2650E+01
  11         1         6         9       0.7335E-02       0.2650E+01
  12        20        21        19       0.5379E-02       0.2650E+01
  13        19        22        19       0.6150E-02       0.2650E+01
  14        18        23        19       0.7335E-02       0.2650E+01
  15        11        13        21       0.5379E-02       0.2650E+01
  16        10        14        21       0.7335E-02       0.2650E+01
  17         9        15        21       0.3912E-02       0.2650E+01


NO. OF EQUATIONS =  72
BANDWIDTH        =   6


**************************************************************


1TIME DEPENDENT ANALYSIS OF SEGMENTAL BRIDGES
 DATE: 03-25-84    TIME: 22:03:14


 GHALI EXAMPLE

 STAGE =  1              ERECTION DATE =     2.0


 TEMPERATURE AT TOP     =   0.0
 TEMPERATURE AT BOTTOM. =   0.0


 SEGMENTS ASSEMBLED
                              CASTING
 ELMT   NOD-I   NOD-J           DATE
    7       7       8          -28.0
    8       8       9          -28.0


 TENDONS STRESSED

 TEND   EMT-I   EMT-J
    1       7       8


 SUPPORT CONDITIONS

 NODE   X-SUP   Y-SUP   R-SUP
    8       1       1       1


 CONSTRUCTION LOADS

 NODE           X-LOAD           Y-LOAD           MOMENT


**************************************************************


1TIME DEPENDENT ANALYSIS OF SEGMENTAL BRIDGES
 DATE: 03-25-84    TIME: 22:03:14


 GHALI EXAMPLE

 STAGE =  1              ERECTION DATE =     2.0


 ELASTIC ANALYSIS


 NODE DISPLACEMENTS

 NODE                 X-DISP          Y-DISP            ROT'N
    7             0.3833E-03      0.9673E-03      -0.2422E-03
    8             0.1917E-27     -0.3948E-12      -0.4039E-27
    9            -0.3833E-03      0.9673E-03       0.2422E-03


 ELEMENT FORCES
                       AXIAL           SHEAR          BENDING
 ELMT  NODE            FORCE           FORCE           MOMENT
    7     7      -0.1587E+04     -0.4595E+02       0.1418E+04
    7     8      -0.1593E+04      0.1513E+03       0.9804E+03
    8     8      -0.1593E+04     -0.1513E+03       0.9804E+03
    8     9      -0.1587E+04      0.4595E+02       0.1418E+04


 ELEMENT STRESSES
                      STRESS          STRESS            SHEAR
 ELMT  NODE           AT TOP          AT BOT           STRESS
    7     7      -0.2724E+03      0.5767E+02     -0.0
    7     8      -0.2198E+03     -0.3510E+02      0.0
    8     8      -0.2198E+03     -0.3510E+02     -0.0
    8     9      -0.2724E+03      0.5767E+02      0.0


 SUPPORT REACTIONS

 NODE                X-FORCE         Y-FORCE           MOMENT
    8            -0.1917E-12      0.3948E+03       0.4039E-12


**************************************************************
```

```
1TIME DEPENDENT ANALYSIS OF SEGMENTAL BRIDGES
 DATE: 03-25-84    TIME: 22:03:14


 GHALI EXAMPLE

 STAGE =  2              ERECTION DATE =     5.0


 TEMPERATURE AT TOP     =   0.0
 TEMPERATURE AT BOTTOM =   0.0


 SEGMENTS ASSEMBLED
                                 CASTING
 ELMT   NOD-I   NOD-J             DATE


 TENDONS STRESSED

 TEND   EMT-I   EMT-J


 SUPPORT CONDITIONS

 NODE   X-SUP   Y-SUP   R-SUP
    8       1       1       1


 CONSTRUCTION LOADS

 NODE           X-LOAD          Y-LOAD           MOMENT


 ************************************************************


1TIME DEPENDENT ANALYSIS OF SEGMENTAL BRIDGES
 DATE: 03-25-84    TIME: 22:03:14


 GHALI EXAMPLE

 STAGE =  2              ERECTION DATE =     5.0


 ELASTIC ANALYSIS


 NODE DISPLACEMENTS

 NODE                 X-DISP           Y-DISP            ROT'N
    7            0.3633E-03       0.8673E-03      -0.2422E-03
    8            0.1917E-27      -0.3848E-12      -0.4038E-27
    9           -0.3633E-03       0.8673E-03       0.2422E-03


 ELEMENT FORCES
                       AXIAL            SHEAR          BENDING
 ELMT  NODE            FORCE            FORCE           MOMENT
    7     7      -0.1587E+04      -0.4595E+02       0.1418E+04
    7     8      -0.1593E+04       0.1513E+03       0.8804E+03
    8     8      -0.1593E+04      -0.1513E+03       0.8804E+03
    8     9      -0.1587E+04       0.4595E+02       0.1418E+04


 ELEMENT STRESSES
                      STRESS           STRESS            SHEAR
 ELMT  NODE           AT TOP           AT BOT           STRESS
    7     7      -0.2724E+03       0.5787E+02      -0.0
    7     8      -0.2188E+03      -0.3810E+02       0.0
    8     8      -0.2188E+03      -0.3810E+02      -0.0
    8     9      -0.2724E+03       0.5787E+02       0.0


 SUPPORT REACTIONS

 NODE                X-FORCE          Y-FORCE           MOMENT
    8           -0.1917E-12       0.3848E+03       0.4038E-12


 ************************************************************


1TIME DEPENDENT ANALYSIS OF SEGMENTAL BRIDGES
 DATE: 03-25-84    TIME: 22:03:14


 GHALI EXAMPLE

 STAGE = 21              ERECTION DATE =    35.0


 TEMPERATURE AT TOP     =   0.0
 TEMPERATURE AT BOTTOM =   0.0


 SEGMENTS ASSEMBLED
                                 CASTING
 ELMT   NOD-I   NOD-J             DATE
   12      12      13            -28.0


 TENDONS STRESSED

 TEND   EMT-I   EMT-J
   15      11      13
   16      10      14
   17       9      15


 SUPPORT CONDITIONS

 NODE   X-SUP   Y-SUP   R-SUP
    1       0       1       0
    8       1       1       0
   17       0       1       0
   24       0       1       0


 CONSTRUCTION LOADS

 NODE           X-LOAD            Y-LOAD            MOMENT


 ******************************************************************


1TIME DEPENDENT ANALYSIS OF SEGMENTAL BRIDGES
 DATE: 03-25-84     TIME: 22:03:14


 GHALI EXAMPLE

 STAGE = 21              ERECTION DATE =    35.0


 ELASTIC ANALYSIS


 NODE DISPLACEMENTS

 NODE                  X-DISP             Y-DISP              ROT'N
    1             0.2450E-02        -0.3718E-12          0.4884E-03
    2             0.2264E-02         0.2823E-02          0.4066E-03
    3             0.1845E-02         0.5470E-02          0.3082E-03
    4             0.1982E-02        -0.1114E-01          0.7833E-03
    5             0.2114E-02        -0.8027E-02          0.5057E-03
    6             0.1803E-02        -0.2835E-02          0.2018E-03
    7             0.1186E-02        -0.1409E-04         -0.2201E-04
    8            -0.4057E-26        -0.1422E-11         -0.1043E-03
    9            -0.1131E-02        -0.1902E-02         -0.2247E-03
   10            -0.1532E-02        -0.5578E-02         -0.4314E-03
   11            -0.1828E-02        -0.1342E-01         -0.7538E-03
   12            -0.1583E-02        -0.1872E-01         -0.1110E-02
   13            -0.5763E-03        -0.1872E-01          0.1110E-02
   14            -0.4306E-03        -0.1342E-01          0.7538E-03
   15            -0.8272E-03        -0.5578E-02          0.4314E-03
   16            -0.1128E-02        -0.1902E-02          0.2247E-03
   17            -0.2259E-02        -0.1422E-11          0.1043E-03
   18            -0.3445E-02        -0.1409E-04          0.2201E-04
   19            -0.4062E-02        -0.2835E-02         -0.2018E-03
   20            -0.4373E-02        -0.8027E-02         -0.5057E-03
   21            -0.4241E-02        -0.1114E-01         -0.7833E-03
   22            -0.4105E-02         0.5470E-02         -0.3082E-03
   23            -0.4523E-02         0.2823E-02         -0.4068E-03
   24            -0.4708E-02        -0.3718E-12         -0.4884E-03


 ELEMENT FORCES
                       AXIAL              SHEAR            BENDING
 ELMT  NODE            FORCE              FORCE             MOMENT
    1     1      -0.9242E+03        -0.3718E+03        -0.1649E+04
    1     2      -0.9242E+03        -0.2300E+03         0.5791E+03
    2     2      -0.1951E+04        -0.2300E+03        -0.1142E+04
    2     3      -0.1951E+04        -0.7892E+02         0.2127E+02
    3     3      -0.2629E+04        -0.7892E+02        -0.1115E+04
    3     4      -0.2629E+04         0.7722E+02        -0.1108E+04
    4     4      -0.3634E+04         0.7722E+02        -0.3298E+03
    4     5      -0.3634E+04         0.2263E+03        -0.1480E+04
    5     5      -0.4465E+04         0.2263E+03         0.8230E+03
    5     6      -0.4465E+04         0.3795E+03        -0.1465E+04
    6     6      -0.4952E+04         0.3013E+03         0.1423E+04
    6     7      -0.4954E+04         0.4801E+03        -0.1434E+04
    7     7      -0.5623E+04         0.3757E+03         0.1422E+04
    7     8      -0.5628E+04         0.5730E+03        -0.2613E+04
    8     8      -0.5627E+04        -0.5235E+03        -0.2613E+04
    8     9      -0.5621E+04        -0.3262E+03         0.1000E+04
    9     9      -0.4522E+04        -0.4174E+03        -0.1185E+04
    9    10      -0.4519E+04        -0.2585E+03         0.1350E+04
   10    10      -0.3831E+04        -0.3300E+03        -0.1388E+04
   10    11      -0.3831E+04        -0.1788E+03         0.8497E+03
   11    11      -0.3100E+04        -0.1788E+03        -0.1754E+04
   11    12      -0.3100E+04        -0.2770E+02        -0.9761E+03
   12    12      -0.2095E+04        -0.2770E+02        -0.1754E+04
   12    13      -0.2095E+04         0.2770E+02        -0.1754E+04
   13    13      -0.3100E+04         0.2770E+02        -0.9761E+03
   13    14      -0.3100E+04         0.1788E+03        -0.1754E+04
   14    14      -0.3831E+04         0.1788E+03         0.8497E+03
   14    15      -0.3831E+04         0.3300E+03        -0.1388E+04
   15    15      -0.4519E+04         0.2585E+03         0.1350E+04
   15    16      -0.4522E+04         0.4174E+03        -0.1185E+04
   16    16      -0.5621E+04         0.3262E+03         0.1000E+04
   16    17      -0.5627E+04         0.5235E+03        -0.2613E+04
   17    17      -0.5628E+04        -0.5730E+03        -0.2613E+04
   17    18      -0.5623E+04        -0.3757E+03         0.1422E+04
   18    18      -0.4954E+04        -0.4801E+03        -0.1434E+04
   18    19      -0.4952E+04        -0.3013E+03         0.1423E+04
   19    19      -0.4465E+04        -0.3795E+03        -0.1465E+04
   19    20      -0.4465E+04        -0.2263E+03         0.8230E+03
   20    20      -0.3634E+04        -0.2263E+03        -0.1480E+04
   20    21      -0.3634E+04        -0.7722E+02        -0.3298E+03
   21    21      -0.2629E+04        -0.7722E+02        -0.1108E+04
   21    22      -0.2629E+04         0.7892E+02        -0.1115E+04
   22    22      -0.1951E+04         0.7892E+02         0.2127E+02
   22    23      -0.1951E+04         0.2300E+03        -0.1142E+04
   23    23      -0.9242E+03         0.2300E+03         0.5791E+03
   23    24      -0.9242E+03         0.3718E+03        -0.1649E+04


 ELEMENT STRESSES
                      STRESS             STRESS              SHEAR
 ELMT  NODE           AT TOP             AT BOT             STRESS
    1     1       0.5790E+02        -0.3733E+03        -0.0
    1     2      -0.1482E+03         0.1303E+02         0.0
    2     2      -0.8384E+02        -0.4018E+03        -0.0
```

```
             2      3     -0.1985E+03     -0.1908E+03      0.0
             3      3     -0.1540E+03     -0.4843E+03     -0.0
             3      4     -0.1547E+03     -0.4831E+03      0.0
             4      4     -0.3302E+03     -0.4220E+03     -0.0
             4      5     -0.2188E+03     -0.5308E+03      0.0
             5      5     -0.5246E+03     -0.2955E+03     -0.0
             5      6     -0.3030E+03     -0.7110E+03      0.0
             6      6     -0.6312E+03     -0.2351E+03     -0.0
             6      7     -0.3178E+03     -0.6517E+03      0.0
             7      7     -0.6379E+03     -0.3087E+03     -0.0
             7      8     -0.2318E+03     -0.7218E+03      0.0
             8      8     -0.2317E+03     -0.7213E+03     -0.0
             8      9     -0.5994E+03     -0.3865E+03      0.0
             9      9     -0.3013E+03     -0.5773E+03     -0.0
             9     10     -0.5811E+03     -0.2052E+03      0.0
            10     10     -0.2594E+03     -0.6397E+03     -0.0
            10     11     -0.4449E+03     -0.2919E+03      0.0
            11     11     -0.1391E+03     -0.6273E+03     -0.0
            11     12     -0.2144E+03     -0.4862E+03      0.0
            12     12     -0.3867E+02     -0.5272E+03     -0.0
            12     13     -0.3867E+02     -0.5272E+03      0.0
            13     13     -0.2144E+03     -0.4862E+03     -0.0
            13     14     -0.1391E+03     -0.6273E+03      0.0
            14     14     -0.4449E+03     -0.2919E+03     -0.0
            14     15     -0.2594E+03     -0.6397E+03      0.0
            15     15     -0.5811E+03     -0.2052E+03     -0.0
            15     16     -0.3013E+03     -0.5773E+03      0.0
            16     16     -0.5994E+03     -0.3865E+03     -0.0
            16     17     -0.2317E+03     -0.7213E+03      0.0
            17     17     -0.2318E+03     -0.7218E+03     -0.0
            17     18     -0.6379E+03     -0.3087E+03      0.0
            18     18     -0.3178E+03     -0.6517E+03     -0.0
            18     19     -0.6312E+03     -0.2351E+03      0.0
            19     19     -0.3030E+03     -0.7110E+03     -0.0
            19     20     -0.5246E+03     -0.2955E+03      0.0
            20     20     -0.2188E+03     -0.5308E+03     -0.0
            20     21     -0.3302E+03     -0.4220E+03      0.0
            21     21     -0.1547E+03     -0.4831E+03     -0.0
            21     22     -0.1540E+03     -0.4843E+03      0.0
            22     22     -0.1985E+03     -0.1908E+03     -0.0
            22     23     -0.8384E+02     -0.4018E+03      0.0
            23     23     -0.1482E+03      0.1303E+02     -0.0
            23     24      0.5790E+02     -0.3733E+03      0.0


       SUPPORT REACTIONS

       NODE                X-FORCE          Y-FORCE          MOMENT
          1           -0.0              0.3718E+03     -0.0
          8            0.4057E-11       0.1422E+04     -0.0
         17           -0.0              0.1422E+04     -0.0
         24           -0.0              0.3718E+03     -0.0
End of file
```

Appendix E

BOXGIRD user's manual

IDENTIFICATION

BOXGIRD: Transverse Analysis of Box Girder Bridges
Programmed by K W Shushkewich, Jan 1984.

PURPOSE

The program computes the node displacements and element forces for open or cellular folded plate structures having simple spans and being subjected to self weight, surcharge, truck loads, lane loads, temperature, and prestressing.

RESTRICTIONS

Dimension statements limit the program to structures with no more than 25 nodes, 30 elements, and 10 load cases. In addition, the storage occupied by the structure stiffness matrix may not exceed 4000 locations. The capacity can easily be expanded.

DESCRIPTION

The program utilizes folded plate theory and is based on the direct stiffness method. The element stiffnesses are evaluated using the Goldberg-Leve equations, and a harmonic analysis with an appropriate number of Fourier series terms is used for the loads. For comparison purposes, a unit length of structure is analysed using plane frame theory.

STRUCTURAL IDEALIZATION

The structure is defined by a series of nodes (joints) connected by one-dimensional elements (members) possessing both membrane and plate bending stiffness. The nodes must be numbered, and this numbering should be chosen to minimize the largest node number difference within the elements. The elements must also be numbered, but in any convenient manner.

Two right-handed orthogonal Cartesian coordinate systems are used:

(a) Global system (X,Y,Z) - An arbitrary point is chosen as the origin such that the structure lies in the Y-Z plane. Node displacements are expressed in the global system.

(b) Local system (x,y,z) - Each element has a local coordinate system whose y axis is directed along the centroidal axis of the element from node I to node J. The global X and local x axes have the same direction. The local x and y axes define the direction of the local z axis. Element forces are expressed in the local system.

INPUT DATA

The following sequence of data numerically defines the problem. Consistent units must be used.

A. PROBLEM TITLE (20A4) - One card
Columns 1-80: Problem title to be printed with output

B. CONTROL INFORMATION (4I5) - One card
Columns 1- 5: Number of nodes (max. 25)
6-10: Number of elements (max. 30)
11-15: Number of load cases (max. 10)
16-20: Plane frame code 0=analysis included
1=analysis not included

C. GENERAL DATA (6E10.0) - One card
Columns 1-10: Span length
11-20: Modulus of elasticity
21-30: Poisson's ratio
31-40: Mass density
41-50: Thermal coefficient
51-60: X-ordinate

D. NODE DATA (I5,5X,2E10.0,2I5) - One card for each node
Columns 1- 5: Node number
11-20: Y coordinate
21-30: Z coordinate
31-35: Support code in Y direction 0=no support
36-40: Support code in Z direction 1=support
(supports are for frame analysis only!)

E. ELEMENT DATA (3I5,5X,2E10.0) - One card for each element
Columns 1- 5: Element number
6-10: Node I
11-15: Node J
21-30: Thickness at node I
31-40: Thickness at node J
(blank taken as thickness at I)

F. LOAD DATA - One set of cards for each load case

(a) CONTROL INFORMATION (A4,8X,I3,5X,15A4) - One card
Columns 1- 4: Load type
(SELF, SURC, TRUC, LANE, TEMP, PRES)
13-15: Number of element loads
21-80: Load case title printed with output

(b) ELEMENT LOADS - One card for each element load

(1) SELF WEIGHT (no cards required)

(2) SURCHARGE (I5,5X,3E10.0)
Columns 1- 5: Element number
11-20: Uniform load W
21-30: Distance Y1 from I end
31-40: Distance Y2 from I end
(blank taken as length of element)

(3) TRUCK LOAD (I5,5X,3E10.0)
Columns 1- 5: Element number
11-20: Concentrated load P
21-30: Distance Y1 from I end
31-40: Distance X0

(4) LANE LOAD (I5,5X,3E10.0)
Columns 1- 5: Element number
11-20: Uniform load W
21-30: Concentrated load P
31-40: Distance Y1 from I end

(5) TEMPERATURE (I5,5X,2E10.0)
Columns 1- 5: Element number
11-20: Temperature T1
21-30: Temperature T2

(6) PRESTRESS (I5,5X,3E10.0)
Columns 1- 5: Element number
11-20: Prestressing force P
21-30: Distance Z1
31-40: Distance Z2

G. NEXT PROBLEM

Any number of problems may be entered and the data is terminated by two blank cards.

OUTPUT INFORMATION

The following information is printed by the program.

A. Echo of the input data

B. Node displacements

C. Element forces (all forces per unit length)

Nxx - longitudinal membrane force
Nxy - membrane shear force
Nyy - transverse membrane force
Qyy - transverse normal shear force
Myy - transverse bending moment

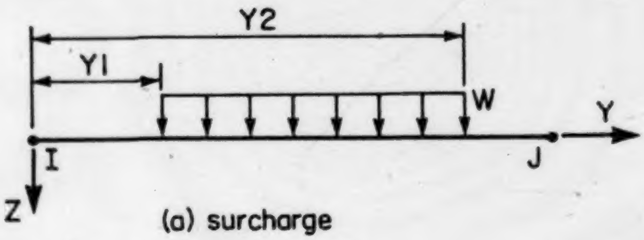

(a) surcharge

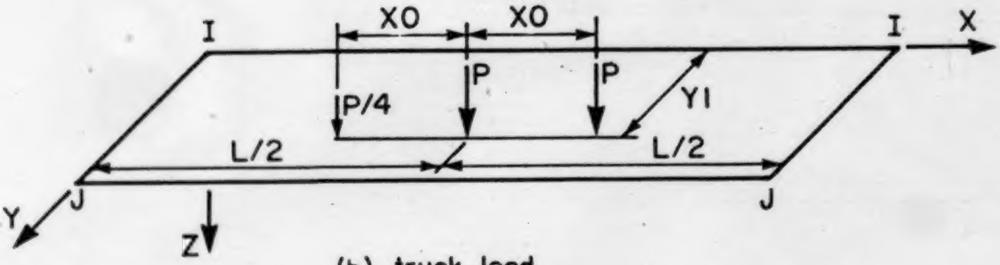
I
XO
XO
I
X
P
P
P/4
YI
L/2
L/2
Y
J
J
Z

(b) truck load

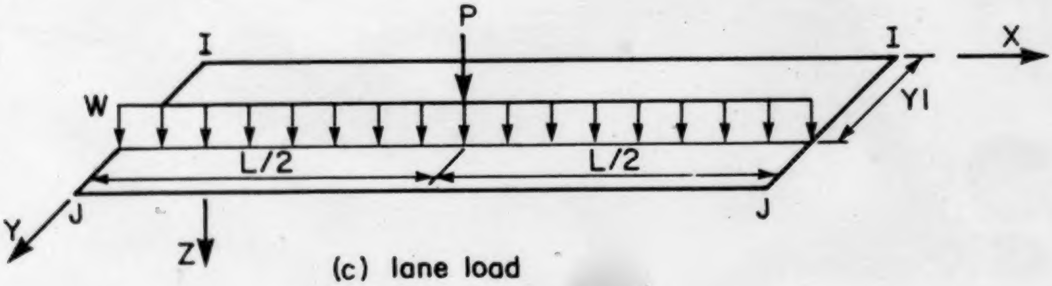
P
I
I
X
W
YI
L/2
L/2
Y
J
J
Z

(c) lane load

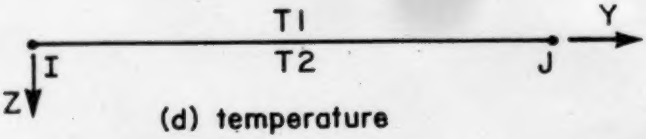

(d) temperature

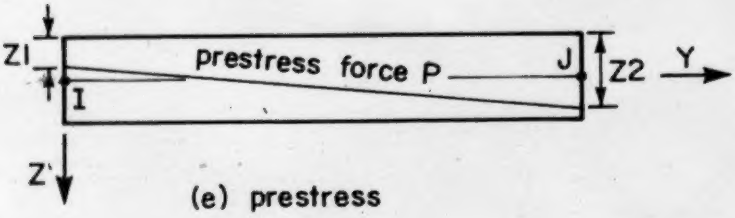
ZI
prestress force P
J
Z2
Y
I
Z

(e) prestress

Figure E.1 - Sign conventions for element loads

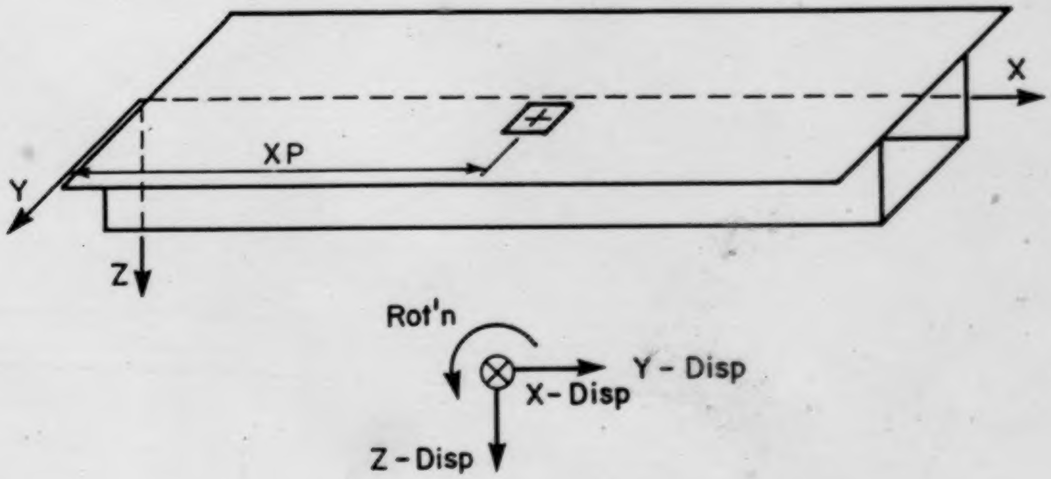
X
XP
Y
Z
Rot'n
Y - Disp
X - Disp
Z - Disp

(a) node displacements

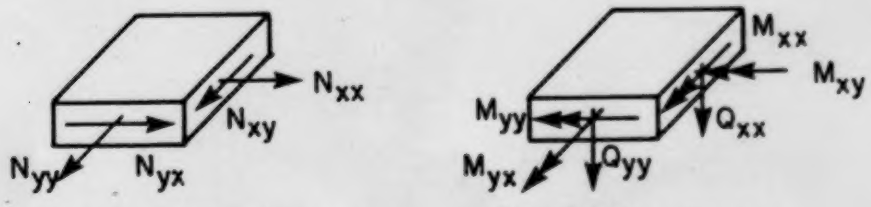
N_{xx}
N_{xy}
N_{yy}
N_{yx}
M_{xx}
M_{xy}
M_{yy}
Q_{xx}
M_{yx}
Q_{yy}

membrane forces plate bending forces

(b) element forces in general

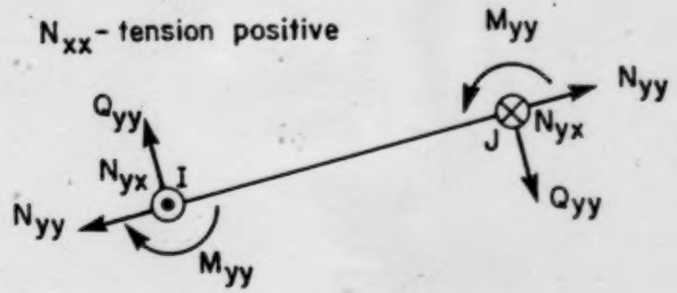
N_{xx} - tension positive
M_{yy}
N_{yy}
Q_{yy}
N_{yx}
I
J
N_{yx}
Q_{yy}
N_{yy}
M_{yy}

(c) element forces in particular

Figure E.2 - Sign conventions for node displacements and element forces

Appendix F

FORTRAN listing of BOXGIRD

```
C     PROGRAM BOXGIRD (INPUT,OUTPUT,TAPE5=INPUT,TAPE6=OUTPUT)
C
C     ****************************************************************
C     *                                                              *
C     *  BOXGIRD:  TRANSVERSE ANALYSIS OF BOX GIRDER BRIDGES         *
C     *            PROGRAMMED BY K W SHUSHKEWICH, JAN 1984.          *
C     *                                                              *
C     ****************************************************************
C
      COMMON /CNL/  DAT,TIM,HED(20),XL,E,U,RO,TC,XP,PI,NH,KODE,KPF
      COMMON /NOD/  Y(25),Z(25),NSUP(25,2),NN
      COMMON /EMT/  NODI(30),NODJ(30),TI(30),TJ(30),NE
      COMMON /SEC/  B(30),D(30),H(30),V(30)
      COMMON /CAS/  CAS(15),NL(30),WL(30,3),NLC,NC,NTYP,NLE
      COMMON /STF/  SK(6,6),A(6,6),SKA(30,6,6),RP(30,6),LM(30,6)
      COMMON /FRC/  SN(25,4,10),FE(30,10,10)
      COMMON /SOL/  R(100),NEQ,MBAND,MAXL
C
      COMMON SK(4000)
      MAXL=4000
C
      PI=ARCOS(-1.0)
      CALL TIME(10,0,DAT)
      CALL TIME( 4,0,TIM)
   10 CALL READ
      DO 30 NC=1,NLC
      CALL CASE
      IF (KPF.EQ.1) GO TO 15
      KODE=1
      NH=1
      CALL STIF(SK,NEQ,MBAND)
      CALL SOLV(SK,R,NEQ,MBAND,1)
      CALL LOAD
      CALL SOLV(SK,R,NEQ,MBAND,2)
      CALL FORC
      CALL RITE
   15 KODE=2
      MAX=9
      INC=2
      IF (NTYP.EQ.3) MAX=99
      IF (NTYP.EQ.3) INC=1
      DO 20 NH=1,MAX,INC
      CALL STIF(SK,NEQ,MBAND)
      CALL SOLV(SK,R,NEQ,MBAND,1)
      CALL LOAD
      CALL SOLV(SK,R,NEQ,MBAND,2)
      CALL FORC
   20 CONTINUE
      CALL RITE
   30 CONTINUE
      GO TO 10
C
      END
C     ****************************************************************
      SUBROUTINE READ
C
      COMMON /CNL/  DAT,TIM,HED(20),XL,E,U,RO,TC,XP,PI,NH,KODE,KPF
      COMMON /NOD/  Y(25),Z(25),NSUP(25,2),NN
      COMMON /EMT/  NODI(30),NODJ(30),TI(30),TJ(30),NE
      COMMON /SEC/  B(30),D(30),H(30),V(30)
      COMMON /CAS/  CAS(15),NL(30),WL(30,3),NLC,NC,NTYP,NLE
      COMMON /STF/  SK(6,6),A(6,6),SKA(30,6,6),RP(30,6),LM(30,6)
      COMMON /FRC/  SN(25,4,10),FE(30,10,10)
      COMMON /SOL/  R(100),NEQ,MBAND,MAXL
C
C     READ & WRITE CONTROL INFORMATION
C
      READ  (5,10) HED,NN,NE,NLC,KPF,XL,E,U,RO,TC,XP
   10 FORMAT(20A4/4I5/6E10.0)
      IF (NN.EQ.0) CALL EXIT
      WRITE (6,20) DAT,TIM,HED,NN,NE,NLC,XL,E,U,RO,TC,XP
   20 FORMAT(43H1TRANSVERSE ANALYSIS OF BOX GIRDER BRIDGES/
     1       1H ,6HDATE: ,A8,4X,6HTIME: ,A8//1H ,20A4//
     2       24H NO. OF NODES           =,I4/
     3       24H NO. OF ELEMENTS        =,I4/
     4       24H NO. OF LOAD CASES      =,I4//
     5       24H SPAN LENGTH            =,E12.4/
     6       24H MODULUS OF ELASTICITY  =,E12.4/
     7       24H POISSON'S RATIO        =,E12.4/
     8       24H MASS DENSITY           =,E12.4/
     9       24H THERMAL COEFFICIENT    =,E12.4/
     X       24H X-ORDINATE             =,E12.4)
C
C     READ & WRITE NODE DATA
C
      READ  (5,30) (N,Y(N),Z(N),(NSUP(N,L),L=1,2),N=1,NN)
   30 FORMAT(I5,5X,2E10.0,2I5)
      WRITE (6,40) (N,Y(N),Z(N),(NSUP(N,L),L=1,2),N=1,NN)
   40 FORMAT(//10H NODE DATA//
     1        5H NODE,11X,5HY-ORD,11X,5HZ-ORD,3X,5HY-SUP,3X,5HZ-SUP/
     2        (I5,2E16.4,2I8))
C
C     READ & WRITE ELEMENT DATA
C
      READ  (5,50) (N,NODI(N),NODJ(N),TI(N),TJ(N),N=1,NE)
   50 FORMAT(3I5,5X,2E10.0)
      DO 60 N=1,NE
   60 IF (TJ(N).EQ.0.0) TJ(N)=TI(N)
      WRITE (6,70) (N,NODI(N),NODJ(N),TI(N),TJ(N),N=1,NE)
   70 FORMAT(//13H ELEMENT DATA//
     1        5H ELMT,3X,5HNOD-I,3X,5HNOD-J,11X,5HTHK-I,11X,5HTHK-J/
     2        (I5,2I8,2E16.4))
C
C     FIND B, H, V, & D
C
      DO 80 N=1,NE
      NI=NODI(N)
      NJ=NODJ(N)
      B(N)=(TI(N)+TJ(N))/2.
      H(N)=Y(NJ)-Y(NI)
      V(N)=Z(NI)-Z(NJ)
      D(N)=SQRT(H(N)**2+V(N)**2)
      H(N)=H(N)/D(N)
   80 V(N)=V(N)/D(N)
C
C     FIND LOCATION MATRIX
C
      DO 90 N=1,NE
      NI=4*(NODI(N)-1)
      NJ=4*(NODJ(N)-1)
      DO 90 K=1,4
      LM(N,K  )=NI+K
   90 LM(N,K+4)=NJ+K
C
C     DETERMINE BANDWIDTH
C
      NEQ=4*NN
      MBAND=0
      DO 100 N=1,NE
      MM=IABS(NODI(N)-NODJ(N))
      IF (MBAND.LT.MM) MBAND=MM
  100 CONTINUE
      MBAND=4*(MBAND+1)
      WRITE (6,110) NEQ,MBAND
  110 FORMAT(//19H NO. OF EQUATIONS =,I3/
     1         19H BANDWIDTH        =,I3)
      L=NEQ*MBAND
      IF (L.LE.MAXL) RETURN
      WRITE (6,120)
  120 FORMAT(///27H STIFFNESS MATRIX TOO LARGE)
      CALL EXIT
C
      RETURN
      END
C     ******************************************************************
      SUBROUTINE CASE
C
      COMMON /CNL/  DAT,TIM,HED(20),XL,E,U,RO,TC,XP,PI,NN,KODE,KPF
      COMMON /NOD/  Y(25),Z(25),NSUP(25,2),NN
      COMMON /EMT/  NODI(30),NODJ(30),TI(30),TJ(30),NE
      COMMON /SEC/  B(30),D(30),H(30),V(30)
      COMMON /CAS/  CAS(15),NL(30),WL(30,3),NLC,NC,NTYP,NLE
      COMMON /STF/  EK(8,8),A(8,8),EKA(30,8,8),RP(30,8),LM(30,8)
      COMMON /FRC/  DN(25,4,10),FE(30,10,10)
      COMMON /SOL/  R(100),NEQ,MBAND,MAXL
C
      DIMENSION TYPE(6)
      DATA TYPE /4HSELF,4HSURC,4HTRUC,4HLANE,4HTEMP,4HPRES/
C
C     READ & WRITE LOAD DATA
C
      READ  (5,10) TYP,NLE,CAS
   10 FORMAT(A4,6X,I3,5X,15A4)
      DO 20 NTYP=1,6
      IF (TYP.EQ.TYPE(NTYP)) GO TO 40
   20 CONTINUE
      WRITE (6,30) TYP
   30 FORMAT(11H1LOAD TYPE ,A4,15H NOT RECOGNIZED)
      CALL EXIT
   40 IF (NTYP.EQ.1) GO TO 140
      READ  (5,50) (NL(N),(WL(N,M),M=1,3),N=1,NLE)
   50 FORMAT(I5,5X,3E10.0)
      WRITE (6,60) DAT,TIM,HED,CAS
   60 FORMAT(42H1TRANSVERSE ANALYSIS OF BOX GIRDER BRIDGES/
     1         1H ,6HDATE: ,A8,4X,6HTIME: ,A8///1H ,20A4//1H ,15A4)
      WRITE (6,70)
   70 FORMAT(//10H LOAD DATA/)
      IF (NTYP.EQ.2) WRITE (6, 80)
      IF (NTYP.EQ.3) WRITE (6, 90)
      IF (NTYP.EQ.4) WRITE (6,100)
      IF (NTYP.EQ.5) WRITE (6,110)
      IF (NTYP.EQ.6) WRITE (6,120)
   80 FORMAT(5H ELMT,15X,1HW,14X,2HY1,14X,2HY2)
   90 FORMAT(5H ELMT,15X,1HP,14X,2HY1,14X,2HX0)
  100 FORMAT(5H ELMT,15X,1HW,14X,2H P,14X,2HY1)
  110 FORMAT(5H ELMT,          14X,2HT1,14X,2HT2)
  120 FORMAT(5H ELMT,15X,1HP,14X,2HZ1,14X,2HZ2)
      WRITE (6,130) (NL(N),(WL(N,M),M=1,3),N=1,NLE)
  130 FORMAT(I5,3E15.4)
  140 CONTINUE
C
      RETURN
      END
C     ******************************************************************
      SUBROUTINE STIF(SK,NNN,MMM)
C
      COMMON /CNL/  DAT,TIM,HED(20),XL,E,U,RO,TC,XP,PI,NN,KODE,KPF
      COMMON /NOD/  Y(25),Z(25),NSUP(25,2),NN
      COMMON /EMT/  NODI(30),NODJ(30),TI(30),TJ(30),NE
      COMMON /SEC/  B(30),D(30),H(30),V(30)
      COMMON /CAS/  CAS(15),NL(30),WL(30,3),NLC,NC,NTYP,NLE
      COMMON /STF/  EK(8,8),A(8,8),EKA(30,8,8),RP(30,8),LM(30,8)
      COMMON /FRC/  DN(25,4,10),FE(30,10,10)
      COMMON /SOL/  R(100),NEQ,MBAND,MAXL
C
      DIMENSION SK(NNN,MMM)
C
C     INITIALIZE STRUCTURE STIFFNESSES
C
      DO 10 I=1,NEQ
      DO 10 J=1,MBAND
   10 SK(I,J)=0.0
C
      DO 100 N=1,NE
C
C     INITIALIZE ELEMENT STIFFNESSES
C
      DO 20 I=1,8
      DO 20 J=1,8
      EK(I,J)=0.0
   20 A(I,J)=0.0
C
      IF (KODE.EQ.2) GO TO 24
C
C     FORM ELEMENT FRAME STIFFNESS MATRIX EK
C
```

```
      EI=E*B(N)**3/12.0
      EA=E*B(N)
      PL=D(N)
C
      EK(1,1)=+4.0*EI/PL
      EK(1,2)=-2.0*EI/PL
      EK(1,3)=-6.0*EI/PL**2
      EK(1,4)=-6.0*EI/PL**2
      EK(2,2)=+EK(1,1)
      EK(2,3)=-EK(1,4)
      EK(2,4)=-EK(1,3)
      EK(3,3)=+12.0*EI/PL**3
      EK(3,4)=+12.0*EI/PL**3
      EK(4,4)=+EK(3,3)
      EK(5,5)=+EA/PL
      EK(5,6)=+EA/PL
      EK(6,6)=+EK(5,5)
      GO TO 26
C
C     FORM ELEMENT PLATE STIFFNESS MATRIX EK
C
   24 D1=E*B(N)**3/(12.0*(1.0-U**2))
      D2=E*B(N)/((1.0+U)**2)
      W1=NN*PI/XL
      W2=W1**2
      W3=W1**3
      S=W1*D(N)/2.0
      CC=COSH(S)
      SS=SINH(S)
      CS=CC*SS
      CC=CC*CC
      SS=SS*SS
      G1=S+CS
      G2=S-CS
      G4=CS*(3.0-U)/(1.0+U)
      G3=S+G4
      G4=S-G4
C
      EK(1,1)=+D1*W1*(CC/G1-SS/G2)
      EK(1,2)=+D1*W1*(CC/G1+SS/G2)
      EK(1,3)=-D1*W2*(CS/G1-CS/G2-1.0+U)
      EK(1,4)=+D1*W2*(CS/G1+CS/G2)
      EK(2,2)=+EK(1,1)
      EK(2,3)=-EK(1,4)
      EK(2,4)=-EK(1,3)
      EK(3,3)=+D1*W3*(SS/G1-CC/G2)
      EK(3,4)=-D1*W3*(SS/G1+CC/G2)
      EK(4,4)=+EK(3,3)
      EK(5,5)=+D2*W1*(SS/G3-CC/G4)
      EK(5,6)=-D2*W1*(SS/G3+CC/G4)
      EK(5,7)=-D2*W1*(CS/G3-CS/G4-1.0-U)
      EK(5,8)=-D2*W1*(CS/G3+CS/G4)
      EK(6,6)=+EK(5,5)
      EK(6,7)=-EK(5,8)
      EK(6,8)=-EK(5,7)
      EK(7,7)=+D2*W1*(CC/G3-SS/G4)
      EK(7,8)=+D2*W1*(CC/G3+SS/G4)
      EK(8,8)=+EK(7,7)
C
   26 DO 30 I=1,8
      DO 30 J=1,8
   30 EK(J,I)=EK(I,J)
C
C     FORM TRANSFORMATION MATRIX A
C
      HD=H(N)
      VD=V(N)
C
      A(1,3)=-1.0
      A(2,7)=+1.0
      A(3,1)=-VD
      A(3,2)=-HD
      A(4,5)=+VD
      A(4,6)=+HD
      A(5,1)=-HD
      A(5,2)=+VD
      A(6,5)=+HD
      A(6,6)=-VD
      A(7,4)=-1.0
      A(8,8)=+1.0
C
C     FORM EK*A
C
      DO 50 I=1,8
      DO 50 J=1,8
      TEMP=0.0
      DO 40 K=1,8
   40 TEMP=TEMP+EK(I,K)*A(K,J)
   50 EKA(N,I,J)=TEMP
C
C     FORM AT*EK*A
C
      DO 70 I=1,8
      DO 70 J=1,8
      TEMP=0.0
      DO 60 K=1,8
   60 TEMP=TEMP+A(K,I)*EKA(N,K,J)
   70 EK(I,J)=TEMP
C
C     ADD ELEMENT STIFFNESS TO STRUCTURE STIFFNESS MATRIX SK
C
      DO 90 I=1,8
      II=LM(N,I)
      DO 90 J=1,8
      JJ=LM(N,J)-II+1
      IF (JJ.LE.0) GO TO 90
      SK(II,JJ)=SK(II,JJ)+EK(I,J)
   90 CONTINUE
C
  100 CONTINUE
C
C     ADD SUPPORT STIFFNESS TO STRUCTURE STIFFNESS MATRIX SK
C
```

```
      IF (KODE.EQ.2) GO TO 110
      DO 110 N=1,NN
      K=4*(N-1)
      IF (NSUP(N,1).EQ.1) SK(K+1,1)=SK(K+1,1)+1.E+15
      IF (NSUP(N,2).EQ.1) SK(K+2,1)=SK(K+2,1)+1.E+15
      SK(K+4,1)=SK(K+4,1)+1.E+15
  110 CONTINUE
C
      RETURN
      END
C     ****************************************************************
      SUBROUTINE LOAD
C
      COMMON /CNL/  DAT,TIM,HED(20),XL,E,U,RO,TC,XP,PI,NH,KODE,KPF
      COMMON /NOD/  Y(25),Z(25),NSUP(25,2),NN
      COMMON /EMT/  NODI(30),NODJ(30),TI(30),TJ(30),NE
      COMMON /SEC/  B(30),D(30),H(30),V(30)
      COMMON /CAS/  CAS(15),NL(30),WL(30,3),NLC,NC,NTYP,NLE
      COMMON /STF/  EK(6,6),A(6,6),EKA(30,6,6),RP(30,6),LM(30,6)
      COMMON /FRC/  DN(25,4,10),FE(30,10,10)
      COMMON /SOL/  R(100),NEQ,MBAND,MAXL
C
C     INITIALIZE STRUCTURE LOADS
C
      DO 10 I=1,NEQ
   10 R(I)=0.0
C
C     INITIALIZE ELEMENT LOADS
C
      DO 20 I=1,NE
      DO 20 J=1,6
   20 RP(I,J)=0.0
C
C     FORM ELEMENT LOAD VECTOR RP (IN LOCAL COORDINATES)
C
      FACT=4.0/(NH*PI)
      IF (KODE.EQ.1) FACT=1.0
      GO TO (30,50,70,90,110,130),NTYP
C
C-----SELF WEIGHT
C
   30 DO 40 N=1,NE
      W1=FACT*RO*TI(N)
      W2=FACT*RO*TJ(N)
      R1=(6.0*W1+4.0*W2)*D(N)**2/120.0*H(N)
      R2=(4.0*W1+6.0*W2)*D(N)**2/120.0*H(N)
      R3=(7.0*W1+3.0*W2)*D(N)/20.0
      R4=(3.0*W1+7.0*W2)*D(N)/20.0
      HD=H(N)
      VD=V(N)
      RP(N,1)=+R1
      RP(N,2)=+R2
      RP(N,3)=-HD*R3
      RP(N,4)=+HD*R4
      RP(N,5)=+VD*R3
   40 RP(N,6)=-VD*R4
      GO TO 150
C
C-----SURCHARGE
C
   50 DO 60 M=1,NLE
      N=NL(M)
      W =WL(M,1)*FACT
      Y1=WL(M,2)
      Y2=WL(M,3)
      IF (Y2.EQ.0.0) Y2=H(N)*D(N)
      YL=H(N)*D(N)
      YA=Y1
      YB=YL-Y2
      YC=YL-YA-YB
      YAL=YA/YL
      YBL=YB/YL
      SC=W*YL**2/12.
      SL=W*YA**2/12.*(6.-8.*YAL+3.*YAL**2)
      SR=W*YB**2/12.*(    4.*YBL-3.*YBL**2)
      R1=SC-SL-SR
      SL=W*YA**2/12.*(    4.*YAL-3.*YAL**2)
      SR=W*YB**2/12.*(6.-8.*YBL+3.*YBL**2)
      R2=SC-SL-SR
      R3=(R1-R2+W*YC*(YB+YC/2.))/YL
      R4=(R2-R1+W*YC*(YA+YC/2.))/YL
      HD=H(N)
      VD=V(N)
      RP(N,1)=RP(N,1)+R1
      RP(N,2)=RP(N,2)+R2
      RP(N,3)=RP(N,3)-HD*R3
      RP(N,4)=RP(N,4)+HD*R4
      RP(N,5)=RP(N,5)+VD*R3
   60 RP(N,6)=RP(N,6)-VD*R4
      GO TO 150
C
C-----TRUCK LOAD
C
   70 DO 80 M=1,NLE
      N=NL(M)
      P =WL(M,1)
      Y1=WL(M,2)
      XO=WL(M,3)
      IF (KODE.EQ.2) GO TO 75
      YL=H(N)*D(N)
      YA=Y1
      YB=YL-Y1
      R1=P*YA*YB**2/YL**2
      R2=P*YB*YA**2/YL**2
      R3=(R1-R2+P*YB)/YL
      R4=(R2-R1+P*YA)/YL
      HD=H(N)
      VD=V(N)
      RP(N,1)=RP(N,1)+R1
      RP(N,2)=RP(N,2)+R2
      RP(N,3)=RP(N,3)-HD*R3
      RP(N,4)=RP(N,4)+HD*R4
      RP(N,5)=RP(N,5)+VD*R3
      RP(N,6)=RP(N,6)-VD*R4
      GO TO 80
   75 W1=NN*PI/XL
      B1=W1*H(N)*D(N)
      E1=W1*Y1
      E2=B1-E1
      SB1=SINH(B1)
      SE1=SINH(E1)
      SE2=SINH(E2)
      CE1=COSH(E1)
      CE2=COSH(E2)
      A1=SB1**2-B1**2
      U1=SE2+E1*CE2
      U2=SE1+E2*CE1
      X1=XL/2.0
      X2=X1+X0
      X3=X1-X0
      SX1=SIN(W1*X1)+SIN(W1*X2)+SIN(W1*X3)*0.25
      RP(N,1)=RP(N,1)+2.0*P/(NN*PI*A1)*(E1*SB1*SE2-B1*E2*SE1)*SX1
      RP(N,2)=RP(N,2)+2.0*P/(NN*PI*A1)*(E2*SB1*SE1-B1*E1*SE2)*SX1
      RP(N,3)=RP(N,3)-2.0*P/(XL*A1)*(U1*SB1-B1*U2)*SX1
      RP(N,4)=RP(N,4)+2.0*P/(XL*A1)*(U2*SB1-B1*U1)*SX1
   80 CONTINUE
      GO TO 150
C
C-----LANE LOAD
C
   90 DO 100 M=1,NLE
      N=NL(M)
      W =WL(M,1)*FACT
      P =WL(M,2)*(-1.0)**((NN+3)/2)*2.0/XL
      Y1=WL(M,3)
      WP=W+P
      YL=H(N)*D(N)
      YA=Y1
      YB=YL-Y1
      R1=WP*YA*YB**2/YL**2
      R2=WP*YB*YA**2/YL**2
      R3=(R1-R2+WP*YB)/YL
      R4=(R2-R1+WP*YA)/YL
      HD=H(N)
      VD=V(N)
      RP(N,1)=RP(N,1)+R1
      RP(N,2)=RP(N,2)+R2
      RP(N,3)=RP(N,3)-HD*R3
      RP(N,4)=RP(N,4)+HD*R4
      RP(N,5)=RP(N,5)+VD*R3
  100 RP(N,6)=RP(N,6)-VD*R4
      GO TO 150
C
C-----TEMPERATURE
C
  110 DO 120 M=1,NLE
      N=NL(M)
      T1=WL(M,1)*FACT
      T2=WL(M,2)*FACT
      TN=E*TC*(T1+T2)*B(N)/2.
      TM=E*TC*(T1-T2)*B(N)**2/12.
      RP(N,1)=-TM
      RP(N,2)=-TM
      RP(N,5)=+TN
  120 RP(N,6)=+TN
      GO TO 150
C
C-----PRESTRESS
C
  130 DO 140 M=1,NLE
      N=NL(M)
      P =WL(M,1)*FACT
      Z1=WL(M,2)
      Z2=WL(M,3)
      EI=TI(N)/2.-Z1
      EJ=TJ(N)/2.-Z2
      EY=D(N)
      EZ=EJ-EI
      EL=SQRT(EY**2+EZ**2)
      CC=EY/EL
      SS=EZ/EL
      RP(N,1)=-P*EI
      RP(N,2)=-P*EJ
      RP(N,3)=+P*SS
      RP(N,4)=+P*SS
      RP(N,5)=+P*CC
  140 RP(N,6)=+P*CC
C
C     ADD ELEMENT LOAD VECTOR TO STRUCTURE LOAD VECTOR R
C
  150 DO 160 N=1,NE
      HD=H(N)
      VD=V(N)
      K=4*(NODI(N)-1)
      R(K+1)=R(K+1)-VD*RP(N,3)-HD*RP(N,5)
      R(K+2)=R(K+2)-HD*RP(N,3)+VD*RP(N,5)
      R(K+3)=R(K+3)-RP(N,1)
      K=4*(NODJ(N)-1)
      R(K+1)=R(K+1)+VD*RP(N,4)+HD*RP(N,6)
      R(K+2)=R(K+2)+HD*RP(N,4)-VD*RP(N,6)
  160 R(K+3)=R(K+3)+RP(N,2)
C
      IF (NTYP.NE.6) GO TO 180
      DO 170 I=1,NE
      DO 170 J=1,6
  170 RP(I,J)=0.0
  180 CONTINUE
C
      RETURN
      END
C     ****************************************************************
      SUBROUTINE FORC
C
      COMMON /CNL/  DAT,TIM,HED(20),XL,E,U,RO,TC,XP,PI,NN,KODE,KPF
      COMMON /NOD/  Y(25),Z(25),NSUP(25,2),NN
      COMMON /EMT/  NODI(30),NODJ(30),TI(30),TJ(30),NE
      COMMON /SEC/  B(30),D(30),H(30),V(30)
      COMMON /CAS/  CAS(15),NL(30),WL(30,3),NLC,NC,NTYP,NLE
      COMMON /STF/  EK(8,8),A(8,8),EKA(30,8,8),RP(30,8),LM(30,8)
      COMMON /FRC/  DN(25,4,10),FE(30,10,10)
      COMMON /SOL/  R(100),NEQ,NBAND,MAXL
C
      DIMENSION RS(8)
C
C     INITIALIZE NODE DISPLACEMENTS
C
      IF (NH.NE.1) GO TO 30
      DO 10 I=1,NN
      DO 10 J=1,4
   10 DN(I,J,NC)=0.0
C
C     INITIALIZE ELEMENT FORCES
C
      DO 20 I=1,NE
      DO 20 J=1,10
   20 FE(I,J,NC)=0.0
C
C     ADD SINGLE HARMONIC NODE DISPLACEMENTS TO TOTAL NODE DISPLACEMENTS
C
   30 G=NH*PI*XP/XL
      CC=COS(G)
      SS=SIN(G)
      DO 40 N=1,NN
      DN(N,1,NC)=DN(N,1,NC)+R(4*N-3)*SS
      DN(N,2,NC)=DN(N,2,NC)+R(4*N-2)*SS
      DN(N,3,NC)=DN(N,3,NC)+R(4*N-1)*SS
   40 DN(N,4,NC)=DN(N,4,NC)+R(4*N  )*CC
      CALL TRNC(DN,NN,25,4,NC)
C
C     FIND SINGLE HARMONIC ELEMENT FORCES
C
      DO 50 N=1,NE
      DO 50 I=1,8
      RS(I)=0.0
      DO 50 J=1,8
      JJ=LM(N,J)
   50 RS(I)=RS(I)+EKA(N,I,J)*R(JJ)
C
C     ADD SINGLE HARMONIC ELEMENT FORCES TO TOTAL ELEMENT FORCES
C
      D1=E*B(N)**3/(12.0*(1.0-U**2))
      W1=NH*PI/XL
      PR=U
      IF (KODE.EQ.1) W1=0.0
      IF (KODE.EQ.1) PR=0.0
      F1=E*B(N)*W1*R(LM(N,4))+PR*(RS(5)-RP(N,5))
      F2=E*B(N)*W1*R(LM(N,8))+PR*(RS(6)-RP(N,6))
      F3=D1*W1**2*(1.0-U)*R(LM(N,3))
      F4=D1*W1**2*(1.0-U)*R(LM(N,7))
      FE(N, 1,NC)=FE(N, 1,NC)+F1*SS
      FE(N, 2,NC)=FE(N, 2,NC)+(RS(7)-RP(N,7))*CC
      FE(N, 3,NC)=FE(N, 3,NC)+(RS(5)-RP(N,5))*SS
      FE(N, 4,NC)=FE(N, 4,NC)+(RS(3)-RP(N,3))*SS+F3*SS
      FE(N, 5,NC)=FE(N, 5,NC)+(RS(1)-RP(N,1))*SS
      FE(N, 6,NC)=FE(N, 6,NC)+F2*SS
      FE(N, 7,NC)=FE(N, 7,NC)+(RS(8)-RP(N,8))*CC
      FE(N, 8,NC)=FE(N, 8,NC)+(RS(6)-RP(N,6))*SS
      FE(N, 9,NC)=FE(N, 9,NC)+(RS(4)-RP(N,4))*SS+F4*SS
   60 FE(N,10,NC)=FE(N,10,NC)+(RS(2)-RP(N,2))*SS
      CALL TRNC(FE,NE,30,10,NC)
C
      RETURN
      END
C     ****************************************************************
      SUBROUTINE RITE
C
      COMMON /CNL/  DAT,TIM,HED(20),XL,E,U,RO,TC,XP,PI,NH,KODE,KPF
      COMMON /NOD/  Y(25),Z(25),NSUP(25,2),NN
      COMMON /EMT/  NODI(30),NODJ(30),TI(30),TJ(30),NE
      COMMON /SEC/  B(30),D(30),H(30),V(30)
      COMMON /CAS/  CAS(15),NL(30),WL(30,3),NLC,NC,NTYP,NLE
      COMMON /STF/  EK(8,8),A(8,8),EKA(30,8,8),RP(30,8),LM(30,8)
      COMMON /FRC/  DN(25,4,10),FE(30,10,10)
      COMMON /SOL/  R(100),NEQ,NBAND,MAXL
C
C     WRITE HEADING
C
      WRITE (6,10) DAT,TIM,HED,CAS
   10 FORMAT(42H1TRANSVERSE ANALYSIS OF BOX GIRDER BRIDGES/
     1        1H ,6HDATE: ,A8,4X,6HTIME: ,A8///1H ,20A4//1H ,15A4)
      IF (KODE.EQ.1) WRITE(6,14)
      IF (KODE.EQ.2) WRITE(6,16) XP
   14 FORMAT(//19H PLANE FRAME THEORY)
   16 FORMAT(//20H FOLDED PLATE THEORY,19X,12HX-ORDINATE =,E12.4)
C
C     WRITE NODE DISPLACEMENTS
C
      WRITE (6,20) (N,(DN(N,M,NC),M=1,4),N=1,NN)
   20 FORMAT(//19H NODE DISPLACEMENTS//
     1 5H NODE,16X,6HY-DISP,6X,6HZ-DISP,7X,5HROT'N,6X,6HX-DISP/
     2 (I5,10X,4E12.4))
C
C     WRITE ELEMENT FORCES
C
      WRITE (6,30) (N,NODI(N),(FE(N,M,NC),M=1, 5),
     1              N,NODJ(N),(FE(N,M,NC),M=6,10),N=1,NE)
   30 FORMAT(//15H ELEMENT FORCES//
     1 11H ELMT  NODE,13X,3HNXX,9X,3HNXY,9X,3HNYY,9X,3HQYY,9X,3HMYY/
     2 (I5,I6,4X,5E12.4))
C
      RETURN
      END
C     ****************************************************************
      SUBROUTINE SOLV(A,B,NN,MM,KK)
C
      DIMENSION A(NN,MM),B(NN)
C
      GO TO (10,70), KK
C
```

```
C     REDUCE STIFFNESS MATRIX
C
   10 DO 60 N=1,NN
      IF (A(N,1).GT.0.001) GO TO 30
      WRITE (6,20) N
   20 FORMAT(///30H ZERO ON DIAGONAL FOR EQUATION,I4)
      CALL EXIT
   30 DO 50 M=2,MM
      FACT=A(N,M)/A(N,1)
      I=N+M-1
      IF (I.GT.NN) GO TO 50
      J=0
      DO 40 K=M,MM
      J=J+1
   40 A(I,J)=A(I,J)-FACT*A(N,K)
   50 A(N,M)=FACT
   60 CONTINUE
      GO TO 120
C
C     REDUCE LOAD VECTOR
C
   70 DO 90 N=1,NN
      DO 80 M=2,MM
      I=N+M-1
      IF (I.GT.NN) GO TO 90
   80 B(I)=B(I)-A(N,M)*B(N)
   90 B(N)=B(N)/A(N,1)
C
C     BACK SUBSTITUTE
C
      N=NN
  100 N=N-1
      IF (N.EQ.0) GO TO 120
      DO 110 M=2,MM
      I=N+M-1
      IF (I.GT.NN) GO TO 110
      B(N)=B(N)-A(N,M)*B(I)
  110 CONTINUE
      GO TO 100
C
  120 RETURN
      END
C     ******************************************************************
      SUBROUTINE TRNC(A,N,L,M,K)
C
      DIMENSION A(L,M,1)
C
      DO 20 J=1,M
      AMAX=0.0
      DO 10 I=1,N
      AA=ABS(A(I,J,K))
      IF (AMAX.LT.AA) AMAX=AA
   10 CONTINUE
      AMAX=AMAX*1.E-03
      DO 20 I=1,N
      AA=ABS(A(I,J,K))
      IF (AA.LT.AMAX) A(I,J,K)=0.0
   20 CONTINUE
C
      RETURN
      END
End of file
```

Appendix G

Listing of input data for BOXGIRD

```
 1      ISLINGTON AVENUE EXTENSION
 2         14    14     8
 3      156.0       576000.0  0.15       0.150      0.000006  75.0
 4          1       -22.50    0.00
 5          2       -19.50    0.00
 6          3       -12.00    0.00
 7          4       -12.00    3.375
 8          5       -12.00    6.75             1     1
 9          6        -6.75    0.00
10          7         0.00    0.00
11          8         0.00    6.75
12          9        +6.75    0.00
13         10       +12.00    0.00
14         11       +12.00    3.375
15         12       +12.00    6.75             0     1
16         13       +19.50    0.00
17         14       +22.50    0.00
18          1     1     2     0.667     0.667
19          2     2     3     0.667     1.500
20          3     3     6     1.500     0.833
21          4     6     7     0.833     0.833
22          5     7     9     0.833     0.833
23          6     9    10     0.833     1.500
24          7    10    13     1.500     0.667
25          8    13    14     0.667     0.667
26          9     5     8     0.750
27         10     8    12     0.750
28         11     3     4     1.500
29         12     4     5     1.500
30         13    10    11     1.500
31         14    11    12     1.500
32      SELF WEIGHT           SELF WEIGHT
33      SURCHARGE      12     SUPERIMPOSED DEAD LOAD
34          1      0.038
35          2      0.038
36          3      0.038
37          4      0.038
38          5      0.038
39          6      0.038
40          7      0.038
41          8      0.038
42          1      0.087      0.0       3.0
43          2      0.087      0.0       3.0
44          8      0.087      1.0       3.0
45          1      5.750      0.0       0.1
46      SURCHARGE       2     SIDEWALK LIVE LOAD
47          1      0.085      0.0       3.0
48          2      0.085      0.0       3.0
49      TRUCK LOAD      2     TRUCK LOAD 1 (NEGATIVE CANTILEVER MOMENT)
50          7      26.0       1.5       14.0
51          7      26.0       7.5       14.0
52      TRUCK LOAD      4     TRUCK LOAD 2 (NEGATIVE INTERIOR MOMENT)
53          3      26.0       4.0       14.0
54          4      26.0       4.75      14.0
55          5      26.0       2.0       14.0
56          6      26.0       1.25      14.0
57      TRUCK LOAD      4     TRUCK LOAD 3 (POSITIVE INTERIOR MOMENT)
58          3      26.0       2.0       14.0
59          4      26.0       2.75      14.0
60          5      26.0       0.0       14.0
61          5      26.0       6.0       14.0
62      TEMPERATURE     8     TEMPERATURE 1 (TOP SURFACE 40 F ABOVE DATUM)
63          1      40.0       0.0
64          2      40.0       0.0
65          3      40.0       0.0
66          4      40.0       0.0
67          5      40.0       0.0
68          6      40.0       0.0
69          7      40.0       0.0
70          8      40.0       0.0
71      TEMPERATURE    10     TEMPERATURE 2 (INTERIOR SURFACE 20 F ABOVE DATUM)
72          3      0.0        20.0
73          4      0.0        20.0
74          5      0.0        20.0
75          6      0.0        20.0
76          9      20.0       0.0
77         10      20.0       0.0
78         11      20.0       0.0
79         12      20.0       0.0
80         13      0.0        20.0
81         14      0.0        20.0
82      PRESTRESS       8     TRANSVERSE PRESTRESS
83          1      17.34      0.333     0.333
84          2      17.34      0.333     0.198
85          3      17.34      0.198     0.552
86          4      17.34      0.552     0.552
87          5      17.34      0.552     0.552
88          6      17.34      0.552     0.198
89          7      17.34      0.198     0.333
90          8      17.34      0.333     0.333
91
92
93
End of file
```

Appendix H

Listing of output information for BOXGIRD

```
1TRANSVERSE ANALYSIS OF BOX GIRDER BRIDGES
 DATE: 03-25-84    TIME: 22:05:38

 ISLINGTON AVENUE EXTENSION

 NO. OF NODES            =  14
 NO. OF ELEMENTS         =  14
 NO. OF LOAD CASES       =   9

 SPAN LENGTH             =  0.1560E+03
 MODULUS OF ELASTICITY   =  0.5760E+06
 POISSON'S RATIO         =  0.1500E+00
 MASS DENSITY            =  0.1500E+00
 THERMAL COEFFICIENT     =  0.6000E-05
 X-ORDINATE              =  0.7800E+02


 NODE DATA

 NODE          Y-ORD               Z-ORD   Y-SUP   Z-SUP
    1     -0.2250E+02     0.0                 0       0
    2     -0.1650E+02     0.0                 0       0
    3     -0.1200E+02     0.0                 0       0
    4     -0.1200E+02     0.3375E+01          0       0
    5     -0.1200E+02     0.6750E+01          1       1
    6     -0.6750E+01     0.0                 0       0
    7      0.0            0.0                 0       0
    8      0.0            0.6750E+01          0       0
    9      0.6750E+01     0.0                 0       0
   10      0.1200E+02     0.0                 0       0
   11      0.1200E+02     0.3375E+01          0       0
   12      0.1200E+02     0.6750E+01          0       1
   13      0.1650E+02     0.0                 0       0
   14      0.2250E+02     0.0                 0       0


 ELEMENT DATA

 ELMT   NOD-I   NOD-J            THK-I          THK-J
    1       1       2      0.6670E+00     0.6670E+00
    2       2       3      0.6670E+00     0.1500E+01
    3       3       6      0.1500E+01     0.8330E+00
    4       6       7      0.8330E+00     0.8330E+00
    5       7       9      0.8330E+00     0.8330E+00
    6       9      10      0.8330E+00     0.1500E+01
    7      10      13      0.1500E+01     0.6670E+00
    8      13      14      0.6670E+00     0.6670E+00
    9       6       8      0.7500E+00     0.7500E+00
   10       9      12      0.7500E+00     0.7500E+00
   11       3       4      0.1500E+01     0.1500E+01
   12       4       5      0.1500E+01     0.1500E+01
   13      10      11      0.1500E+01     0.1500E+01
   14      11      12      0.1500E+01     0.1500E+01


 NO. OF EQUATIONS = 56
 BANDWIDTH        = 20


 **************************************************************


1TRANSVERSE ANALYSIS OF BOX GIRDER BRIDGES
 DATE: 03-25-84    TIME: 22:05:38.


 ISLINGTON AVENUE EXTENSION

 SELF WEIGHT


 PLANE FRAME THEORY


 NODE DISPLACEMENTS

 NODE                 Y-DISP      Z-DISP       ROT'N       X-DISP
    1            0.3621E-04  0.2537E-02  0.3365E-03  0.0
    2            0.3621E-04  0.1646E-02  0.3098E-03  0.0
    3            0.3621E-04  0.2890E-04  0.1584E-04  0.0
    4            0.5582E-04  0.1471E-04  0.3356E-05  0.0
    5            0.0         0.0        -0.6323E-04  0.0
    6            0.3220E-04  0.6961E-03 -0.2073E-03  0.0
    7            0.2137E-04  0.1730E-02  0.0         0.0
    8            0.2137E-04  0.4468E-02  0.0         0.0
    9            0.1055E-04  0.6961E-03  0.2073E-03  0.0
   10            0.4537E-05  0.2890E-04 -0.1584E-04  0.0
   11           -0.4307E-04  0.1471E-04 -0.3356E-05  0.0
   12            0.4275E-04  0.0         0.6323E-04  0.0
   13            0.4537E-05  0.1646E-02 -0.3098E-03  0.0
   14            0.4537E-05  0.2537E-02 -0.3365E-03  0.0


 ELEMENT FORCES

 ELMT  NODE            NXX           NXY           NYY          QYY          MYY
    1     1     0.0          0.0          0.0          0.0          0.0
    1     2     0.0          0.0          0.0         -0.3001E+00  -0.4502E+00
    2     2     0.0          0.0          0.0         -0.3002E+00  -0.4502E+00
    2     3     0.0          0.0          0.0         -0.1519E+01  -0.6687E+01
    3     3     0.0          0.0         -0.5030E+00   0.1762E+01  -0.7507E+01
    3     6     0.0          0.0         -0.5030E+00   0.8434E+00  -0.6877E+00
    4     6     0.0          0.0         -0.5030E+00   0.8434E+00  -0.6877E+00
    4     7     0.0          0.0         -0.5030E+00   0.0           0.1948E+01
    5     7     0.0          0.0         -0.5030E+00   0.0           0.1948E+01
    5     9     0.0          0.0         -0.5030E+00  -0.8434E+00  -0.6877E+00
    6     9     0.0          0.0         -0.5030E+00  -0.8434E+00  -0.6877E+00
    6    10     0.0          0.0         -0.5030E+00  -0.1762E+01  -0.7507E+01
    7    10     0.0          0.0          0.0          0.1519E+01  -0.6687E+01
    7    13     0.0          0.0          0.0          0.3002E+00  -0.4502E+00
    8    13     0.0          0.0          0.0          0.3001E+00  -0.4502E+00
    8    14     0.0          0.0          0.0          0.0          0.0
    9     6     0.0          0.0          0.5030E+00   0.1350E+01  -0.5275E+01
```

```
      9     8      0.0          0.0          0.9030E+00  0.0          0.2828E+01
     10     8      0.0          0.0          0.9030E+00  0.0          0.2828E+01
     10    12      0.0          0.0          0.9030E+00 -0.1360E+01  -0.5275E+01
     11     3      0.0          0.0         -0.3281E+01 -0.9030E+00   0.8205E+00
     11     4      0.0          0.0         -0.4040E+01 -0.9030E+00  -0.2227E+01
     12     4      0.0          0.0         -0.4040E+01 -0.9030E+00  -0.2227E+01
     12     5      0.0          0.0         -0.4800E+01 -0.9030E+00  -0.5275E+01
     13    10      0.0          0.0         -0.3281E+01  0.9030E+00  -0.8205E+00
     13    11      0.0          0.0         -0.4040E+01  0.9030E+00   0.2227E+01
     14    11      0.0          0.0         -0.4040E+01  0.9030E+00   0.2227E+01
     14    12      0.0          0.0         -0.4800E+01  0.9030E+00   0.5275E+01


 **************************************************************************

1TRANSVERSE ANALYSIS OF BOX GIRDER BRIDGES
 DATE: 03-25-84     TIME: 22:05:36


 ISLINGTON AVENUE EXTENSION

 SELF WEIGHT


 FOLDED PLATE THEORY                       X-ORDINATE =  0.7800E+02


 NODE DISPLACEMENTS

 NODE             Y-DISP      Z-DISP       ROT'N      X-DISP
    1        -0.8324E-03  0.2303E+00  0.5980E-03 -0.1831E-17
    2        -0.5481E-03  0.2286E+00  0.5340E-03 -0.1841E-17
    3        -0.3253E-03  0.2257E+00  0.1518E-03 -0.1705E-17
    4         0.1827E-03  0.2257E+00  0.1402E-03  0.7780E-18
    5         0.6602E-03  0.2256E+00  0.7448E-04  0.3264E-17
    6        -0.1741E-03  0.2258E+00 -0.1340E-03 -0.1658E-17
    7         0.0         0.2268E+00  0.0        -0.1632E-17
    8         0.0         0.2292E+00  0.0         0.3101E-17
    9         0.1741E-03  0.2258E+00  0.1340E-03 -0.1658E-17
   10         0.3253E-03  0.2257E+00 -0.1518E-03 -0.1705E-17
   11        -0.1827E-03  0.2257E+00 -0.1402E-03  0.7780E-18
   12        -0.6602E-03  0.2256E+00 -0.7448E-04  0.3264E-17
   13         0.5481E-03  0.2286E+00 -0.5340E-03 -0.1841E-17
   14         0.8324E-03  0.2303E+00 -0.5980E-03 -0.1831E-17


 ELEMENT FORCES

 ELMT  NODE              NXX         NXY         NYY         QYY         MYY
    1     1      -0.8398E+02  0.0         0.0         0.4309E-02  0.0
    1     2      -0.8450E+02 -0.7136E-15  0.1241E+00 -0.3107E+00 -0.4468E+00
    2     2      -0.8450E+02 -0.7136E-15  0.1241E+00 -0.2981E+00 -0.4468E+00
    2     3      -0.1970E+03 -0.4013E-14  0.2053E+01 -0.1581E+01 -0.6734E+01
    3     3      -0.1972E+03  0.4575E-14  0.1114E+01  0.1837E+01 -0.7817E+01
    3     6      -0.1068E+03  0.2009E-14 -0.8109E+00  0.8820E+00 -0.8405E+00
    4     6      -0.1068E+03  0.2009E-14 -0.8109E+00  0.8709E+00 -0.8405E+00
    4     7      -0.1052E+03  0.0        -0.1595E+01  0.0         0.2059E+01
    5     7      -0.1052E+03  0.0        -0.1595E+01  0.0         0.2059E+01
    5     9      -0.1068E+03 -0.2009E-14 -0.8109E+00 -0.8709E+00 -0.8405E+00
    6     9      -0.1068E+03 -0.2009E-14 -0.8109E+00 -0.8820E+00 -0.8405E+00
    6    10      -0.1972E+03 -0.4575E-14  0.1114E+01 -0.1837E+01 -0.7817E+01
    7    10      -0.1970E+03  0.4013E-14  0.2053E+01  0.1581E+01 -0.6734E+01
    7    13      -0.8450E+02  0.7136E-15  0.1241E+00  0.2981E+00 -0.4468E+00
    8    13      -0.8450E+02  0.7136E-15  0.1241E+00  0.3107E+00 -0.4468E+00
    8    14      -0.8398E+02  0.0         0.0        -0.4309E-02  0.0
    9     5       0.1890E+03 -0.6490E-14  0.9407E+00  0.1408E+01 -0.5368E+01
    9     8       0.1803E+03  0.0         0.5223E+01  0.0         0.2868E+01
   10     8       0.1803E+03  0.0         0.5223E+01  0.0         0.2868E+01
   10    12       0.1890E+03  0.6490E-14  0.9407E+00 -0.1408E+01 -0.5368E+01
   11     3      -0.1878E+03 -0.5589E-14 -0.3418E+01 -0.9308E+00  0.8838E+00
   11     4       0.8872E+02 -0.9325E-14 -0.8275E+00 -0.9307E+00 -0.2225E+01
   12     4       0.8872E+02 -0.9325E-14 -0.8275E+00 -0.9307E+00 -0.2225E+01
   12     5       0.3780E+03 -0.6490E-14  0.1408E+01 -0.9428E+00 -0.5368E+01
   13    10      -0.1878E+03 -0.5589E-14 -0.3418E+01  0.9308E+00 -0.8838E+00
   13    11       0.8872E+02 -0.9325E-14 -0.8275E+00  0.9307E+00  0.2225E+01
   14    11       0.8872E+02 -0.9325E-14 -0.8275E+00  0.9307E+00  0.2225E+01
   14    12       0.3780E+03 -0.6490E-14  0.1408E+01  0.9428E+00  0.5368E+01


 **************************************************************************


1TRANSVERSE ANALYSIS OF BOX GIRDER BRIDGES
 DATE: 03-25-84     TIME: 22:05:36


 ISLINGTON AVENUE EXTENSION

 SUPERIMPOSED DEAD LOAD


 LOAD DATA

 ELMT             W             Y1              Y2
    1      0.3600E-01     0.0             0.0
    2      0.3600E-01     0.0             0.0
    3      0.3600E-01     0.0             0.0
    4      0.3600E-01     0.0             0.0
    5      0.3600E-01     0.0             0.0
    6      0.3600E-01     0.0             0.0
    7      0.3600E-01     0.0             0.0
    8      0.3600E-01     0.0             0.0
    1      0.8700E-01     0.0             0.3000E+01
    2      0.8700E-01     0.0             0.3000E+01
    8      0.8700E-01     0.1000E+01      0.3000E+01
    1      0.8750E+01     0.0             0.1000E+00


 **************************************************************************


1TRANSVERSE ANALYSIS OF BOX GIRDER BRIDGES
```

```
DATE: 03-26-84    TIME: 22:05:36


ISLINGTON AVENUE EXTENSION

SUPERIMPOSED DEAD LOAD


PLANE FRAME THEORY


NODE DISPLACEMENTS

NODE                 Y-DISP      Z-DISP         ROT'N       X-DISP
   1             -0.1347E-02  0.8482E-02  0.1282E-02  0.0
   2             -0.1347E-02  0.5815E-02  0.1072E-02  0.0
   3             -0.1347E-02  0.1567E-04  0.2688E-03  0.0
   4             -0.5536E-03  0.0         0.1906E-03  0.0
   5              0.0         0.0         0.1483E-03  0.0
   6             -0.1341E-02 -0.7601E-03  0.4073E-04  0.0
   7             -0.1330E-02  0.0        -0.1642E-03  0.0
   8             -0.2118E-04  0.1748E-03 -0.8772E-04  0.0
   9             -0.1320E-02  0.5078E-03  0.5248E-04  0.0
  10             -0.1314E-02  0.0         0.1362E-03  0.0
  11             -0.7356E-03  0.0         0.1873E-03  0.0
  12             -0.4238E-04  0.0         0.2048E-03  0.0
  13             -0.1314E-02 -0.3855E-04 -0.8832E-04  0.0
  14             -0.1314E-02  0.2393E-03 -0.1011E-03  0.0


ELEMENT FORCES

ELMT  NODE             NXX             NXY           NYY           QYY           MYY
   1     1     0.0          0.0          0.0          0.0          0.0
   1     2     0.0          0.0          0.0         -0.1050E+01 -0.2854E+01
   2     2     0.0          0.0          0.0         -0.1050E+01 -0.2854E+01
   2     3     0.0          0.0          0.0         -0.1595E+01 -0.1205E+02
   3     3     0.0          0.0          0.8854E+00  0.7573E+00 -0.8035E+01
   3     5     0.0          0.0          0.8854E+00  0.5578E+00 -0.2583E+01
   4     5     0.0          0.0          0.8854E+00  0.5578E+00 -0.2583E+01
   4     7     0.0          0.0          0.8854E+00  0.3013E+00  0.2109E+00
   5     7     0.0          0.0          0.8854E+00  0.3013E+00  0.2109E+00
   5     9     0.0          0.0          0.8854E+00  0.4479E-01  0.1485E+01
   6     9     0.0          0.0          0.8854E+00  0.4479E-01  0.1485E+01
   6    10     0.0          0.0          0.8854E+00 -0.1547E+00  0.1195E+01
   7    10     0.0          0.0          0.0          0.5730E+00 -0.2748E+01
   7    12     0.0          0.0          0.0          0.2880E+00 -0.5190E+00
   8    13     0.0          0.0          0.0          0.2880E+00 -0.5190E+00
   8    14     0.0          0.0          0.0          0.0          0.0
   9     5     0.0          0.0         -0.8854E+00  0.8888E-01 -0.8847E+00
   9     8     0.0          0.0         -0.8854E+00  0.8888E-01  0.5789E-01
  10     8     0.0          0.0         -0.8854E+00  0.8888E-01  0.5789E-01
  10    12     0.0          0.0         -0.8854E+00  0.8888E-01  0.1100E+01
  11     3     0.0          0.0         -0.2353E+01  0.8854E+00 -0.7028E+01
  11     4     0.0          0.0         -0.2353E+01  0.8854E+00 -0.4007E+01
  12     4     0.0          0.0         -0.2353E+01  0.8854E+00 -0.4007E+01
  12     5     0.0          0.0         -0.2353E+01  0.8854E+00 -0.8847E+00
  13    10     0.0          0.0         -0.7277E+00 -0.8854E+00  0.4844E+01
  13    11     0.0          0.0         -0.7277E+00 -0.8854E+00  0.1823E+01
  14    11     0.0          0.0         -0.7277E+00 -0.8854E+00  0.1823E+01
  14    12     0.0          0.0         -0.7277E+00 -0.8854E+00 -0.1100E+01



*****************************************************************************


1TRANSVERSE ANALYSIS OF BOX GIRDER BRIDGES
 DATE: 03-26-84    TIME: 22:05:36


 ISLINGTON AVENUE EXTENSION

 SUPERIMPOSED DEAD LOAD


 FOLDED PLATE THEORY                          X-ORDINATE =  0.7800E+02


 NODE DISPLACEMENTS

 NODE                 Y-DISP      Z-DISP         ROT'N       X-DISP
    1             -0.5825E-03  0.5623E-01  0.1260E-02 -0.4058E-15
    2             -0.5713E-03  0.5455E-01  0.1065E-02 -0.4134E-15
    3             -0.5147E-03  0.5488E-01  0.2579E-03 -0.4363E-15
    4              0.1233E-03  0.5686E-01  0.1272E-03  0.2000E-15
    5              0.4579E-03  0.5685E-01  0.8800E-04  0.8299E-15
    6             -0.4845E-03  0.5774E-01  0.1834E-03 -0.4244E-15
    7             -0.4044E-03  0.5665E-01  0.1905E-03 -0.4103E-15
    8              0.2783E-03  0.5570E-01  0.2226E-03  0.7802E-15
    9             -0.3805E-03  0.5526E-01  0.1605E-03 -0.4084E-15
   10             -0.3100E-03  0.5485E-01  0.4803E-04 -0.4156E-15
   11             -0.1162E-03  0.5455E-01  0.8801E-04  0.1807E-15
   12              0.1234E-03  0.5453E-01  0.7814E-04  0.8015E-15
   13             -0.2547E-03  0.5535E-01 -0.1788E-03 -0.4120E-15
   14             -0.2334E-03  0.5597E-01 -0.2210E-03 -0.4130E-15


 ELEMENT FORCES

 ELMT  NODE             NXX         NXY           NYY           QYY           MYY
    1     1     -0.2085E+02  0.0          0.0          0.1378E-01  0.0
    1     2     -0.2128E+02 -0.1557E-15  0.2901E-01 -0.1098E+01 -0.2828E+01
    2     2     -0.2128E+02 -0.1557E-15  0.2901E-01 -0.1098E+01 -0.2828E+01
    2     3     -0.5066E+02 -0.5554E-15  0.4938E+00 -0.1550E+01 -0.1323E+02
    3     3     -0.5042E+02  0.1758E-14  0.2213E+01  0.4848E+00 -0.2178E+01
    3     5     -0.2710E+02  0.1093E-14  0.1379E+01  0.2377E+00 -0.3542E+00
    4     5     -0.2710E+02  0.1093E-14  0.1375E+01  0.2375E+00 -0.3542E+00
    4     7     -0.2828E+02  0.5730E-15  0.7277E+00 -0.2885E-01  0.3471E+00
    5     7     -0.2828E+02  0.5730E-15  0.7277E+00 -0.2885E-01  0.3471E+00
    5     8     -0.2825E+02  0.6228E-15  0.4783E+00 -0.2851E+00 -0.7242E+00
    6     8     -0.2825E+02  0.6228E-15  0.4783E+00 -0.2801E+00 -0.7242E+00
    6    10     -0.4835E+02 -0.5523E-15  0.5085E+00 -0.5041E+00 -0.2772E+01
    7    10     -0.4830E+02  0.5740E-15  0.5185E+00  0.5982E+00 -0.3838E+01
    340          7    13   -0.21208E+02  0.17838E-15  0.31488E-01  0.38808E+00 -0.53488E+00
    341          8    13   -0.21208E+02  0.17838E-15  0.31488E-01  0.30208E+00 -0.53488E+00
    342          8    14   -0.21268E+02  0.0          0.0          0.0          0.0
    343          9     5    0.48378E+02 -0.22338E-14 -0.17188E+01 -0.52278E-01  0.58108E+00
    344          9     8    0.48188E+02 -0.88888E-15  0.17728E+00 -0.48818E-01  0.83188E-01
    345         10     8    0.48188E+02 -0.88888E-15  0.17728E+00 -0.48818E-01  0.83188E-01
    346         10    13    0.48288E+02  0.10348E-14 -0.82788E-01 -0.47288E-01 -0.80078E+00
    347         11     3   -0.81078E+02 -0.27238E-14 -0.21148E+01  0.17278E+01 -0.11088E+02
    348         11     4    0.23018E+02 -0.28318E-14 -0.10488E+01  0.17238E+01 -0.81778E+01
    349         12     4    0.23018E+02 -0.28318E-14 -0.10488E+01  0.17238E+01 -0.81778E+01
    350         12     6    0.97248E+02 -0.22338E-14 -0.92838E-01  0.17208E+01  0.88108E+00
    351         12    10   -0.48818E+02 -0.15288E-14 -0.11048E+01 -0.48378E-01  0.10888E+01
    352         13    11    0.21988E+02 -0.18488E-14 -0.48358E+00 -0.88188E-01  0.78138E+00
    353         14    11    0.21988E+02 -0.18488E-14 -0.48358E+00 -0.88188E-01  0.78138E+00
    354         14    13    0.82788E+02 -0.10348E-14  0.47878E-01 -0.87848E-01  0.80078E+00
End of file
```

Appendix I

FORTRAN listing of PREBEAM

```
      C     PROGRAM PREBEAM (INPUT,OUTPUT,TAPE5=INPUT,TAPE6=OUTPUT)
      C
      C     ****************************************************************
      C     *                                                              *
      C     *  PREBEAM:  ANALYSIS OF PARTIALLY PRESTRESSED CONCRETE BEAMS  *
      C     *            PROGRAMMED BY K W SHUSHKEWICH, JAN 1984.          *
      C     *                                                              *
      C     ****************************************************************
      C
            DIMENSION CURV(5,2),HED(20)
            DATA CURV / 274.0 , 239.2 , 1.06 , 0.0105 , 7.447 ,
           1            156.6 , 148.0 , 1.02 , 0.0043 , 4.190 /
            REAL NP,NS,NSP,NPM1,NSM1,NSPM1,N,M,NU,MU,IUC,ICR,MCR,KK
      C
      C     READ & WRITE INPUT DATA (UNITS ARE INCHES AND KIPS)
      C
            CALL TIME(10,0,DAT)
            CALL TIME( 4,0,TIM)
         10 READ  (5, 20) HED,KODE1,KODE2
         20 FORMAT(20A4/2I5)
            IF (KODE1.EQ.0) CALL EXIT
            WRITE (6, 30) DAT,TIM,HED
         30 FORMAT(48H1ANALYSIS OF PARTIALLY PRESTRESSED CONCRETE BEAMS/
           1       1H ,8HDATE: ,A8,4X,8HTIME: ,A8/1H ,20A4/
           2       12H INPUT DATA:)
            READ  (5, 40) FCP,FPU,FSY,FSPY
         40 FORMAT(4F10.0)
            WRITE (6, 50) FCP,FPU,FSY,FSPY
         50 FORMAT(7H  FC' =,F10.1,7H  FPU =,F10.1,
           1       7H  FSY =,F10.1,7H  FSY'=,F10.1)
            READ  (5, 60) EC,EP,ES,ESP
         60 FORMAT(4F10.0)
            WRITE (6, 70) EC,EP,ES,ESP
         70 FORMAT(7H  EC  =,F10.1,7H  EP  =,F10.1,
           1       7H  ES  =,F10.1,7H  ES' =,F10.1)
            READ  (5, 80) B,D,B1,D1,B2,D2
         80 FORMAT(2F10.0)
            WRITE (6, 90) B,D,B1,D1,B2,D2
         90 FORMAT(7H  B   =,F10.3,7H  D   =,F10.3/
           1       7H  B1  =,F10.3,7H  D1  =,F10.3/
           2       7H  B2  =,F10.3,7H  D2  =,F10.3)
            IF (B1.LT.B) B1=B
            IF (B2.LT.B) B2=B
            READ  (5,100) AP,DP,AS,DS,ASP,DSP
        100 FORMAT(2F10.0)
            WRITE (6,110) AP,DP,AS,DS,ASP,DSP
        110 FORMAT(7H  AP  =,F10.3,7H  DP  =,F10.3/
           1       7H  AS  =,F10.3,7H  DS  =,F10.3/
           2       7H  AS' =,F10.3,7H  DS' =,F10.3)
            IF (AP .EQ.0.0) EP =0.0
            IF (AS .EQ.0.0) ES =0.0
            IF (ASP.EQ.0.0) ESP=0.0
            READ  (5,120) N,M,F,NU,MU,PHI
        120 FORMAT(3F10.0)
            WRITE (6,130) N,M,F,NU,MU,PHI
        130 FORMAT(7H  N'  =,F10.3,7H  M'  =,F10.3,7H  F   =,F10.3/
           1       7H  NU  =,F10.3,7H  MU  =,F10.3,7H  PHI =,F10.3)
      C
            NP =EP /EC
            NS =ES /EC
            NSP=ESP/EC
            NPM1 =NP -1.
            NSM1 =NS -1.
            NSPM1=NSP-1.
            B1B=B1-B
            B2B=B2-B
      C
      C     UNCRACKED SECTION
      C
            WRITE (6,140)
        140 FORMAT(19H UNCRACKED SECTION:)
            IF (KODE1.EQ.1) WRITE (6,144)
            IF (KODE1.EQ.2) WRITE (6,146)
        144 FORMAT(27H (GROSS SECTION PROPERTIES))
        146 FORMAT(33H (TRANSFORMED SECTION PROPERTIES))
      C
            AUC=        B*D    +       B1B*D1    +       B2B*D2
            QUC=1./2.*B*D**2+1./2.*B1B*D1**2-1./2.*B2B*D2**2+B2B*D2*D
            IUC=1./3.*B*D**3+1./3.*B1B*D1**3+1./3.*B2B*D2**3+B2B*D2*D*(D-D2)
            IF (KODE1.EQ.1) GO TO 150
            AUC=AUC+NSPM1*ASP         +NSM1*AS        +NPM1*AP
            QUC=QUC+NSPM1*ASP*DSP     +NSM1*AS*DS     +NPM1*AP*DP
            IUC=IUC+NSPM1*ASP*DSP**2+NSM1*AS*DS**2+NPM1*AP*DP**2
      C
        150 YT=QUC/AUC
            YB=D-YT
            IUC=IUC-AUC*YT**2
            ST=IUC/YT
            SB=IUC/YB
            R=F*(1.0+NP*AP/AUC*(1.0+(DP-YT)**2/(IUC/AUC)))
            MCR=F*(SB/AUC+DP-YT)-N*(SB/AUC)
            FT=-F/AUC+F*(DP-YT)/ST+N/AUC-M/ST
            FB=-F/AUC-F*(DP-YT)/SB+N/AUC+M/SB
            Y=FT/(FT-FB)*D
            FSP=-NSP*(DSP-Y)/Y*FT
            FS =-NS *(DS -Y)/Y*FT
            FP =-NP *(DP -Y)/Y*FT
      C
            WRITE (6,160) YT,YB,AUC,IUC,MCR,FT,FB,FP,FS,FSP
        160 FORMAT(7H  YT  =,F10.3,7H  YB  =,F10.3/
           1       7H  AUC =,F10.3,7H  IUC =,F10.3/
           2       7H  MCR =,F10.3/7H  FT  =,F10.3,
           3       7H  FB  =,F10.3/7H  FP  =,F10.3,
           4       7H  FS  =,F10.3,7H  FS' =,F10.3)
      C
      C     CRACKED SECTION
      C
            IF (MCR.GT.M) GO TO 200
            WRITE (6,170)
        170 FORMAT(17H CRACKED SECTION:)
      C
            M=M+N*YT-R*DP
            N=R-N
```

```
C
      ALPHA=        B1B*D1    +NSPM1*ASP         +NS*AS      +NP*AP
      BETA =1./2.*B1B*D1**2+NSPM1*ASP*DSP    +NS*AS*DS    +NP*AP*DP
      GAMMA=1./3.*B1B*D1**3+NSPM1*ASP*DSP**2+NS*AS*DS**2+NP*AP*DP**2
C
      Y=(SQRT(ALPHA**2+2.*B*BETA)-ALPHA)/B
C
      IF (N.EQ.0.0) GO TO 180
C
      A0=-(GAMMA*N+BETA *M)
      A1=+(BETA *N+ALPHA*M)
      A2=+1./2.*B*M
      A3=+1./6.*B*N
      CALL ROOT(A0,A1,A2,A3,Y)
C
  180 FC =M*Y/(1./6.*B*Y**3+BETA*Y-GAMMA)
      FSP=-NSP*(DSP-Y)/Y*FC
      FS =-NS *(DS -Y)/Y*FC
      FP =-NP *(DP -Y)/Y*FC+R/AP
C
      ACR=       B*Y    +ALPHA
      QCR=1./2.*B*Y**2+BETA
      ICR=1./3.*B*Y**3+GAMMA
      YCR=QCR/ACR
      ICR=ICR-ACR*YCR**2
C
      WRITE (6,190) R,N,M,Y,YCR,ACR,ICR,FC,FP,FS,FSP
  190 FORMAT(7H  R    =,F10.3/7H  N    =,F10.3,7H  M    =,F10.3/
     1         7H  YNA =,F10.3,7H  YCR =,F10.3/
     2         7H  ACR =,F10.3,7H  ICR =,F10.3/
     3         7H  FC  =,F10.3/7H  FP  =,F10.3,
     4         7H  FS  =,F10.3,7H  FS' =,F10.3)
C
C     ULTIMATE STRENGTH
C
  200 WRITE (6,210)
  210 FORMAT(18H ULTIMATE STRENGTH:)
      IF (KODE2.EQ.1) WRITE (6,214)
      IF (KODE2.EQ.2) WRITE (6,216)
  214 FORMAT(18H (270 KSI STRANDS))
  216 FORMAT(15H (160 KSI BARS))
C
      L=KODE2
      FPU=CURV(1,L)
      FPY=CURV(2,L)
      KK =CURV(3,L)
      QQ =CURV(4,L)
      RR =CURV(5,L)
C
      I=0
      A=D/10.
      BETA1=0.85
      IF (FCP.GT.4.0) BETA1=0.85-0.05*(FCP-4.0)
  220 C=A/BETA1
      ZSP=0.003*(DSP-C)/C
      ZS =0.003*(DS -C)/C
      ZP =0.003*(DP -C)/C+R/(EP*AP)
      FSP=ESP*ZSP
      IF (ABS(FSP).GT.FSPY) FSP=FSPY*FSP/ABS(FSP)
      FS=ES*ZS
      IF (ABS(FS).GT.FSY) FS=FSY*FS/ABS(FS)
      FACT=(1.0+((EP*ABS(ZP))/(KK*FPY))**RR)**(1.0/RR)
      FP=EP*ZP*(QQ+(1.0-QQ)/FACT)
      T1=ASP*FSP
      T2=AS *FS
      T3=AP *FP
      C1=-0.85*FCP*B
      C2=-0.85*FCP*(B1-B)
      ANEW=-(T1+T2+T3-NU/PHI)/(C1+C2)
      IF (A.GT.D1) ANEW=-(T1+T2+T3+C2*D1-NU/PHI)/C1
      X=ANEW
      IF (A.GT.D1) X=D1
      TEST=(ANEW-A)/ANEW
      I=I+1
      A=ANEW
      WRITE (6,230) I,A,FP
  230 FORMAT(I7,2F10.3)
      IF (I.GT.10) GO TO 240
      IF (ABS(TEST).GT.0.001) GO TO 220
  240 NU=PHI*(T1+T2+T3+C1*A+C2*X)
      MU=PHI*(T1*DSP+T2*DS+T3*DP+C1*A**2/2.0+C2*X**2/2.0)-NU*YT
      WRITE (6,250) A,C,FP,FS,FSP,NU,MU,PHI
  250 FORMAT(7H  A    =,F10.3,7H  C    =,F10.3/
     1         7H  FP  =,F10.3,7H  FS  =,F10.3,7H  FS' =,F10.3/
     2         7H  NU  =,F10.3,7H  MU  =,F10.3,7H  PHI =,F10.3)
      GO TO 10
C
      END
C     **************************************************************
      SUBROUTINE ROOT(A0,A1,A2,A3,Y)
C
      I=0
      Y=0.0
   10 FY=A0+Y*(A1+Y*(A2+Y*A3))
      FYP=A1+Y*(2.*A2+Y*3.*A3)
      YNEW=Y-FY/FYP
      TEST=(YNEW-Y)/YNEW
      I=I+1
      Y=YNEW
      WRITE (6,20) I,Y
   20 FORMAT(I7,F10.3)
      IF (I.GT.10) RETURN
      IF (ABS(TEST).GT.0.001) GO TO 10
C
      RETURN
      END
End of file
```

Appendix J

Listing of output information for PREBEAM

```
1ANALYSIS OF PARTIALLY PRESTRESSED CONCRETE BEAMS
 DATE: 03-28-84    TIME: 22:08:57
 NILSON - P.100 - PARTIALLY PRESTRESSED T BEAM
 INPUT DATA:
  FC' =       4.0  FPU =     270.0  FSY =      60.0  FSY'=      60.0
  EC  =    3610.0  EP  =   27000.0  ES  =   29000.0  ES' =   29000.0
  B   =     4.000  D   =    30.000
  B1  =    16.000  D1  =     5.000
  B2  =     8.000  D2  =     8.000
  AP  =     0.863  DP  =    25.000
  AS  =     1.570  DS  =    27.000
  AS' =     0.0    DS' =     0.0
  N'  =     0.0    M'  =  3744.000  F   =   123.000
  NU  =     0.0    MU  =     0.0    PHI =     0.900
 UNCRACKED SECTION:
 (GROSS SECTION PROPERTIES)
  YT  =    13.123  YB  =    16.877
  AUC =   212.000  IUC = 21785.478
  MCR =  2210.173
  FT  =    -1.885  FB  =     1.186
  FP  =     4.868  FS  =     7.017  FS' =    -0.0
 CRACKED SECTION:
        1    17.227
        2    14.192
        3    13.836
        4    13.835
  R   =   131.883
  N   =   131.883  M   =   446.913
  YNA =    13.835  YCR =     7.717
  ACR =   134.806  ICR =  9308.821
  FC  =    -2.192
  FP  =   185.841  FS  =    18.513  FS' =    -0.0
 ULTIMATE STRENGTH:
 (270 KSI STRANDS)
        1     6.818   257.838
        2     7.882   252.704
        3     7.354   243.126
        4     7.585   246.765
        5     7.503   245.472
        6     7.533   245.944
        7     7.522   245.773
        8     7.526   245.835
  A   =     7.526  C   =     8.850
  FP  =   245.835  FS  =    60.000  FS' =     0.0
  NU  =     0.000  MU  =  6256.906  PHI =     0.900
End of file
```

Appendix K

Derivation of equations 3.22 and 3.23

Appendix K - Derivation of equations 3.22 and 3.23

The principle of superposition allows the total creep strain at any time t_n to be obtained as the sum of independent creep strains produced by stress changes at different ages for different durations of time.

$$\epsilon(t_n) = \sum_{j=1}^{n} \Delta\sigma(t_j)\, C(t_j, t_n)$$

$$\begin{aligned}\epsilon(t_n) &= \Delta\sigma_1 \quad C(t_1, t_n) \\ &+ \Delta\sigma_2 \quad C(t_2, t_n) \\ &+ \ldots \\ &+ \Delta\sigma_{n-1}\, C(t_{n-1}, t_n)\end{aligned}$$

Substituting for creep compliance expressed as a Dirichlet series

$$\begin{aligned}\epsilon(t_n) &= \Delta\sigma_1 \sum_{i=1}^{m} a_i(t_1) \quad [1 - e^{-\lambda_i(t_n - t_1)}] \\ &+ \Delta\sigma_2 \sum_{i=1}^{m} a_i(t_2) \quad [1 - e^{-\lambda_i(t_n - t_2)}] \\ &+ \ldots \\ &+ \Delta\sigma_{n-1} \sum_{i=1}^{m} a_i(t_{n-1})\, [1 - e^{-\lambda_i(t_n - t_{n-1})}]\end{aligned}$$

Rearraranging (note that $\Delta t_i = t_{i+1} - t_i$)

$$\begin{aligned}\epsilon(t_n) &= \Delta\sigma_1 \sum_{i=1}^{m} a_i(t_1) \quad [1 - e^{-\lambda_i \Delta t_1 - \lambda_i \Delta t_2 - \ldots - \lambda_i \Delta t_{n-1}}] \\ &+ \Delta\sigma_2 \sum_{i=1}^{m} a_i(t_2) \quad [1 - e^{-\lambda_i \Delta t_2 - \ldots - \lambda_i \Delta t_{n-1}}] \\ &+ \ldots \\ &+ \Delta\sigma_{n-1} \sum_{i=1}^{m} a_i(t_{n-1})\, [1 - e^{-\lambda_i \Delta t_{n-1}}]\end{aligned}$$

Similarly

$$\epsilon(t_{n+1}) = \Delta\sigma_1 \sum_{i=1}^{m} a_i(t_1)\,[1 - e^{-\lambda_i \Delta t_1 - \lambda_i \Delta t_2 - \ldots - \lambda_i \Delta t_n}]$$

$$+ \Delta\sigma_2 \sum_{i=1}^{m} a_i(t_2)\,[1 - e^{-\lambda_i \Delta t_2 - \ldots - \lambda_i \Delta t_n}]$$

$$+ \ldots$$

$$+ \Delta\sigma_n \sum_{i=1}^{m} a_i(t_n)\,[1 - e^{-\lambda_i \Delta t_n}]$$

Subtracting

$$\Delta\epsilon = \epsilon(t_{n+1}) - \epsilon(t_n)$$

$$= \Delta\sigma_1 \sum_{i=1}^{m} a_i(t_1)\, e^{-\lambda_i \Delta t_1 - \ldots - \lambda_i \Delta t_{n-1}}\,[1 - e^{-\lambda_i \Delta t_n}]$$

$$+ \Delta\sigma_2 \sum_{i=1}^{m} a_i(t_2)\, e^{-\lambda_i \Delta t_2 - \ldots - \lambda_i \Delta t_{n-1}}\,[1 - e^{-\lambda_i \Delta t_n}]$$

$$+ \ldots$$

$$+ \Delta\sigma_{n-1} \sum_{i=1}^{m} a_i(t_{n-1})\, e^{-\lambda_i \Delta t_{n-1}}\,[1 - e^{-\lambda_i \Delta t_n}]$$

$$+ \Delta\sigma_n \sum_{i=1}^{m} a_i(t_n)\,[1 - \epsilon^{-\lambda_i \Delta t_n}]$$

Simplifying

$$\Delta\epsilon = \sum_{i=1}^{m} A_{in}\,[1 - e^{-\lambda_i \Delta t_n}]$$

where

$$A_{in} = A_{i,n-1}\, e^{-\lambda_i \Delta t_{n-1}} + \Delta\sigma_n\, a_i(t_n)$$

In terms of axial strain and curvature

$$\Delta\epsilon = \sum_{i=1}^{m\quad N} A_{in}\,[1 - e^{-\lambda_i \Delta t_n}]$$

$$\Delta\phi = \sum_{i=1}^{m} A^{M}_{in} \left[1 - e^{-\lambda_i \Delta t_n}\right]$$

where

$$A^{N}_{in} = A^{N}_{i,n-1}\, e^{-\lambda_i \Delta t_{n-1}} + \frac{\Delta N}{Ac}\, a_i(t_n)$$

$$A^{M}_{in} = A^{M}_{i,n-1}\, e^{-\lambda_i \Delta t_{n-1}} + \frac{\Delta M}{Ic}\, a_i(t_n)$$

These equations are similar to those given in equations 3.22 and 3.23.

Appendix L

Membrane forces acting on a box girder bridge

Appendix L - Membrane forces acting on a box girder bridge

The membrane forces acting on a box girder bridge can be determined by simple strength of material relationships. Consider the simply supported box girder shown in Figure L.1(a). A uniform load of 1/2 w is applied at each web. The span length is L and the distance between the webs is B. The cantilever has a thickness of t1 while the top and bottom slabs have thicknesses of t2 and t3 respectively. Note that St and Sb are defined as the section moduli at the top and bottom of the section respectively.

Let us first consider the cantilever. In order to reference points on the cantilever, the x and y coordinate system is defined. An incremental element is located so that its right side is adjacent to the free edge of the cantilever. By treating the box girder as a beam, the longitudinal bending moment can be found as

$$M = 1/2\ w\ x\ (L - x) \qquad (L.1)$$

If the effects of shear lag are neglected, the compressive stress at the top fibre is given by

$$\sigma xx = M / St \qquad (L.2)$$

The longitudinal membrane force in the cantilever is

$$Nxx = \sigma xx\ t1 \qquad (L.3)$$

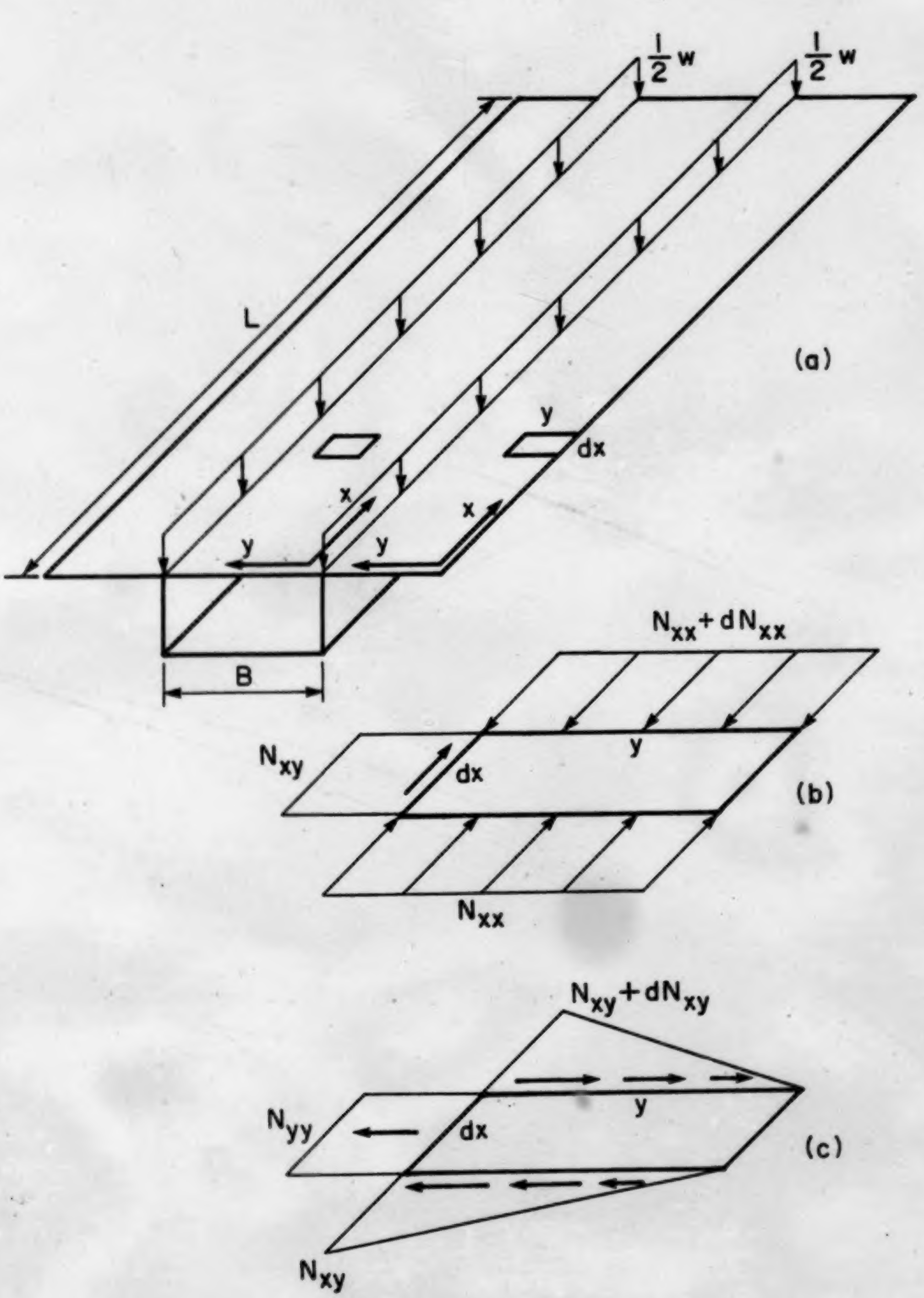
$\frac{1}{2}w$
$\frac{1}{2}w$
L
(a)
y
dx
x
x
y
y
B
$N_{xx}+dN_{xx}$
N_{xy}
dx
y
(b)
N_{xx}
$N_{xy}+dN_{xy}$
N_{yy}
dx
y
(c)
N_{xy}

Figure L.1 - Membrane forces acting on a box girder bridge

The membrane shear force can be found by referring to the free body diagram shown in Figure L.1(b). Considering equilibrium in the x direction, we get

$$Nxy = \frac{dNxx}{dx} y \tag{L.4}$$

The transverse membrane force can be found by referring to the free body diagram shown in Figure L.1(c). Considering equilibrium in the y direction, we get

$$Nyy = - \frac{dNxy}{dx} \frac{y}{2} \tag{L.5}$$

Algebraic manipulation of the previous relationships gives three equations which can be used to determine the membrane forces at any point (x,y) on the cantilever.

$$Nxx = 1/2\ w\ x\ (L - x)\ t1\ /\ St \tag{L.6}$$

$$Nxy = 1/2\ w\ (L - 2\ x)\ y\ t1\ /\ St \tag{L.7}$$

$$Nyy = 1/2\ w\ y^2\ t1\ /\ St \tag{L.8}$$

Let us now consider the top slab. An x and y coordinate system is defined at the corner of the top slab. An incremental element is located so that its right side is adjacent to the centerline of symmetry. Hence Nxy is zero at the right side of the element just as it was for the cantilever. Derivation of the equations are similar to those for the cantilever except that now the incremental element is located at y = B/2 rather than y = 0. The following three equations can be used to determine the membrane forces at any point (x,y) on the top slab.

$$Nxx = 1/2\ w\ x\ (L - x)\ t2\ /\ St \qquad (L.9)$$

$$Nxy = 1/4\ w\ (L - 2\ x)\ (B - 2\ y)\ t2\ /\ St \qquad (L.10)$$

$$Nyy = 1/2\ w\ y\ (B - y)\ t2\ /\ St \qquad (L.11)$$

Let us now consider the bottom slab. If t2 is replaced by t3 and St is replaced by Sb in the preceding equations, the membrane forces at any point (x,y) on the bottom slab can be found.

$$Nxx = 1/2\ w\ x\ (L - x)\ t3\ /\ Sb \qquad (L.12)$$

$$Nxy = 1/4\ w\ (L - 2\ x)\ (B - 2\ y)\ t3\ /\ Sb \qquad (L.13)$$

$$Nyy = 1/2\ w\ y\ (B - y)\ t3\ /\ Sb \qquad (L.14)$$

These three sets of equations are a general function of x and y. Nxx has a quadratic distribution in the longitudinal direction and a constant value in the transverse direction. Conversely, Nyy has a constant value in the longitudinal direction and a quadratic distribution in the transverse direction. Nxy has a linear distribution in both directions.

Let us now refer to the transverse membrane force (axial force) diagram (Nyy) for self weight (Figure 4.22). The significant differences between the folded plate and plane frame results are due to the fact that plane frame theory neglects the interaction of the membrane forces (Nxx, Nxy, Nyy). Figure L.2 shows that if the results given by the previous equations are added to the plane frame results, the folded plate results can be found.

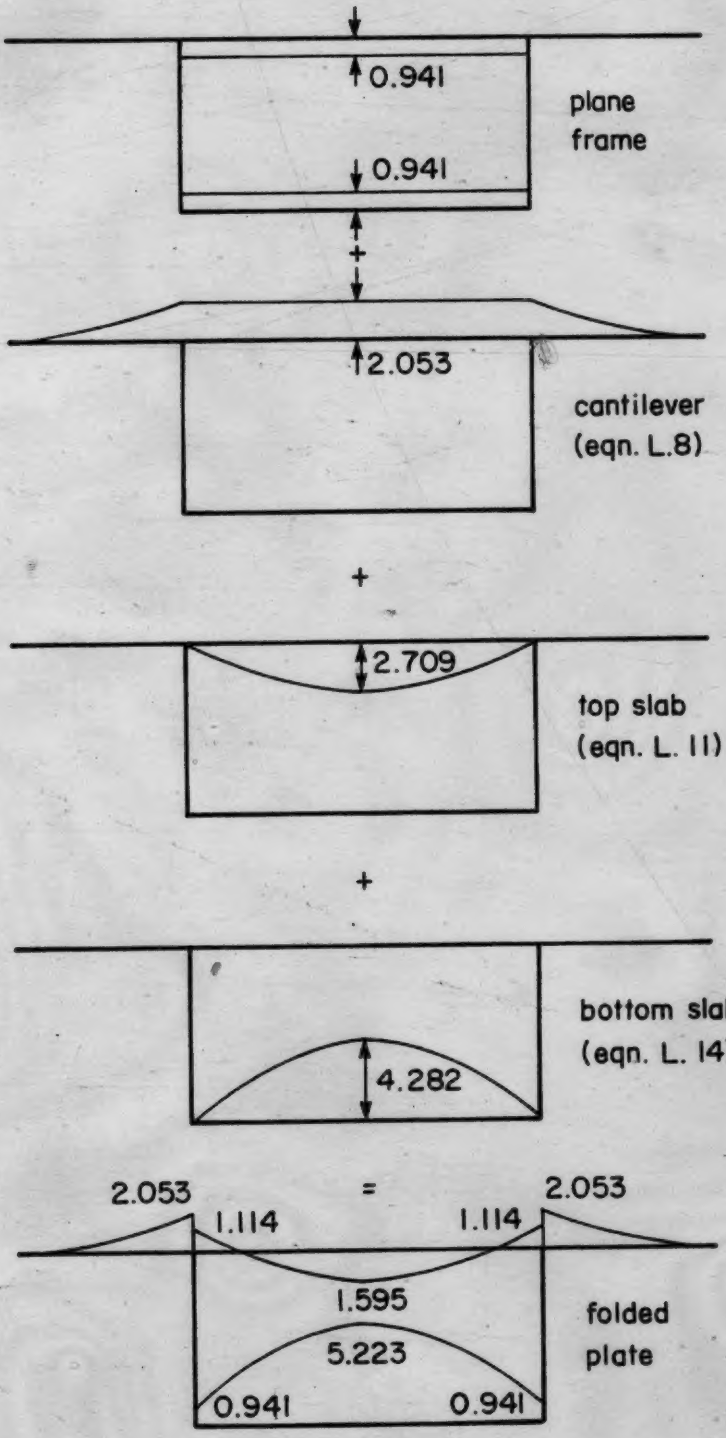
0.941
plane
frame
0.941
+
2.053
cantilever
(eqn. L.8)
+
2.709
top slab
(eqn. L. 11)
+
bottom slab
(eqn. L. 14)
4.282
=
2.053
1.114
1.114
2.053
1.595
5.223
folded
plate
0.941
0.941

Figure L.2 - Transverse membrane forces due to self weight